Final Report

FDOT Contract No: BDK75-977-46
UF Contract No. 00093705

Bottom Side Grouting of Drilled Shafts Prior to Tip Grouting

Principal Investigators: Michael C. McVay
John L. Schwartz III

Department of Civil and Coastal Engineering
University of Florida
Gainesville, Florida 32611 – 6580

Developed for the

Project Managers: Rodrigo Herrera, P.E.
Peter Lai, P.E. (retired)

December 2013

DISCLAIMER

CONVERSION FACTORS

APPROXIMATE CONVERSIONS TO SI UNITS

SYMBOL	WHEN YOU KNOW	MULTIPLY BY	TO FIND	SYMBOL
LENGTH				
in	inches	25.4	millimeters	mm
ft	feet	0.305	meters	m
yd	yards	0.914	meters	m
mi	miles	1.61	kilometers	km

SYMBOL	WHEN YOU KNOW	MULTIPLY BY	TO FIND	SYMBOL
AREA				
in^2	square inches	645.2	square millimeters	mm^2
ft^2	square feet	0.093	square meters	m^2
yd^2	square yard	0.836	square meters	m^2
ac	acres	0.405	hectares	ha
mi^2	square miles	2.59	square kilometers	km^2

SYMBOL	WHEN YOU KNOW	MULTIPLY BY	TO FIND	SYMBOL
VOLUME				
fl oz	fluid ounces	29.57	milliliters	mL
gal	gallons	3.785	liters	L
ft^3	cubic feet	0.028	cubic meters	m^3
yd^3	cubic yards	0.765	cubic meters	m^3
NOTE: volumes greater than 1000 L shall be shown in m^3				

SYMBOL	WHEN YOU KNOW	MULTIPLY BY	TO FIND	SYMBOL
MASS				
oz	ounces	28.35	grams	g
lb	pounds	0.454	kilograms	kg
T	short tons (2000 lb)	0.907	megagrams (or "metric ton")	Mg (or "t")

SYMBOL	WHEN YOU KNOW	MULTIPLY BY	TO FIND	SYMBOL
TEMPERATURE (exact degrees)				
ºF	Fahrenheit	5 (F-32)/9 or (F-32)/1.8	Celsius	ºC

SYMBOL	WHEN YOU KNOW	MULTIPLY BY	TO FIND	SYMBOL
FORCE and PRESSURE or STRESS				
lbf	pound force	4.45	newtons	N
lbf/in^2	pound force per square inch	6.89	kilopascals	kPa
lbf	pound force	0.001	kip (kilopounds)	kip

APPROXIMATE CONVERSIONS TO SI UNITS

SYMBOL	WHEN YOU KNOW	MULTIPLY BY	TO FIND	SYMBOL
LENGTH				
mm	millimeters	0.039	inches	in
m	meters	3.28	feet	ft
m	meters	1.09	yards	yd
km	kilometers	0.621	miles	mi

SYMBOL	WHEN YOU KNOW	MULTIPLY BY	TO FIND	SYMBOL
AREA				
mm^2	square millimeters	0.0016	square inches	in^2
m^2	square meters	10.764	square feet	ft^2
m^2	square meters	1.195	square yards	yd^2
ha	hectares	2.47	acres	ac
km^2	square kilometers	0.386	square miles	mi^2

SYMBOL	WHEN YOU KNOW	MULTIPLY BY	TO FIND	SYMBOL
VOLUME				
mL	milliliters	0.034	fluid ounces	fl oz
L	liters	0.264	gallons	gal
m^3	cubic meters	35.314	cubic feet	ft^3
m^3	cubic meters	1.307	cubic yards	yd^3

SYMBOL	WHEN YOU KNOW	MULTIPLY BY	TO FIND	SYMBOL
MASS				
g	grams	0.035	ounces	oz
kg	kilograms	2.202	pounds	lb
Mg (or "t")	megagrams (or "metric ton")	1.103	short tons (2000 lb)	T

SYMBOL	WHEN YOU KNOW	MULTIPLY BY	TO FIND	SYMBOL
TEMPERATURE (exact degrees)				
ºC	Celsius	1.8C+32	Fahrenheit	ºF

SYMBOL	WHEN YOU KNOW	MULTIPLY BY	TO FIND	SYMBOL
FORCE and PRESSURE or STRESS				
N	newtons	0.225	pound force	lbf
kPa	kilopascals	0.145	pound force per square inch	lbf/in^2
kip	kip (kilopounds)	1000	pound force	lbf

TECHNICAL REPORT DOCUMENTATION PAGE

1. Report No.	2. Government Accession No.	3. Recipient's Catalog No.

4. Title and Subtitle	5. Report Date
Bottom Side Grouting of Drilled Shafts Prior to Tip Grouting	March 2014
	6. Performing Organization Code
7. Author(s) Michael C. McVay and John L. Schwartz III	8. Performing Organization Report No. UF Project 93705
9. Performing Organization Name and Address Department of Civil and Coastal Engineering University of Gainesville Gainesville, Florida 32611	10. Work Unit No. (TRAIS) 11. Contract or Grant No. BDK75-977-46
12. Sponsoring Agency Name and Address Florida Department of Transportation 605 Suwannee Street, MS 30 Tallahassee, FL 32366 – 6580	13. Type of Report and Period Covered Final Report April 2011 – December 2013 14. Sponsoring Agency Code

15. Supplementary Notes

16. Abstract: Drilled shaft used as a foundation beneath structures (bridges, buildings, etc.) is common in urban areas (e.g., vibration issues) or where large lateral loading is expected in limited right-of-way areas. Unfortunately in sands and silts, the axial resistance of a drilled shaft is generally lower than similarly sized driven large-displacement piles. To increase the axial capacity of drilled shafts, post grouting of drilled shaft tips/bottoms is seeing increased use in Florida. However, tip grouting alone just preloads the tip and may result in grout flow upward alongside the soil-shaft interface, thus reducing side friction during grouting. Recognizing that grouting has the potential to significantly increase the stress state and axial capacity of a drilled shaft, the Florida Department of Transportation [FDOT] funded this research to develop a side and tip grout system for drilled shafts in loose silts and sands. The experimental efforts were scaled up from small proof of concept to large shaft test in a controlled environment (FDOT test chamber), finally to full-scale testing at an FDOT field site. The side grout system is composed of the following components: (1) tube-a-manchettes for grout delivery; (2) flexible top and bottom seals; (3) polypropylene membrane; (4) colloidal grout; and (5) multiple set of steel rings (hold membrane, seals, etc.). The new side grout system allows a contractor to cast the new shaft with traditional practices, (i.e., drill hole, place rebar cage, and concrete the shaft), but allows for sequential grouting (seals, membrane, and tip) after construction. Measurements of grout pressures and volumes in both the large-scale chamber and full-scale field tests showed that it is possible to develop cavity expansion limit pressures: cylindrical alongside the shaft and spherical below the tip of the shaft. Subsequent load testing, including top-down static and Statnamic, revealed the new side-and-tip-grouted drilled shaft is capable of mobilizing three times the static resistance (side and tip) of a conventional ungrouted shaft at conservative service settlements (e.g., 1"). For design, recommendations on estimating side and tip resistance are presented based on in situ testing (e.g., Standard Penetration Test (SPT) and Pressuremeter Test (PMT)), and/or newer method (i.e., K_g) using the existing vertical effective stress in the grout zone.

17. Key Word	18. Distribution Statement
Deep Foundations, Drilled Shafts, Side and Tip Grouting, Axial Capacity, Cavity Expansion, Chamber Testing, Static Load Testing, Statnamic Testing, In situ Testing (SPT, CPT, PMT)	No Restrictions.

19. Security Classif. (of this report)	20. Security Classif. (of this page)	21. No. of Pages	22. Price
Unclassified	Unclassified	262	

ACKNOWLEDGEMENTS

The researchers would first like to thank the Florida Department of Transportation [FDOT] for the financial support to carry out this research as well as the guidance of the project managers for its successful outcome. The researchers would also like to thank University of Florida faculty, graduate assistances, and administration, for their efforts made it possible to complete the project. In addition, this research could not have been completed without the aid of the State Materials Office, who performed the laboratory testing (e.g., concrete and grout unconfined compression testing, as well as testing the load cell and readout system), installation of pressures cells in the field, and conducted all in situ testing (SPT, CPT, DMT, and PMT tests). Next, the researchers would like to thank Loadtest Inc. for the use of their data acquisition system, Reliable Constructors Inc. for excavation and shaft construction, and especially Applied Foundation Testing Inc. for providing grouting equipment, grouting services, and contributing equipment and labor for Statnamic testing. Finally, the researchers would like to recognize the Coastal Engineering Laboratory lab technicians for assisting with fabrication, construction, grouting processes, and load tests.

EXECUTIVE SUMMARY

Drilled shaft use as a foundation beneath structures (bridges, buildings, etc.) is common in urban areas (e.g., because of vibration issues) or where large lateral loading is expected in limited right-of-way areas. Unfortunately in sands and silts, the axial resistance of drilled shafts is generally lower than that of similarly sized driven large-displacement piles. To increase the axial capacity of drilled shafts, post grouting of drilled shaft tips/bottoms (Mullins et al, 2006) is seeing increased use in Florida and throughout the United States. Tip grouting of the shaft serves two functions (Thiyyakkandi et al., 2013a and 2013b; McVay et al., 2009): (1) it preloads the tip or it increases the shaft tip mobilization (i.e., reloading) at the onset of axial top loading; and (2) it gives an estimate of axial shaft capacity (i.e., grout pressure times cross-sectional tip area). However during tip grouting, it has been found (Florida Department of Transportation [FDOT] report BD545-31), that grout first fills the ring void beneath the shaft and then flows in the weakest direction, usually up alongside the soil-shaft interface (low radial stress around shaft), reducing side friction during the grouting process (i.e., fluid grout between soil-shaft interface).

The FDOT readily recognized that grouting had the potential to significantly increase the axial capacity of a drilled shaft. Specifically if the stress states (side and tip) could be increased (e.g., cavity expansion), significant side and tip resistance of a drilled shaft could be developed vs. conventional or tip-grouted approaches. Consequently, the focus of this research was to develop/introduce materials and construction practices which would allow a traditional drilled shaft to be cast (e.g., hole, rebar cage placement, and concreting), then side-grouted, and finally tip grouted with sufficient wait times for concrete and grout hydration. As with the development of any new technology, the experimental effort was scaled up from small proof of concept to larger tests in a controlled environment (i.e., FDOT test chamber), then to full-scale testing at an FDOT field site. The final side-and-tip-grouted drilled shaft was constructed as two separate systems: (1) side grout system and (2) tip grout system.

The side grout system is composed of the following components: (1) tube-a-manchettes for grout delivery; (2) flexible top and bottom seals; (3) polypropylene membrane; (4) colloidal grout (cement, fly ash, and water); and (5) multiple sets of steel rings (hold side membrane, seals, etc.). Easily fabricated using thermal welding techniques, the polypropylene membrane has a number of functions: (1) prevents mixing of grout and soil (loss of grout strength and grout-shaft concrete bond); and (2) limits grout flow, i.e., impermeable membrane. The top and bottom membrane seals had three important functions: (1) inflated with air during shaft construction, which prevents concrete flow outside of the membrane; (2) separate the membrane from the concrete shaft in first stage of grouting; and (3) provide a top and bottom constraints during side grouting.

The tip grouting system follows construction methods similar to that of conventional tip-grouted shafts and has the following components: (1) tube-a-manchettes for grout delivery; (2) steel base plate and bottom ring; (3) steel feet (cage support and bottom manchette protection); (4) bottom membrane; and (5) colloidal grout (cement, fly ash, and water). The tube-a-manchettes exiting the top and bottom of the shaft should be constructed from schedule 80 pipe because tip grout pressures may exceed 1,000 pound per square inch (psi). The steel bottom plate, steel ring, and steel feet are strongly recommended to provide support (i.e., minimize rebar cage settlement) and protect the tube-a-manchettes when the cage is placed in the drilled shaft hole (e.g., clogged with loose soil and/or embedded in concrete).

A large-scale test shaft (36" x 25') was constructed and subsequently side and tip grouted in the FDOT test chamber. Recorded side and tip grout pressures either equaled or exceeded the expected spherical (tip) and cylindrical (side) cavity expansion limit pressures (Salgado and Randolph, 2001) at grout volumes approaching one and a half times the initial shaft diameter (1 ½ D or 1.5 D). In the case of a full-scale test shaft (42" x 25') conducted in the field (Keystone Heights, Florida), measured side grout pressures (420 psi) were in reasonable agreement with cylindrical cavity expansion values (399 psi), and tip grout pressures (620 psi) were less than the spherical limit pressures due to the limited allowed vertical movement (0.3") of the shaft. Subsequent Statnamic testing of the field shaft showed the static capacity of the shaft in excess of 2,650 kip (side – 1,350 kip; tip – 1,300 kip) at 1.5" of vertical movement.

The side resistance (after side grouting) was estimated using one of four methods: (1) K_g method (Thiyyakkandi et al., 2013b); (2) in situ Pressuremeter Test (PMT); (3) measured in situ soil pressure cell data; and/or (4) measured tip grouting pressures during construction. Total capacity was estimated as at least twice the estimated side resistance (mobilized during tip grouting). Comparison of capacity estimation methods versus the observed side resistance generally showed them to be conservative (i.e., underpredicts side friction). This was attributed to the mobilization of end bearing on the top or bottom of the side membrane (i.e., end bearing on the shelf/ledge created by increased diameter along the side grouted zone). Finally, the new side-and-tip-grouted drilled shaft is conservatively shown to have a capacity three times greater than a conventional ungrouted drilled shaft at service settlements (e.g., 1").

TABLE OF CONTENTS

LIST OF FIGURES

LIST OF TABLES

CHAPTER 1
INTRODUCTION

1.1 Background and Literature Review

1.1.1 Background and Previous Research

Drilled shafts are widely used around the world to support bridges, buildings, signage, walls, and so on. They are typically used in residential areas that are unfavorable for driven piles (i.e., sensitive to seismic vibrations), sites that require embedment into rock layers, or large lateral resistance (i.e., large moment of inertia). Drilled shafts support axial loads through side shear alongside the shaft and tip resistance beneath the shaft. The side and tip resistance of a drilled shaft are mobilized quite differently; generally, the tip resistance requires large vertical displacements to become fully mobilized, as shown in Figure 1-1 on the next page. Mobilization of the side resistance component can be 50% of the ultimate at displacements of approximately 0.2% of the shaft diameter, D, (AASHTO, 2010) and fully developed at displacements in the range of 0.5% to 1.0% of D (Bruce, 1986; Mullins et al., 2006). On the other hand, a displacement of about 2.0% is required to mobilize 50% of the ultimate tip resistance (AASHTO, 2010) and fully mobilized in the range of 10% to 15% of D (Bruce, 1986). In the case of ultimate unit side friction for cohesionless soils, a drilled shaft will develop 25% to 100% smaller resistance than a driven pile (H, solid square, etc.) depending on the relative density, depth, and so on.

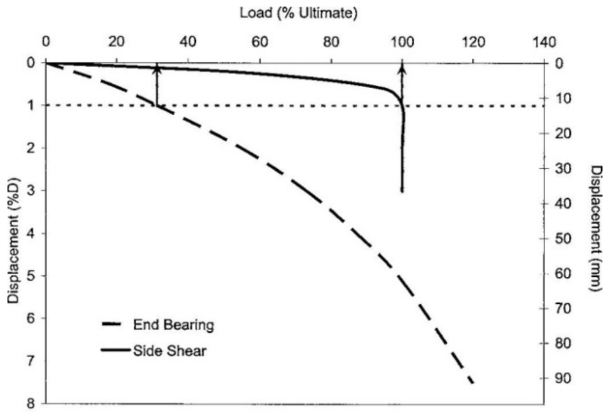

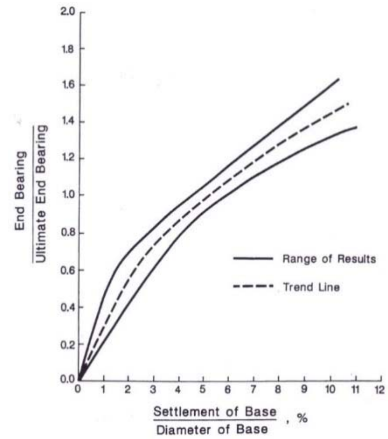

Figure 1-1: Left figure (Mullins et al., 2006) - typical mobilization of the side and tip resistance for a drilled shaft in a cohesionless soil (42 inch diameter); Right figure (Reese and O'Neill, 1988) - Ultimate end bearing for an allowable displacement of 5% of shaft diameter

Since large displacements, i.e., exceeding the structural tolerance limits, are required to mobilize significant tip resistance as well as soil disturbance issues during construction, typical designs for drilled shaft in weathered rock neglect the tip resistance contribution to the axial capacity (FDOT Soils and Foundations Handbook, 2012; AASHTO, 2010; FHWA, 2010). To utilize a significant part of tip resistance under tolerable/serviceable settlement, post grouting the drilled shaft tip has been introduced and has become common practice in the United States in the last decade. Specifically, cement grout is pumped under pressure to the tip of the shaft after the shaft construction, i.e., 14 to 28 days for concrete hydration. The pressurized grout fills any voids and compresses the soil below the tip (preloading). Since the grout exerts bi-directional force, side resistance of the shaft is mobilized in an upward direction during the tip grouting process. Since the applied grout pressure is balanced by the mobilized side friction and self-weight of shaft, the maximum grout pressure is limited by the available side resistance of the shaft.

Tip grouting is inherently also a proof test of the shaft's side resistance, i.e., it verifies the minimum axial capacity, which is equal to two times the resultant tip force (grout pressure times shaft tip area) during grouting (Mullins et al., 2006). Since the soil beneath shaft's tip is preloaded to the applied grout pressure, the tip resistance follows a reloading path (stiffer) up to the applied grout pressure during subsequent top-down loading (Mullins et al., 2006). That is, a large quantity of tip resistance is mobilized under small displacements depending on the applied grout pressure. The pre-loading of soil beneath a drilled shaft's tip during conventional post grouting processes and the stiffer reloading path during axial loading is illustrated in Figure 1-2 below. The tip grouting process occurs between points (1) and (2), steady state reached after tip grouting stopped between points (2) and (3), and during axial loading, the mobilized side and tip resistance of a conventional post grouted drilled shaft between points (3) and (4).

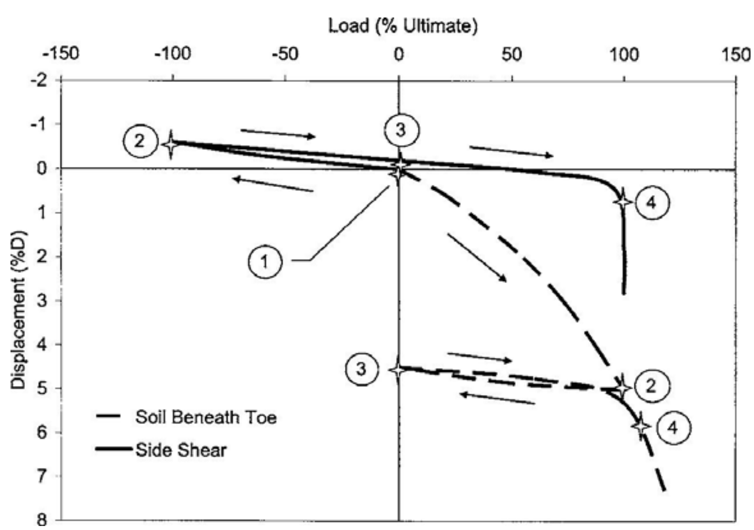

Figure 1-2: Illustration of pre-loading soil beneath drilled shaft tip resulting from conventional tip grouting process (Mullins et al., 2006)

Post tip grouting of a drilled shaft does not necessarily improve the soil's properties (i.e., angle of internal friction) or stress state (mean stress), and thus, tip grouting alone has no influence on the ultimate resistance of drilled shafts (McVay et al., 2009). The tip capacity under small displacement is improved only by preloading effect and possible increased tip area (Thiyyakkandi et al., 2013a and 2013b). McVay et al. (2009) also identified that the increase in tip area was by the accumulation of upward flowing grout and not by a cavity expansion process. During post grouting processes, the grout tries to flow along the path of least resistance (Figure 1-3), which is normally along the soil-shaft interface due to the low lateral stress (minor principal stress).

Figure 1-3: Conventional tip-grouted shafts (left - McVay and Thiyyakkandi, 2010; right - Mullins and Winters, 2004)

However, the soil stress states below the shaft tip can be improved by developing spherical cavity expansion stresses during post grouting steps (McVay et al., 2009). The latter requires that the radial stress be increased first alongside the shaft (i.e., side grouting) prior to tip grouting. For instance, Salgado and Randolph (2001) identified that significant cylindrical cavity expansion pressures (i.e., radial stresses) could be developed, e.g., pressuremeter testing, in cohesionless soil depending on depth of embedment. Similarly, if a membrane and side grout zone were introduced to a drilled shaft, significant uniform radial stresses (i.e., grout pressures) could be developed. As result of increasing the radial stress, the side friction alongside the shaft in the grout zone would also increase appreciably.

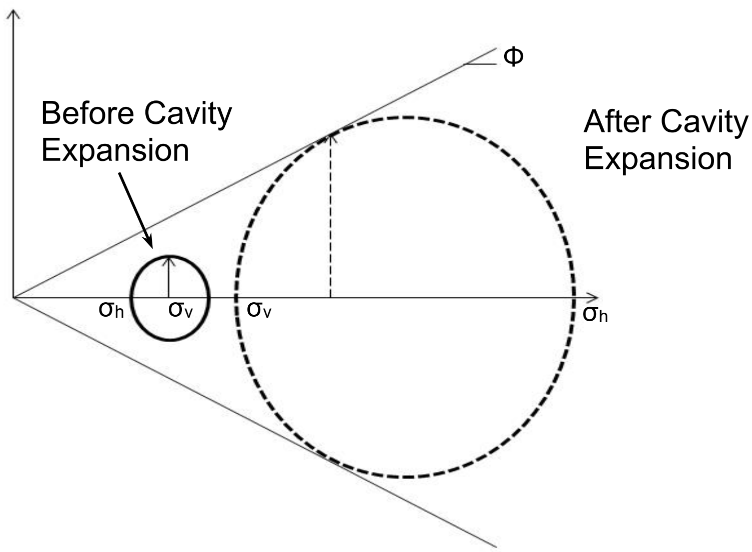

Figure 1-4: Illustration of the change in stress state during cavity expansion using Mohr-Coulomb circle

Shown in Figure 1-4 (solid circle) is the expected principal stresses near a drilled shaft (i.e., $\sigma_v > \sigma_h$) after a typical drilled shaft installation. Generally during tip grouting, the horizontal stress would not increase during tip grouting (McVay et al., 2009), but instead, the vertical stress, σ_v, would increases until failure (i.e., circle touches strength envelope). However, with sufficient side grouting (sufficient length of zone and pressure), the horizontal stress during grouting would increase along with the vertical stress and shown by the dashed circle in Figure 1-4. The increase in horizontal and vertical stresses results in the Mohr circle being shifted to the right until failure, thus resulting in greater mobilized shear resistance at failure.

Another component that adds to the increased shaft capacity is the size of the grout regions around the shaft. In the case of side grouting, the grout bulb expands out radially, i.e., increasing the surface area alongside the shaft which further increases side resistance when combined with the increased lateral stress. Similarly during subsequent tip grouting, cavity expansion will results in an increase in tip stresses and the development of a spherical bulb (increased tip area) at the tip of the shaft, resulting in a significant increase in ultimate tip capacity. Also note, the greater the side resistance (i.e., side friction and the additional weight of grout), the higher grout pressures (spherical cavity expansion) are achievable below the tip of the shaft.

1.1.2 Summary of State-of-the-Art

A drilled shaft's axial capacity in cohesionless soils may be improved by increasing the soils' stress states along the bottom side and below the shaft tip during side and tip grouting processes. The improved stress state of the soil is achieved through the development of cylindrical cavity expansion pressures during side grouting (i.e., new processes) and spherical cavity expansion pressures during tip grouting (i.e., new outcome). By improving the soil stress state around the bottom side, greater side and tip resistance can be mobilized during service loading conditions. Additionally, axial resistance (side and tip) are developed due to increased areas (surface – side; cross-sectional – tip) as a result of the grouting sequence (i.e., side followed by tip) (McVay et al., 2009).

A new side grouting technique is proposed for drilled shafts which employs membrane seals and an impermeable side membrane. Both the membrane seals and side membrane are discussed further in Chapters 2 and 3. By controlling grout flow during side grouting, cylindrical cavity expansion pressures (Salgado and Randolph, 2001) can develop along the bottom side of the shaft (above the tip). Cavity expansion process increases the horizontal stress state surrounding the shaft such that the horizontal stress becomes major principal stress (Figure 1-4). The increased stress state near the bottom of the shaft restricts grout flow vertically upwards along the soil-shaft interface during subsequent tip grouting, so higher grout pressures and cavity expansion stresses (i.e., available tip stresses) can develop during subsequent tip grouting. It is expected that tip grouted pressures under the proposed process are much greater than that of conventional tip grouting stresses (i.e., no side grouting).

1.2 Objectives

The overall scope of this project was to improve the axial capacity of drilled shafts in cohesionless soils by developing cavity expansion pressures alongside and beneath the bottom of the shaft. The scope of the project was separated into four main tasks: (1) develop technology to allow side grouting of a cast in situ drilled shaft; (2) compare theoretical cavity expansion pressures (cylindrical and spherical) with the observed grout pressures (side and tip); (3) perform static and Statnamic (field shaft only) load tests on the side-and-tip-grouted drilled shafts; and (4) compare the measured capacities of the side-and-tip-grouted drilled shafts with the estimated capacities using in situ data (Standard Penetration Test (SPT) and Pressuremeter Test (PMT)) and grout pressures observed during construction.

To investigate side and tip grouting of drilled shafts, three full scale test shafts were constructed and tested. First, the construction and implementation of the side and tip grouting system was verified with a 36" x 6' test shaft and will be referred to as the short shaft throughout this report. Next, an instrumented 36" x 25' test shaft (referred to as the long shaft) was constructed in the FDOT/UF test chamber and tested under static loading conditions to measure force-deformation, soil stresses, and shape (exhumed shaft). The final shaft was an instrumented 42" x 25' test shaft (referred to as the field shaft) and constructed in the field by a contractor and tested under static and Statnamic loading conditions. A discussion of each follows.

1.2.1 Short Test Shaft in FDOT Test Chamber (Short Shaft – 36" x 6')

The focus of the short shaft was to demonstrate the ability to develop cavity expansion pressures during side and tip grouting processes and ensure proper attachment of the various grout systems (i.e., membrane seals, side membrane, and tip grout system). The rebar cage and various grouting systems were constructed at UF Coastal Engineering Laboratory (coastal lab), with the shaft construction and post grouting processes performed in the FDOT test chamber also located at the coastal lab. Details of the coastal lab and FDOT test chamber are discussed in section 1.3 (Methodology: Equipment and Test Facilities). The short shaft was exhumed after the post grouting processes and visually examined to identify the effectiveness of the grout system and any areas of concern that should be improved. Of great interest was the flow direction of the grout during the side and tip grouting phases.

1.2.2 Long Test Shaft in FDOT Test Chamber (Long Shaft – 36" x 25')

The focus of the larger test shaft was to validate the side and tip grouting processes at stress states representative of the field. Of great interest was the stress state of the soil and mobilized side and tip resistance before, during, and after the grouting processes. Again, the rebar cage and various grouting systems were constructed at the UF coastal lab, and the shaft construction and post grouting processes were completed in the FDOT test chamber. A static top-down load test was performed on the shaft to assess the axial response to static loading (i.e., under service loading conditions). The internal strain and shaft displacement was monitored throughout the test to quantify the load-displacement behavior of the side-and-tip-grouted shaft. Following the load test, the shaft was exhumed and visually examined to identify the effectiveness of the grout system and any areas of concern that should be improved.

1.2.3 Full-Scale Test Shaft at FDOT Test Site (Field Shaft – 42" x 25')

The focus of the field shaft was to execute the side and tip grouting processes in field conditions while monitoring the soil stress around the grouted zones and internal strains (vibrating wire) along the shaft during all phases (i.e., grouting and load testing). The rebar cage and various grouting systems were constructed on UF campus at the coastal lab, but the shaft construction and post grouting processes took place at the FDOT test site located near Keystone Heights, Florida (a.k.a., Kingsley Borrow Pit). The FDOT test site is discussed in section 1.3 (Methodology: Equipment and Test Facilities).

1.2.4 Static Load Test on Shaft at FDOT Test Site (Field Shaft – 42" x 25')

A top-down load test (static load test) was performed on the field shaft to assess the axial response to static loading (i.e., under service loading conditions). The internal strain and shaft displacement was monitored throughout the test to quantify the load-displacement behavior of the side-and-tip-grouted shaft. For this test, two 48" x 55' reaction drilled shafts were used. Of great interest, the mobilized side and tip resistance were obtained from the internal strain data. Strain gauges were cast into the shaft just above the side grout zone and at the tip of the shaft (below the side grout zone).

1.2.5 Statnamic Load Test on Shaft at FDOT Test Site (Field Shaft – 42" x 25')

Due to the limited uplift capacity of the reaction shafts (section 1.2.4), an additional load test, i.e., Statnamic, was performed on the field shaft. Since the vibrating wire strain gauges (section 1.2.3) could not record continuously during Statnamic loading, additional foil strain gauges and a tip accelerometer were post installed, i.e., two - 3" x 25' cores were drilled into the shaft, gauges placed, and holes grouted. For the Statnamic test, a 2,000 kip device was setup by Applied Foundation Testing Inc. (AFT) with strain, forces, accelerations, and deformations monitored by AFT during the test.

1.2.6 Design Recommendations for Side-and-Tip-Grouted Drilled Shafts in Cohesionless Soils

The focus of this task was to provide design recommendation given the results of the three full-scale test shafts (short, long, and field). Design recommendations include site investigation and data analysis for SPT and PMT, grout system assembly (materials and dimensions), grouting procedures (volumes and pressures), quality control (monitoring), capacity calculations (side and tip resistance before and after grouting), and prediction of total shaft capacity vs. top displacement.

1.3 Methodology

1.3.1 Experimental Design and Preface

Performance, reliability, and constructability were the main focus throughout the design evolution of the new side grout system. The new side grout system was designed to prevent grout flow vertically upwards during the side grouting phase, allowing for higher grout pressures and cavity expansion to develop. An impermeable membrane was used to contain the grout during the side grouting phase. Because the side membrane must be cast-in-place along with the rebar cage, the possibility of embedding the side membrane, rendering it useless during shaft construction had to be prevented. Consequently, a torus-shaped seal (membrane seal) was developed to prevent concrete from flowing outside of the side membrane. The membrane seal was constructed using high pressure layflat discharge hose.

The membrane seal was placed at the top of the side membrane between the rebar cage and side membrane, and then pressurized with air while concrete was placed. As the membrane seal was pressurized, the torus expands outwards pressing the side membrane against the wall of the shaft creating a “seal” that prevented concrete flow between the side membrane and shaft wall (i.e., flow outside of the side membrane). It was later decided to employ a second membrane seal located at the bottom of the side membrane to prevent concrete from flowing around the bottom of the rebar cage and up along the side membrane. The design evolution of the membrane seals and side membrane will be discussed further throughout Chapters 2 and 3.

The short shaft was constructed and post grouting processes were completed to confirm the potential for developing cavity expansions during side and tip grouting processes (i.e., test preliminary design). Of concern was the performance of the membrane seals in preventing concrete from embedding the side membrane during shaft construction and side membrane in restricting grout from flowing vertically upwards during the side grouting and subsequent tip grouting phases. The material type and fabrication method for the membrane seals and side membrane were investigated before implementing with the short shaft (section 2.1.1). The observations made during shaft construction and post grouting processes were used in conjunction with the exhumed shaft and visual examination of the post grouted short shaft to facilitate the design improvements implemented on the long shaft.

The long shaft was constructed and post grouting processes were completed to quantify the influence of the side and tip grouting processes had on the surrounding soil and measure the load-displacement behavior under axial loading. Of concern was the stress state of the soil surrounding the side and tip grouted zones and the mobilized side and tip resistances during axial loading. Further testing of the material type and fabrication method for the membrane seals and side membrane were investigated before constructing the long shaft (section 2.2.1). The observations and data collected during shaft construction and post grouting processes were used in conjunction with the excavation and visual examination of the post grouted long shaft to facilitate the design improvements implemented on the field shaft.

The field shaft was constructed and post grouting processes were completed to confirm the constructability of the side-and-tip-grouted drilled shaft in field conditions and to again quantify the influence of the side and tip grouting processes on the surrounding soil and measure the load-displacement behavior under axial loading. Of concern was the construction time for the side-and-tip-grouted drilled shaft (i.e., time to complete shaft construction, post grouting processes, and allow sufficient hydration before applying service loads), and again, the stress state of the soil surrounding the side and tip grouted zones and the mobilized side and tip resistances during axial loading. The observations and data collected during shaft construction and post grouting processes were used in conjunction with the results obtained from the short and long test shafts to develop the design recommendations for side-and-tip-grouted drilled shafts in cohesionless soils (section 6.2).

1.3.2 Equipment and Test Facilities

Earth pressure cells were used with the long and field shafts to quantify the influence of the side and tip grouting processes has on the surrounding soil (i.e., measure soil stresses). The long shaft was tested in the FDOT test chamber, and Geokon earth pressure cells (Model 4800) were placed throughout the test chamber at various depths, distances away from the shaft, and in different orientations (vertical and horizontal). Testing and placement of these pressure cells throughout the test chamber is discussed in section 2.2.2. The field shaft was tested at the FDOT test site, and RST push-in pressure cells (Model VW-2100) were used to monitor the soil stress around the side and tip grouted zones. Testing and placement of these pressure cells in the field is discussed in section 3.1.2. Both the Geokon and RST pressure cells used vibrating wire technology to measure stresses.

Embedded strain gauges were used with the long and field shafts to quantify the mobilized side resistance during tip grouting and axial loading (i.e., measure strain along the shaft). On the long shaft, four strain gauges were attached to the rebar cage and cast-in-place, with two gauges (180° apart) placed above the side membrane and two gauges (180° apart) placed below the side membrane (tip). By placing gauges above and below the side membrane, the mobilized side resistance along the side grouted zone could be calculated, and by placing the gauges 180° apart, bending forces were calculated. The types of strain gauges used on the long shaft were Geokon (Model 4200) concrete embedment gauges which use vibrating wire technology to measure the strain. The location of the embedded strain gauges on the long shaft will be discussed in section 2.2.3.

On the field shaft, eight strain gauges were attached to the rebar cage and cast-in-place. Two types of strain gauges were used on the field shaft (orthogonal to each other): four Geokon (Model 4200) concrete embedment gauges which use vibrating wire technology to measure the strain, and four Vishay (Model EGP-5-350) concrete embedment gauges which use resistance wire technology to measure the strain. Again, two gauges (of each type) were placed above the side membrane and two gauges (of each type) were placed below the side membrane (tip), with gauges 180° apart (of the same type). By placing gauges above and below the side membrane, the mobilized side resistance along the side grouted zone could be calculated, and by placing the gauges 180° apart, bending forces were calculated. The location of the embedded strain gauges will be discussed in section 3.1.3. Additionally, one five volt accelerometer (± 20 times gravity) and five Vishay (Model EGP-5-350) concrete embedment gauges were installed after shaft construction, so a complete analysis of Statnamic load test could be done (i.e., calculate inertial and damping forces). The location and installation of these six gauges will be discussed in section 3.1.5.

The data acquisition system used collect the pressure cell data and vibrating wire strain data during the post grouting processes and top-down load tests consisted of a multiplexer, data logger, and a computer with the MultiLogger program installed. The instrumentation (i.e., pressure cells and strain gauges) were connected to the multiplexer to be read in sequential order. The data logger automatically reads each channel on the multiplexer and saves the data (readings) to an internal storage device, and a computer was used to control the MultiLogger program. The data acquisition system allows for automated data collection during post grouting processes and top-down load tests, so less personnel was required during these phases (i.e., do not need to manually collect pressure cell and strain data). The data acquisition system will be discussed further in sections 2.2.2 and 3.1.2.

Digital dial gauges were used to measure vertical displacements of the shaft and soil during post grouting processes and top-down load tests. These gauges were not connected to an automated data collection system but instead read manually during grouting and load tests. The digital dial gauges had an accuracy of ± 0.0001 inch. By measuring the displacements during post grouting processes and top-down load tests, the percent mobilized side and tip resistance could be estimated and the load-displacement behavior could be characterized. The location of the digital dial gauges during various grouting processes and load tests are discussed in Chapters 2 and 3.

Performance and reliability based tests performed on the membrane seals and side membrane, fabrication of the three grout systems (i.e., membrane seals, side grout system, and tip grout system), construction of the rebar cage, and attaching the various grout systems to the rebar cage all took place at the Coastal Engineering Laboratory (coastal lab) or in the Soil Mechanics Laboratory on UF campus (soils lab). Material property measurements and load cell calibrations were completed in the Structure Laboratory on UF campus or in the Structure Laboratory at the State Materials Office (SMO) located in Gainesville, Florida. Both were structure labs, so modern equipment and knowledgeable staff were available to ensure accurate valuation of the load cells and the measurement of material properties like the strength of the side membrane material, unconfined compressive strength of concrete and grout, and Young's modulus and Poisson's ration of concrete and grout. Field technicians from SMO performed the site investigations at the FDOT test site (i.e., SPT, CPT, DMT, and PMT), and the Soil Mechanic Laboratory at SMO provided the soil properties for the soil used in the FDOT test chamber and recovered soil samples from the FDOT test site (i.e., gradation, moisture content, and friction angle). The site investigation and soil properties will be discussed in Chapter 5.

Funded by the Florida Department of Transportation [FDOT] and in collaboration with the University of Florida [UF], a large diameter steel casing (i.e., FDOT/UF test chamber) was installed at the coastal lab to conduct full scale tests in a controlled environment (McVay et al., 2009). Throughout the remainder of this report, the FDOT/UF test chamber will be referred to simply as the "test chamber". The test chamber is 12 feet in diameter and 35 feet deep, with a concrete plug and drain field constructed at the bottom. Two reaction shafts were constructed on either side of the test chamber, so top-down axial load tests could be performed on test piles or shafts constructed within the test chamber. The reaction shafts have a diameter of four feet and an uplift capacity of 300 kip (600 kip total uplift capacity). The first two test shafts (short and long) were constructed and tested in the FDOT test chamber to minimize uncertainties associated with construction method, spatial variability, and soil properties. In addition, the FDOT test chamber allowed precise placement of earth pressure cells in proximity to the test shaft and control of the water table within the test chamber (i.e., controlled saturation within test chamber). The test chamber was filled with a silty-sand (A-2-4 soil), which is typically found in Florida. The soil was placed in lifts to achieve specific soil properties like unit weight, relative density, and friction angle. The soil placement, pressure cell placement, and construction of the sort and long test shafts will be discussed in Chapter 2.

The field shaft was cast, grouted, and loaded axially at the FDOT test site, and throughout the remainder of this report, the site will be referred to simply as “the field,” “test site,” or “Keystone Heights.” The test site is located at the Kingsley Borrow Pit (FDOT District 2) outside of Keystone Heights, Florida. Before construction of the field shaft, two reaction shafts were constructed so that top-down load testing could be performed on the side-and-tip-grouted test shaft (field shaft). The reaction shafts have a diameter of four feet and an estimated individual uplift capacity of 500 kip (1,000 kip total uplift capacity). As stated earlier, a site investigation was conducted across the test site and will be discussed further in Chapters 3 and 5. The predominate soil types (i.e., typical soil stratigraphy across the test site) are clay layer (varying thickness) underlain by silty-sand (varying thickness) followed by dense sand (varying depth).

Shaft construction, post grouting processes, and excavations were completed with the assistance of coastal lab technicians, crane operations, and subcontractors (i.e., Reliable Constructors Inc. and Applied Foundation Testing Inc.). The short shaft was constructed (cast), grouted, and excavated with the assistance of the coastal lab technicians only (relatively small shaft). The long and field shafts (larger shafts) however required crane operations and subcontractors to complete construction, post grouting processes, and excavation of the long shaft. Details of shaft construction post grouting processes, and excavations (if any) of all three test shafts will be discussed in Chapters 2 and 3. Post grouting of the short shaft and grouting of all membrane seals (i.e., membrane seals on all three test shafts) was completed using UF’s grout pump.

The side and tip grouting processes on the long and field shafts was completed with grouting services provided by Applied Foundation Testing Inc. (AFT). Additionally, AFT completed the Statnamic load test performed on the field shaft.

The excavation of the test chamber (twice) and shaft construction in the field was completed by Reliable Constructors Inc. (Reliable). Crane services were required on various phases of the project such as, removal of the casing during long shaft construction (test chamber), removal of the long shaft for visual examination (test chamber), moving the rebar cage with grout systems attached during field shaft construction (test site), setup and breakdown of the reaction system used for top-down load test on field shaft (test site), and setup and breakdown of the reaction system used for statnamic load test on field shaft (test site). A heavy lift forklift (Taylor – 20,000 pound (lb) capacity) was able to execute many heavy lifts throughout the project such as, removal of the short shaft for visual examination (test chamber), placing the casing used during long shaft construction (test chamber), setup and breakdown of the reaction system used for top-down load test on long shaft (test chamber), and placing rebar cage with grout systems attached on a flatbed truck for transport to the test site (coastal lab).

1.3.3 Procedures and Analysis

The evolution of the new side grouting process (i.e., implementation of membrane seals and side membrane) began with an initial design (i.e., material selection, fabrication method, and attaching to the rebar cage). The short shaft testing results facilitated improvements and further testing with the second test shaft (long shaft). The second test shaft was instrumented with embedded strain gauges and test chamber instrumented with pressure cells. The results from the second test shaft facilitated further design improvements, which were implemented on the third test shaft (field shaft). The third test shaft was also instrumented with embedded strain gauges and pressure cells installed around the test shaft. The results from the third test shaft, along with results from the first two test shafts, led to the design recommendations for side-and-tip-grouted drilled shafts in cohesionless soils (section 6.2).

The initial design executed on the short shaft began with investigating materials and fabrication methods for the membrane seals and side membrane. Different tests were conducted to determine the performance, reliability, and constructability of the materials and fabrication methods used. The initial investigation of materials and fabrication methods will be discussed further in section 2.1.1. The short shaft was constructed (cast), side and tip grouted, exhumed, and visually examined to confirm the performance and reliability of the new side grouting process. Of importance were the fabrication methods and shaft construction process (i.e., constructability), predicted grout volumes and pressures vs. observed (actual) grout volumes and pressures, and the overall shapes of the side and tip grout bulb (i.e., grout flow during post grouting processes).

Both the grout volume and pressure are controlled by cavity expansions theory (cylindrical and spherical) and will influence the shape and size of the grout bulb (McVay et al., 2009). The cavity expansion limit pressures, i.e., predicted maximum grout pressures associated with the grouting process, were computed based on

Salgado and Randolph (2001) (see Figures 1-5 and 1-6 at the end of the chapter). The predicted maximum grout pressures were compared to the observed (actual) grout pressures. Calculation of the predicted grout pressures will be discussed further in sections 5.1.4 and 5.2.4.

Grout was pumped under high pressure to develop the cavity expansions along the bottom side and below the drilled shaft tip. All grout was mixed following the grout mix design developed in preceding research (McVay et al., 2009). The grout mix design specifies a water to cement ratio of 0.45 and 2% fly ash by volume. The water to cement ratio is low enough to maintain adequate compressive strength, and the fly ash improved the viscosity of the grout (flowability through grout pipes) and reduced the grout's set time.

Capacity calculations (side resistance) for a conventional (ungrouted) drilled shafts were made for side resistance (i.e., Alpha method for clays and Beta method for sands and silts) and tip resistance following FHWA specifications (FHWA, 2010). Estimation of the improved side resistance along the side-grouted shaft was calculated using four methods: (1) K_g method (Thiyyakkandi et al., 2013a and 2013b); (2) Pressuremeter Test (PMT) method; (3) measured in situ soil pressure cell data; and (4) approach using tip grout pressure observed during construction. The capacity calculations for only tip-grouted drilled shafts (pre-loaded tip resistance) were made following FDOT Soils and Foundations Handbook (2012) (Mullins et al, 2006). A comparison between tip resistance for the three different approaches (i.e., no tip grouting, tip grouting only, and side grouting followed by tip grouting) was also performed (section 5.2.6).

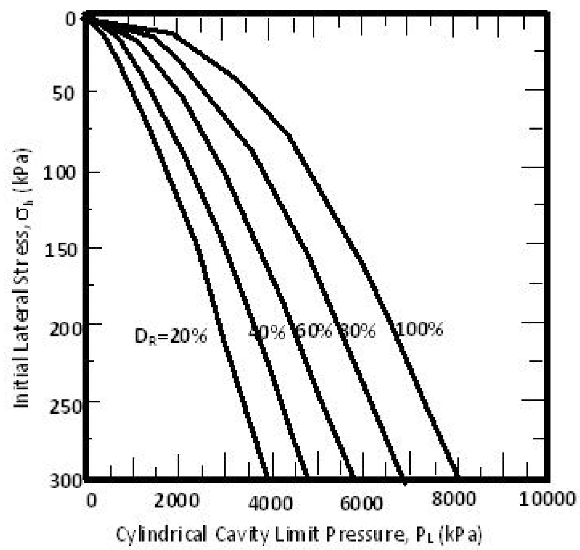

Figure 1-5: Cylindrical cavity expansion limit pressure for a constant volume friction angle, Φ_c, of 30° (Salgado and Randolph, 2001)

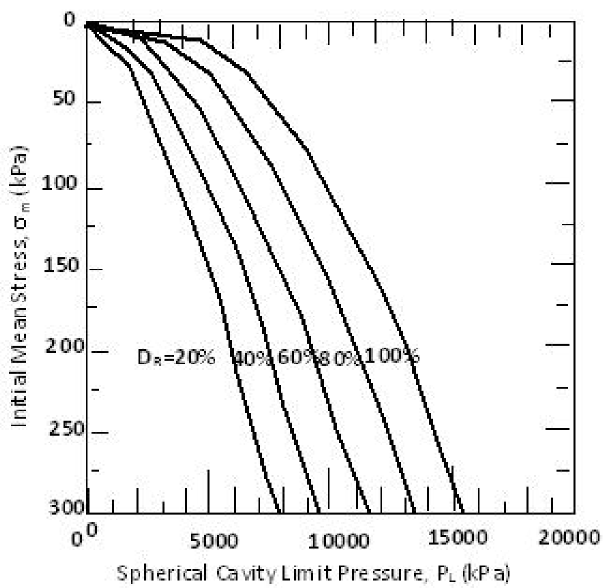

Figure 1-6: Spherical cavity expansion limit pressure for a constant volume friction angle, Φ_c, of 30° (Salgado and Randolph, 2001)

CHAPTER 2
SIDE-AND-TIP-GROUTED DRILLED SHAFT TESTING IN FDOT TEST CHAMBER

2.1 Short Shaft (36" x 6')

The design, construction, post grouting, and load testing of two test shafts (short and long) in the FDOT test chamber are discussed in this chapter. The chapter focuses on the evolution in the design and construction of each shaft; therefore, the analysis of results for each shaft is presented in Chapter 4 (Summary of Data and Presentation of Results). The overall changes (e.g., grout system) are discussed for each in chronological order, e.g., design, construction, and grouting of the short shaft followed by design, construction, grouting, and load testing of the long shaft.

2.1.1 Initial Design: Performance Demands, Material Selection, and Fabrication Methods

The main focus for the short shaft (and overall project scope) was to implement a new side grout system that would promote cavity expansion during side and tip grouting processes; more specifically, promote cylindrical cavity expansion along the bottom side during side grouting and spherical cavity expansion below the shaft tip during tip grouting. Key to accomplishing this task was controlling grout flow during post grouting, which was necessary for sustaining higher grout pressures.

Throughout the design, performance demands, reliability, and constructability influenced the choice of materials and fabrication methods. The focus of this research was not to change the conventional tip grouting system (fabrication and construction) or tip grouting processes, but to improve the outcome of the post tip grouting process (i.e., increase side and tip resistance of drill shafts). Therefore, the tip grout systems used on the test shafts were similar to that of a conventional tip grouting system (i.e., steel base plate and tube-a-manchettes to deliver grout below the shaft tip), and a new side grout system (i.e., membrane seals, side membrane, and side grout delivery system) was developed. The conventional tip grout system will be discussed further here and in Chapter 3 (construction of field shaft). The short test shaft did not use this type of tip grout delivery system, with reasons discussed below.

Performance demands imposed for the new side and tip grout system included effective and reliable containment of grout (i.e., control grout flow) during side and tip grouting processes while being easily constructed and outfitted to a conventional drilled shaft reinforcing steel (rebar cage). Quality of the concrete, reinforcing steel placement, and other shaft construction concerns impact the structural integrity of drilled shafts. The main focus throughout the design was to maximize function and reliability while minimizing interference with conventional drilled shaft construction. Two important considerations were: limit contact with the wall of the drilled hole during placement of the rebar cage and ensure adequate concrete cover on the rebar cage. Less contact with the wall of the hole will minimize scraping the wall, and creating unwanted debris. Similarly, adequate concrete cover on the rebar cage is important to ensure protection (sulfides, chlorides, etc.) of the shaft. Consequently, the grout systems were designed with two geometric constraints: one inch of clearance between the grout system and shaft wall (i.e., hole), and the longitudinal steel will have a minimum concrete cover of three inches (AASHTO, 2010). Additional considerations throughout the design were to ensure the new side grout system would not interfere with conventional shaft construction processes such as casing removal, use of slurries, and concrete placement, as well as being compatible with any size drilled shaft and all methods of drilled shaft construction. Finally, the resulting drilled shaft prior to post grouting should have a uniform cross-section similar to a conventional ungrouted drilled shaft.

The main purpose of the new side grout system and side grouting process was to increase the stress states of the soil above the shaft tip (i.e., cylindrical cavity expansion). To accomplish this, a new side grouting process to limit vertical grout flow was developed. Specifically in the side grouting phase, the grout was contained by an impermeable set of seals and expanding side membrane. Under high pressures, grout follows the path of least resistance, i.e., along the soil-shaft interface; therefore, the grout wants to flow vertically upwards (lower stress state) during the side grouting phase. To prevent grout flow in this direction, an impermeable membrane (side membrane) acts as a boundary, containing the grout, and forces the grout to flow radially outwards. Restricting the grout flow generates the higher grout pressures needed to develop cylindrical cavity expansion. As the grout pressure grows during the side grouting phase, the side membrane expands outward changing the stress state alongside the shaft. Since the stress change is a function of depth, it was decided to restrict the side grouted zone to be equal to one third of the embedment length and have the side grout bulb expand outwards to a final diameter of one and a half times the shaft's initial diameter, D (McVay et al., 2009). The final diameter will be denoted as "1 ½ D or 1.5 D" throughout the remainder of the report.

The side membrane must be free to expand outwards to increase the soil stresses and effectively contain the grout during the side grouting phase. If the side membrane becomes embedded in the shaft during construction, it would no longer function as intended. Therefore, an inflatable seal was proposed to prevent the flow of concrete to the outside of the side membrane during shaft construction (McVay et al., 2009). Putting the seal at the top and inside of the side membrane, the membrane seal was inflated and pushed the side membrane against the wall of the shaft, thus preventing concrete flow outside of the side membrane (discussed in Chapter 1). The design and development of the membrane seal presented a new set of questions and challenges such as: material selection, fabrication method, interference with side and tip grout delivery systems, clearance between rebar cage and shaft wall, reduced cover on the rebar cage, the shaft profile before grouting, subsequent grouting phases, and adverse effect on overall axial capacity. Given the geometry of the rebar cage and drilled shaft, a torus shape (e.g., bicycle inner tube) was ideal for creating a uniform seal on the shaft wall without encroaching on the rebar cage. Once shaft construction was complete however, there would be a void where the membrane seal was located. As a result, it was decided to grout the membrane seal and eliminate said void. Henceforth, the membrane seal system, side grout system, and tip grout system was referred to as the three stage grout system.

A rigid boundary was formed at the top of the side membrane once the membrane seal was grouted, i.e., an upper boundary condition present during the side grouting phase. As the grout tries to flow upward during the side grouting phase, the grouted seal helps to obstruct vertical flow (i.e., rigid boundary condition). That is, the rigid upper boundary impedes the flow and forces the grout to flow radially outward, thus encouraging cylindrical cavity expansion. Moreover, the seal was partially inflated with air during shaft construction (elliptical cross-section) and fully inflated once grouted (circular cross-section). While being grouted, the seal expanded outward into the surrounding soil, and theoretically, changes the stress state within the surrounding soil similar to the cylindrical cavity expansion process. Like the influence of side grouting prior to tip grouting, the stress state around the seal was such the path of least resistance was downward and radially (i.e., soil boundary condition), so during subsequent side grouting, the grout flows downward and radially outwards.

Cavity expansion below the shaft tip during the tip grouting phase was achieved by first changing the stress states (e.g., horizontal) above the shaft tip (i.e., develop cylindrical cavity expansion stresses during the side grouting phase). Because the path of least resistance was no longer vertically upwards, grout should flow vertically downward and radially outwards during tip grouting. As the grout flows in these directions, the volume and grout pressures increase and spherical cavity expansion develops. It was decided to limit the final diameter to 1 ½ D (i.e., limit pressure); but it should be noted that the final cavity stress was completely dependent on the available shaft resistance to upward movement. That is, if the force generated by the tip grout pressure times shaft tip area exceeded the upwards resistance, the shaft will move upward. The two major forces resisting movement in this direction was the self-weight of the shaft and mobilized side friction (above and along the side grouted zone). In addition to self-weight and side resistance, there was an additional resisting force generated by the bearing area between the grouted seal/membrane and the soil. Note, the shaft profile after completing the side grouting phase (i.e., grouted seal and side membrane) created a ledge (¼ D) or shelf where the side grout bulb expanded outwards (i.e., diameter of the side grouted zone was greater than that above the side grouted zone). The resistance generated by this bearing area was not the focus of this research but should be acknowledged; that is, the measured side resistance of the side grouted zone (strain difference across side grouted zone) considered side friction only. Therefore, unit side friction along the side grout zone will only be computed from increased lateral stress multiplied by the surface area of the side grout zone (i.e., conservative estimate if neglect bearing resistance).

The material selection and fabrication methods of the new side grouting system (membrane seal and impermeable side membrane) were determined given the performance demands and geometric constraints described above with emphasis on reliability and constructability. Recall that the performance demands require a reliable containment of the grout (i.e., controlled grout flow) during side and tip grouting processes, and the geometric constraints require no obstruction to shaft construction procedures while being easily constructed and integrated into a conventional drilled shaft reinforcing cage. For this reason, it was decided to use one-inch polyvinyl chloride (PVC) pipes to deliver grout to the various grout systems (seal, side membrane, and tip). This ensured the smallest influence on cross-sectional properties of the shaft, and one-inch PVC was the smallest size which won’t create “sand locking” issues.

The membrane seal was designed to be a torus shape, so the first option considered was to use an inner tube to create a seal. Although airtight and a manufactured product (easily obtained and minimal fabrication), inner tubes rely on a stronger outer boundary (rubber tire) to hold high pressures. Moreover, an inner tube with the desired dimensions is uncommon, expensive, and would still have to be adapted to accept grout delivery through a one-inch pipe. Consequently, a high pressure layflat discharge hose, which is both flexible and able to sustain high pressures, was selected for the membrane seal fabrication (Figure 2-1). The layflat hose used on the short shaft had a maximum working pressure of 150 pounds per square inch (psi). A scale model of this fabrication method, inflation process, and resulting seal was tested and shown in Figure 2-2 on the next page. Note, the seal may be cut in any length, i.e., limiting the final outer diameter (OD) of its expansion (torus shape). Evident from the figure, the layflat hose created an adequate seal and prevented concrete from flowing outside of the side membrane during shaft construction; in addition, the membrane seal did not fail during grouting and created an upper boundary condition during the side grouting phase. This will be discussed further below and in Chapter 4 (Summary of Data and Presentation of Results).

Figure 2-1: High pressure layflat hose (150 psi rated working pressure)

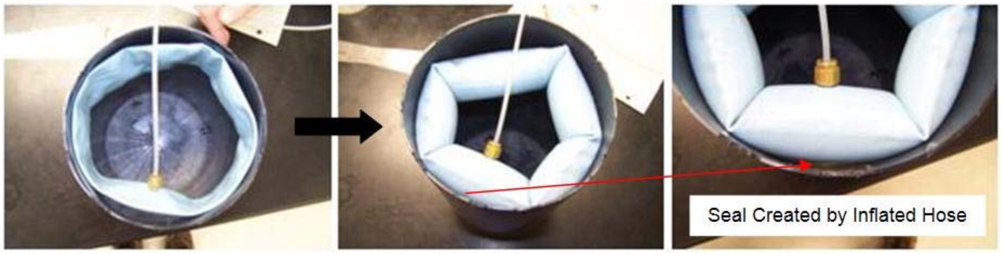

Figure 2-2: Small-scale test to check the seal created by inflated hose (torus shape)

Various materials were investigated for fabricating the side membrane: canvas, Kevlar, and geosynthetic materials. Canvas was the cheapest option but lacked the tensile strength needed to retain grout under high pressures (two kip per square inch (ksi) maximum tensile force). In addition, special equipment and skilled workers are needed to create a stitch that is strong when joins two pieces together. The Kevlar was much stronger with a maximum tensile force of around 40 times that of canvas (80 ksi maximum tensile force), but Kevlar is expensive and also requires special stitching to properly join the material. Other methods of joining fabric-like materials include chemical and thermal bonding. Chemicals are typically expensive and require special handling and disposal, so thermal bonding was favored.

Geosynthetic materials have many applications and a wide range of physical properties like strength, flexibility, and permeability. Capable of being joined with a thermal bond, geomembranes were considered viable. Geomembranes are a type of geosynthetic commonly used in landfills and canals to create an impermeable boundary, and there are different types of geomembranes depending on the application. The two major geomembrane composites are polyethylene and polypropylene, and the strength characteristics of these two materials behave similarly. The application usually depends on the required chemical resistivity, i.e., polyethylene and polypropylene are resistant to different chemicals. Because polypropylene is slightly more flexible than polyethylene, polypropylene was selected as the side membrane material (Figure 2-3). More specifically, a 45 mil thick (one mil = 0.001 inch) reinforced low density polypropylene (LDPP) was investigated. Low density polypropylene is more flexible than high density polypropylene, and the reinforced LDPP has a reinforcing scrim to increase its tensile strength.

Figure 2-3: Piece of reinforced low density polypropylene (45 mil thick)

The tensile strength of the reinforced polypropylene (RPP) was determined by testing strips of the material in tension (Figure 2-4). Strips of material were cut, and the two ends were joined together with a thermal bond (creating a loop). Using a Universal Testing Machine (UTM), the loops were failed in tension to simulate potential failure as the side membrane expands outwards (tensile stresses proportional to hoop stresses during cavity expansion). The average tensile strength of the RPP was 3.7 ksi.

Figure 2-4: Tension test on reinforced low density polypropylene using UTM

It should be noted that the membrane carries the difference between the internal grout pressure and outside soil mean stress; therefore, 3.7 ksi tensile strength was considered sufficient for this application. As the side membrane and grout bulb expand outward, the soil resistance (i.e., soil stresses) and grout pressures increase. If the grout pressures exceeds the soil resistance, the membrane must carry the additional stress until the soil mass realigns (increased resistance) or the grout pressures reaches the cylindrical cavity limit pressure.

The side membrane should take a cylindrical shape unless soil variability is high. A single piece of RPP was used to construct the cylindrical shape with only one seam needed to make the side membrane (vertical seam along the length). To secure the side membrane to the rebar cage, the top and bottom of the membrane was pinched between two steel rings connected to the rebar cage. To prevent grout from flowing between the steel rings and the cast shaft, the steel rings were smaller than the proposed shaft diameter, so the steel rings become embedded during shaft construction. To deliver grout to the side membrane a network of steel and PVC pipes were used and will be discussed later.

As discussed, the shaft tip grouting process used a tube-a-manchettes (PVC pipes). At the shaft tip, the pipes have a series of holes drilled along the length of the pipe with the holes covered by a thick walled rubber sleeve (gum rubber) creating the tube-a-manchette grout delivery system. The purpose of the short test shaft was to prove the ability to develop cavity expansion stresses during post grouting processes on drilled shafts, so the tip grout system used on the short shaft was simplified by using a single PVC pipe centered within the shaft (greatly reducing cost). Although an efficient way to deliver grout to the shaft's tip, results from the short test shaft showed major flaws, such as poor contact area between the grout and shaft tip and no cleanout capability, that prevented it from being a viable tip grouting method and will be discussed further in Chapter 3.

2.1.2 Shaft Construction, Grouting, and Exhume Shaft

The construction of the rebar cage and attachment of the various grout systems took place at the UF coastal lab. The rebar cage was designed for testing purposes and would not be subject to large axial tension loads (i.e., lift during excavation), so there was little reinforcing steel in the shaft (Figure 2-5). A total of five number eight bars (one-inch diameter) were used in the longitudinal direction. The minimum concrete cover on the longitudinal bars was four and a half inch, so the longitudinal bars were evenly spaced such that the diameter of the arrangement was two feet three inch (27 inch). The longitudinal bars were seven feet long to provide grip points during rebar cage placement and shaft removal (exhume). To provide some shear resistance, steel shear rings were made using number three bars (three-eighths-inch diameter) and evenly spaced six inches apart (12 shear rings total).

Figure 2-5: Short shaft rebar cage

The membrane seal and side membrane were fabricated in the soil's lab (UF campus). Using the high pressure layflat discharge hose, torus shapes were fabricated to create the membrane seals (Figure 2-6). Because the layflat hose is not elastic, the required length of hose was simply the outside circumference of the desired torus. In this case, the diameter of the shaft was three feet (36 inch) and the membrane seals were expected to expand four to six inches away from the drilled shaft once grouted. Taking the larger of the two values, the OD of the torus once fully expanded was four feet. With the required length of hose cut, the two ends were brought together to create the torus shape. The two ends were joined together with a thermal bond creating the membrane seal joint.

Figure 2-6: Membrane seal fabrication for short shaft

Before the two ends were bonded together, two entry and exit points for the air/grout delivery were fabricated (Figure 2-7 on the next page). Using various PVC couples, PVC ports similar to a through-wall fitting were made. Holes were drilled through the wall of the layflat hose and PVC ports were secured. A preliminary seal test using low air pressure revealed air leaks at the joint location and both PVC ports. In an attempt to stop the leaks, high strength PVC cement was used. By first putting a vacuum on the membrane seal, the PVC cement was sucked into the areas where air was leaking out. After several applications of the cement using this suction technique, the membrane seals were made more air tight but still leaked slightly. Because the PVC cement is combustible, secondary thermal bonding to further reduce leaks was never attempted.

Figure 2-7: Through-wall port fabrication for short shaft membrane seal

Like the side and tip grouting systems, one-inch PVC pipes were used to deliver grout to the membrane seal (Figure 2-8 left), so the air used to pressurize the membrane seal during shaft construction was delivered through the same pipes. An adapter with a Schrader valve was made to fit on the pipe at the top of the shaft (Figure 2-8 right), so delivering air through the grout pipes required little additional fabrication.

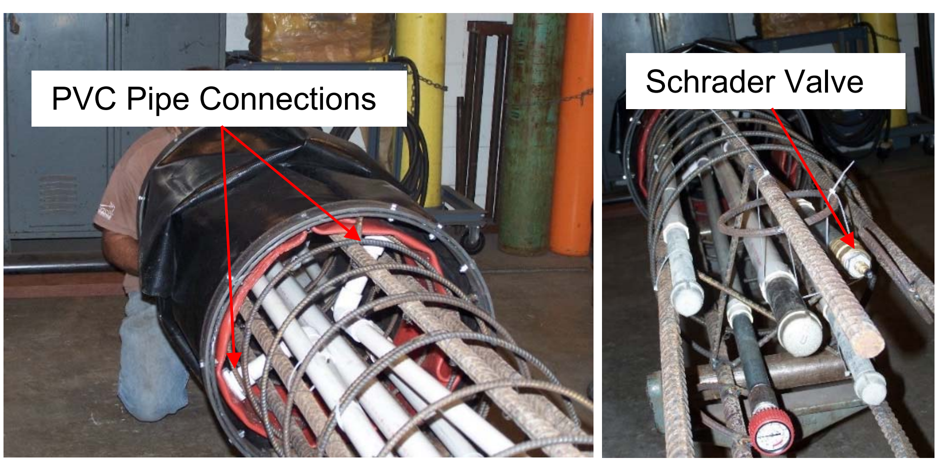

Figure 2-8: Grout and air delivery system to membrane seal for short shaft

The side grout system consists of the membrane seal(s), side membrane, steel rings to secure the membrane to the rebar cage, and an internal PVC network to deliver grout to the side membrane. Constructed to be a cylindrical shell, the side membrane was fabricated using a single piece of reinforced polypropylene (RPP). The RPP was 45 mills thick (0.045 inch), and cut to a length of 15 feet (circumference of the projected side grout bulb) and a width of three and a half feet (height of the projected side grout bulb). The circumference of the projected side grout bulb was 170 inch (1 ½ D), so an extra 10 inch was added to the length to account for seam overlap (cut length of 180 inch or 15 feet). A thermal weld was made along the vertical seam using two hot plates heated to 150 °C, four kilogram (kg) weight to apply a constant pressure, and a four minute hold time. This created an air tight seam and permanently bonded the two edges of the RPP together. Four vertical pleats were made to reduce the circumference of the side membrane from 170 inch (final circumference of projected side grout bulb) to 85 inch (circumference of longitudinal rebar arrangement), as shown in Figure 2-9.

Figure 2-9: Vertical pleats used to reduce circumference of side membrane

With a reduction in circumference, additional material was required in the vertical direction to provide a transition from the steel ring diameter (< D) to the fully expanded membrane (1 ½ D). The height of the transition zone was two feet (24 inch), so an extra 18 inch was added to the width (cut width of 42 inch or three and a half feet), which ensures enough membrane material for full radial expansion to 1 ½ D. A horizontal pleat was added upon attaching to the rebar cage (Figure 2-10), which reduced the height of the side membrane. The direction of the horizontal pleat was such that it did not catch concrete during casting (inside of membrane) and minimized the resistance along the wall of the drilled shaft or casing during placement (outside of membrane).

Figure 2-10: Horizontal pleat used to reduce height of side membrane

Steel rings were fabricated using flat bar and were used to secure the side membrane to the rebar cage (Figure 2-11 on the next page). The flat bar was one quarter inch thick by two and a half inch wide, and the bars were cut into lengths equal to the circumference of the desired ring (e.g., circumference of longitudinal rebar arrangement). Once cut, the flat bar was rolled to create a ring. Two steel rings (inner and outer) were fabricated for the top and bottom of the side membrane, so a total of four rings were fabricated for the side membrane system (two inner rings and two outer rings). Half inch holes were drilled through the steel rings before welding the inner rings to the cage. The inner rings were welded to the rebar cage, and the outer rings were secured to the inner rings using three-eighths-inch bolts.

Figure 2-11: Steel rings used to secure the side membrane to rebar cage

To deliver grout to the side membrane, an internal grout delivery network was constructed (Figure 2-12 on the next page). The internal network included steel nipples at the top of the shaft, one-inch schedule 40 PVC pipe within the shaft, and a PVC tube-a-manchette along the side grouted zone (side-manchette). The steel nipples were used at the top of the shaft to protect the grout delivery system from damage during rebar cage placement and shaft construction, and more importantly, steel nipples were used at the top of the shaft to prevent bursting of the grout pipes during the grouting processes in the open atmosphere. One-inch schedule 40 PVC pipe, with a working pressure rating of 450 psi, was used within the shaft and to construct the side-manchette. The side-manchette extended the length of the side grouted zone (two feet). Three-eighth-inch holes were drilled five inches apart in the PVC pipe, and quarter inch thick gum rubber was used to cover the holes creating a tube-a-manchette (side-manchette). The gum rubber prevents concrete from clogging the side-manchette during shaft construction and allows for back flushing of the grout system without pumping large volumes of water into the side grout bulb. The side grout delivery system was a continuous loop to allow for back flushing if secondary side grouting was required.

Figure 2-12: Grout delivery pipes for side membrane (side-manchette)

The most efficient and cost effective way to deliver grout to the tip of the shaft was a single pipe through the center of the shaft (Figure 2-13 on the next page). Therefore, the tip grout system consisted of a steel nipple at the top of the shaft, three-inch diameter schedule 40 PVC pipe, and a rubber seal at the bottom. The steel nipple was used at the top of the shaft for the same reasons as with the side grout system (protect grout pipes and prevent pipe burst). The three inch PVC pipe was centered in the middle of the rebar cage and extended the length of the shaft. A thin piece of rubber was secured to the bottom of the PVC pipe to create a seal, so the bottom of the pipe would not become clogged with dirt or concrete during shaft construction.


Figure 2-13: Grout delivery pipe for tip grouting

The order in which the grout systems were attached to the rebar cage was developed during the construction of the short test shaft. In general, the tip grouting system was completed first, followed by the membrane seals, and finally the side grout system. If instrumentation was used (i.e., embedded strain gauges), it would be attached before completion of the side grout system. To avoid damage to PVC pipes, the inner steel rings for the side membrane were welded onto the rebar cage before construction of any grout delivery systems. During the fabrication of the membrane seal and side membrane, the grout delivery systems for the side and tip grouting systems were completed. Once the membrane seal was finished, the top seal was attached to the rebar cage, and the membrane seal grout delivery system was then completed. The membrane seal was pleated to reduce its size, so the rebar cage and three stage grout system would fit within the drilled shaft hole or casing. Finally, the pleated side membrane and outer steel rings were added to the rebar cage, along with steel angle to create feet and prevent rebar cage from sinking into the underlying sand (Figure 2-14 on the next page). Tape was used to keep the side membrane closed (not inflated) over the rebar cage and minimize contact with the drilled shaft or casing during placement.

Figure 2-14: Completed short shaft rebar cage with grout systems attached

The short test shaft was constructed using a casing method. A Sonotube was used for the casing (Figure 2-15 on the next page), which is a typical casing used for construction of small diameter columns and piers. The Sonotube is fabricated from a laminated wax paper (cardboard like material). The inside diameter (ID) of the Sonotube used for the short test shaft was three feet (shaft diameter) and six feet in length (embedment length). Soil in the test chamber was excavated, the casing was placed, and the soil was backfilled around the casing. The soil was excavated from the test chamber using hand shovels. Once the Sonotube was in place, the soil was backfilled in lifts and compacted to simulate natural soil in the field. Once the soil was backfilled around the casing, the rebar cage with three stage grout system was lowered into the casing. As intended, there was minimal contact between the grout system and casing, so there was little resistance when placing the rebar cage with grout systems attached.

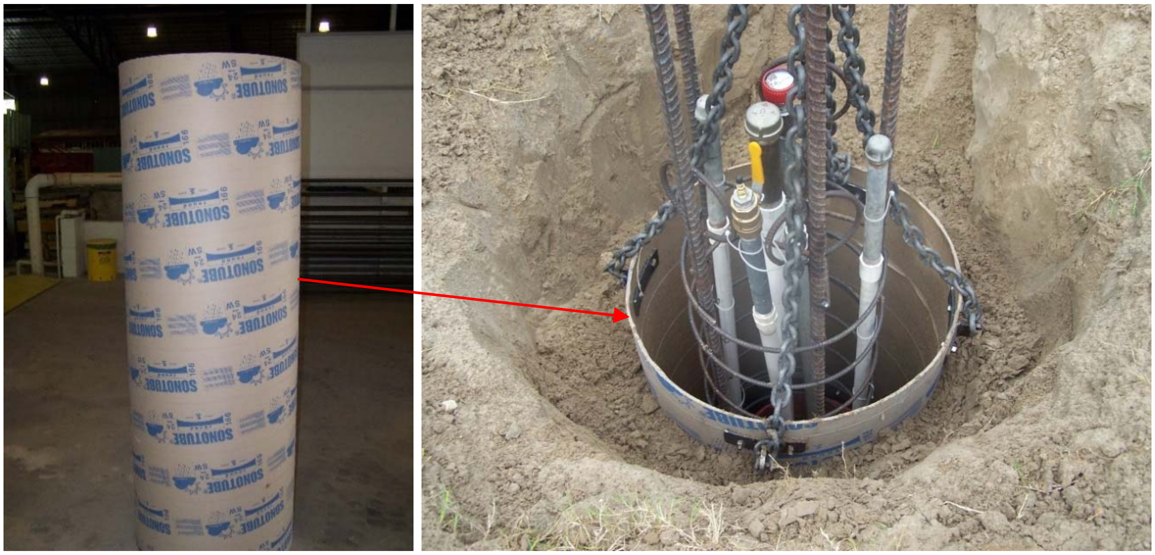

Figure 2-15: Temporary casing used with short shaft

A ready mix concrete truck was used to cast the short test shaft. The concrete mix design was a 5,000 psi mix (compression strength of 5,000 psi after 28 days of hydration). Typically, the Sonotube is left until the concrete starts to hydrate and is removed from the shaft later. For this test, the casing was pulled during concrete placement. Unfortunately, the wall of the Sonotube failed where the pick points were located for the last two and a half feet of embedment. Consequently the Sonotube was left in place until the concrete hydrated for couple of days (Figure 2-16). Then the soil was excavated again, the Sonotube was removed from the shaft, and the soil was backfilled and compacted again (Figure 2-17 on the next page).

Figure 2-16: Failed Sonotube during removal

Figure 2-17: Removed Sonotube and backfill around short shaft

The membrane seal was inflated with air to a pressure of five psi before concrete placement began (Figure 2-18 on the next page). The inflated seal pressed the side membrane against the wall of the Sonotube thus preventing the concrete from flowing to the outside of the side membrane and embedding the side membrane within the shaft. There was a visible volume of air that leaked into the concrete during shaft construction, and the seal had to be re-pressurized through concrete placement to maintain five psi pressure within the seal. Air was seen bubbling at the surface of the concrete and the hold pressure of the seal decreased throughout shaft construction, as seen in Figure 2-19 on the next page. The concrete was placed with a final depth of six and a half feet (six feet embedment depth + a half foot above soil surface). Concrete vibrators were used to remove the majority of entrained air that was trapped during placement of the concrete and the air that had leaked from the membrane seal. Since no axial load test was performed on the short test shaft, three of the five longitudinal bars were left protruding above the casted shaft, which provided pick points while exhuming the shaft. Within 24 hours of shaft construction (concrete placement), water was pumped through the side grout delivery system, and the concrete cover on the side-manchette was spalled off by the water pressure. The water pressure spiked at first (concrete was covering holes) and then dropped (concrete spalled off side-manchette), and the water pressure remained constant at a negligible value (water able to flow freely through side-manchette).

Figure 2-18: Pressurized membrane seal successfully pressing side membrane against wall of shaft

Figure 2-19: Air bubbles observed during shaft construction

Grouting the membrane seal(s) was the first of the three grouting stages and completed seven days after shaft construction. While grouting the membrane seal, the grout volume and pressure were monitored. Pressure was measured using a high pressure pinch valve, with the maximum pressure occurring during the pump stroke. The volume of grout pumped was estimated based on the number of grout pump strokes (approximately three and a half gallons per stroke). The short test shaft had only one seal at the top of the shaft. Grout was pumped into one side of the seal (front end) while air was released out of the other side (back end), i.e., removing air. Once the seal was primed with grout, the valve on the back end was closed and grout pressures were allowed to grow. The grout was pumped until 90% max theoretical volume of the seal was approached (18.7 gallons).

Grouting the side membrane was the second of the three grouting stages and completed 14 days after shaft construction (seven days after grouting membrane seal). During side grouting, the grout volume, grout pressure, and vertical displacement of the shaft were monitored. Again, the pressures recorded were the maximum pressures during the pump stroke (measured using a high pressure pinch valve). The grout was pumped until 90% max theoretical volume was approached (119 gallons). The grout system was again primed with grout but to remove all water (rather than air) from the PVC pipes. Then the valve on the back end was closed, and higher grout pressures developed.

Grouting the tip of the shaft was the third and final stage of the three grouting stages and completed 28 days after shaft construction (14 days after grouting the bottom side). During tip grouting, the grout volume, grout pressure, and vertical displacement of the shaft were monitored (Figure 2-20). Again, the pressure that was recorded was the maximum pressure during the pump stroke, and pressure was measured using a high pressure pinch valve. The grout was pumped until 90% max theoretical volume was approached (321 gallons). Again, the tip grout system was primed to remove all air before grout pressures were allowed to develop.

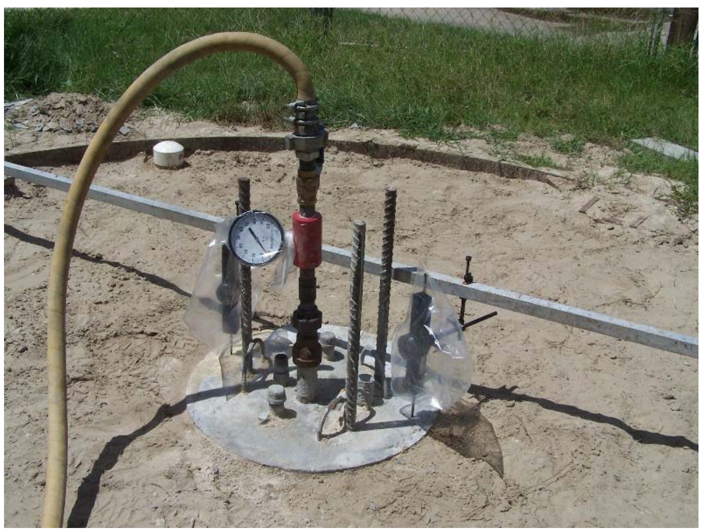

Figure 2-20: Top of short shaft during tip grouting

The short test shaft was removed from the test chamber and visually examined to evaluate the performance of the three stage grout system. More specifically, the performance of the membrane seal and side membrane was evaluated. The tip grouting process was also observed and assessed. The excavation of soil around the short test shaft was completed using hand shovels (Figure 2-21 on the next page). Once the tip grout bulb was exposed (smooth gray surface; bottom right photo in Figure

2-21), the hand excavation stopped. Using the large forklift, the grouted test shaft was lifted from the test chamber (Figure 2-22). When the shaft was lifted from the test chamber, the tip grout bulb broke from the bottom of the shaft and had to be lifted separately from the test chamber. The shaft and grout bulb were cleaned off with water to more easily distinguish the various boundaries and better assess grout flows and will be shown clearly in section 4.1.

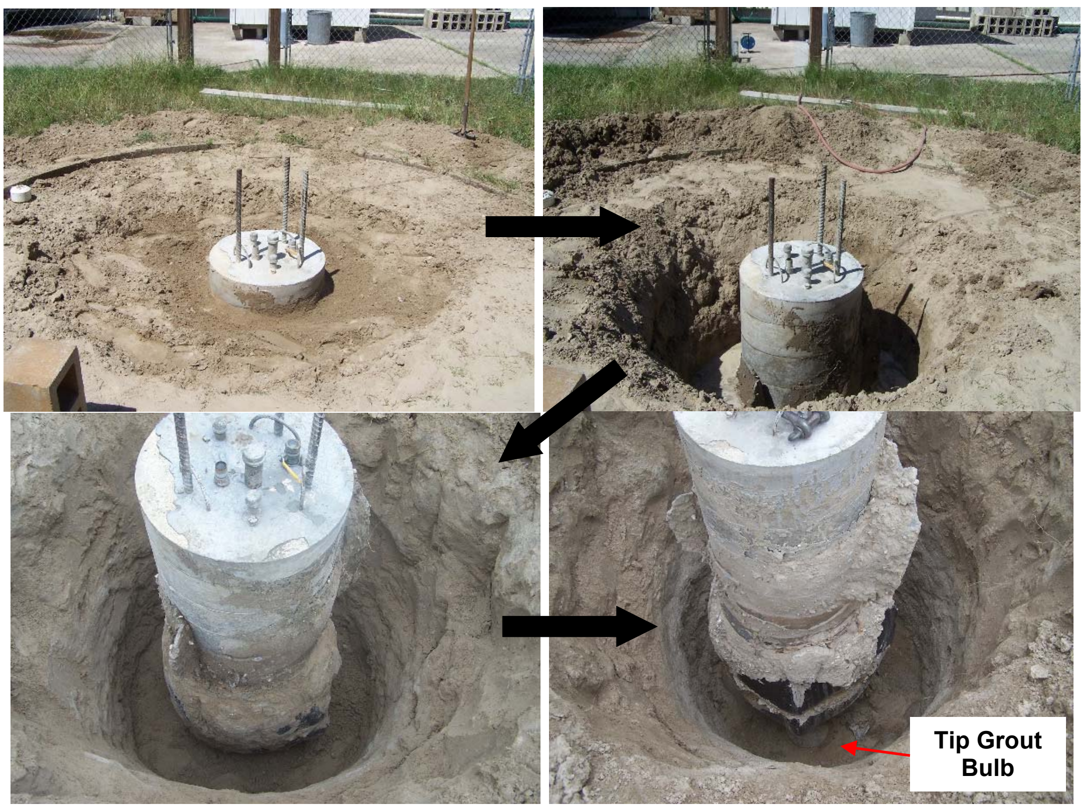

Figure 2-21: Excavate soil around short shaft

Figure 2-22: Large forklift used to remove the short shaft from test chamber

2.2 Long Shaft (36" x 25')

2.2.1 Design Evolution and Improvements

Three major areas of improvement were identified for the membrane seal: (1) stop air leaks; (2) improve reliability; and (3) prevent intrusion into the longitudinal rebar profile during shaft construction when pressurized with air. The membrane seal for the short shaft was not air tight and leaked a considerable amount of air into the concrete during shaft construction. It is important to minimize the amount of entrained air in concrete to ensure strength, so the membrane seals had to be air tight if used for this application. Moreover, the membrane seals must not fail under high pressures. While testing the first membrane seal, the volume of air leaking from the joint increased as the air pressure was increased, i.e., leak became worse. The short shaft test revealed the joint on the membrane seal using a thermal bonding technique was unreliable at high pressures. In addition, while the membrane seal controlled the flow of concrete during shaft construction, the short shaft chamber test revealed the membrane seal expanded inwards on the longitudinal rebar and prevented sufficient concrete cover where the seal was located (Figure 2-18). Accurately predicting the amount of concrete cover on the reinforcing steel is crucial for accurately predicting the capacity of the cast shaft. Consequently, a way to restrict the membrane seal’s inner diameter was required, i.e., encroachment on reinforcing steel during shaft construction.

Stopping air leaks and improving the reliability of the membrane seals was satisfied by changing the method in which the membrane seal joint was fabricated. Rather than using a thermal bond, the ends of the layflat hose were mechanically secured to a rigid member using high torque hose clamps (Figure 2-23). Additionally, the entry and exit points for air/grout were moved to the steel pipe instead of fabricating through-wall fittings. This eliminated the holes in the layflat hose for the through-wall fitting and the potential for leaks at the entry and exit points. Conventional high pressure hose connections use a similar method to create water tight reliable connections (e.g., fire hose connections). Typically, multiple rows of steel banding are used to secure the hose to a fitting or union, which ensures a reliable connection. Due to the geometry constraints (must fit between rebar cage and drilled hole/casing), there was not enough space for multiple rows of banding, so high torque hose clamps were used as an alternative.

Figure 2-23: Membrane seal joint fabrication method used with long shaft

Both PVC and metallic pipe were considered for use as the rigid member. Two deciding factors led to the use of steel (metallic) pipe as the rigid member: (1) moving the entry points for air/grout delivery, i.e., stopping leaks; and (2) the maximum working pressure of the rigid member. With steel or aluminum, a weld can be made to create the connection needed for the air/grout entry and exit points, which is an air tight connection; however, PVC would likely have to be glued or threaded to create the connection needed for the entry and exit points, which could potentially leak regardless.

Furthermore, the maximum working pressure of the six inch steel pipe is much higher than the PVC equivalent. In addition, steel pipe can be ordered with specific dimensions (i.e., OD and wall thickness), so a tight fit is ensured between the layflat hose and steel pipe. Conversely, PVC is manufactured with fixed dimensions and working pressures, so there were no PVC pipes with an OD equal to the ID of the hose that would create a tight fit and have sufficient strength under high pressure (i.e., six inch PVC pipe is an uncommon size).

Once it was decided to use steel pipe to fabricate the joint, various hose clamps were tested to identify what clamp type would create an air tight seal. Three types of hose clamps were compared (Figure 2-24): (1) worm-drive; (2) high-torque bolt; and (3) twin-ring. The worm-drive hose clamp was not a high torque clamp, so the force generated by the clamp was not enough to prevent air leaks. Both the high-torque bolt and twin-ring hose clamps are high pressure clamps which generate higher clamping forces. The high-torque bolt clamp tested had double bolts with inner saddles to provide equal distribution of the clamp force, but due to the discontinuity between the clamp and saddles, air leaked regardless of clamp force. The twin-ring clamp provided a more evenly distributed clamp force, and an air tight membrane seal was created.

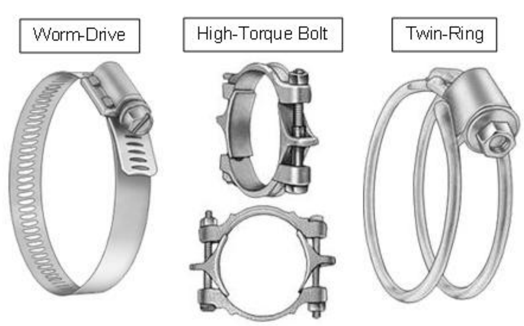

Figure 2-24: Hose clamps tested for membrane seal application

The membrane seal was tested using water under high pressure to determine the reliability of the membrane seal when using the new joint fabrication method (steel pipe and hose clamps). It was found that the boundary conditions present have a direct effect on the maximum hold pressure of the membrane seal (Figure 2-25 on the next page). As the seal becomes pressurized, the water pressure pushes on the walls of the layflat hose, and with no boundary conditions (Figure 2-25 – top left photo), the hose was free to take a linear shape (intended by manufacturer). As the hose takes a linear shape, large tensile forces develop at the joint. The only force resisting failure of the joint is the friction between the hose and steel pipe (normal force generated by hose clamp). With no inner or outer boundary condition (shaft and soil), the maximum hold pressure was 35 psi, and failure occurred at the connection (hose slipped off pipe). To simulate a rigid inner boundary condition (cast shaft), a large diameter conduit pipe was used (OD ≈ 36 inch). With only an inner boundary condition (Figure 2-25 – top right photo), the seal could not form an oblong shape and tensile forces developed at the joint much quicker, so the maximum hold pressure was 20 psi. To simulate an outer boundary condition (surrounding soil in reality), a circular trench was dug to a depth of two feet. With both an inner and outer boundary condition (Figure 2-25 – bottom photo), the outer boundary provided an additional resisting force as the hose tries to take a linear shape, so the maximum hold pressure was over 100 psi. These tests show the importance of the outer boundary (soil mass) condition in preventing failure of the membrane seal.

Figure 2-25: Test the effects of boundary conditions on membrane seal performance

Preventing intrusion of the membrane seals into the longitudinal rebar cage during shaft construction when pressurized with air was the last concern addressed. Steel rings were fabricated to create a rigid boundary between the membrane seal and rebar cage (Figure 2-26 on the next page). Once pressurized with air during shaft construction, the steel rings prevent the membrane seals from inflating inwards and intruding on the reinforcing cage (i.e., preventing adequate concrete cover on the rebar), thus ensuring adequate concrete cover on the reinforcing steel wherever the membrane seals are located.

Figure 2-26: Membrane seal steel rings fabricated to prevent seal from inflating inwards

Besides increasing the stresses alongside the shaft, the side membrane needs to transfer side resistance based on Coulombic friction to the soil. Affecting the mobilized side resistance was the interface friction angle between the soil and RPP, rather than the interface friction angle between the soil and concrete (conventional drilled shaft). Since the interface friction angle between the soil and RPP was of great interest, it was tested in a direct shear apparatus. Various suppliers/manufactures of the RPP material were tested to ensure the greatest tensile strength and interface friction angle between the soil and RPP (Figure 2-27 on the next page). Because tensile strength is so important during the side grouting phase, tensile tests were completed and compared first. The tests were performed in the same method as described in section 2.1.1 (loop tested in tension). The resulting tensile strengths ranged from 2.6 to 3.7 ksi. Unfortunately, the textured sample of RPP, which would likely have the highest interface friction angle, had the lowest tensile strength and was never tested in direct shear.

Figure 2-27: RPP samples from different suppliers

The three samples with the highest tensile strength were tested in direct shear. To estimate the interface friction angle between the soil and RPP, a direct shear test was performed (ASTM D 3080) with a failure surface between the soil and RPP (Figure 2-28 on the next page). To simulate soil conditions for the test, soil was taken from test chamber and prepared to have the same properties as expected in the test chamber (i.e., relative density, moisture content, and unit weight). The RPP was secured to the bottom half of the direct shear apparatus, and the soil sample was prepared in the top half of the direct shear apparatus. Five tests were performed for each material using a normal load of 4, 8, 12, 16, and 20 kg. The resulting interface friction angles for three samples ranged from 19° to 23°, with the material used on the short test shaft around 21° (about two thirds of the peak friction angle, Φ_p, from direct shear test). The results suggested that the mobilized side resistance with a RPP-soil interface is comparable to a concrete-soil interface. Therefore having no apparent adverse effect on the mobilized side resistance, the side membrane material was unchanged, and the same RPP (i.e., manufacturer) was used again with the long test shaft.

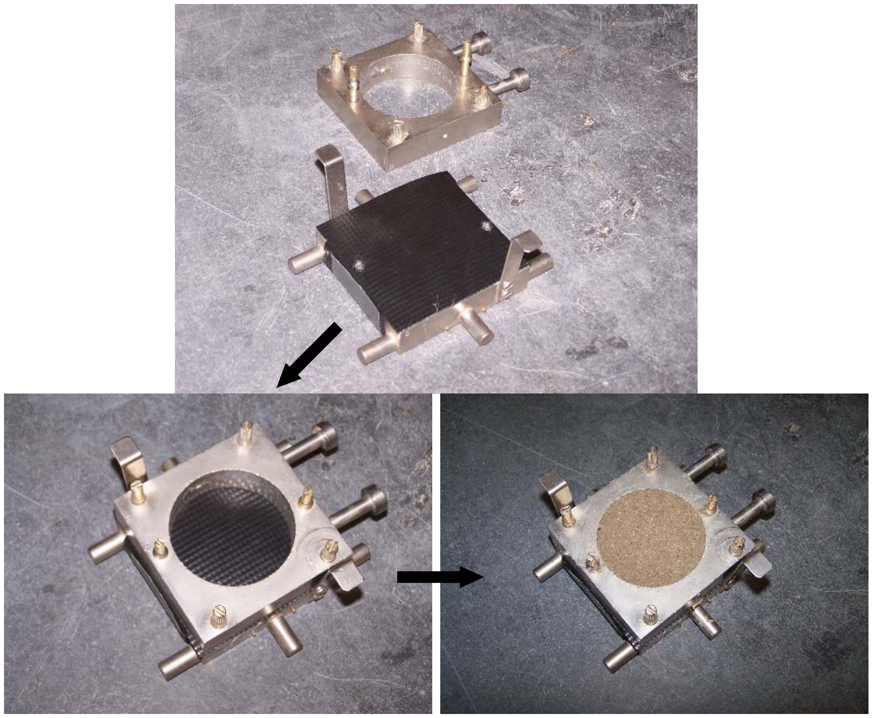

Figure 2-28: Direct shear test with failure surface between RPP and soil

Even though the tip grout bulb on the short shaft was formed below the shaft, there was poor contact between the shaft's tip and grout bulb (discussed further in Chapter 3). Having a uniform contact area is important for load transfer from the shaft to the grout bulb during axial loading. Moreover if the contact area is not centered below the shaft tip during axial loading, the soil reaction forces acting on the grout bulb would create an eccentric force on the shaft's tip and cause internal bending moments. Also of great concern was soil mixing with the grout resulting in a reduced grout tip bulb stiffness and strength. Therefore following similar construction methods for conventional post grouted drilled shafts (no cavity expansion), the tip grout system for the long test shaft included a steel base plate, tube-a-manchette (tip-manchette), steel ring below the base plate, and a rubber seal to protect the tip-manchette and help generate initial grout pressures. Pictures of the tip grout system used on the long shaft can be seen in section 2.2.3.

Since much higher grout pressures were expected with the long shaft, schedule 80 PVC pipe was used to construct the tip-manchette (630 psi max working pressure), and instead of steel nipples, high pressure hoses were used at the top of the shaft (3,000 psi max working pressure). The steel base plate has multiple functions, which include: protect the tip-manchette from being damaged by falling concrete during shaft construction; provide a uniform contact surface for concrete creating a uniform shaft tip (known area); and provide a uniform contact surface for grout creating a uniform load transfer area between the shaft’s tip and grout bulb. The addition of the steel base plate greatly improves the quality and consistency of the shaft’s tip, which allows for more accurate predictions about the final profile of the shaft’s tip and assumed load transfer areas. To protect the tip-manchette from being clogged with sand or crushed from the weight of concrete, the tip-manchette was surrounded by a steel ring and covered by a rubber seal. The steel ring was welded below the base plate and a rubber seal was attached to create a void around and below the tip-manchette, in which initial grout pressures can develop. To protect the tip-manchette from being crushed by the weight of concrete, shaft feet were constructed to minimize the settlement of the rebar cage during shaft construction. The shaft feet should also help transfer axial loads from the shaft’s tip to the grout bulb below (section 2.2.3).

2.2.2 Test Chamber Preparation

The FDOT test chamber was re-instrumented with earth pressure cells and the casing placed while the rebar cage and grout systems were fabricated. Soil within the test chamber had to be excavated to recover the earth pressure cells, which were used during previous research. Once all the pressure cells were removed from the test chamber, they were all tested, repaired, rewired, tested again, and re-placed throughout the test chamber. In conjunction, construction of the casing had to be completed and casing placed in the test chamber, for the casing and pressure cells had to be in place before the test chamber could be backfilled with soil. Test chamber preparation was essential for creating a controlled testing environment, thus validating results.

The soil was excavated from the test chamber using a track mounted drill rig (Figure 2-29 on the next page). The drill rig had a telescoping boom, and various size auger bits were used to remove the soil from the test chamber. Drilling had to stop periodically, so earth pressure cells could be located by hand and secured to the edge of the test chamber (Figure 2-30 on the next page). It took one day to excavate the test chamber to a depth of 26 feet below the top of the test chamber. The earth pressure cells recovered from the test chamber and used with the long shaft were Geokon Model 4800 earth pressure cells (Figure 2-31 on the next page). These gauges measure total stress within the soil and were used to measure the stress change around and below the test shaft. Depending on the orientation of the gauge, stress can be measured in any direction. There were a total of 22 gauges recovered from the test chamber. Once all of the gauges and wires were removed from the test chamber, the PVC conduit and steel racks were inspected and repaired. The PVC conduit protects the gauge wires from water and heavy equipment, and the steel racks protect the PVC conduit from heavy equipment and were used to secure the gauges while soil was excavated or backfilled.

Figure 2-29: Track-mounted drill rig used to excavate soil from test chamber

Figure 2-30: Recovered pressure cell secured to steel racks along sides of test chamber

Figure 2-31: Geokon earth pressure cells (model 4800)

To ensure the pressure cells were providing accurate measurements, all cells were tested in a pressure vessel (Figure 2-32). The pressure vessel was constructed out of steel and can test up to six gauges at one time. Using air, the vessel was pressurized and depressurized while each pressure cell was monitored. The airline supplying pressure to the vessel had two separate air pressure gauges on it to confirm air pressure within the vessel (one gauge on air compressor regulator and a second inline). The vessel was pressurized to 20, 40, 60, and 80 psi, and then depressurized to 40 and 0 psi. By depressurizing the vessel and taking readings, the readings before and after pressurizing can be compared. If there was much difference between the two zero readings, it would have indicated a rebound issue with the gauge and raise concerns about the gauge accuracy. However, all of the gauges provided similar pressure readings during the tests, so the gauges were within tolerable limits (< 1% error) and considered to be working accurately (Figure 2-33 on the next page).

Figure 2-32: Pressure vessel used to test earth pressure cells

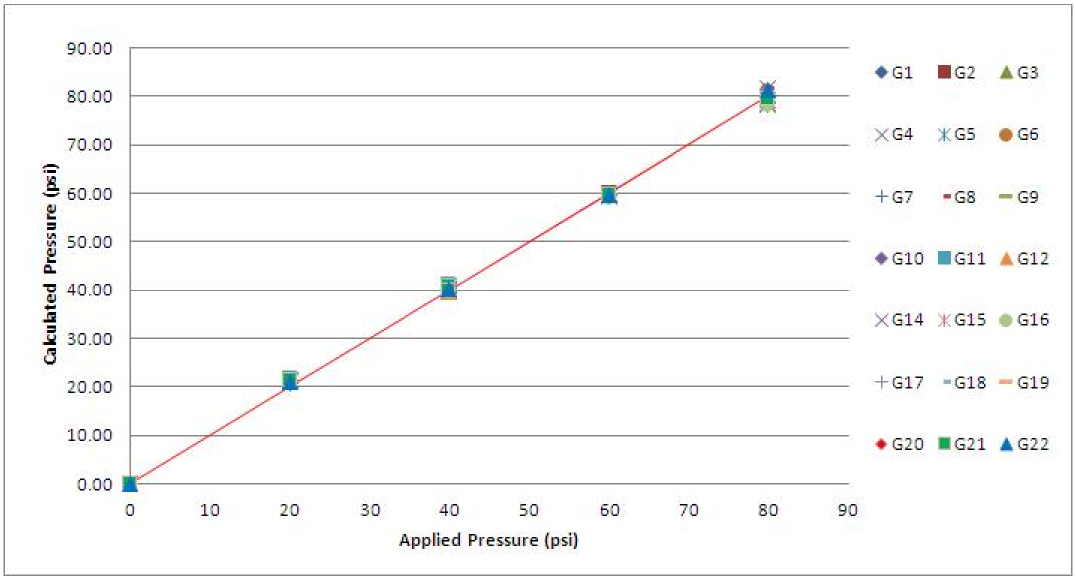

Figure 2-33: Results from pressure vessel test

After confirming all pressure cells were reading accurately, the gauge wires had to be inspected and repaired. New wire lengths had to be determined for every gauge, since the gauge location differs from their original positions. To avoid potential issues from having multiple wire splices on a single gauge, every gauge wire was cut, the old splice removed, and a single new splice was made. Once all splices were finished and pressure cells re-numbered, a zero reading was taken and compared to the zero reading before wire repairs. The changes in the zero readings after repairs were within 1% of the zero reading before wire repairs (Figure 2-34 on the next page), which suggests that the accuracy of the gauges had not changed and a second pressure vessel test was not required.

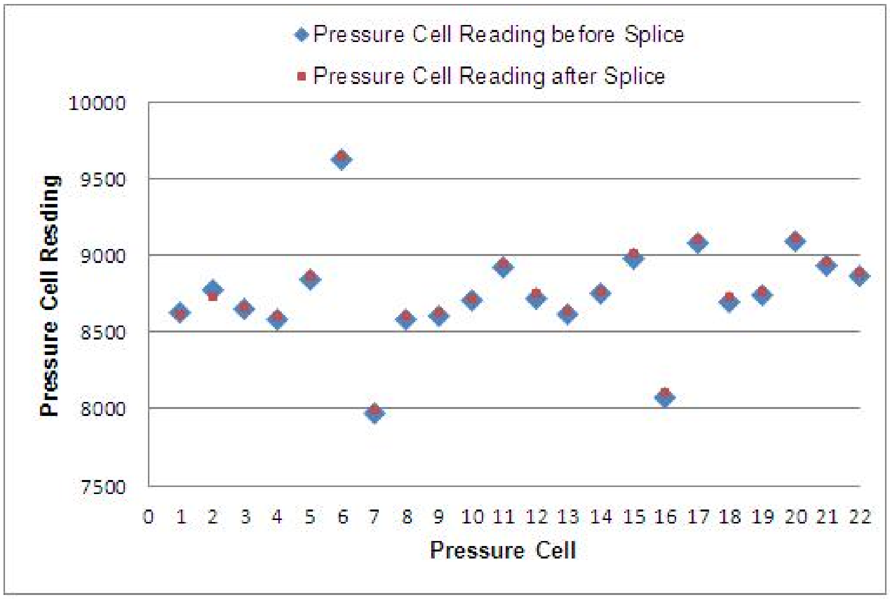

Figure 2-34: Zero reading before and after wire splicing

With all pressure cell wires repaired, the cells were secured to the steel racks and wires pulled back through the PVC conduit (Figure 2-35 on the next page). The PVC conduit convened to a shed, so the ends of the wires and pressure cell reading equipment could stay dry (Figure 2-36 on the next page). As discussed in section 1.3.2 (Equipment and Test Facilities), the gauges were wired to a multiplexer, so the gauges could be read in sequence (Figure 2-37 on the next page). The multiplexer is connected to a data-logger which automatically takes readings from the multiplexer in sequential order. Using the MultiLogger computer program, the multiplexer channel numbers (gauge location), all of the gauge correction factors, and the data logger information was entered in to the program. This allowed for automated data collection and storage during grouting processes and top-down testing.

Figure 2-35: Securing the pressure cells to steel racks before backfilling soil

Figure 2-36: Shed where pressure cell wires convene

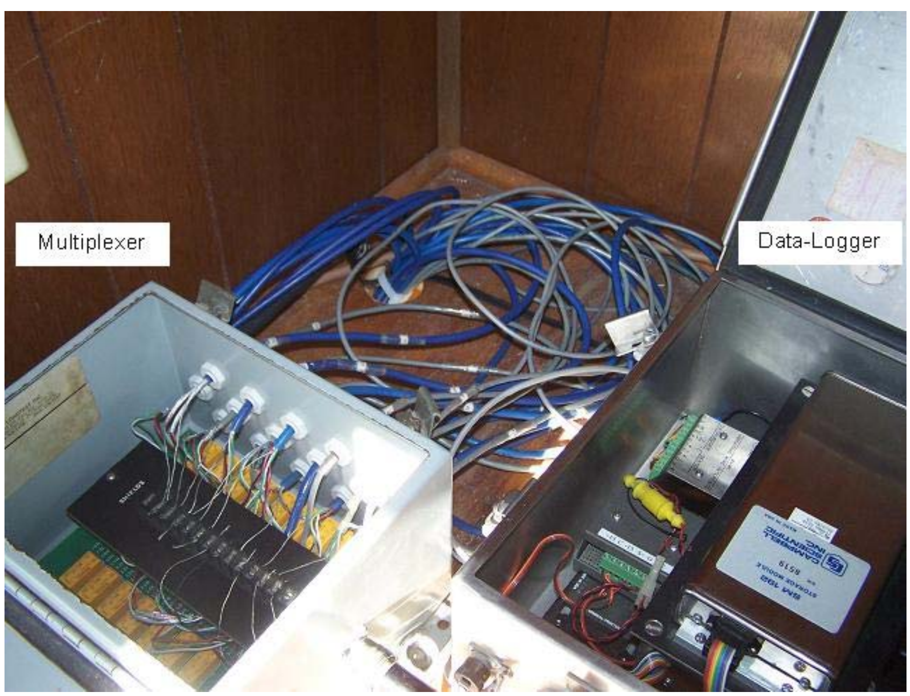

Figure 2-37: Data acquisition system (inside shed)

A temporary casing was used during the construction of the long test shaft (Figure 2-38 on the next page). The casing simplified the construction since no slurry was required for hole stability and eliminated the possibility of damaging the pressure cells during shaft construction (i.e., drilling equipment). Furthermore, the shaft profile and location of pressure cells relative to the proposed shaft were better defined with the use of a temporary casing. When using a tremie or concrete pump to pour concrete, it is difficult to continue placing concrete once the casing is pulled several feet into the air; therefore, the casing was constructed using three separate sections, so a section could be removed once it was pulled to the applicable height. The casing sections were constructed using eight rectangular steel sheets that were ten gauge (about one eighth inch thick) and had dimensions of four feet by nine and a half feet, which gave the desired circumference of 9.42 feet (diameter of three feet). The steel sheets were rolled in cylindrical shells and welded along the vertical seams (Figure 2-38 – top two photos). The eight shells were sized and welded along the horizontal seam to create three cylindrical shells with dimensions of three feet by eight feet tall (Figure 2-38 – bottom photo). Steel brackets were fabricated and welded to the three shells, so the three sections could be bolted together and unbolted to remove a section during shaft construction.

Figure 2-38: Temporary casing used with long shaft

In addition to the shaft casing, a form was fabricated for the top of the shaft (Figure 2-39) that was above the ground surface. Since the casing was to be removed after the concrete hydrated, it was constructed in two pieces, i.e., instead of welding along the vertical seam (permanent), and the seam was held together with bolts. This way, the form was able to be unbolted and easily removed after the concrete hardened.

Figure 2-39: Removable shaft form used with long shaft

Once the casing was complete, the soil level in the test chamber was raised to a depth of 25 feet below the top of the test chamber (bottom of proposed shaft). The two pressure cells directly below the proposed test shaft were placed as the soil was compacted in lifts within the test chamber. Using the test chamber as a reference, a circle with a diameter of three feet was centered at the bottom of the test chamber (top left Figure 2-40). The casing was lowered into the test chamber, and the top of the casing was secured to the sides of the top of the test chamber (bottom right Figure 2-40) with turn buckles, preventing the casing from shifting during compaction of the soil lifts.

Figure 2-40: Casing placement before backfilling soil

With the casing in place, soil was backfilled around the casing in 18 inch lifts and compacted using vibratory method (Figure 2-41 on the next page – left photo). The soil was compacted for a specified time to ensure a constant relative density of 50%. After every two to three lifts, a nuclear density test was performed (Figure 2-41 – right photo) to confirm, unit weight, moisture content, and the appropriate relative density (results of the nuclear density tests can be seen in section 5.1.1).

Figure 2-41: Backfilling soil in test chamber

Also as the soil was placed in lifts, the soil pressure cells were placed at the appropriate locations. The location and orientation of the pressure cells were such that the horizontal and vertical stress could be monitored at key areas of interest (Figure 2-42). The important areas of interest were above the side grouted zone, along the side grouted zone at various distances away from the shaft, below the side grouted zone, and below the tip. Using the top of the test chamber for the vertical datum and the casing for the horizontal reference, the location of the gauges with respect to the shaft were placed within ± 2 inch. Note that the gauges were located vertically, horizontally, as well as relative to true north (Figure 2-42).

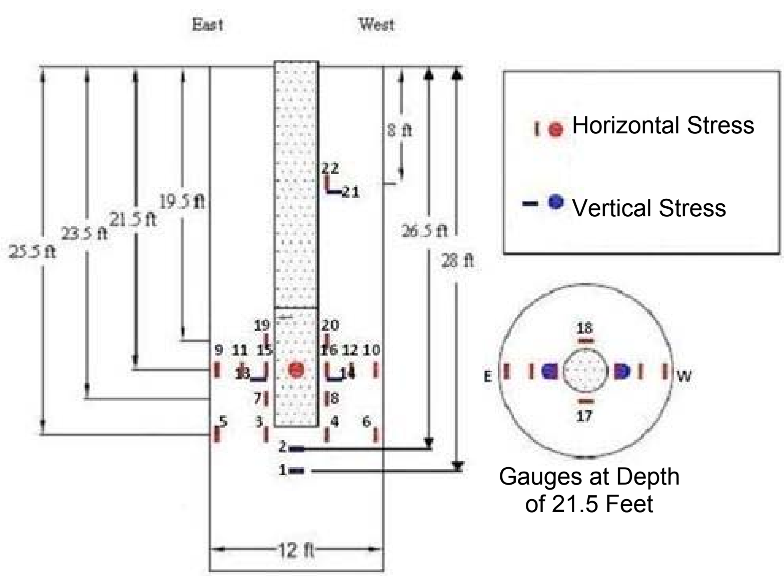

Figure 2-42: Location of 22 pressure cells through test chamber

2.2.3 Shaft Construction and Grouting

The construction of the rebar cage and the attachment of the grout systems took place at the coastal lab. The rebar cage was designed considering both axial loading and bending (AASHTO, 2010). Using thirteen number 10 bars (one-and-a-quarter-inch diameter) in the longitudinal direction, the reinforcement represented approximately 2% (Figure 2-43) of cross-sectional area. Using a minimum concrete cover of six inches, the longitudinal bars were evenly spaced such that the outer diameter of the arrangement was two feet. Using number three bars (three-eighths-inch diameter) for shear reinforcement, the shear steel was evenly spaced 12 inches apart center to center. The test shaft was designed for axial loading only (no lateral or torsional loading), so little shear steel was needed.

Figure 2-43: Long shaft rebar cage

The membrane seals and side membrane were constructed in the soil's lab (UF campus). The two membrane seals were fabricated using the same method that resulted in an air tight and more reliable membrane seal joint (steel pipe and hose clamps). The steel pipe had an OD equal to the ID of the layflat hose creating a tight connection at the joint. The length of the steel pipe was four inches long, so the joint could recess into the rebar cage (between longitudinal steel) giving sufficient clearance during cage placement (Figure 2-44). One-inch holes were drilled in the steel pipe, and a short length (two inch) of one-inch treaded steel pipe was welded to create an air tight port for air and grout to flow. The treaded steel pipe used to fabricate the joint had National Pipe Thread (NPT), so it was compatible with PVC pipe treads (Figure 2-45 on the next page). It was decided to inflate only the top seal during shaft construction. If the membrane seals were to fail, failure would occur at the joint, so by having only one joint on the bottom seal, there would be one less potential failure site (no exit point needed for air to escape while priming the seal with grout). After the membrane seals were completed, they were tested under air pressure and checked for leaks with soapy water. The inner steel rings for the membrane seals were fabricated using steel flat bar that was one-eighth-inch thick and three-inch width (Figure 2-46 on the next page). The layflat hose is about nine inches wide while flat, so two rings were spaced three inches apart to create inner steel rings that were nine inches wide.

Figure 2-44: Membrane seal joint recess between longitudinal steel


Figure 2-45: Grout delivery pipe connection to membrane seal


Figure 2-46: Securing membrane seals to inner steel rings

The same RPP that was used for the short shaft was used to fabricate the side membrane for the long test shaft. The required size of RPP needed was estimated in the same way as the short shaft (circumference and height of the side grout zone equated to the length and width of the cut RPP). The same method of thermal bonding was used to make the vertical seam and create a cylindrical shell (Figure 2-47 on the next page). The steel rings used to secure the side membrane to the rebar cage were fabricated in the same fashion as well. The side grout system was similar to the short shaft but the side-manchette only extended the bottom two thirds of the side grouted zone (bottom six feet). The side-manchette was constructed with the same size grout holes, grout hole spacing, and gum rubber (Figure 2-48 on the next page). The side-manchette was attached to the rebar cage following the tip grout system and before the membrane seals. The side membrane was again pleated vertically and horizontally to reduce stress within the membrane as it expanded outwards during side grouting and attached to the rebar cage by securing it between two steel rings at either end of the side membrane (Figure 2-49 on the next page).

Figure 2-47: RPP used to fabricate side membrane used with long shaft

Figure 2-48: Side-manchette


Figure 2-49: Pleated side membrane secured to cage by steel rings

All welding had to be completed on the rebar cage before PVC and instruments were added to avoid damage from the welding process (i.e., excess heat or welding slag). Therefore, the steel base plate, steel ring for the base plate, and shaft feet were all attached to the rebar cage first. The inner steel rings for the side membrane were also welded to the cage at this time. The steel ring for the base plate was fabricated using steel flat bar that was one-quarter-inch thick and four-inch width (Figure 2-50 on the next page). Using schedule 80 PVC, the tip-manchette was constructed with the same size grout holes, grout hole spacing, and gum rubber as the side-manchette. The required area for the shaft feet was determined using Terzaghi's bearing capacity for a circular footing, with an applied load equal to the weight of the rebar cage and concrete. Using an equivalent area, four square shaft feet were fabricated using steel flat plate (Figure 2-51 on the next page). The shaft feet prevent the rebar cage from sinking too far into the soil during shaft construction and possibly crushing or clogging the tip-manchette. The shaft feet also help transfer loads from the shaft to the tip grout bulb (compressive forces during axial loading or tensile forces during shaft removal).

Figure 2-50: Tip grout system fabrication with steel base plate, steel ring, and tip-manchette (bottom membrane not shown)

Figure 2-51: Shaft feet

The grout systems were added to the rebar cage in the same order as with the short shaft. The tip grout system was completed first, followed by the membrane seals, and finally the side grout system. Completing the tip grout system consisted of attaching the tip-manchette and high pressure hoses at the top of the cage. The inner steel rings for the membrane seals were spaced three inches away from the longitudinal rebar to ensure adequate concrete cover. The rings were secured to the rebar cage using U-bolts (Figure 2-52 on the next page), and the membrane seals were pleated around the rings. The seal joints recessed into the rebar cage giving sufficient clearance when placing cage. Using 90° PVC elbows (threaded to socket), the PVC grout pipes were connected to the membrane seals (shown above in Figure 2-45), followed by the steel nipples at the top of the cage.

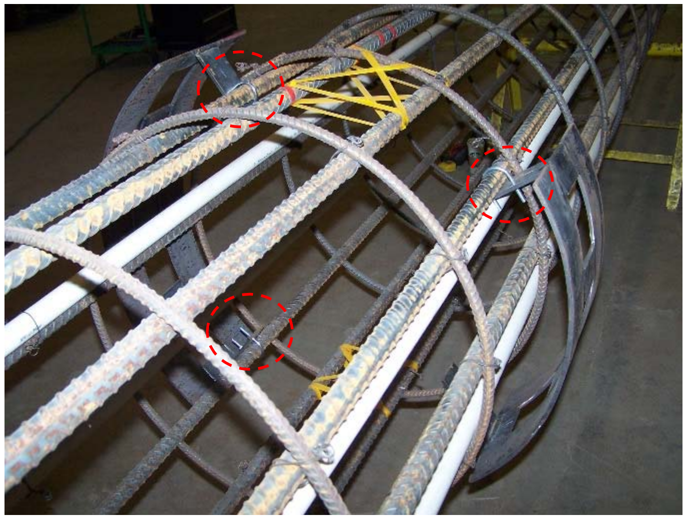

Figure 2-52: Inner rings for membrane seals attached to rebar cage using U-bolts

Before the side membrane was attached, the rebar cage was instrumented with four embedded vibrating wire strain gauges (Figure 2-53), two above the side grouted zone and two below the side grouted zone (shaft tip). The embedded strain gauges were crucial for quantifying the internal forces and load distribution within the shaft during grouting processes and top-down testing. Because the strain gauges were vibrating wire type, they were able to be connected to the same data collection as the Geokon pressure cells, so the strain gauge data could be automatically collected during grouting processes and top-down testing.

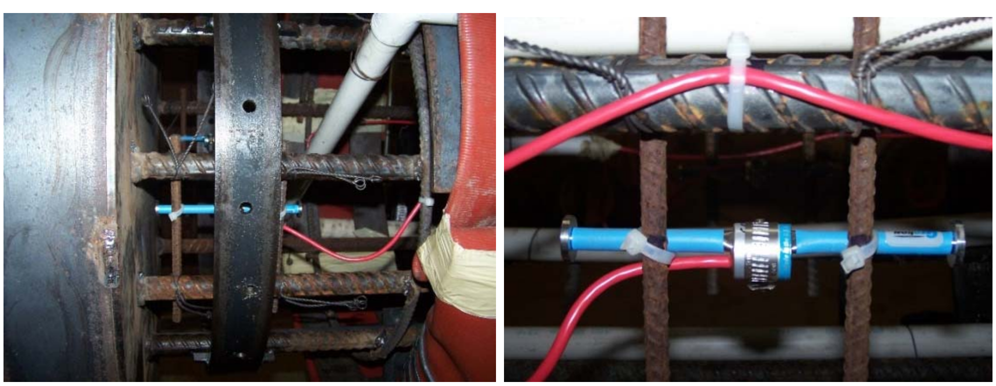

Figure 2-53: Mounted strain gauge below side membrane (left) and above side membrane (right)

Finally, the side-manchette, steel nipples, and high pressure flexible hose were attached to the cage (Figure 2-54), and then, the side membrane was pleated and secured to the cage. The side membrane was pleated around the inner rings (four vertical pleats), a horizontal pleat was made to reduce the height of the side membrane, and the outer rings were secured to the inner rings using half-inch bolts. Again, the side membrane was secured close to the rebar cage to maximize clearance during cage placement (Figure 2-55). The last thing attached to the rebar cage was the bottom seal on the shaft tip, which was secured to the base plate steel ring using metal banding.

Figure 2-54: Steel nipples and high pressure hydraulic hose at the top of rebar cage

Figure 2-55: Completed long shaft rebar cage with grout systems attached

Concerned with large side friction on the casing when pulling and potentially failing the bolts holding the sections together, the test chamber was fully saturated to reduce the effective stress within the soil around the casing, thus reducing lateral stress and mobilized side resistance. The rebar cage with the grout systems attached was lowered into the casing (Figure 2-56). A 5,000 psi ready mix batch of concrete was used to cast the long test shaft (5,000 psi max compression strength after 28 days). Using a concrete pump and fabricated tremie pipe, concrete was placed from the bottom up (Figure 2-57).

Figure 2-56: Placing long shaft rebar cage with grout systems attached in casing

Figure 2-57: Concrete pump (right) and tremie (left) used to place concrete during long shaft construction

After placing a few feet of concrete, the casing was pulled a few feet using a crane (keeping the level of concrete above the bottom of the casing). This process was repeated throughout shaft construction, with the top section of casing removed once above the soil surface (Figure 2-58). Once the concrete level in the shaft was nearing the top of the side membrane, the casing was pulled above the top membrane seal (minimize friction on inside of casing), the top membrane seal was pressurized (pressing the side membrane against the wall of the shaft), and concrete placement continued. Before the last section of casing was removed, the shaft form was partially secured around the casing, the last section of casing was removed, and the shaft form was fully secured around the shaft (Figure 2-59 on the next page). Concrete was added to the form until the desired height was reached. About seven cubic yards of concrete was used to cast the long test shaft.

Figure 2-58: Removing temporary casing during concrete placement

Figure 2-59: Securing the shaft form at the end of shaft construction

Cylindrical concrete specimens were collected during the shaft construction to determine concrete properties, such as the 28 day compression strength, Young's Modulus, and Poison's Ratio. Within 24 hours of shaft construction, water was pumped through the side grout system to spall the concrete cover from the side-manchette. Top of shaft was covered with plastic and kept saturated for two weeks after shaft construction. The test chamber was de-watered after shaft construction, so the tests could be run in the dry (no pore pressure instrumentation in chamber).

Seven days after shaft construction, grouting of the membrane seals was undertaken. The grout volume and pressure was monitored in the same way as the short shaft. In addition to monitoring volume and pressure, the earth pressure cells were also monitored. The bottom seal was grouted before the top seal. The PVC grout pipe was primed by hand using a funnel to remove air before developing grout pressures (Figure 2-60 on the next page).


Figure 2-60: Filling grout pipes (priming) with grout before pumping under pressure

14 days after shaft construction (seven days after grouting membrane seals), side grouting was completed. Because a large volume of grout is needed and higher grout pressures were expected, the grout was pumped using a conventional high pressure grout pump (Figure 2-61 on the next page). The pumping rate throughout the side grouting phase was around two gallons per minute (gpm). The grout volume and pressure was monitored at the grout pump, with a second pinch valve at the top of the shaft (measure pressure loss from pump to shaft). The volume of grout pumped was measured based on grout level in the grout pump reservoir (i.e., one inch = 0.436 ft^3 = 3.26 gallons). In addition to monitoring the grout volume and pressure, the earth pressure cells, embedded strain gauges, and displacements (shaft and soil) were monitored throughout and again two hours after the side grouting phase. Eight digital dial gauges were used to monitor the shaft and soil displacements (Figure 2-62 on the next page).

Figure 2-61: Conventional high pressure grout mixer and pump

Figure 2-62: Digital dial gauge setup during side grouting

Forty-two days after shaft construction (28 days after side grouting), tip grouting was completed. Again, the grout was pumped using a conventional high pressure grout pump (Figure 2-61), and the pumping rate throughout the tip grouting phase was two gpm. The grout volume and pressure was monitored at the grout pump, with a second pinch valve at the top of the shaft to measure pressure losses from pump to shaft. The volume of grout was again measured based on the grout level in the grout pump reservoir. Again, the earth pressure cells, embedded strain gauges, and displacements (shaft and soil) were monitored throughout and two hours after tip grouting. Eight digital dial gauges were used to monitor the shaft and soil displacements during grouting (Figure 2-63). The tip grout system was primed to remove all air before grout pumping was initiated.

Figure 2-63: Digital dial gauge setup during tip grouting

2.2.4 Static Load Test and Exhume Shaft

To prepare for the top-down axial load test (static), the load test cell was tested and the load reaction system was set up at the coastal lab. The load cell was tested in a Universal Testing Machine (UTM) (Figure 2-64). The load cell was loaded and unloaded to identify any hysteresis and compared to the actual applied load from the UTM (Figure 2-65). The load cell readings were within tolerable limits (< 1% error).

Figure 2-64: Check load cell and readout box using UTM

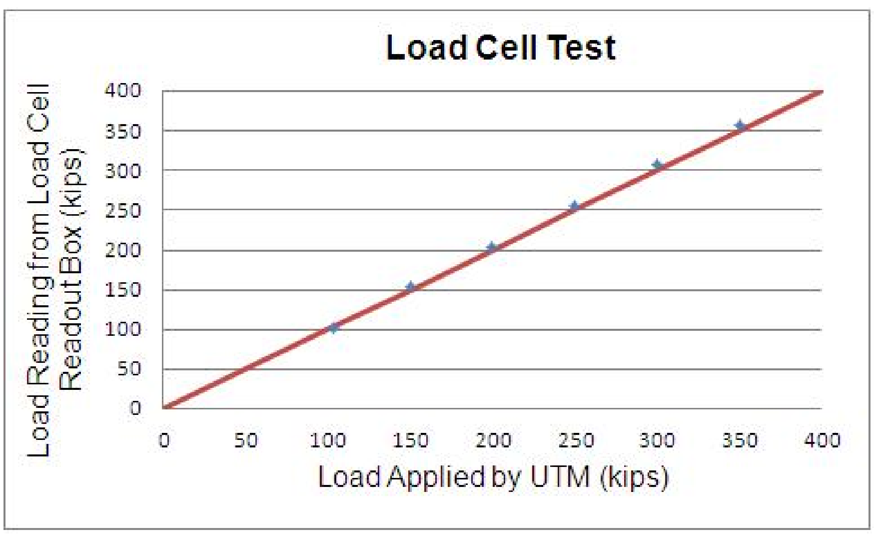

Figure 2-65: Results of load cell test

To transfer the applied load to the test shaft, a reaction system was set up. The beam/girder was secured to the two reaction shafts using steel plates and Dywidag bars (Figure 2-66). A hydraulic jack with a maximum lift capacity of 600 kip was used to apply loads to the shaft during the top-down test (Figure 2-67). The load cell was placed between the jack and reaction beam with a hemispherical bearing plate on top. Between the reaction beam and load cell were three steel plates to transfer the shear force to the reaction beam.

Figure 2-66: Setup reaction system for static load test

Figure 2-67: Load application setup for static test

Throughout the top-down test, the load cell, soil stress gages, embedded strain gauges, and digital dial gauges were monitored. Eight digital dial gauges were used to monitor the shaft, soil, and reaction shaft displacements (Figure 2-68). The top-down test performed was similar to the quick maintained test procedure recommended by the Federal Highway Administration [FHWA] (ASTM 1143-81). During the top-down test, the shaft was initially loaded to 20 kip, and the load was increased by 20 kip intervals with a five minute hold time at each increment (Figure 2-69 on the next page). Once the max load was reached (380 kip), the shaft was unloaded to 250 kip, and the load was reduced by 50 kip intervals with a five minute hold time at each increment.

Figure 2-68: Digital dial gauge setup during static load test (test shaft and soil – top photo; reaction shafts – bottom photos)

Figure 2-69: Applied load during static load test

Shortly after completing the load test, the soil was excavated around the test shaft and long shaft removed from the test chamber. Excavation of the soil from the test chamber was undertaken using a track mounted drill rig and various size auger bits (similar to tank excavation before long shaft construction), with the excavation stopping periodically to locate and remove the Geokon soil pressure cells (Figure 2-70 on the next page). The estimated weight of the shaft was around 23 ton, so the grouted shaft had to be lifted using a crane (Figure 2-71 on the next page). Both the shaft and tip grout bulb were removed together from the test chamber. The actual weight of the grouted shaft was 22 ton (measured by load cell on crane). Once removed from the test chamber, the grouted shaft was rinsed off with water and visually inspected.

Figure 2-70: Excavate soil from test chamber using track-mounted drill rig

Figure 2-71: Crane used to exhume shaft from test chamber

CHAPTER 3
FIELD TESTING OF SIDE-AND-TIP-GROUTED DRILLED SHAFT

3.1 Field Shaft (42" x 25')

The design, construction, post grouting, and load testing (static and Statnamic) of the field shaft (42" x 25') is presented in this chapter and was located near Keystone Heights, Florida (FDOT test site). The process (construction, grouting, etc.) is presented in detail since the field shaft was one of the focuses/tasks of the research. Discussion of the data collected and analysis of the field test results will be presented in section 4.3.

3.1.1 Design Evolution and Improvements

A major area of concern for side grouted drilled shafts was the membrane seals. The seals were designed for three functions: (1) prevent concrete from flowing to the outside of the side membrane during the casting; (2) separate the hydrating concrete from membrane; and (3) provide an upper and lower boundary condition during the side grouting process. The seals were a torus shape and constructed from layflat hose using a small length of steel pipe as a “joint” for air and grout to enter or exit the seals. High torque wire hose clamps were used to secure the layflat hose to the steel pipe. Unlike other clamp types tested, the wire hose clamps create an airtight joint, so air was prevented from escaping into the concrete during casting. However, the steel pipe used to fabricate the joints on the long shaft seals had a smooth surface, so the maximum friction between the hose and steel pipe was less than desirable. In an unconfined test with air, the maximum pressure before leakage of the joint was 35 psi (section 2.2.1).

To improve the friction at the seal joint (between hose and rigid pipe), a barbed union was used instead of the smooth surfaced steel pipe (Figure 3-1). In addition, two hose clamps were used to attach each end of the layflat hose to the barbed union instead of using a single hose clamp per side (Figure 3-2 on the next page). The center of union had a one-inch national pipe tread (NPT) pipe connector welded on to supply air and/or grout to the hose (similar to long shaft). The performance of the new joint fabrication was tested with an inner and outer boundary condition (Figure 3-3 on the next page). That is, the seal was tested in a circular trench dug 18 inches into the ground. For this series of tests, the four wire hose clamps were used to secure the hose to the barbed union, but the hose clamps were not tightened to their maximum torque of 60 foot pounds (ft-lb). The membrane seal held a pressure of 150 psi (rated working pressure), and no leaks were observed (Figure 3-4 on the next page).

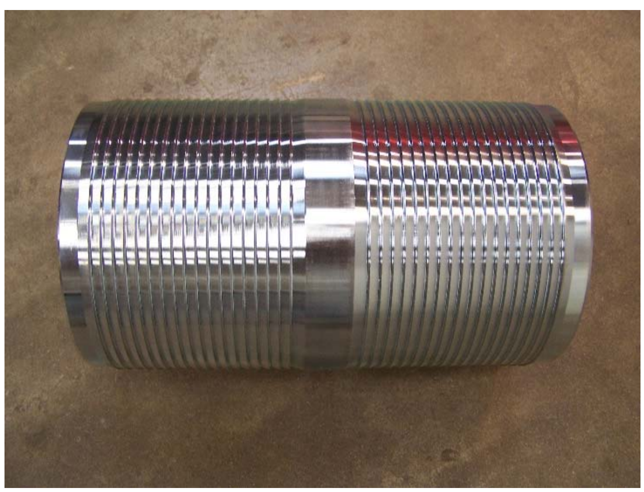

Figure 3-1: Barbed union used to fabricate membrane seal joint

Figure 3-2: Membrane seal joint fabrication method used with field shaft

Figure 3-3: Test the improved membrane seal design with inner and outer boundary conditions

Figure 3-4: No leaks observed during initial test of improved membrane seal design

After the successful test, construction of top and bottom seals began for the full scale test shaft. Once the barbed union was fabricated, it was discovered there was not enough space for two hose clamps at each end of the union to fit between the longitudinal rebar. Therefore, an additional field test using one wire hose clamp on each end was conducted to check the performance and reliability of the joint. For this test, the hose clamps were tightened to their maximum torque of 60 ft-lb. Since grout pressures were expected to exceed 150 psi (e.g., 220 psi observed while grouting the bottom seal on the large chamber test shaft), it was decided to test the bottom membrane seal at pressures higher than 150 psi (higher than rated pressure). For safety concerns, the seal was placed in a circular trench excavated to depth of 30 inches (Figure 3-5). The seal was pressurized to 150 psi, and again, no leaks were observed. The pressure within the seal was then raised, and once the pressure reached 170 psi, the membrane seal failed via hose rupture (Figure 3-6 on the next page).


Figure 3-5: Test the improved membrane seal design with two hose clamps

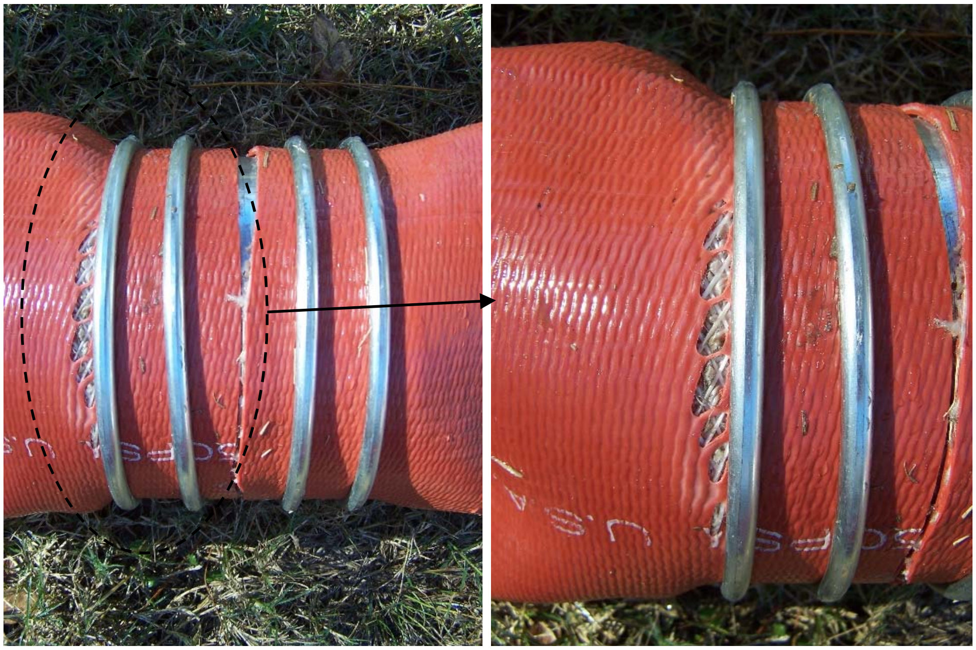

Figure 3-6: Hose failure via rupture

Interestingly, the failure mode was unlike the failure mode previously observed (i.e., the ends of the hose slip off due to insufficient friction between hose and union). Instead, the hose ruptured next to one of the wire hose clamps (Figure 3-6 above). Further investigation concluded that this failure mode was caused by a combination of the stress concentration created next to the wire hose clamp and damage to the hose by the high torque wire clamps (not typically used with barbed union). The permanent distortion of the hose due to the high torque wire clamps (tightened 60 ft-lb torque) is shown in Figure 3-7 on the next page, and the damage caused by the high torque wire clamps and barbed union is shown in Figure 3-8 on the next page.

Figure 3-7: Permanent distortion of the hose due to the high torque wire clamps

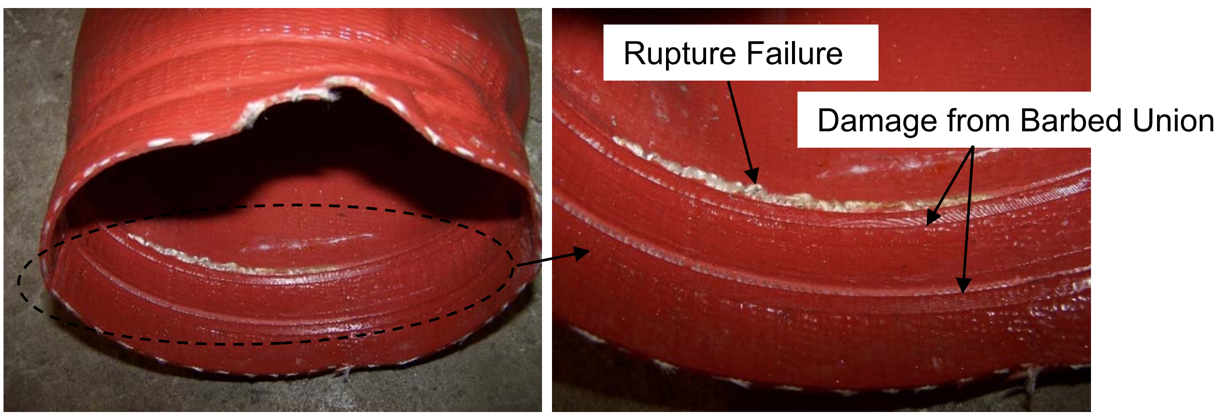

Figure 3-8: Damage to hose caused by the high torque wire clamps and barbed union

The test in the trench was repeated using the same length of layflat hose (already pressurized several times) and tightening the hose clamps to a torque of 20 ft-lb. Unexpectedly, the membrane seal ruptured before 150 psi was reached. Since testing the membrane seals in the trench was labor intensive, an alternative testing method was developed to identify a reliable solution to the new rupture failure mode being observed. Using scrap pieces of the barbed unions, an apparatus was made to test the "slip vs. rupture" failure modes observed (Figure 3-9 on the next page). New layflat hose was ordered and used with the apparatus to eliminate rupture failure caused by hose fatigue.

Figure 3-9: Apparatus used to test the failure mode for joint fabrication method

To prevent damage to the hose, the twin-ring hose clamps were replaced with steel banding (recommended hardware for the layflat hose and barbed union). The banding was tested with a new piece of hose, and leaking water was observed at 70 psi, well before the “slip” failure mode was observed. Because the banding cannot be torqued sufficiently (banding clamp fails under very high torque), t-bolt hose clamps were used to generate greater friction and prevent the “slip” failure mode (Figure 3-10 on the next page). Using two t-bolt hose clamps on either end of the hose, a maximum pressure of 200 psi was maintained without failure (complete failure was avoided for safety reasons; Figure 3-11 on the next page). Unlike the twin-ring wire hose clamps, the t-bolt hose clamps evenly distribute the clamping force across more of the barbs, and unlike the less expensive steel banding, the clamping force of the t-bolt hose clamps was much greater and easily measured (i.e., torque wrench).

Figure 3-10: Test setup with steel banding (left) and t-bolt hose clamp (right)

Figure 3-11: Final membrane seal joint fabrication method

The t-bolt hose clamps were then tested at full scale in the trench (Figure 3-12 on the next page). To simulate the boundary conditions expected at greater depths, the trench was dug to a depth of 36 inches and soil was packed around the seal before pressurization began. The membrane seal failed at 150 psi with a "rupture" failure of the hose (rated working pressure of the hose; Figure 3-13 on the next page). The failure at a pressure less than 200 psi is likely due to the additional tensile stresses (circular shape). Subsequently, a layflat hose with a higher rated working pressure of 310 psi was used (blue hose; Figure 3-14).

Figure 3-12: Test final membrane seal joint fabrication method with inner and outer boundary conditions

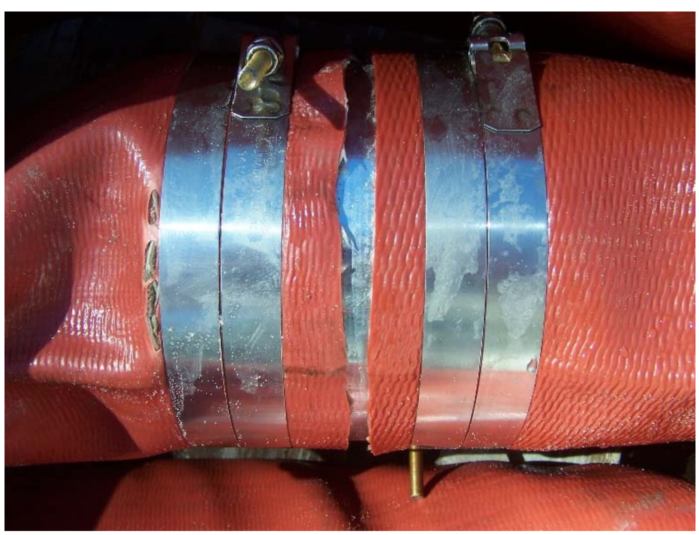

Figure 3-13: Rupture failure observed with final membrane seal joint fabrication method

Figure 3-14: Blue layflat hose (310 psi rated working pressure)

Another area of concern with the membrane seal design was the stress at the connection between the grout delivery pipes (embedded in concrete) and membrane seal joint (expands outwards when grouted). To minimize this stress, it was decided to use a flexible connection that would allow the membrane seals to expand outward after shaft construction (i.e., separating membrane from shaft). To ensure that a new failure mode was not being introduced (i.e., flexible connection could be the weakest point), a flexible connection with a rated working pressure far beyond the layflat hose and barbed union was selected. The flexible connection will be discussed further section 3.1.3. To ensure that the flexible connection does not become embedded during concrete placement, the flexible connection was covered with Styrofoam (discussed further in section 3.1.3), so the flexible connection would be free to move while grouting the membrane seals.

Improvements were also made to the side grouting system. Longer radius elbows were added to improve grout flow (reduce likelihood of “sand locking” under higher pressure) and ensure easy cleanout if needed (Figure 3-15 on the next page). Also, additional side grout delivery systems (single side-manchettes) were added to the rebar cage for grouting (Figures 3-16 and 3-17 on the next page). Instead of a continuous PVC loop, four single PVC pipes were installed, which could be cleaned out from the top. Because much of the plumbing was completed at this point, there was only one feasible location for the additional side-manchettes, approximately 22.5° away from the original side-manchette (continuous loop). The new side-manchettes were placed orthogonal to one another. Note, the additional grout pipes allowed grout to be delivered to all four sides of the shaft if needed (i.e., north, south, east, and west). This approach also minimized the amount of plumbing that crossed the rebar cage (i.e., minimizes potential for damage to side-manchette during concrete placement).

Figure 3-15: Replace short radius 45° elbows (left) with long radius 45° elbows (right)

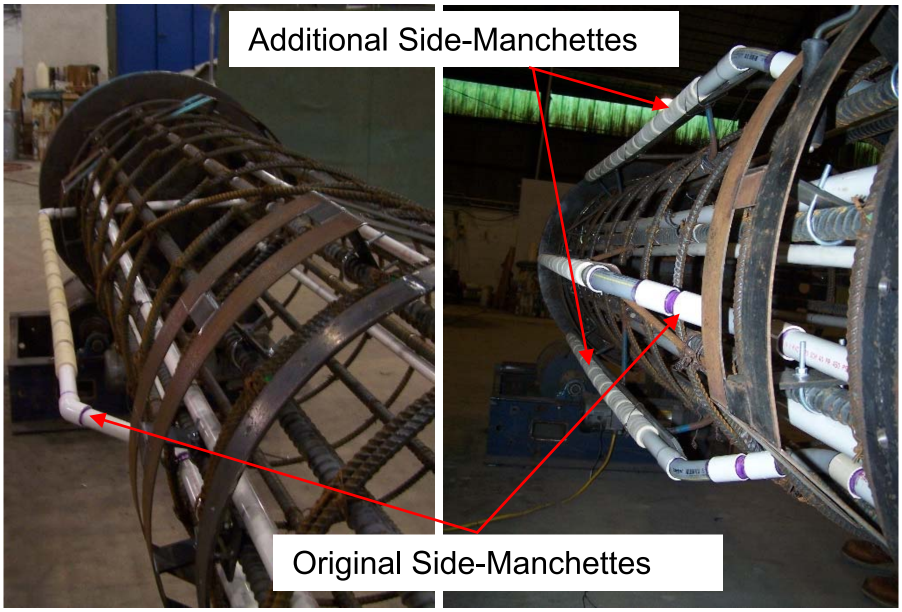

Figure 3-16: Additional side-manchettes added (right) to the original single side-manchette (left)


Figure 3-17: Bottom of side-manchettes (original – continuous loop; additional – capped at ends)

Unlike the first two test shafts which were constructed using the casing method, the full scale test at Keystone Heights was constructed using the wet hole or slurry method of construction. Of concern was the potential for scraping and/or disturbing the walls of the drilled shaft during the placement of the rebar cage. Moreover, the displacement of the slurry during concrete placement is different than temporary casing filled with water. After careful discussion with the contractor and FDOT, the decision was made to allow for one inch of clear cover for both the base plate and pleated side membrane with the side of the hole. One inch of cover over the side membrane would allow the concrete to be spalled over the grout pipes after casting. For corrosion issues, the longitudinal rebar would remain six inches from the side of the hole and conventional shaft spacers which attach to the rebar cage would be used to center the rebar cage within the hole. Additionally, it was decided that the steel rings used to attach the side membrane (bottom) to the rebar cage would be located at least four inches above the steel base plate. The latter ensures that the drilling slurry would easily flow around the solid steel base plate and up through the center of rebar cage as the cage was lowered into the hole. Furthermore, the four inch gap between the steel base plate and bottom of side membrane would allow concrete to flow easily around the rebar and create a desired uniform shaft tip with fully embedded strain gauges. Note, the bottom seal would prevent the fluid concrete from enveloping the membrane. In addition, the gap provides a location to secure instrumentation (embedded strain gauges), which was outside side grouting zone to separate side friction from tip resistance.

The tip grouting system used with the field shaft was nearly identical to the tip grout system used with the long shaft (i.e., conventional tip grout system). Because higher grout pressures were expected with the field shaft, it was decided to use steel pipe to fabricate the tip-manchette rather than schedule 80 PVC pipe used with the long shaft. To minimize cost, steel pipe was also used at the top of the shaft rather than the flexible hydraulic lines used with the long shaft.

The observations and experience gained from the first two shaft (long and short) helped develop effective grouting procedures. Uniform grout flow during the side grouting phase was crucial for generating cylindrical cavity expansion stresses and desirable side grout shape (cylindrical). To encourage the grout to flow both radially and circumferentially around the shaft, the grout should be pumped at a low flow rate. With the grout mix (cement, fly ash, and water) and slower flow rate (e.g., two gpm), the grout that was pumped initially flows upwards to the top of membrane and begins to hydrate (i.e., increased viscosity), which helps to anchor of the membrane and provides a barrier preventing further flow. As additional grout was pumped at higher pressures, grout flowed beneath the hydrating grout (preventing further flow), thus causing the fresh grout to flow radially outward and circumferentially around the shaft expanding the membrane outwards (i.e., develop cylindrical cavity expansion). If the side grouting process was occurring successfully (i.e., cavity expansion), the grout pressure should increase approximately linearly with the grout volume pumped. The expected grout pressure vs. grout volume trend will be discussed further in Chapter 5.

3.1.2 Site Preparation

In conjunction with another FDOT funded project (BDK75-977-41), two reaction shafts were constructed to provide reaction during static load test (Figure 3-18). The two reaction shafts each have a diameter of four feet and embedment depth of 55 feet (plus one foot above soil surface). Each reaction shaft has a design capacity of 400 kip (800 kip total reaction force).

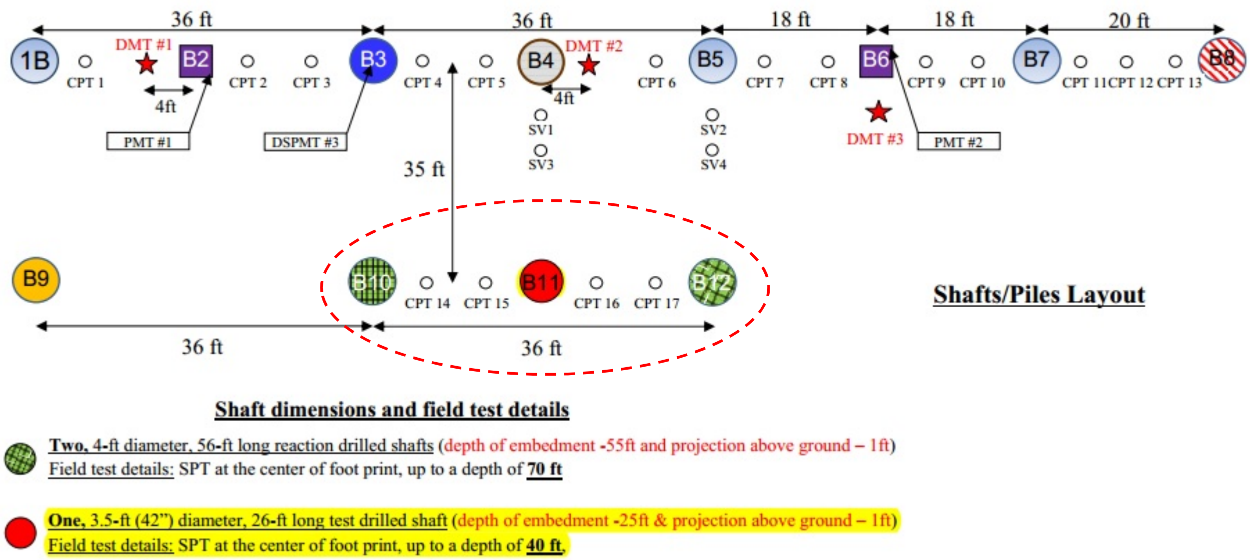

Figure 3-18: Location of field shaft and reaction shafts

A Pressuremeter Test (PMT) was conducted in the proposed shaft's footprint (center) by FDOT SMO personnel (Figure 3-19 on the next page). The depth of the first PMT corresponded to the middle of side membrane of the drilled shaft. At a depth of 19 feet 10 inches (middle of side cavity), the first PMT was completed and results shown in Figure 3-20 on the next page. The Pressuremeter (probe) was pressurized to 281 psi, and the volume of fluid in the probe was at 42 square centimeters (i.e., uncorrected volume). The volume was held for 15 minutes and the recorded pressure dropped to 254.1 psi. Next, an attempt was made to advance the probe to a depth of 25 feet 8 inches (tip cavity). The maximum permissible truck dead load was exerted on the probe (over eight ton or around 72,000 kN) at depth of 20 feet with little to any penetration observed. Consequently, no PMT data was available at the tip (only SPT).

Figure 3-19: PMT test in center of field shaft footprint

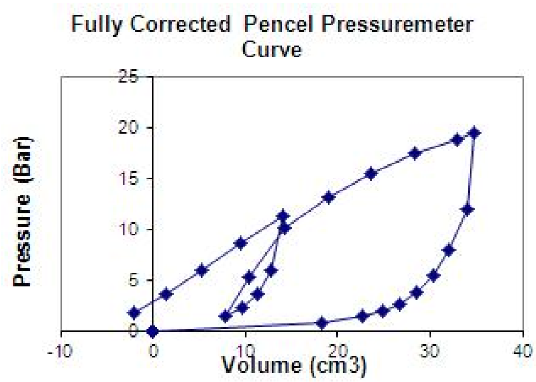

Figure 3-20: PMT results

Supplemental funds were provided by the Florida Department of Transportation to monitor soil stresses during all phases of shaft construction, grouting, and subsequent top-down testing. The additional funding was sufficient to purchase five push-in pressure cells manufactured by RST Instruments (Figure 3-21 on the next page). The pressure cells measure total soil stress perpendicular to plane in which they are installed. The cells have a thermistor and piezometer to measure the temperature and pore water pressure, so effective stresses can be calculated (total stress minus pore water pressure). Concerned with potentially high lateral stresses and deflections from the grouting process, the width of the pressure cells was increased from six millimeters (mm) (standard width) to 12 mm. The pressure cells were placed vertically around the shaft to measure horizontal stresses at various depths in the ground (side and tip grouted zones). The proposed location of the pressure cells is shown in Figure 3-22.


Figure 3-21: Push-in pressure cell manufactured by RST Instruments

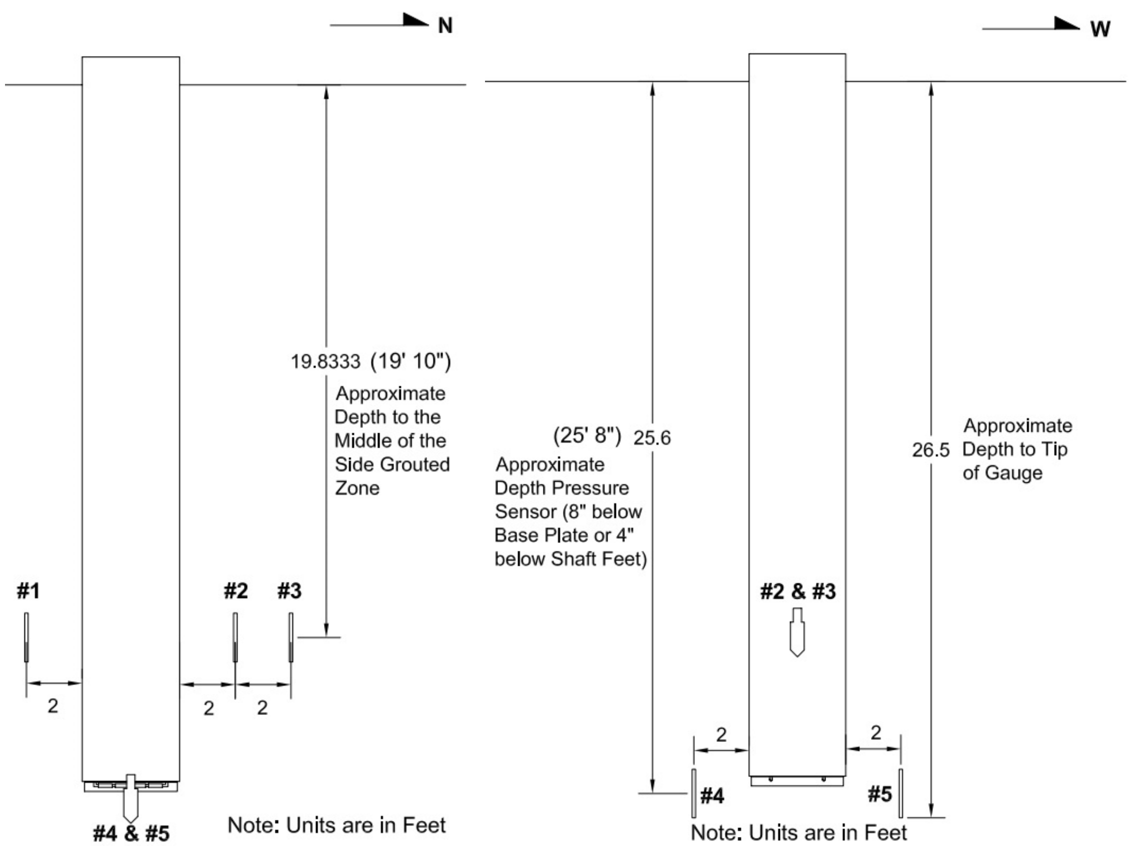

Figure 3-22: Proposed push-in pressure cell locations

After receiving the five push-in pressure cells from RST, the pressure cells were tested and calibrated with the MultiLogger data acquisition program prior to field installation. Since the instruments were not a Geokon product, they were first tested using the Geokon readout box (i.e., checked zero reading). Both the pressure cell and piezometer use vibrating wire technology, so the Geokon readout box was capable of reading both. The zero readings measured with the Geokon were compared to the zero readings provided on the calibration sheets for each gauge (Table 3-1 on the next page). Next, the thermistors were tested using an ohmmeter, and the temperatures were calculated using the conversion table provided along with the instruction manual (Table 3-2 on the next page). The temperatures measured by the ohmmeter (gauge temperature reading) did not exactly match the temperatures measured by a typical outdoor thermometer. The temperatures measured by the push-in pressure cells (ohmmeter) varied from 19 to 20 degrees Celsius (°C) (± 200 Ω). The temperature measured by the outdoor thermometer however was about 18 °C. Sources of error include the outdoor thermometer used to estimate the actual air temperature (i.e., accuracy ± 1°C) and the accuracy of the ohmmeter used to measure the thermistor resistance (i.e., accuracy ± 1 kΩ).

Table 3-1: Pressure cell zero readings

All Zero Values are in B-Units

Gauge #	Pressue Cell		Piezometer	
	Average Zero from Clibration Sheet	Zero Reading using Geokon Readout Box	Regresion Zero from Clibration Sheet	Zero Reading using Geokon Readout Box
1	8799	8794	9012	9006
2	8931	8921	8998	8994
3	8968	8960	8797	8794
4	8805	8797	8899	8894
5	8726	8712	8780	8777

Temperature at Time of Calibration was 17.6 °C
Temperature when Measuring with Geokon Box was 23.3 °C

Table 3-2: Pressure cell temperature readings

Gauge #	Thermistor	
	Measures Resistance (kΩ)	Temperature Range (°C)
1	3900	19 - 20
2	3900	19 - 20
3	3800	19 - 20
4	3700	19 - 20
5	3800	19 - 20

Temperature when Measuring with Ohmmeter was 23.3 °C

After ensuring that the push-in pressure cells were functioning, their accuracy was checked using the pressure vessel. First, the pressure cells were connected to MultiLogger data acquisition system. Because these were not Geokon pressure cells, the gauge specifications had to be manually selected (i.e., excitation frequency and voltage). The values read using the Geokon readout box have units of "B" (a.k.a., "B-Units"). The B-Units are calculated given equation 3.1:

$$B\text{-}Units = \frac{Excitation\ Frequency\ (Hz)^2}{1000} \tag{3.1}$$

Where the excitation frequency is the frequency in which the vibrating wire is plucked and measured in hertz (Hz). For example, the excitation frequency for a readout box value of 9,000 B-Units is 3,000 Hz. Therefore, the high excitation frequency was selected in the MultiLogger program (i.e., RST gauges range from 2,000 to 4,200 Hz). The low and middle excitation frequencies (i.e., 400 to 1,000 Hz and 1,000 to 2,500 Hz respectively) were outside the B-Unit range observed on the calibration sheets (i.e., 9,000 to 4,000). For any of the excitation frequencies (low, middle, and high), a five volt or 12 volt excitation can be used. Since the gauge wire length is relatively short, there were no splices in the wires, and no expected electrical interferences, the five volt excitation was selected in the MultiLogger program. Additionally, a five volt excitation is recommended to minimize wear on the gauges, and in some cases (other instrumentation), the 12 volt excitation can permanently damage the instrument. Using the calibration sheets for each gauge, the calibration factors were entered and saved in the MultiLogger program.

With the pressure cells connected to the data acquisition system (Figure 3-23), a series of pressure tests were conducted. Shown in Figures 3-24 and 3-25 on the next page are the results of the pressure vessel test. The results showed that all sensors exhibit linear behavior and were within the manufacture's specifications.

Figure 3-23: Pressure vessel test with RST push-in pressure cells

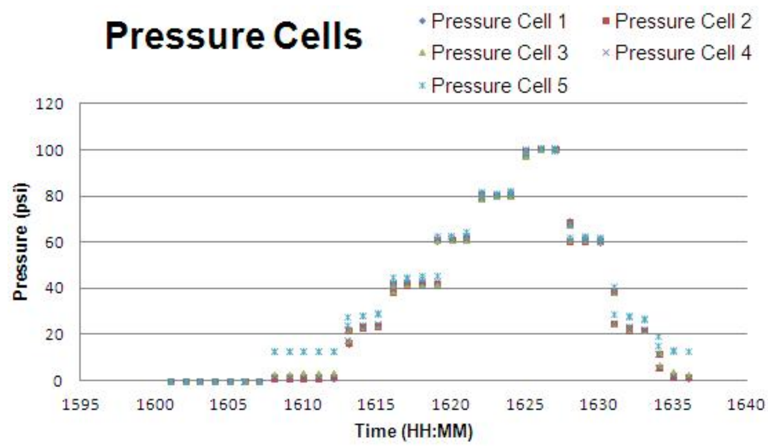

Figure 3-24: Pressure cell reading during pressure vessel test

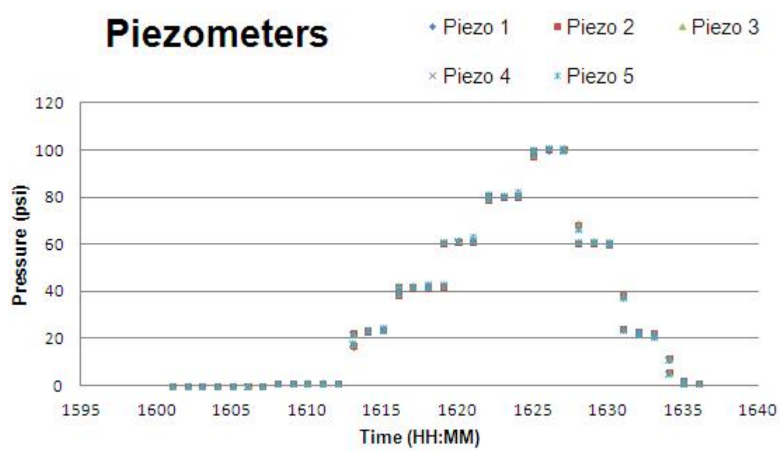

Figure 3-25: Piezometer reading during pressure vessel test

Next, the push-in pressure cells were installed in the field by FDOT SMO personnel. Due to difficulties with the PMT test (i.e., refusal around 20 feet), it was decided to pre drill the holes and push the soil stress cells the last foot. Therefore, SMO's SPT drill rig was used to drill and push the pressure cells in the field. Once the gauges were installed, the gauge wires were run through PVC conduit and buried two feet below the soil surface. The conduit was run to a weather resistant box four feet from the shaft (Figure 3-26 on the next page). The box housed the multiplexer with each pressure cell connected to the desired channel on the multiplexer. During shaft construction and grouting, a single cable from the data acquisition to the multiplexer allowed the instrumentation to be read automatically. The embedded strain gauges were also connected to the multiplexer before grouting and load tests and disconnected afterwards, so the weather resistant box housing the multiplexer could remain closed.

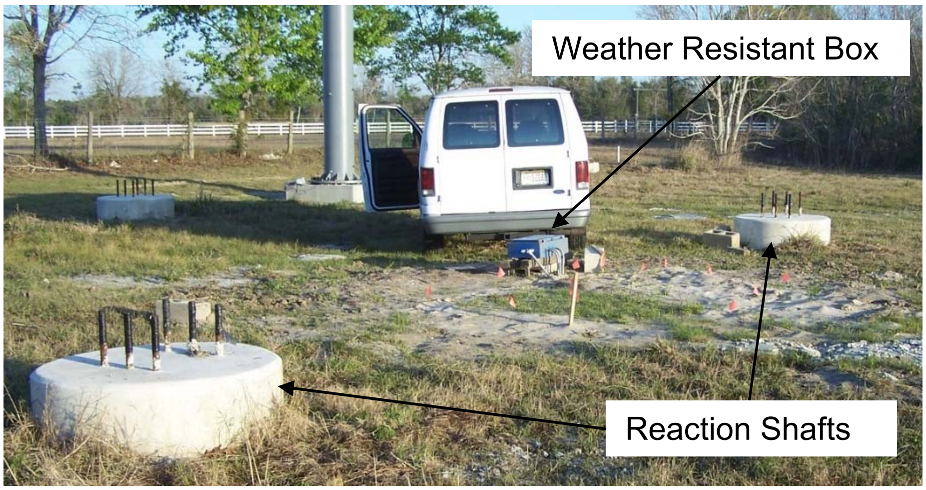

Figure 3-26: Test site before field shaft construction

3.1.3 Shaft Construction and Grouting

The construction experience learned from the test chamber testing was used in the construction of the full scale field test shaft. For example, any welding done on the rebar cage was completed prior to placing PVC grout pipes or instrumentation. Otherwise, excess heat or slag (molten metal) could damage the PVC pipes or embedded gauge wires. Overall, the tip grouting system was completed first, followed by the membrane seals, then embedded strain gauges (instrumentation), and finally the side grouting system.

The reinforcement cage for the field shaft is shown in Figure 3-27 on the next page. The pre-grout dimensions of the shaft was 42 inches by 25 feet with at steel ratio of 1.06%. Twelve number 10 bars (one-and-a-quarter-inch diameter) were used in the longitudinal direction and 26 number five bars (five-eights-inch diameter) were used for the shear reinforcement, spaced every 12 inches along the cage. The longitudinal bar center to center spacing was 7.44 inches, which was sufficient to accommodate PVC grout delivery pipes and the membrane seal joints (recess into the rebar cage). The steel base plate was centered and attached to one end of the rebar cage (Figure 3-28). The diameter of the base plate was 40 inches with one inch of clearance between the base plate and drilled shaft wall (42 inch diameter). The base plate had four holes for supply and return of two separate grout lines (i.e., tip-manchettes). The four holes were located such that the grout delivery pipes could be attached to the longitudinal rebar and pass through the base plate without any bends (ensures easier flow and cleanout).

Figure 3-27: Field shaft rebar cage

Figure 3-28: Steel base plate used with field shaft

Rather than relying on the weld strength between the longitudinal rebar and the steel base plate (i.e., rebar is not weldable grade steel), a mechanical connection was used along with a welded connection to the base plate (Figure 3-29). The mechanical connection included set screws that secured the longitudinal rebar to a thick walled steel pipe (weldable). Holes were drilled and treaded along the thick walled pipe with the thick walled pipe welded to the base plate. Note, the tip grout delivery system was already attached to the rebar cage, which would be picked up from the top and inserted into the drilled shaft hole with a crane.

Figure 3-29: Base plate connection to rebar cage

Three steel feet were attached to the bottom base plate (Figure 3-30 on the next page). The size of shaft feet was calculated based on bearing capacity and soil conditions expected below the shaft tip (bottom of drilled hole). Note, the rebar cage was designed to rest on the bottom of the drilled shaft (hole) before concrete placement, so the shaft feet help protect the tip-manchette during shaft construction (prevent crushing under weight of concrete). The feet also ensure that a space exists below the base plate, so grout flow will initiate beneath the tip of the shaft. The rubber seal covering the tip manchettes was attached to the base plate before moving the cage to the test site.

Figure 3-30: Shaft feet

The tip grouting system included grout delivery pipes, steel base plate, steel ring, tube-a-manchette (tip-manchette), and bottom rubber seal. Using steel flat bar, a steel ring was rolled and attached to the bottom of the base plate (Figure 3-31 on the next page). The dimension of the flat bar was four inches by one-quarter-inch thick. The bar was cut and rolled to make a steel ring four inches high with an OD of 40 inches (i.e., equal to the base plate diameter). The rubber seal was attached to bottom of the steel ring. The base plate, steel ring, steel feet, and rubber seal create a void around the tip-manchette. The tip-manchette was fabricated using steel pipe rather than PVC pipe. Further investigation of the cost versus reliability for PVC and steel pipe revealed that steel pipe had a higher working pressure versus the overall cost. Consequently, one-inch schedule 80 steel pipe was purchased, cut to the desired lengths, and threaded to construct the two tip-manchettes beneath the steel base plate (Figure 3-31 - left). Holes were drilled in the steel pipe and covered with gum-rubber to create the final tip-manchette (i.e., tube-a-manchette). In addition, steel nipples were fabricated from the same steel pipe and extend one foot above the base plate (one foot above shaft tip), so the connection to the embedded PVC pipes would have adequate concrete cover (Figure 3-31 - right). One-inch schedule 40 PVC pipe was used within the shaft to deliver grout from the top of the shaft to the tip-manchette. Since the grout delivery system was embedded with a minimum of six inches of concrete cover, schedule 40 PVC pipe was acceptable within the shaft (additional strength provided by concrete).

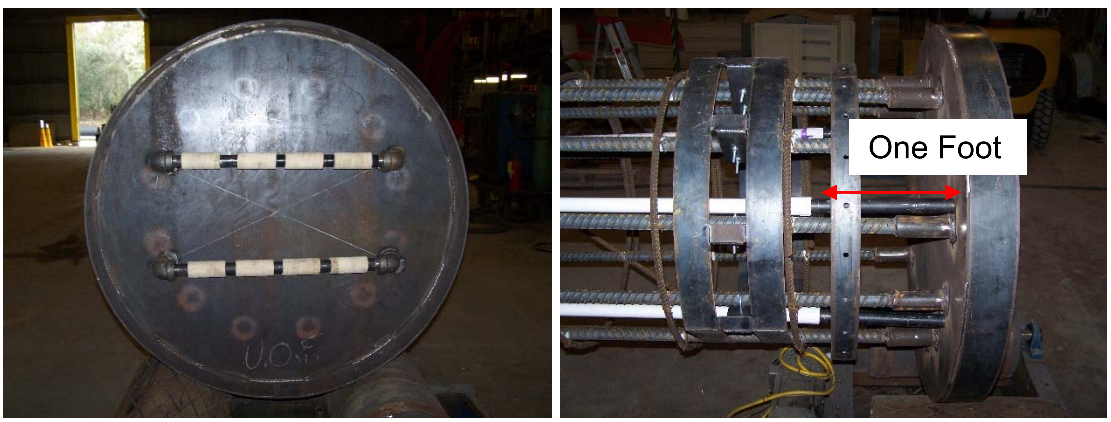

Figure 3-31: Tip grout delivery system

To prevent the membrane seals from expanding inward during shaft construction and reduce the shaft's concrete cover where the seals are located, steel rings were fabricated and secured to the rebar cage. Using the same size steel flat bar, rings were fabricated similarly to the long shaft (see section 2.2.3). Rather than welding the rings to the cage, the ring sections were secured using steel stand-offs and U-bolts (Figure 3-32 on the next page). The stand-offs were welded to the inside of the ring sections, and U-bolts were used to secure the stand-offs to the longitudinal rebar (mechanical connection). To prevent damaging the membrane seals on the sharp end of the ring sections, an additional piece of flat bar extends from the ends of the ring sections to the next longitudinal rebar leaving space (gap between longitudinal bars) for the membrane seal joint to recess (Figure 3-32).

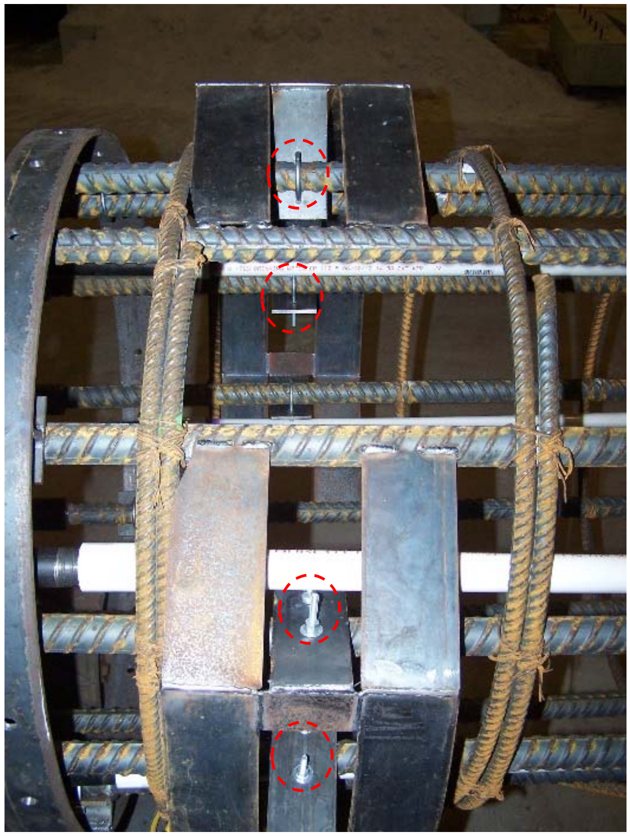

Figure 3-32: Inner steel ring for membrane seals attached to cage using U-bolts

Shown in Figures 3-33 and 3-34 on the next page, the membrane seals were fabricated using both the red hose (150 working pressure) and blue hose (310 psi working pressure). The blue hose was used to fabricate the bottom seal because of the higher expected grout pressures (Figure 3-33). When ordering the high pressure layflat hoses, the minimum length of hose that could be purchase was 25 feet. Consequently, the remaining length of blue hose (from bottom seal) and remaining red layflat hose from apparatus test (section 3.1.1) were used to fabricate the top membrane seal (Figure 3-34).

Figure 3-33: Bottom membrane seal fabricated for field shaft

Figure 3-34: Top membrane seal fabricated for field shaft

Once the seals were completed, they were attached to the rebar cage. The seals were pleated around the steel rings and secured using tape. To allow the membrane seal to expand outwards while being grouted, flexible hydraulic hose was used (Figure 3-35 on the next page). To prevent the flexible hydraulic hose from becoming embedded in concrete during shaft construction, Styrofoam was used to cover the flexible hydraulic hose (Figure 3-36 on the next page).

Figure 3-35: Flexible hydraulic hose used to allow membrane seal to expand outwards unrestricted

Figure 3-36: Styrofoam used to prevent flexible hose from becoming embedded in shaft

The side grouting system included grout delivery pipes, side membrane, and steel rings. Fabricated from steel flat bar (see 2.2.3), the steel rings were used to hold the membrane and position it outside the rebar cage.   Before grout PVC pipes were attached, the inner rings were attached to the rebar cage using U-bolds, which mechanically attached the side membrane to the rebar cage (Figure 3-37 on the next page). Since the rings were located horizontally outward from the rebar cage, steel spacers were welded to the rings. The rings were spaced approximately nine feet apart on the rebar cage (i.e., length of side grouted zone).

Figure 3-37: Mechanical connection used to secure inner side membrane steel rings

Schedule 40 PVC pipe was used to deliver grout to the side membrane (Figure 3-38 on the next page). The PVC pipes were attached to the longitudinal rebar, but extend outside the rebar cage in the side grouted zone (i.e., tube-a-manchette). The PVC pipes extend four inches outside the rebar cage, resulting in one inch of clearance between pipe and shaft wall. The latter distance was agreed on after discussions with FDOT and contractor for ease of placement of the rebar cage and grout systems in the drilled shaft hole prior to concrete placement. The side-manchette grout system extends in the bottom two thirds of the side grouted zone (i.e., bottom six feet of side grouted zone). Steel spacers were attached between the side-manchettes and longitudinal rebar to limit flexure of the side-manchettes during transportation, rebar cage placement, and shaft construction (Figure 3-38). To prevent damage to the bottom PVC loop (crosses the center of rebar cage) during concrete placement, a piece of steel flat bar was welded above the PVC pipe section (Figure 3-39). The piece extended horizontally across the rebar cage and prevented the contractor's tremie pipe and/or falling concrete from damaging the PVC pipe.

Figure 3-38: Side membrane grout delivery pipes with steel reinforcing members

Figure 3-39: Bottom of continuous loop side membrane grout delivery system with reinforcing member

Identical to the long shaft side membrane fabrication, the side membrane was fabricated again using 45 mil reinforced polypropylene (Figure 3-40 on the next page). The vertical seam was completed first. The horizontal pleat was made before placing the side membrane on the cage. Once the side membrane was on the cage, vertical pleats were made to secure the membrane to the steel rings, located at the top and bottom of the side membrane. Tape was used to keep the side membrane uninflated, i.e., minimize contact between the membrane and wall of the drilled hole during placement.

Figure 3-40: Side membrane pleated and secured to rebar cage

Before attaching the side membrane, the rebar cage was instrumented with two types of embedded strain gauges, vibrating wire and resistance wire (Figure 3-41 on the next page). A total of eight gauges were used (four above the side membrane and four below), with four vibrating wire (two above the side membrane and two below, Figure 3-41 top two photos) and four resistance gauges (two above the side membrane and two below, Figure 3-41 bottom two photos). The vibrating wire gauges were mounted orthogonal to the resistance gauges such that the vibrating wire gauges measure bending moment above and below the side membrane in the one direction and resistance gauges measure bending moment above and below the side membrane orthogonal to the vibratory gages. All embedded strain gauge wires run through their own half-inch PVC conduit to the top of the shaft to prevent damage during construction from lifting the cage, tremie pipe, concreting, and so on. At the top of the cage, the wires were stored in three inch PVC pipes (Figure 3-42 on the next page). This protects the wire ends during shaft construction and provides a dry storage place while not in use. The pipes were secured inside the cage during transport and placement of the rebar cage (Figure 3-42 – right photo).

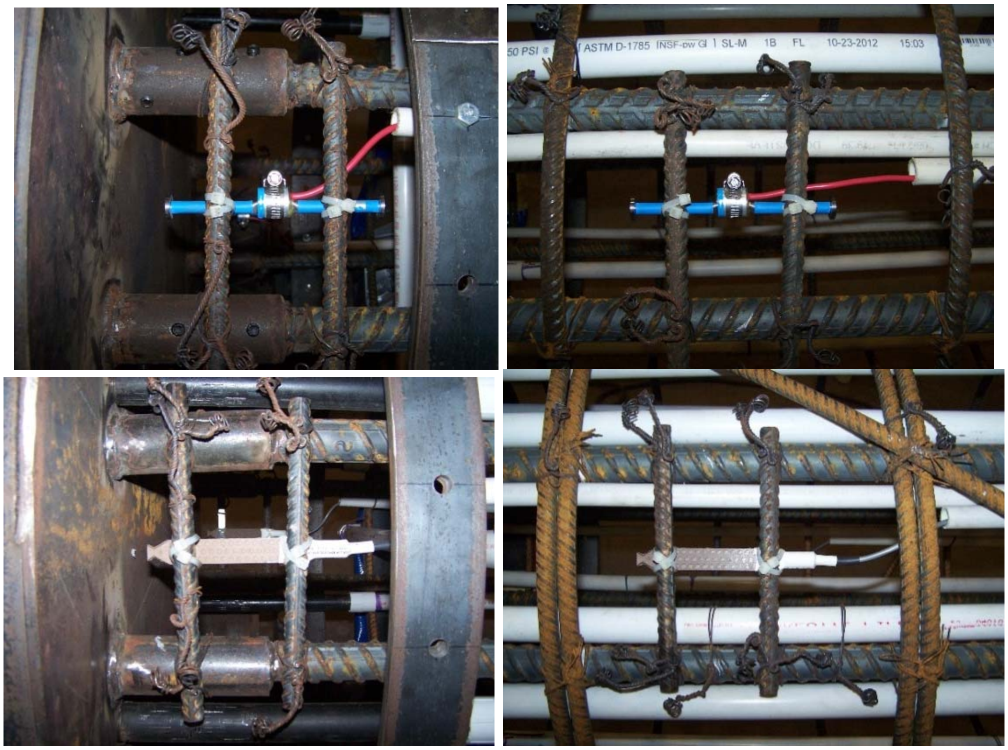

Figure 3-41: Top two photos – vibrating wire strain gauges below side membrane (left) and above side membrane (right). Bottom two photos – resistance wire strain gauges below side membrane (left) and above side membrane (right).

Figure 3-42: PVC pipes used to store and protect embedded strain gauge wires

For the grout system and cage instrumentation, steel nipples were fabricated and attached to the ends of pipes at the top of the rebar cage (Figure 3-43 on the next page). The steel nipples for high pressure grout lines extend one foot below the top of shaft. For the side and tip grout delivery pipes, each nipple was constructed from schedule 80 steel pipe with a working pressure greater than 2,000 psi. For the membrane seal grout delivery pipes, schedule 40 steel nipples were used since much lower grout pressures were expected. Additionally, the flexible grout lines from the grout pump to the shaft nipples were rated at 2,000 psi working pressure. It should be noted that while many grout lines were expected to have grout pressures greater than 600 psi (max 1,000 psi), flash setting of the grout or “sand locking” may result in the possibility of pressure spikes (>1,000psi) due to displacement nature of the grout pump. It was primarily used as a precaution to prevent injury to workers due to bursting of grout lines at working pressures of 2,000 psi for lines above ground. To ensure the desired grout pipe was identified correctly after shaft construction, all of the grout pipe steel caps were labeled three ways (Figure 3-44 on the next page): (1) steel punch; (2) indelible marker; and (3) bi-color tape. Also, the steel caps were used to cover the pipes and keep them clean during shaft construction. In addition to labeling the steel caps, the schematic (i.e., relative location) of the various pipes ensured the correct grout pipe was selected and grout pumped to desired location (e.g., seal, side, or tip).

Figure 3-43: Steel nipples at the top of cage

Figure 3-44: Grout pipe identifying marks (left – punch and marker; right – colored tape and schematic)

Shaft construction began on Thursday, March 7th, 2013 by Reliable Contractors Inc. (Reliable). A truck-mounted drill rig was used to drill the hole (Figure 3-45). The hole was drilled without slurry (open hole) to a depth of about eight feet. By implementing open hole construction initially, the hole acted as the slurry reservoir, so the larger shaft casing (typically used) was not used at the top of the shaft, thus ensuring the shaft had a constant diameter and cross-section at the end of construction.

Figure 3-45: Truck-mounted drill rig used to drill hole

Shortly after drilling began, at a depth of three and a half feet, buried debris (i.e., galvanized steel pipe) was encountered and prevented drilling from progressing (Figure 3-46). Attempts were made to pull the debris from the hole but were unsuccessful. To avoid impacting the quality of the hole or damaging nearby soil pressure cells, the steel debris in the shaft's footprint (i.e., footprint of the auger) was cut out and removed from the hole manually. The sharp edges on the debris on the wall of the hole (outside of the footprint) were hammered inward to avoid cutting the side membrane while placing the cage in the hole.

Figure 3-46: Debris struck at three-foot drilling depth

With the debris removed, drilling continued to a depth of about five and a half feet when more buried debris (i.e., steel plate) was encountered and prevented drilling from progressing (Figure 3-47 on the next page). Because the hole was still open (i.e., no slurry), the debris could be reached with cutting tools and removed manually again. However, the steel plate was much larger and thicker than the galvanized steel pipe struck earlier, requiring five and a half hours to cut and remove the steel plate from the hole. As a result, shaft construction had to be continued the following day.

Figure 3-47: Debris struck at five and a half foot drilling depth

The following day (Friday, March 8th, 2013), drilling continued. The hole was drilled to a depth of about eight feet and slurry was added to maintain hole stability (Figure 3-48). Polymer slurry was used, and the slurry quality was checked throughout the remaining drilling process (Figures 3-49 to 3-51). The hole was drilled to an approximate depth of 25 feet and four inches.

Figure 3-48: Use drilling slurry after drilling to depth of eight feet

Figure 3-49: Equipment used to check slurry quality

Figure 3-50: Recover slurry sample for quality check

Figure 3-51: Checking slurry quality during shaft construction

Next, the shaft's surface casing was centered over the hole and leveled (Figure 3-52 on the next page). The surface casing was positioned to result in one foot of exposure of the constructed shaft and the final ground surface elevation (i.e., 25 foot embedment depth with one foot above the soil surface). After measuring the distance from the top of the surface casing and the bottom of shaft hole, the instrumented rebar cage with attached grout systems was picked up from its top (Figure 3-53 on the next page), centered over the hole (Figure 3-53, bottom right), and lowered into the hole

(Figure 3-54 on the next page). The slurry easily flowed around the base plate and into the center of the rebar cage as the cage was lowered into the hole (one foot spacing between base plate and membrane rings; Figure 3-31).

Figure 3-52: Shaft form centered and leveled at top of hole (42 inch diameter)

Figure 3-53: Lift rebar cage and maneuvered to hole


Figure 3-54: Lower cage with grout systems attached into hole

Once the cage was resting on the bottom of the hole, the three inch PVC pipes housing the embedded strain gauge wires were all fixed in the upright position (Figure 3-54 – bottom right photo) and both membrane seals were pressurized with air (Figure 3-55). The air (20 psi top seal; 30 psi bottom seal) was provided by an onsite air compressor, and air pressures were decided based on the expected hydrostatic pressure generated by the fluid concrete, which were estimated to be 27 psi at the tip (26 feet of concrete) and 17 psi at the top seal (16 feet of concrete). Hydrostatic pressure generated were estimated using a unit weight of 150 pounds per cubic foot (pcf) for the concrete.

Figure 3-55: Air compressor (left) and pressurize membrane seals (right)

Next, a concrete pump was used to place the concrete (Figure 3-56 on the next page). The line carrying concrete was divided into two lines after leaving the pump. The two lines were wired together and lowered down to the bottom of the cage with a crane. The velocity of concrete exiting each line was about half of the flow normally exiting a single line as concrete is pumped (i.e., reduce disturbance). Two concrete trucks were needed to cast the shaft (estimated 9.3 cubic yards needed). The actual volume of concrete used, measured by FDOT inspector, was 10.3 cubic yards. The increase, 11% was attributed to the hole diameter being slightly larger than 42 inches (typical as auger goes in and out of the hole) and voids created after cutting and removing the debris. Quality of the concrete for each truck was tested before concrete was placed (i.e., slump and air entrainment; Figure 3-57). Nine concrete cylinder specimens were collected from each truck. These samples were used to determine properties of the concrete after three and 28 days of hydration. The concrete testing was performed at SMO with the properties given in Table 3-3 on the next page. Grout specimens were also collected during the post grouting stages and will be discussed later in this report. The grout properties are given in Table 3-4 on the next page.

Figure 3-56: Concrete pump (left) used to place concrete with split tremie (right)

Figure 3-57: Check slump of concrete mix (top left) and prepare test cylinders

Table 3-3: Field shaft concrete properties

Days of Hydration	Compressive Strength (psi)	Modulus of Elaticity (psi)	Poisson's Ratio
3	3020	N/A	N/A
	3470		
11	4900	N/A	N/A
	5093		
	5360		
	5358		
28	5980	N/A	N/A
	6447		
	6220	3850000	0.28
	6556	3950000	0.25
	6059	3950000	0.28
	6375	4200000	0.30

Table 3-4: Field shaft grout properties

Days of Hydration	Specimen (Source)	Compressive Strength (psi)	Modulus of Elaticity (psi)	Poisson's Ratio
5	Seals (UF)	4885	N/A	N/A
7	Side Grout (AFT)	5172	N/A	N/A
	Side Grout (AFT)	5025		
28	Side Grout (AFT)	6300	2000000	0.27
	Side Grout (AFT)	6941	2000000	0.27
	Tip Grout (AFT)	4595	N/A	N/A
	Tip Grout (AFT)	5416		
	Tip Grout (AFT)	5314	1883333	0.28
	Tip Grout (AFT)	5628	1883333	0.28
	Tip Grout (AFT)	5409	2000000	0.29
	Tip Grout (AFT)	5899	1950000	0.28
31	Seals (UF)	6853	N/A	N/A
	Seals (UF)	7512		
	Seals (UF)	6758	2200000	0.32
	Seals (UF)	7764	2300000	0.31

Less than 24 hours after shaft construction (Saturday, March 9th, 2013), both membrane seals were grouted. Before grouting the seals, all six side-manchettes were cleaned out (i.e., pumped small volume of water through side-manchettes to break off concrete cover). Once the side-manchettes were cleaned out, the top seal was grouted first, followed by the bottom seal. Since both seals had an inlet and exit pipe to the surface (i.e., front end and back end), the grout was pumped into the front end with the back end open until grout flowed to the top (i.e., remove air from grout lines). The exit back end was then closed and pumping continued until 90% of theoretical volume was reached with grout pressure being recorded throughout. Note, the steel form at the top of the shaft was still attached to the shaft during seal grouting (Figure 3-58).

Figure 3-58: Top of shaft before grouting membrane seals

Side grouting was scheduled to be completed three days following the shaft construction, given the compressive strength of the concrete was at acceptable value (i.e., concrete strength greater than stresses exerted by the fluid grout during the side grouting phase). The average unconfined compressive strength (ASTM C-39) of the concrete after three days of hydration was 3,245 psi. The three-day concrete strength was compared with the stress state exerted on the shaft from the side grouted zone during side grouting (e.g., minimum vertical confining pressure along the side grouted zone). Given a conservative height of concrete to the top seal (15 ft) and unit weight of concrete (150 pcf), the vertical stress in the shaft at the top of the side grouted zone is

2,250 pounds per square foot (psf) or 15.625 psi. Given the observed grout pressures during side grouting on the large-scale shaft (includes boundary effects of test chamber), a maximum grout pressure of 600 psi was conservatively taken as the expected maximum horizontal stress (Figure 3-59). Comparing the Mohr circles at failure (compressive strength) and the expected stress state during the side grouting phase, it was believed that the concrete strength after three days of hydration was sufficient to prevent concrete distress during the side grouting phase.

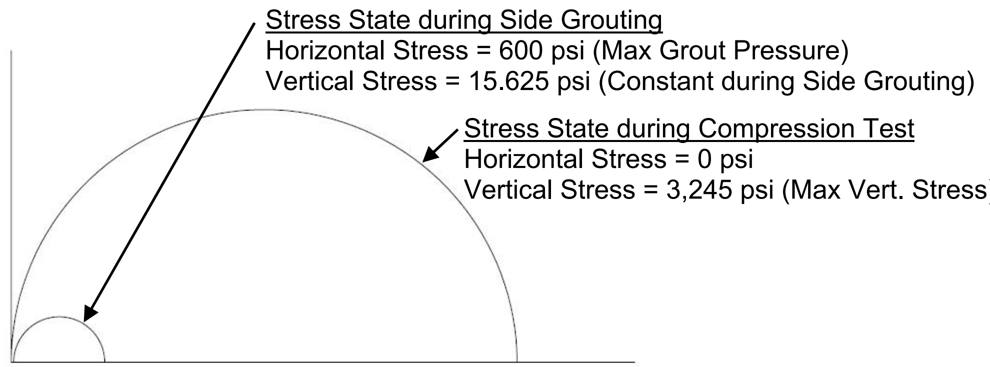

Figure 3-59: Comparing concrete stress state at failure

The side grouting of the shaft began Tuesday, March 12th, 2013 (four days after shaft construction). Side grouting initiated with AFT's grout pump by pumping 425 gallons of grout through two of the four orthogonal dead end side-manchettes (Figure 3-60 on the next page). Grout was pumped at two gallons per minute (gpm) (i.e., low pressure setting) with a linear increase with grout pressure vs. volume for one and a half hours, but before side grout was completed, the grout flow became erratic (i.e., little to no flow rate with alternating high pressure to low or no pressure during consecutive pump strokes). Discussions with AFT personnel suggested the pump's ball valve was not operating properly (i.e., not sealing). Grouting was stopped and the pump's valve was dissembled and cleaned. Subsequently, the pumping was reinitiated with the high pressure setting on the pump (exceeding 650 psi with a higher flow rate of four gpm), but the grout pressure dropped from 600 psi (above cylindrical cavity limit pressure) to 300 psi with an additional 100 gallons of grout pumped. With concern of membrane damage from observed pressure drop, it was decided to stop pumping and look for leaks (i.e., grout flow to the soil surface or through other grout pipes). Inspection of top of shaft showed no fluid grout exiting the ground surface nor was any grout evident in the open grout pipes not being used (side and tip). Given the late time, it was decided to continue grouting the next day. Since AFT wasn't available shortly after, grouting continued on Thursday, March 14th, 2013 (six days after shaft construction) using UF's grout pump and rented concrete/grout mixer (Figure 3-60 - right). Grout was then pumped through the other two of the four orthogonal dead end side-manchettes and finally through the original side-manchette (continuous loop).

Figure 3-60: Side grouting using AFT's grout pump (left) and UF's grout pump (right)

Grout was pumped at approximately two gpm for approximately one hour, with 85 gallons being pumped. The observed pressure increased from AFT's recorded last values as grout volume increased. Next, the grout lines were detached and subsequently attached to the last set of side grout lines (original side-manchette). An additional 105 gallons was pumped (total grout volume 615 gallons) with increasing pressure when side grouting was stopped (> 90% theoretical volume).

Tip grouting was scheduled to be completed seven days after the side grouting phase (10 days after shaft construction), if side grout strength was sufficient to transfer shear from shaft to the surrounding soil (i.e., sufficient grout bond/shear strength between the side grout bulb and shaft). The average unconfined compressive strength (ASTM C-39) of the grout after seven days of hydration was 5,099 psi. Given the seven day unconfined compressive strength of the grout (f_c'), the shear resistance or bond strength between the concrete and side grout bulb was estimated using equation 3.2:

$$Shear\ Strength, \tau = 2\ x \sqrt{f_c'} \tag{3.2}$$

The resulting seven day shear strength of the grout was 142.8 psi. Assuming a conservative bond area between the concrete and side grout bulb (i.e., bulb height of 8.5 feet), the mobilized shear resistance along the side grot bulb is about 1,921 kip. Using a maximum tip grout pressure of 600 psi (observed during tip grouting of long shaft in the test chamber) and base area of 8.7 square feet (base plate diameter equal to 40 inches), the maximum force exerted on the tip is 754 kip for a factor of safety of 2.5.

With adequate bond/shear strength between the side grout bulb and shaft, tip grouting began seven days after the side grouting, i.e., Thursday, March 21st, 2013 (14 days after shaft construction). Tip grouting was completed using AFT's grout and pumping through both tip-manchettes (both loops). Grout was pump through one tip-manchette first, grouting stopping and grout pump cleaned out, and the remaining grout was pumped through the other tip-manchette until upward vertical movement of the top of the shaft exceed allowable movement (0.3"). The latter movement was used to obtain a conservative estimate of mobilized side friction, i.e., only alongside the membrane but not including bearing resistance at the top of the side grouted zone.

3.1.4 Static Load Test

The load cell and readout boxes were tested prior to performing the top-down test to ensure the load was being applied and measured accurately (Figure 3-61). The load cell and readout boxes were tested at the SMO using their testing machine (SATEC Instron). The Instron can test a specimen in tension or compression and is capable of exerting 800 kip (400 ton) of compressive force.

Figure 3-61: Checking load cell and readout boxes at SMO

The two readout boxes were calibrated previously for use on another project (FDOT BDK75-977-41), so this test was to confirm proper calibration. Looking at Figure 3-62, readout box one displays the load in ton and has a working range between zero and 750 kip, and readout box two displays the load in kip and has a working range between zero and 999 kip (display limited to three digit numbers). Neither readout box had been calibrated up to the range of 800 kip due to prior capability of machine used to check load cell (500 kip max load at UF campus) and maximum load during a previous top-down test (375 kip max load).

Figure 3-62: Readout box one (right) and readout box two (left)

During the test at SMO, the load cell was loaded and unloaded incrementally in 200 kip increments up to 800 kip. The results of the load cell test are shown in Figures 3-63 and 3-64 on the next page. The applied load (value recorded from Instron display) and readout box values were recorded at the same time interval (± one second). The load cell and both readout boxes provide an accurate measurement of the applied load (i.e., < 1% error during loading and ≤ 2% error during unloading). The error during unloading was due to the load cell rebound time and not the readout boxes. As the load cell was loaded in compression, the load cell flexes and deforms developing hysteresis with the change in loading direction (i.e., compression to tension). The hysteresis results in slight difference in calibration based on direction of loading. However, the measured error during the unloading phase was still acceptable for this application (i.e., ≤ 2% error during unloading) which was less than typical error with strain gauges (i.e., 2% of full range ~ 1,000 ton).

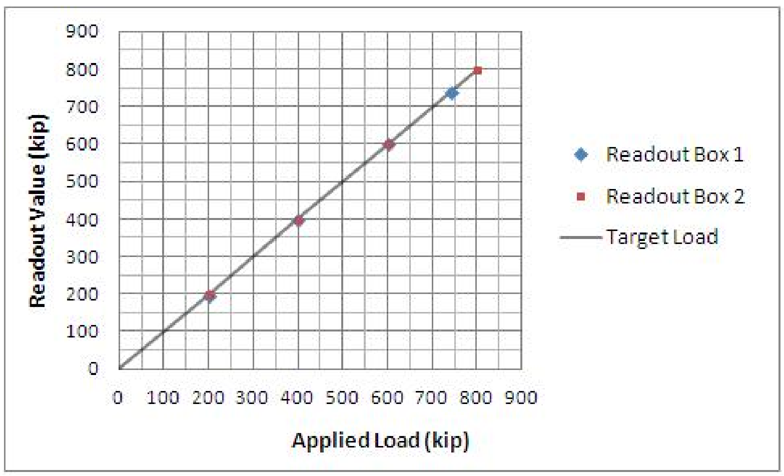

Figure 3-63: Load cell test results during loading phase

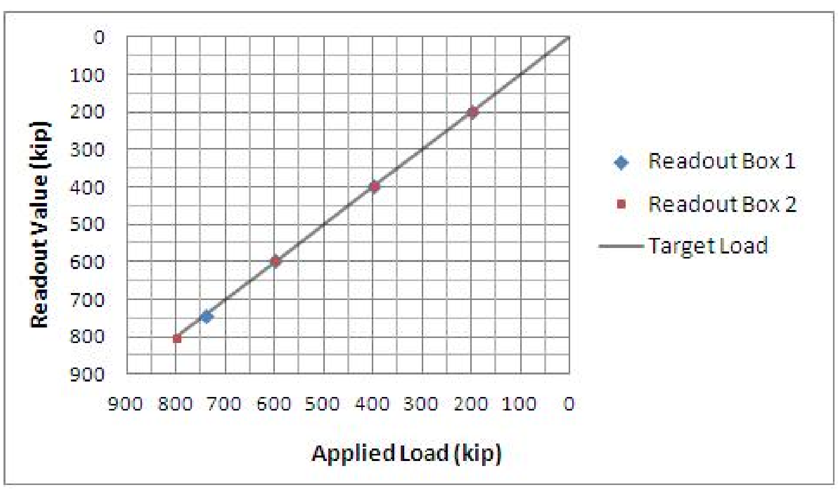

Figure 3-64: Load cell test results during unloading phase

The reaction system and load transfer can be seen in (Figure 3-65). Two steel girders (reaction beams) were used to transfer the load generated by the hydraulic jack to the reaction shafts through Dywidag bars. Using a crane, the reaction system was disassembled from another test shaft location (FDOT BDK75-977-41) and moved to the side-and-tip-grouted drilled shaft.

Figure 3-65: Field reaction system used for static load test

Next a wooden frame (Figure 3-66 on the next page) was setup to secure digital dial gauges (i.e., rigid structure to attach the dial gauges). Also used on the other project (BDK75-977-41), the wooded frame was built such that the frame was independent from the reaction system and sits on the ground a minimum of five diameters away from the test shaft (ASTM D1143). Secured to the wooden frame, steel square tubing was used to attach the digital dial gauges used to monitor the shaft displacement (Figure 3-67 on the next page). Similarly, digital dial gauges were used to monitor reaction shaft displacements (Figure 3-67 on the next page) and were independent of the reaction system and wooden frame.

Figure 3-66: Wooden frame used to support digital dial gauges

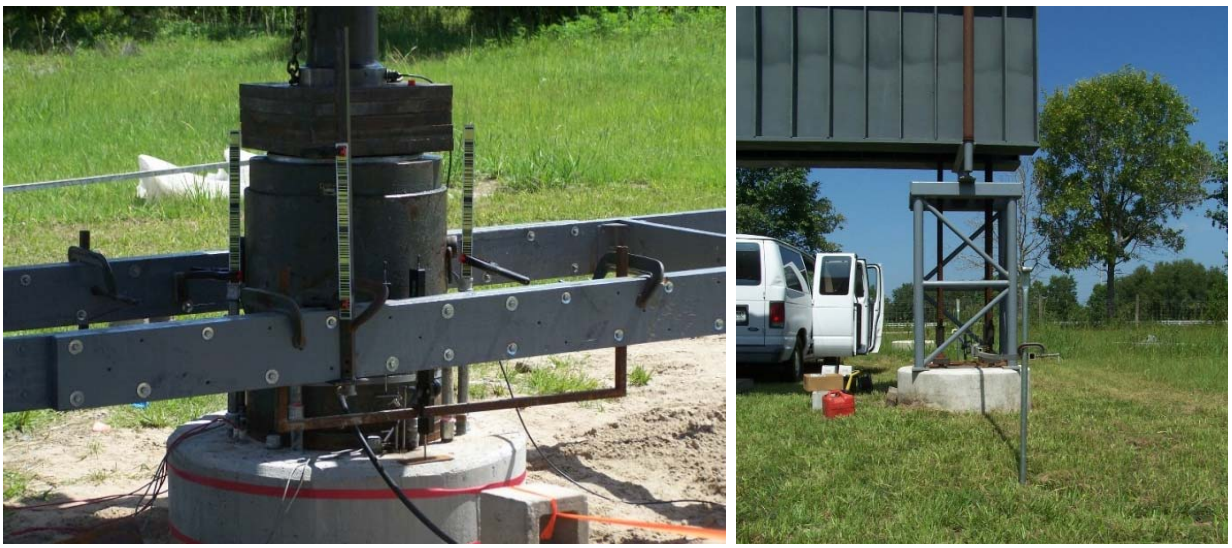

Figure 3-67: Digital dial gauge setup during static load test (left - grouted shaft; right - reaction shaft)

Four digital dial gauges and three digital levels were used to monitor displacements during axial loading (i.e., displacement of test shaft, displacement of reaction shafts, and displacement of the wooden frame used to support the digital dial gauges). Two dial gauges were used to monitor the top of the test shaft, and one dial gauge was used on each reaction shaft (center of shaft; Figure 3-67 above). The digital dial gauge readings were taken manually after each load increment, two minutes after the load step and two minutes before the next load increment. The three digital levels were connected to a single data collection system with readings collected in 15-second interval. Two digital levels were used to monitor the displacement of the top of the test shaft, and one digital level was used to monitor the displacement of the wooden frame (e.g., thermal expansion or contraction of wood; Figure 3-68). Monitoring the movement of the wooden frame was important to accurately interpret the dial gauge readings. The digital dial gauges were set up outside the zone of the loaded shaft (10 D). The digital level readings of the wooden frame were used to correct the dial gauge readings and compared with digital level readings of the shaft.

Figure 3-68: Digital levels used to monitor shaft and wooden frame displacements

Embedded strain gauge readings were collected throughout the top-down test as well. The embedded strain gauges were located above and below the side grouted zone, so the mobilized side resistance above and along the side grouted zone could be obtained along with the tip resistance. Strain gauge readings were collected in 30-second intervals along with reading from the push-in pressure cells.

After setting up the instruments, the top-down axial load test was conducted with UF personnel to measure the load displacement behavior and axial capacity of the side-and-tip-grouted drilled shaft (field shaft). The shaft was loaded in increments which were sustained for approximately 10 minutes (i.e., quick static load test). The shaft was loaded initially to 25 kip (held for 10 min), increased to 50 kip (held for 10 min), and loaded in 50 kip increments thereafter. At the last load increment (total load of 850 kip), the south reaction shaft underwent 0.25" upward movement (total movement 0.576"), so the loading phase was stopped. During the unloading phase, the shaft was unloaded in 200 kip decrements with the final unloading decrement of 50 kip (held for 10 min), and then, the shaft was unloaded to zero with additional set of readings taken after 10 minutes.

3.1.5 Statnamic Load Test

The statnamic load test was not originally part of the project; however, the static load test moved the shaft only 0.18" at 850 kip static axial load. Since the FDOT was interested in assessing the capacity of the shaft, additional supplement was provided to conduct a Statnamic load test. Since four of the embedded strain gauges were vibrating wire resistance type, additional instrumentation was also needed (i.e., vibrating strain cannot capture internal load during Statnamic loading). The gauges ordered were 350 ohm resistance embedded strain gauges (five total) and a five volt accelerometer with a working range of ± 50 time gravity. Note, the resistance strain gauges are required to collect continuous strain data (e.g., 1,000 readings per second) and the accelerometer was required to calculate the inertial and damping forces generated during Statnamic loading.

The Statnamic test along with the data collection was to be performed by AFT. Therefore, the instrumentation was ordered and shipped to AFT for further preparations, i.e., additional cabling, water proofing, and so on. To minimize fabrication costs, additional cable was spliced by AFT rather than by the manufacture. The accelerometer needed to be contained/housed for placement within grout (i.e., made water proof), so the gauge was embedded in a water proof media by AFT.

Since, the instrumentation was not originally installed (i.e., attached to rebar cage before shaft construction), two holes were drilled along the length of the shaft for placement of instrumentation, which would be subsequently grouted. The holes were drilled by SMO personnel using a SPT rig and can be seen in Figure 3-69 on the next page. The two holes were evenly spaced along the diameter of the shaft (i.e., 14 inch spacing) using a two inch core barrel. The final diameter of the holes were three inches, and both holes were drilled to an approximate depth of 25 feet four inches (nine inches above the steel base plate at the tip of shaft). Both holes were thoroughly flushed with water to remove cutting debris, and the remaining water was pumped out using the SPT rig before placing instrumentation and grout.

Figure 3-69: Drilled holes for additional instrumentation (strain and accelerometer)

During drilling, concrete cores were recovered along the length of the shaft (approximately two inches by five feet) and shown in Figure 3-70. Six cores samples were tested (three form each hole) at the SMO facility. The cores were tested in compression to estimate the unconfined compressive strength of the concrete for the Statnamic load test (Figure 3-71 on the next page). The cores samples tested were recovered from depths corresponding the proposed strain gauge locations (i.e., top of shaft, above side grouted zone, and tip of shaft), and the average unconfined compressive strength of the six core samples tested was 7,089 psi.

Figure 3-70: Recovered cores from field shaft

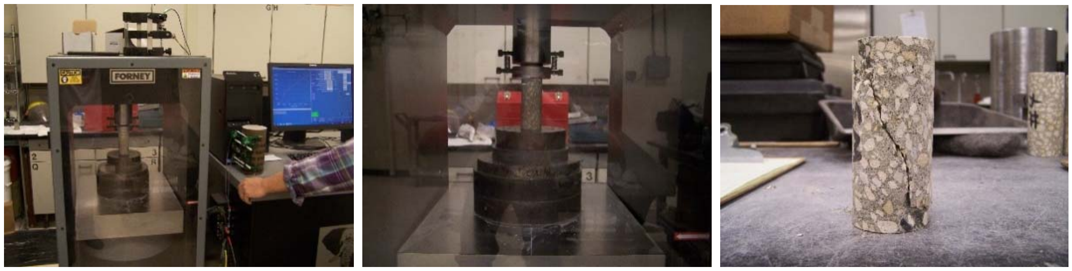

Figure 3-71: Unconfined compression test on recovered core sample

A frame (rigid structure) was needed to orient (vertical and center) the gauges within the drilled holes prior to grouting. Also, the grout needed to be placed from the bottom up (i.e., placed with tremie) to displace any water within the holes and minimize any air voids during grout placement. Because of the limited space in the hole, it was decided to fabricate a ridged tremie in which the instrumentation could be attached. To ensure the section properties (i.e., shaft cross-section) were unchanged after the installation of the instruments, PVC pipe were used as the tremie and frame (vs. steel pipe). An initial PVC tremie/frame can be seen in Figure 3-72 on the next page. Because of the limited space within the holes, three quarter inch PVC pipes were used to fabricate the tremie/frame. To keep the PVC pipe aligned vertically and orient the gauges along the shaft, rings were cut from two and a half inch PVC pipe (i.e., OD less than the hole diameter and ID greater than the OD of tremie/frame pipe). The rings were secured to the tremie/frame using zip-ties, and the strain gauges were then secured to the rings using zip-ties. The PVC rings also help keep the PVC pipe aligned vertically within the hole.

Figure 3-72: Initial tremie/frame

Since the tremie must act as a frame in which the gauges were secured, the tremie could not be pulled up as the level of grout rises within the hole (typical tremie process). Therefore, an investigation was done to determine the flowability of the grout during installation (i.e., confirm that the grout will flow down the tremie/frame, exit the bottom of the tremie/frame, and fill the drilled holes from the bottom-up). The investigation was done using the FDOT/UF test chamber at the coastal lab (Figure 3-73 on the next page). To simulate the drilled holes in the field (holes drilled in shaft), a steel pipe was used which was two inches by 26 feet (i.e., previously fabricated tremie pipe used to place concrete during construction of the long test shaft). A large container was suspended from the top of the test chamber to catch any grout. The steel pipe was capped at the bottom, suspended from the top of the test chamber, and rested on the bottom of the container (to catch any grout). To simulate potential flow restrictions caused by the PVC rings and attached strain gauges, PVC rings were cut from one and a half inch PVC pipe (OD less than steel pipe diameter and ID greater than the OD of tremie/frame pipe) and aluminum blocks (anomalies) were used to simulate obstruction cause by the strain gauges (Figure 3-72 on the previous page). At the bottom of the PVC pipe, vertical slits were cut to allow unrestricted flow as the grout exits the tremie (Figure 3-72 on the previous page). The three quarter inch PVC pipe (tremie/frame) with rings and anomalies attached was then lowered into the two inch steel pipe (hole), and the steel pipe was filled with water (Figure 3-74).

Figure 3-73: Suspend pipe from edge of test chamber with catch container below bottom of pipe

Figure 3-74: Fill pipe with water before placing grout

Two small batches of non-shrink grout were mixed using five gallon buckets with a hand drill and a mixing bit (Figure 3-75 - left). Grout was placed through a funnel at the top of the tremie/frame pipe (i.e., gravity driven grout flow; Figure 3-75 - right). Once the grout level in the steel pipe (hole) reached about 17 feet (nine feet from top of the hole/funnel), the grout flow stopped. This suggests that the grout will not flow and fill the drilled holes in the field shaft unless the funnel elevation above the shaft is greater than nine feet. Because of the results of this investigation, it was decided to use a pump (rather than gravity) to generate the pressure needed to ensure grout flow that would completely fill the holes during installation. Various pump options were considered such as buying a used hand grout pump, renting a hand grout pump, or modifying the UF grout pump for use as a manual pump. Fortunately, AFT was able provide grout services to install instrumentation and place grout caps at the top of the drilled shaft.

Figure 3-75: Small batches of non-shrink grout (left) and gravity-driven grout flow through tremie/frame (right)

In the field (gauge installation), the embedded strain gauges were secured to the PVC pipe (tremie/frame) using two and a half inch PVC rings and zip-ties (Figure 3-76 - left). Three PVC pipes (three-quarter inch by 10 feet long) were used to fabricate each tremie/frame (two total). The PVC pipes were connected in three sections. The bottom section was cut to seven feet, so the second gauge (above the side membrane) would not be secured where the two PVC pipes connect (i.e., PVC union that connects two pipes may misalign the strain gauge or effect the concrete cover around the gauge). The middle and top sections were full length sections (10 feet), with the top section cut off at the top once fully lowered in each hole (Figure 3-76 - right).


Figure 3-76: Final tremie/frame with instruments attached (left) and tremie/frame with instrumentation attached fully lowered in holes before grouting (right)

The top sections were cut off twice; first for placing the grout (left above the top of shaft), and again for the grout cap (cut flush with top of shaft). The accelerometer and two strain gauges (locate at tip and top of shaft) were placed in the west hole, and the other three strain gauges (locate at tip, above side membrane, and top of shaft) were placed in the east hole. This evenly divided the number gauges wires exiting each hole and minimized resistance to grout flow within the holes due to the gauges and wires. To further minimize the resistance due to the gauge wires, the wires were taped to the PVC pipe. The strain gauges were located below the side membrane (two gauges), above the side membrane (one gauge), at the top of shaft (two gauges), and the accelerometer was located below the side membrane (tip). The strain gauges below the side membrane (tip) were approximately 24 feet below the soil surface (one foot above steel base plate), the strain gauge above the side membrane was 15 feet below the soil surface, and the top strain gauges were 16 inches below the top of shaft (approximately even with soil surface).

AFT provided grouting services for instrument installation and placement of grout cap over the shaft (needed for Statnamic test). The grout used for gauge installation and cap was a non-shrink grout (Sikagrout 212), with a mix ratio of 1.2 gallons of water per 50 pound bag of cement (w/c ≈ 0.2). Using a small grout pump (Figure 3-77 on the next page), the grout was mixed and pumped down each tremie to completely fill both holes. Form work was then placed around the top of the drilled shaft, the PVC pipes (tremie/frame) were cut flush with the top of shaft, and the grout cap was poured on top of the shaft (Figure 3-77 on the next page). The grout around the instrumentation (embedded strain gauges and accelerometer) and grout caps was allowed to hydrate for two weeks before Statnamic testing was performed.

Figure 3-77: Small grout pump used to grout instruments and place grout for cap (left) and grout cap (right)

Based on tip grouting and in situ data, the axial capacity of the side-and-tip-grouted drilled shaft was estimated to exceed 1,600 kip. After discussions with FDOT, and AFT, a 2,000 kip Statnamic test was selected. The Statnamic test began with the setup of the catch frame (Figure 3-78), concrete dead weights (Figure 3-78 - right), and top instrumentation (dynamic load cell and accelerometers). Subsequently, all the instrumentation (load cells, strain gages, and accelerometers) were connected to a national instruments data acquisition system with a sampling rate of 5,000 samples per second.

Figure 3-78: Statnamic system (crane, catch frame, and dead weights)

Nine pounds of propellant was placed within the reaction chamber, and the test was performed (0.5 sec duration; Figure 3-79). A total Statnamic force of 2,550 kip and peak vertical displacement of 1.5" was recorded during the test. Discussion and analysis of the construction and load tests (static and Statnamic) are presented in section 4.3.

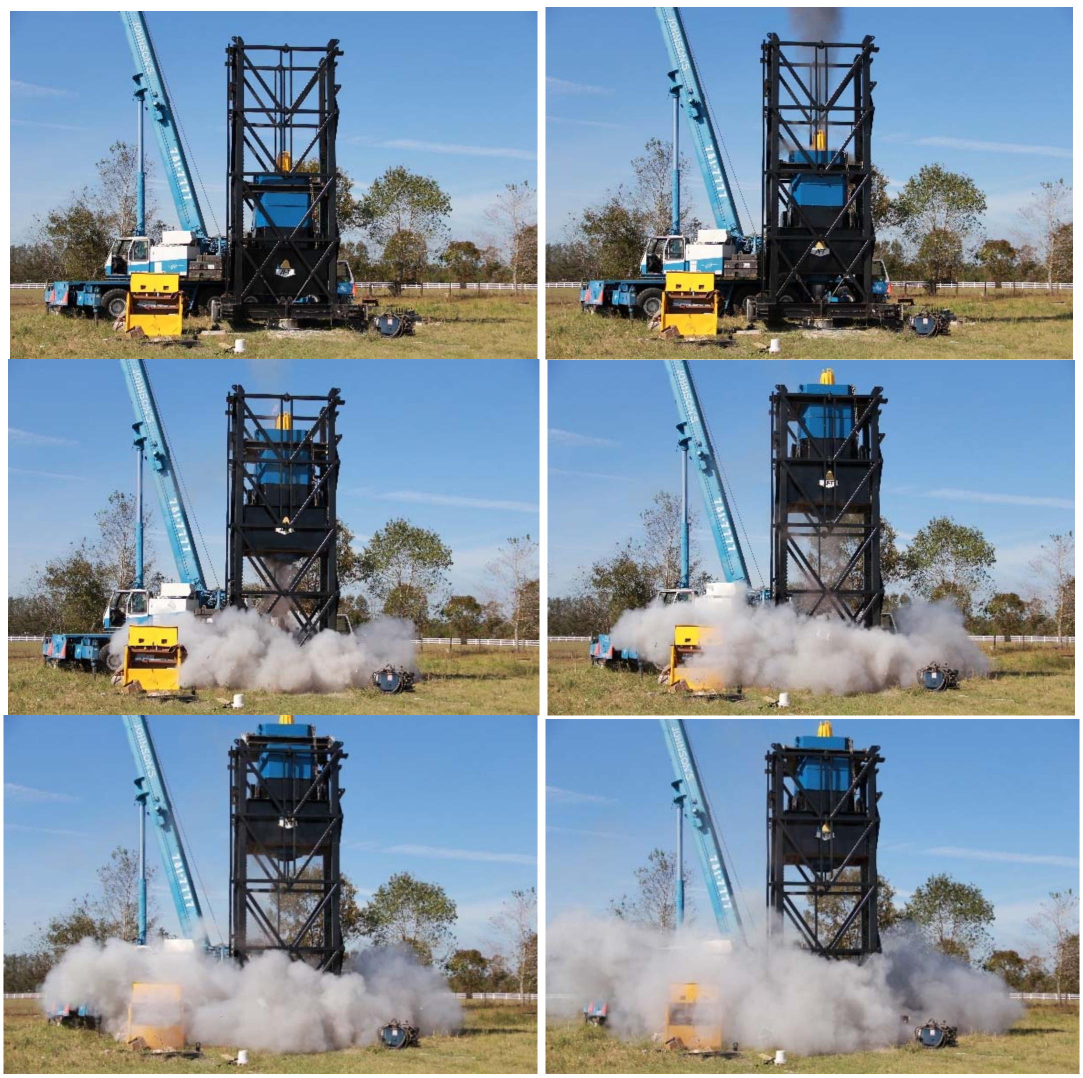

Figure 3-79: Performing the Statnamic test

CHAPTER 4
OBSERVED AND MEASURED RESPONSE OF SIDE-AND-TIP-GROUTED SHAFTS

Presented is the measured grout pressures, soil stresses, and shaft displacements during side and tip grouting; in addition, the measured load transfer (side and tip) during load tests (static and Statnamic) of the large-scale test shafts (long and field). Observed side and tip grout bulb from the test chamber shafts (short and long) are also presented. Estimation of side and tip resistance for grouted drilled shafts will be presented in Chapter 5 along with soil characterization (laboratory and in situ data).

4.1 Short Shaft (36" x 6')

4.1.1 Shaft Construction and Membrane Seal Grouting

The membrane seal prevented nearly all of the concrete from flowing to the outside of the membrane during construction of the short test shaft (i.e., concrete placement during shaft construction). This was shown by the negligible amount of concrete on the outside of the side membrane, which is distinguished by concrete aggregate (Figure 4-1 on the next page).

Although the membrane seal prevented concrete from flowing outside of the membrane, the seal was not air tight and air leaked during concrete placement, i.e., shaft construction (recall air bubbles shown in Figure 2-19). The entrained air caused by the leaking membrane seal creates voids within the concrete, reducing the overall shaft quality. However, those void within the membrane zone may have been subsequently filled during side grouting.

Figure 4-1: Short test shaft being removed from test chamber (tip grout bulb not shown)

During grouting of the seal, grout pressure increased with volume of grout pumped into the seal. At 60 psi of pressure and 12.25 gallons of grout, the pressure jumped (80 psi) and the grouting was stopped to prevent seal failure (70% max volume). After grouting stopped, the grout pressure remained constant initially and then decreased over time. Note, since the grout is incompressible, any change in volume (e.g., soil creep), a drop in pressure is expected. Also, if the maximum volume of the seal was reached but grout pressure did not increase or spike, this would suggest that the seal had a leak, and if the pressure spikes and then dropped significantly, this would suggest that the seal had ruptured/failed.

4.1.2 Side Grouting

The grout pressure increased while pumping the first 15 gallons of grout (Figure 4-2), and then, the pressures remained constant (100 psi) while grout volume increased. Observed peak pressures were110 psi with lows of 75 psi, and grouting stopped when the final volume reached 100 gallons (80% of theoretical volume). Based on initial soil stresses, the steady state grout pressure of 100 psi compared favorably with the cylindrical cavity expansion limit pressure of 94 psi (Salgado and Randolph, 2001; Figure 1-5).

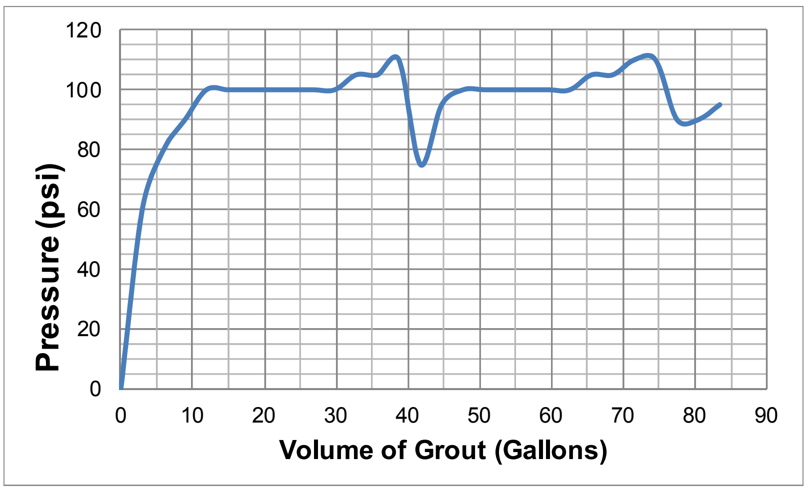

Figure 4-2: Grout volume vs. grout pressure during side grouting of short shaft

Figure 4-3: Ground surface during side grouting of short shaft

No grout flow to the ground surface was observed during side grouting, Figure 4-3 above; however, upward movement (0.3") of the shaft was observed. This movement was attributed to the hydrostatic (i.e., equal all around) grout pressure acting inside the membrane and on the membrane seal during the side grouting phase (Figure 4-4). The horizontal component (i.e., lateral stress) of the fluid grout was resisted by movement outward thus increased the lateral soil stresses. The vertical upward component was carried by the soil above the membrane (bearing) but mostly by the grouted seal (rigid boundary) and side membrane (impermeable), both of which were attached to the shaft; therefore, the vertical upward component transferred the load to the shaft and vertical upward movement was observed. Note, no grout was evident in the tip grout pipe during side grouting, which suggested grout did not flow beneath the shaft.

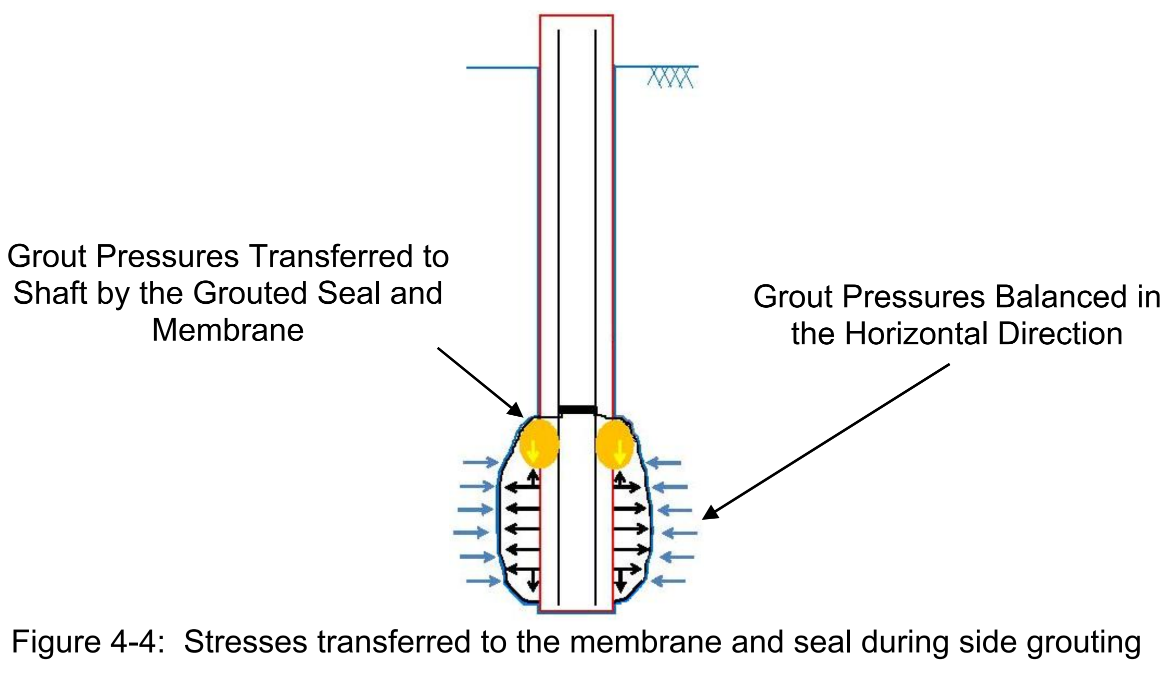

Figure 4-4: Stresses transferred to the membrane and seal during side grouting

Visual inspection of the exhumed shaft, shown in Figure 4-1, suggested that cylindrical cavity expansion was achieved. That is during side grouting, the side membrane expanded outward to a final diameter of four-and-a-half feet (i.e., 1 ½ D) with negligible grout flow above the membrane seal. The vertical pleats were only visible at the top and bottom of the membrane (secured by steel rings). The horizontal pleat was still visible but was reduced considerably as the side membrane expanded outward with grout flow. Note, the pleats allowed the membrane to expand outwards without developing excessive tensile stresses within the side membrane.

4.1.3 Tip Grouting

Grout pressures increased throughout the tip grouting process as the volume of grout pumped to the tip increased (Figure 4-5). The maximum recorded pressure was 105 psi, and the final volume of grout pumped was 52 gallons. After pumping six gallons of grout (grout pressure of 42 psi), the shaft started to move vertically upwards (Figure 4-6 on the next page). Grouting stopped because of large observed upward shaft displacement (average 0.65").

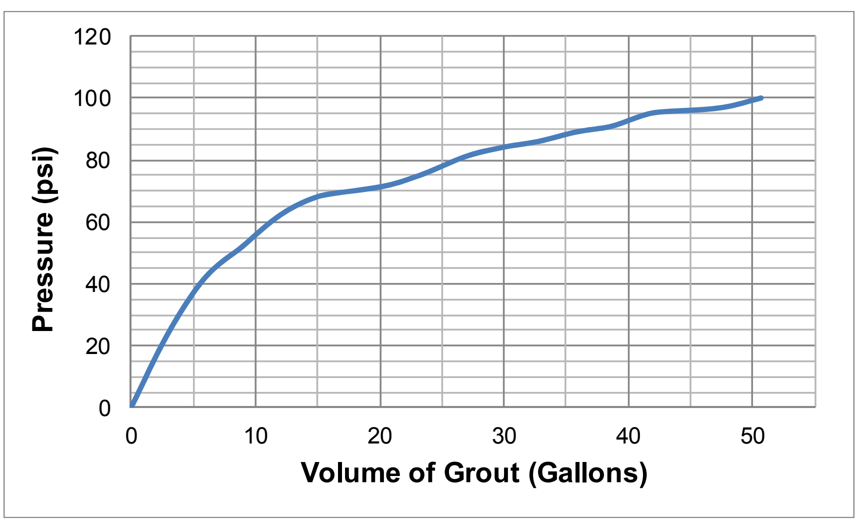

Figure 4-5: Grout volume vs. grout pressure during tip grouting of short shaft

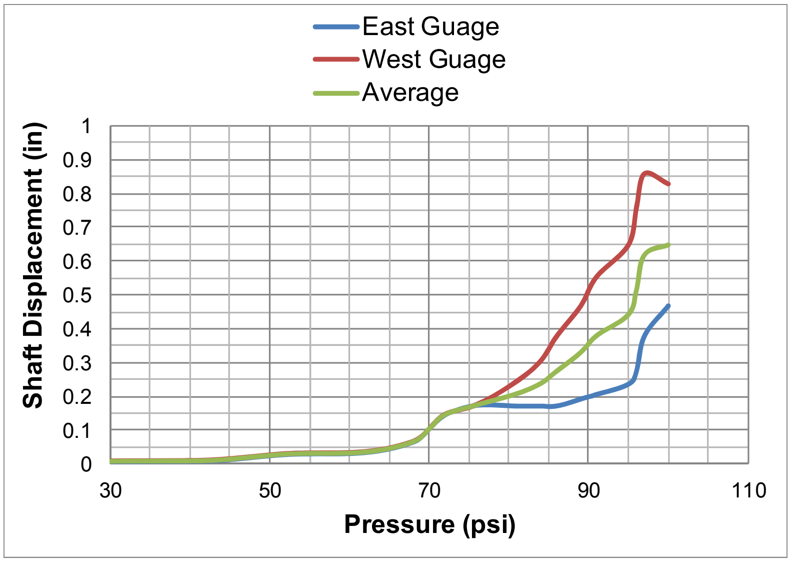

Figure 4-6: Short shaft displacement during tip grouting of short shaft

Excavation of the shaft revealed that there was little to no upward flow of the grout during the tip grouting phase (Figures 4-1 and 4-7 below). Visual inspection of the grouted shaft shows the grout remained below the shaft tip during the tip grouting phase, and there was a clear boundary between the grout bulb and shaft tip (concrete placed during shaft construction). Note, shafts that were tip grouted only showed that the flow of grout was predominantly up along the soil-shaft interface (McVay and Thiyyakkandi, 2010; Mullins et al., 2006). In addition, Figure 4-7 shows a semi-symmetrical shape and smooth surface of the tip grout bulb, suggesting progression toward spherical cavity expansion. Salgado and Randolph (2001) suggested a spherical cavity expansion pressure of 155 psi, which wasn't achieved here due to the limited vertical resistance. Because side resistance is a function of confining stresses and the shaft embedment was shallow, little confining stress and thus side resistance was available to resist the vertical movements during tip grouting.

Evident from Figure 4-7 (exhumed shaft), there was poor surface contact between the tip of the shaft and the tip grout bulb. As grout was being pumped and expanding below the tip (single open grout pipe), a layer of soil was trapped between the tip of the shaft and the grout bulb and prevented bonding and uniform contact between the shaft and grout bulb. Consequently, the tip grout bulb did not remain attached to the shaft while being removed from the test chamber (Figure 4-8).

Figure 4-7: Tip grout bulb on short test shaft

Figure 4-8: Poor contact between the tip grout bulb (left two photos) and bottom of shaft (right photo)

4.2 Long Shaft (36" x 25')

4.2.1 Shaft Construction and Membrane Seal Grouting

Only the top membrane seal was inflated/pressurized during shaft construction (i.e., concrete placement). Evident from visual examination of the excavated shaft (Figure 4-9), the top membrane seal prevented the concrete from flowing to the outside of the side membrane. Also, the top seal maintained air pressure throughout the shaft construction and no air bubbles were observed at the concrete surface, which suggested that the top seal was airtight (validated by maintaining pressure without additional air flow).

Figure 4-9: Top of side membrane/side grouted zone (location of top membrane seal)

There were two membrane seals within the long shaft (top and bottom), and the bottom seal was grouted first. As grouting began, the pressure initially spiked to over 150 psi during the first strokes (Table 4-1 on the next page), but then, the grout pressure dropped as more grout was pumped. The grout pressure increased again to a maximum hold pressure of 80 psi (17.5 gallons). The top seal was subsequently grouted after the bottom seal. Since the top seal had two ports (front and back ends), one port was left open (back end) to allow air to escape while the PVC grouting system was filled through the front end (zero hold pressure at the end of pump stroke). Then, the back end was closed to allow pressures to grow. The volume of grout pumped into the top seal was 18.1 gallons (87% max volume), and the maximum hold pressure at the end was 80 psi.

Table 4-1: Grout pressures during seal grouting on long shaft

Membrane Seal	Pump Stroke #	Volume during Stroke (gal)	Max Pressure during Stroke (psi)	Hold Pressure after Stroke (psi)	Cumulative Volume (gal)
Bottom Seal	1	3.5	150	75	3.5
	2	3.5	190	50	7
	3	3.5	50	20	10.5
	4	3.5	170	140	14
	5	3.5	220	150	**17.5**
Top Seal	1	3.5	0	0	3.5
	2	3.5	20	0	7
	3	3.5	20	0	10.5
	4	3.5	18	0	14
	5	3.5	100	80	17.5
	6 (Partial)	0.6	110	90	**18.1**

Since the estimated grout volume was approached with no loss in pressure and grout is incompressible, this was a good indication that both seals expanded as predicted (similarly to test performed in trench having both inner and outer boundary conditions). Both seals held a final grout pressure of 80 psi for over 30 minutes, which suggested neither seal had failed. If either seal had failed (e.g., separated at the joint), there would have been no hold pressure after grouting stopped. The pressure spike observed when initial grouting the bottom seal was likely due to partial embedment of seal in the concrete. Note, the bottom seal was not inflated with air during shaft construction; therefore, there was likely a greater amount of concrete cover on the bottom seal, which caused the spike until sufficient pressure spalled the concrete off the seal. This was further validated by inspection of the bottom of the membrane, which revealed pieces of concrete that penetrated the side membrane as shown in Figure 4-10. The latter suggests that both top and bottom membrane seals should be inflated during shaft construction.

Figure 4-10: Side membrane pierced by concrete between seal and side membrane as the bottom membrane seal expanded outwards during seal grouting

The soil stresses were monitored during all phases of shaft construction and grouting. Unfortunately, there were no pressure cells in proximity of the top membrane seal, so the change in stress around top seal could not be observed. However, there were two pressure cells (#7 and #8) near the bottom seal, so the change in horizontal stress around bottom seal during grouting can be seen in Figure 4-11 on the next page.

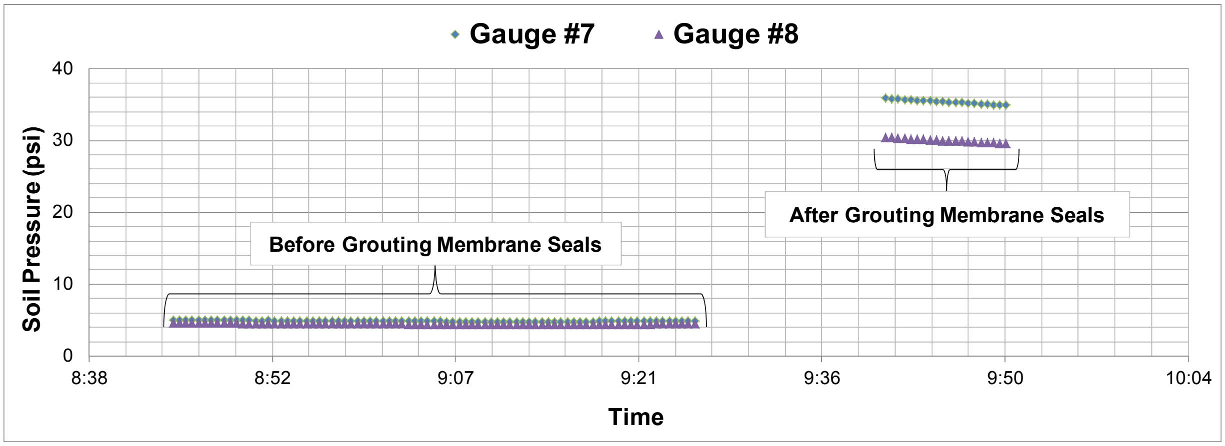

Figure 4-11: Change in horizontal stress around the bottom seal during grouting of long shaft membrane seals

The horizontal stress increased from 4.4 psi to between 30 psi and 35 psi (gauges #7 and #8 respectively). Evident, the stress increase suggest that the membrane (seal underneath) moved out into the soil, i.e., separating the membrane from the shaft. Also, the membrane seals when hydrated creates a rigid upper and lower boundary constraint (e.g., anchor). Subsequently when grouting the side membrane (i.e., next day or later), the seals and membrane will limit the upward and downward flow of the grout, so grout is encouraged to flow radially or horizontally outwards, thus supporting cylindrical cavity expansion.

4.2.2 Side Grouting

Grout pressures increased throughout the side grouting process as the total volume of grout increased (Figure 4-12 on the next page). Grout was pumped to the theoretical volume of 1 ½ D (595 gal) or excessive vertical displacement of the shaft occurred (> 0.2% of D to avoid fully mobilizing side resistance). At grout volume of 425 gallons (71% max volume) with maximum observed pressure of 600 psi, grouting stopped due to the shaft's upward vertical movement of 0.74". For the given overburden stresses (center of bag), cylindrical cavity expansion limit pressure was 261 psi (Salgado and Randolph, 2001). The difference between the measured and theoretical pressure was believed to be caused by the wall of the test chamber. That is, the rigid (steel) wall of the test chamber limited the lateral movement of the soil, resulting in a significant increase in lateral soil stresses between the membrane and the test chamber wall.

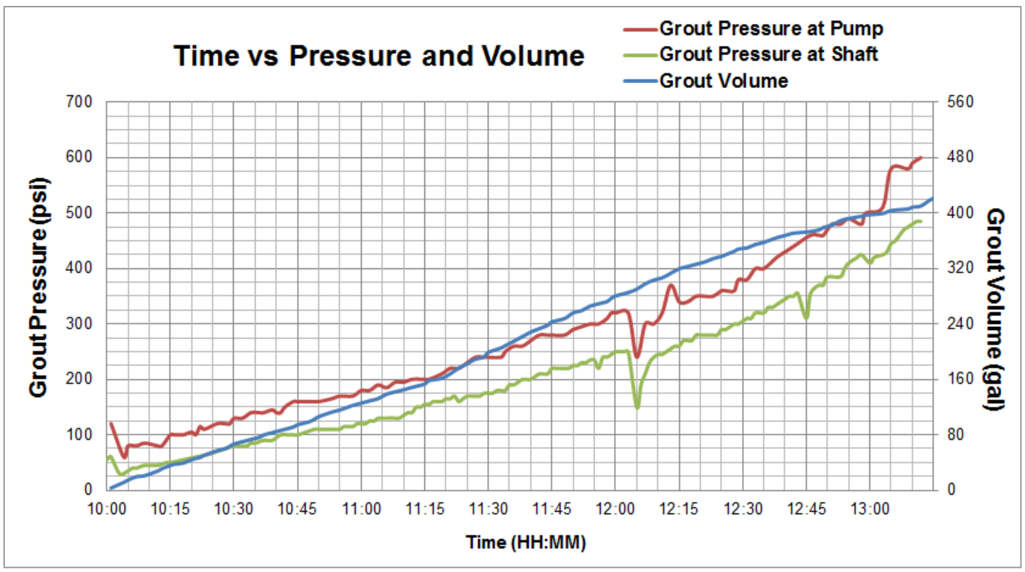

Figure 4-12: Grout pressure and grout volume vs. time during side grouting of long shaft

Side grouting stopped because of the large vertical displacement of the shaft (Figure 4-13 on the next page); however, the soil was also moving upwards. The average shaft and soil displacements at the end of grouting were 0.7389" (shaft), 0.7257" (soil one and a half feet from shaft), and 0.6620" (soil three feet from shaft). The differential displacement between the shaft and soil 3 feet from the shaft was 0.0769" (0.2% D). The upward movement of the soil was likely due to outer boundary (steel wall) of the test chamber, for as the side grout bulb expanded outward, the soil moved vertically because of the limited horizontal space (about four-and-a-half feet between shaft and test chamber wall). Since the vertical constraint was limited (i.e., friction on the wall), both the soil and shaft moved upwards together (note the small differential displacement between shaft and soil). At the end of grouting, the shaft and soil differential displacement was less than 0.1".

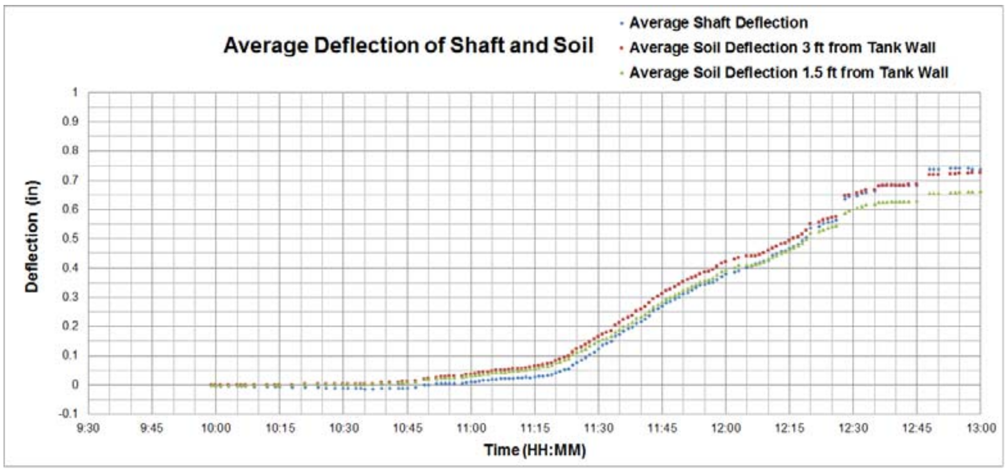

Figure 4-13: Shaft and soil displacements during side grouting of long shaft

Supporting the displacement (soil and shaft) were measured horizontal and vertical soil stresses within the test chamber during side grouting (Figure 4-14 and 4-15 on the next page). The pressure cell working range was 0 to 100 psi, so once stresses exceeded this limit, the gauges would no longer provide readings (gap in data). The gauges closest to the side grouted zone are shown in Figure 4-14 (horizontal stress) and 4-15 (vertical stress). As expected, the rate of horizontal stress increase closest to the side membrane (#15, #16, #17, and #18) was the largest, followed by gauges further away from the side membrane (#9, #10, #11, and #12).

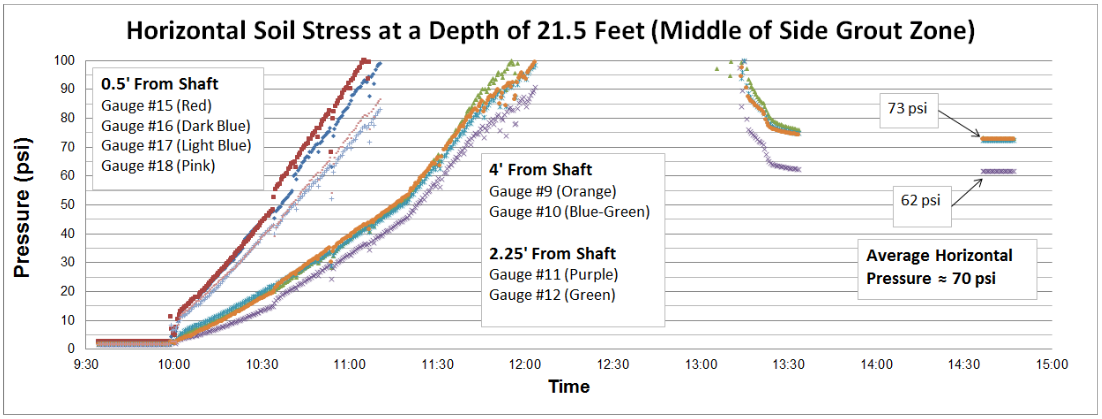

Figure 4-14: Change in horizontal stress near side grouted zone of long shaft

Along with the horizontal stress, a vertical stress increase was observed in the side grouted zone near the membrane (cavity expansion). Also of interest, the average horizontal stress was greater than the vertical stress multiple days after grouting. Even though the gauges closest to the side membrane (#15, #16, #17, and #18) no longer provided data since the stress was greater than 100 psi or damaged during side grouting, the average horizontal stress was greater than 70 psi (gauges #9, #10, #11, and #12) while the observed vertical stress was 67 psi (gauge #13). Note, due to chamber wall affects, the stresses may too high by a factor of two or more.

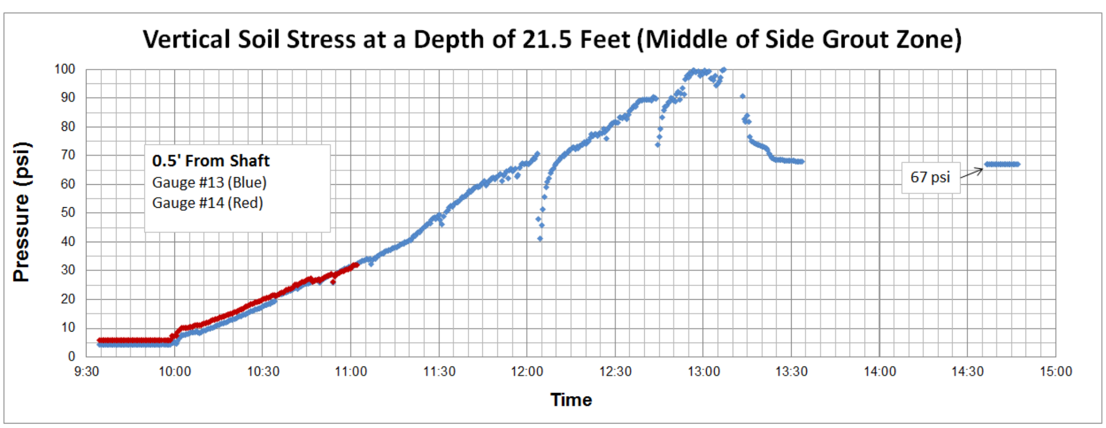

Figure 4-15: Change in vertical stress near side grouted zone of long shaft

The two gauges (horizontal and vertical) above the side grout zone near the shaft showed much smaller stress increases and shown in Figure 4-16. Below the shaft tip (pressure cells #1 through #6), the stresses were larger but less than the stresses around the side grouted zone. Again, the horizontal and vertical stress increase near the shaft during side grouting as shown by Figures 4-14 and 4-15, i.e., was expected to prevent vertical grout flow during subsequent tip grouting.

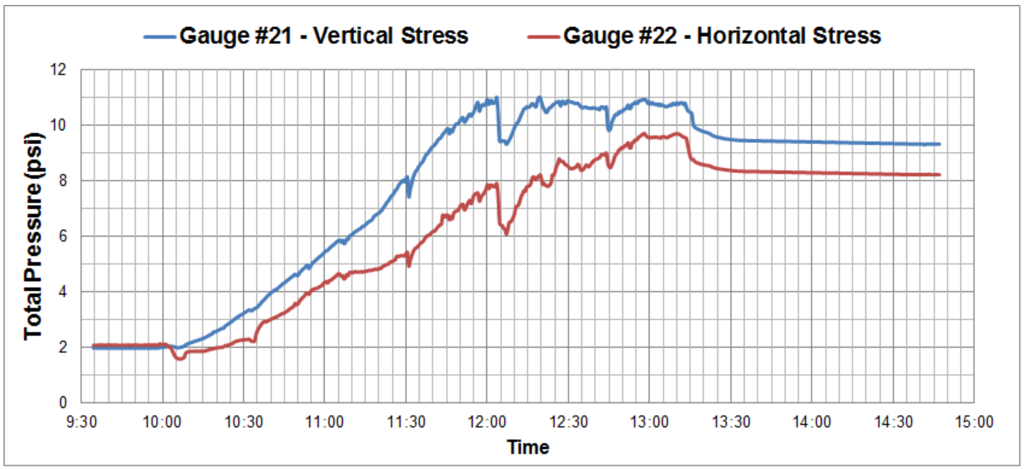

Figure 4-16: Change in vertical and horizontal stress at the top of test chamber during side grouting of long shaft

Visual examination of the side-grouted shaft after excavation shows negligible grout on the outside of the side membrane and a side grout bulb that was cylindrical in shape (Figure 4-17), suggesting that cylindrical cavity expansion during the side grouting did occur. The side grout bulb was larger at the top part of the side grouted zone, so the grout still showed a tendency to flow upward during the side grouting processes. The diameter of the grout bulb at the top of the side grouted zone was four-and-a-half feet (1 ½ D), with an average diameter of four feet across the side grouted zone (1 ⅓ D). The upward flow of the grout also resulted in the stretching of the side membrane at the top part of the side grout zone, as shown by Figure 4-18. Because the pumping rate was slow enough (two gpm), the grout started to hydrate before the side membrane failed and did not actually flow past the side membrane. Had the pumping rate been faster, the higher tensile stresses would have developed sooner (grout still fluid), and the grout may have flowed up along the soil-shaft interface. Regardless, the grout flowed mostly in the radial/horizontal direction rather than upwards along the soil-shaft interface and was evident by the side grout bulb shape, which reflected cylindrical cavity expansion (radial flow).

Figure 4-17: Close up of side grouted zone as long shaft was removed from test chamber

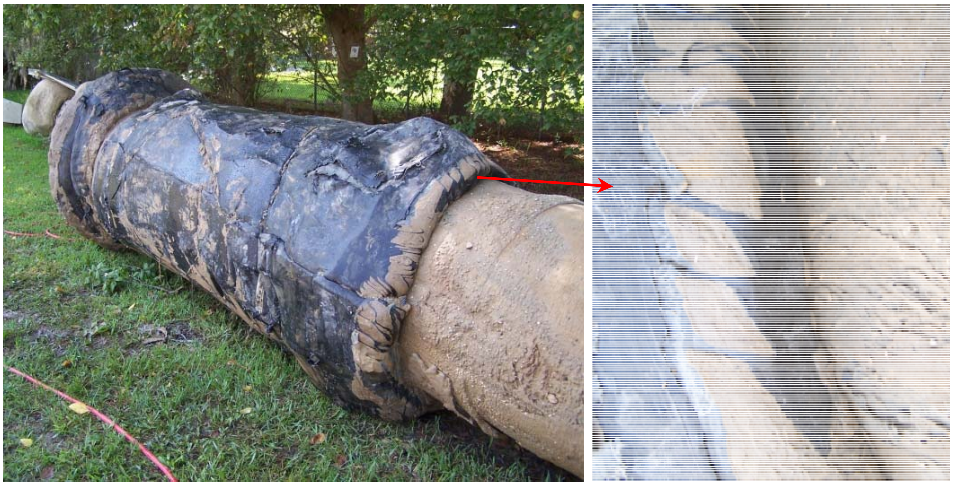

Figure 4-18: Top of side membrane failure as grout flowed upwards during side grouting of long shaft

4.2.3 Tip Grouting

Visual examination of the grouted shaft showed no upward grout flow above the side membrane during the tip grouting phase and a semi-spherical tip grout bulb shape (Figure 4-19). Both suggested spherical cavity expansion during the tip grouting phase. The tip of the shaft can be identified by the concrete aggregate and shown in Figure 4-19, which showed no grout from the tip grouting phase above the shaft's tip. Due to boundary effects caused by the test chamber, grout flow was primarily in the radial/horizontal direction with little grout observed below the shaft feet (Figure 4-20). There was less than 10 feet of soil below the shaft tip, so the soil below the tip quickly compressed during grouting (path of least resistance no longer vertically downward) and forced the grout to flow outward (radial/horizontal).

Figure 4-19: Close-up of tip-grouted zone as long shaft was removed from test chamber

Figure 4-20: Bottom of tip-grouted zone of long shaft

Grout pressures increased throughout the tip grouting process as the total volume of grout increased (Figure 4-21). Grout was planned to be pumped until max theoretical volume was approached (357 gal) or excessive vertical displacement of the shaft occurred (> 0.2% of D to avoid fully mobilizing side resistance). The final volume of grout pumped was 180 gallons (50% max volume), and the maximum pressure observed was 700 psi. The maximum expected grout pressure was 783 psi (spherical cavity limit pressure; Salgado and Randolph, 2001). Note, the maximum tip pressure will be controlled by the spherical cavity expansion or maximum resistance of the shaft (self-weight and side resistance), which will discussed further in Chapter 5.

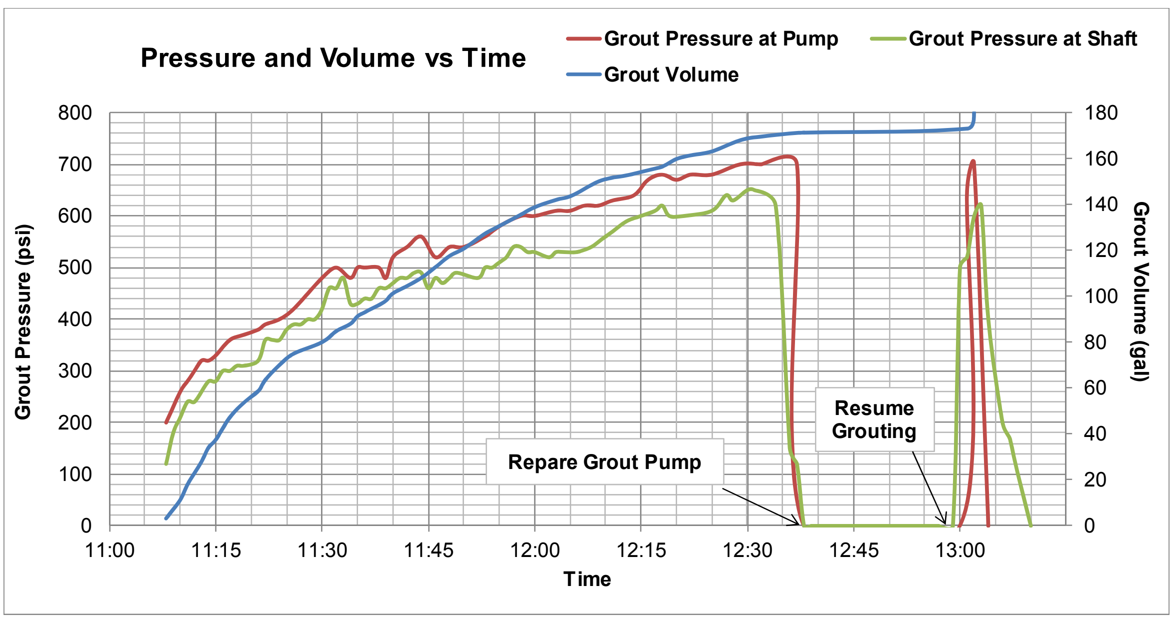

Figure 4-21: Grout pressure and grout volume vs. time during tip-grouting of long shaft

Grouting stopped because of large vertical displacements of the shaft (Figure 4-22 on the next page). The top of the shaft moved upwards to a maximum of 0.4038" and the soil moved upwards to a maximum of 0.2008", or the average differential movement of the shaft with the soil was 0.203" when grouting stopped (0.56% D).

There was much less vertical movement of the soil during the tip grouting phase (i.e., less volume pumped). Also, significant displacements did not occur until grout pressure exceeded 300 psi (Figure 4-23).

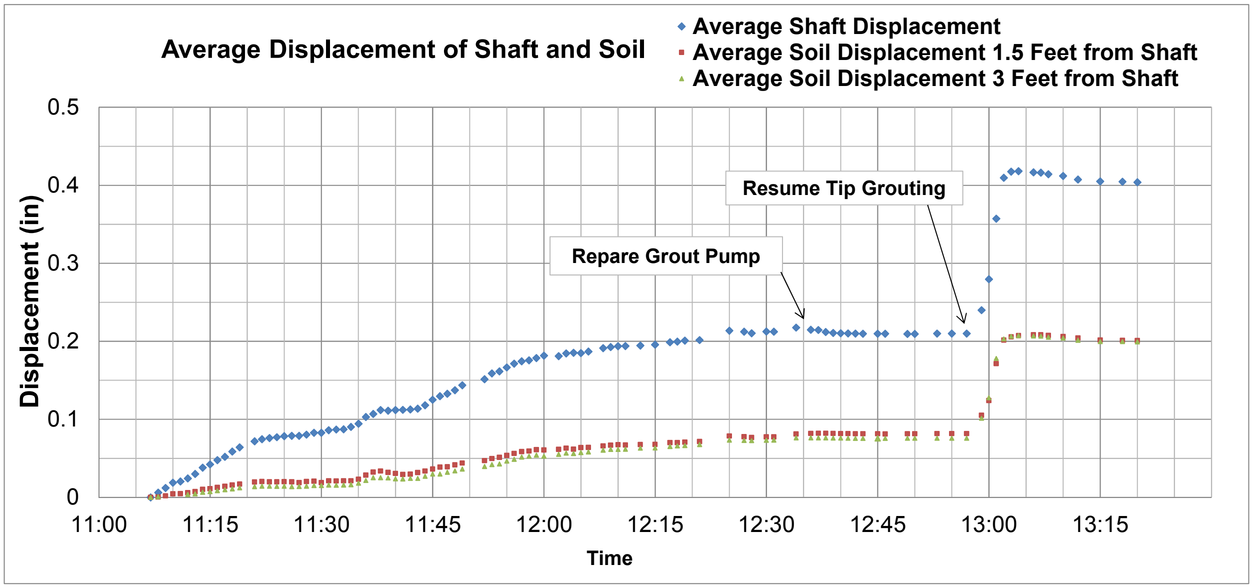

Figure 4-22: Shaft and soil displacements during tip-grouting of long shaft

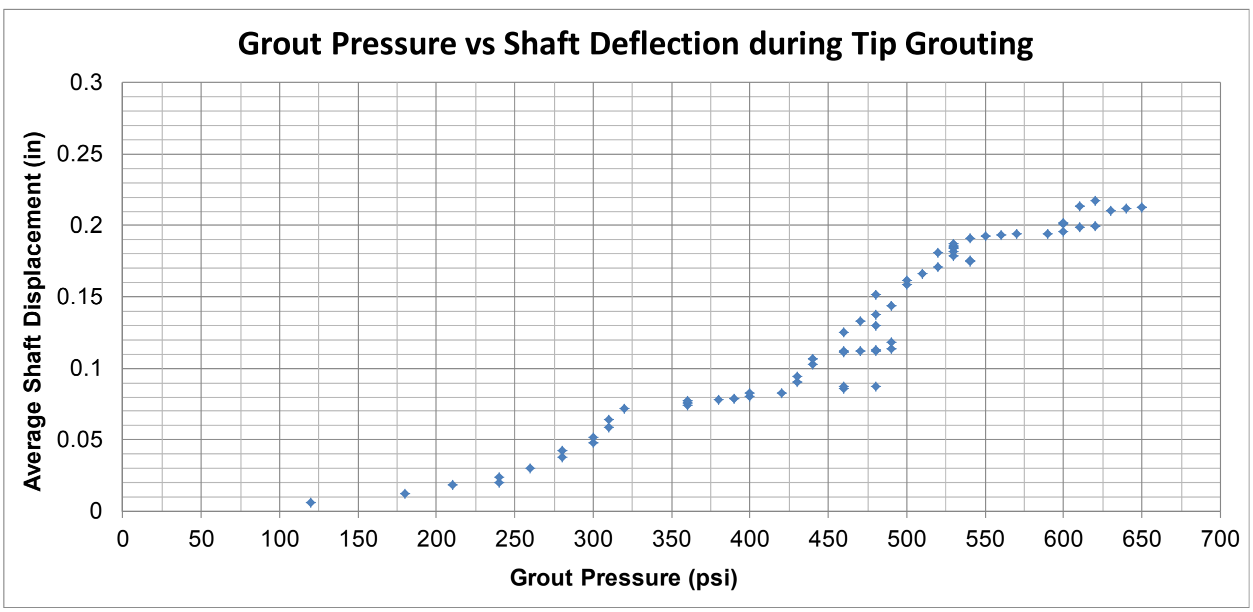

Figure 4-23: Top of shaft displacement during tip-grouting of long shaft

Of great interest was the change in stress throughout the test chamber due to the influence of tip grouting. The gauges closest to the tip grouted zone are shown in Figure 4-24. The Geokon earth pressure cells below the tip (#1 and #2) quickly reached maximum gauge readings (vertical stress). Similarly as the grout volume and pressures grew, the pressure cells next to the shaft tip (#3 and #4) quickly reached maximum gauge readings too (horizontal stress). This means grout did flow radially, and the increased horizontal stress state extended further away from the shaft as the cavity expanded (pressure cells #5 and #6).

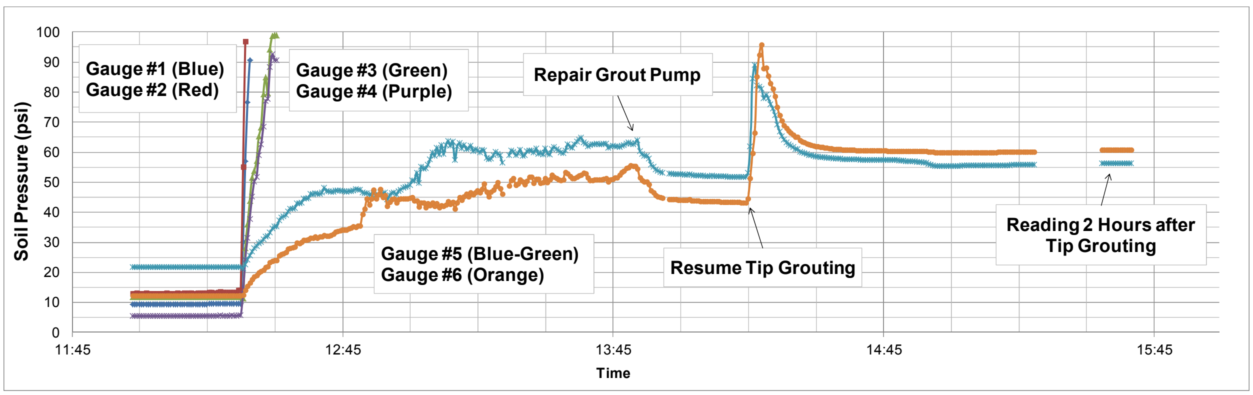

Figure 4-24: Change in vertical and horizontal stress near tip of long shaft

Additionally, the mobilized side resistance along the shaft was of great interest (side grouted zone vs. ungrouted zone), and the internal forces (strain data) and tip forces (grout pressure) are shown in Figure 4-25 on the next page. In the case of the embedded strain data, Young's modulus (concrete samples taken during shaft construction) was multiplied by the original cross-sectional area of the shaft to compute the internal force as well as the estimated force exerted by the grout (pressure multiplied by original cross-sectional area). As expected, the shaft was in compression throughout the tip grouting phase. Before grouting stopped to repair the grout pump, the maximum internal force above the side grouted zone was 50 kip, and the maximum internal force below the side grouted zone was 770 kip (shaft tip), as illustrated in Figure 4-26 (left). Using the maximum grout pressure of 650 psi (grout pressure at shaft) and a contact area of 1,018 in^2 (D = 36 inch), the force exerted on the shaft tip during the tip grouting phase should have been around 662 kip. The difference between the estimated versus observed (662 kip vs. 770 kip measured at the shaft tip) suggested that the tip grout bulb was acting over a larger contact area (see Figure 4-26 below - right).

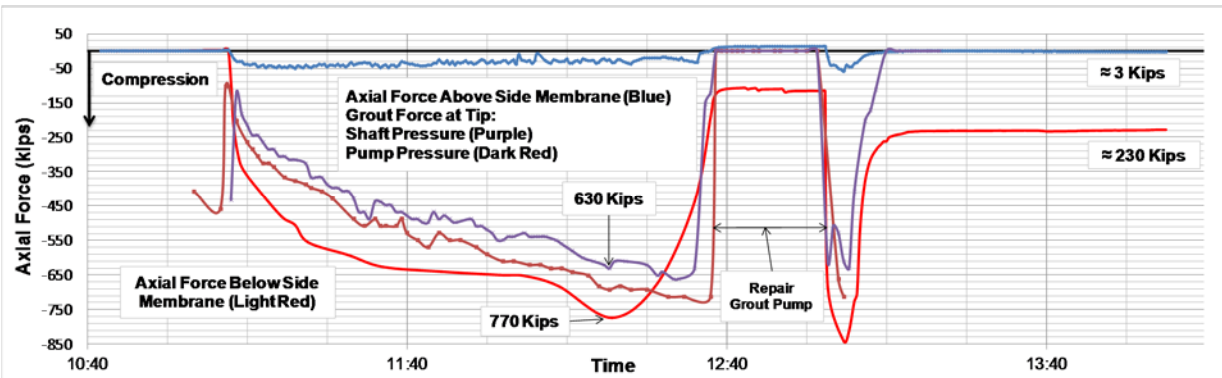

Figure 4-25: Embedded stain data vs. grout pressure during tip-grouting of long shaft

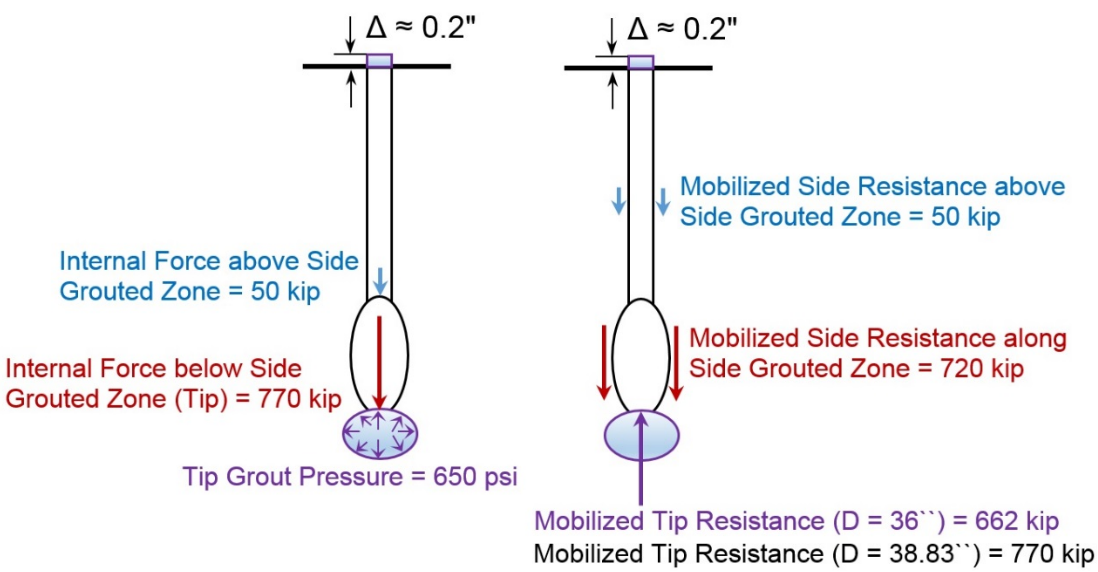

Figure 4-26: Measured internal force and grout pressure (left) and mobilized side and tip resistance (right) during tip grouting of long shaft

The force exerted on the shaft tip by the tip grout was carried by the mobilized side resistance (Figure 4-26 - right). The difference in the internal force above and below the side grouted zone was thus equal to the mobilized side friction along the side grouted zone, and similarly, the difference in internal force above the side grouted zone and top of the shaft was equal to the mobilized side friction above the side grouted zone. Based on the strain gauge data (Figure 4-26 - left), the mobilized side resistance above the side grouted zone was 50 kip (top ⅔ of shaft), and the mobilized side resistance along the side grouted zone was 720 kip (bottom ⅓ of shaft). Using the force of 770 kip measured at the shaft's tip and the maximum grout pressure of 650 psi, the estimated cross-sectional area was about 1,184.2 in^2 (D = 38.83 inch). The side grouted zone mobilized over 15 times the side resistance that was mobilized above the side grouted zone, or the bottom third of the shaft mobilized 93.9% of the total side resistance during tip grouting.

4.2.4 Static Load Test

After tip grouting and setting up the reaction system, a top-down axial load test (static) was performed on the long shaft with displacements, soil stresses, and internal strain recorded. The pressure cells below the tip reached maximum working pressure almost immediately and several pressure cells were still above maximum range from the tip grouting phase, so no useful pressure cell data was collected during the static load test. The applied load was increased during top-down test until the reaction shafts started to fail (upward displacement > 2% D). The loading phase of the test stopped when the west reaction shaft moved 0.0551" (0.15% D). The displacement of the test shaft at the end of loading was 0.069" (0.19% D) and shown in Figure 4-27. During the maximum applied load (380 kip), the average downward displacement of the shaft was 0.0684" and soil was 0.0297", and the average upward displacement of the reaction shafts was 0.0333". After unloading the shaft, the average shaft displacement was 0.0212" and soil was 0.01", and the average displacement of the reaction shafts was 0.008".

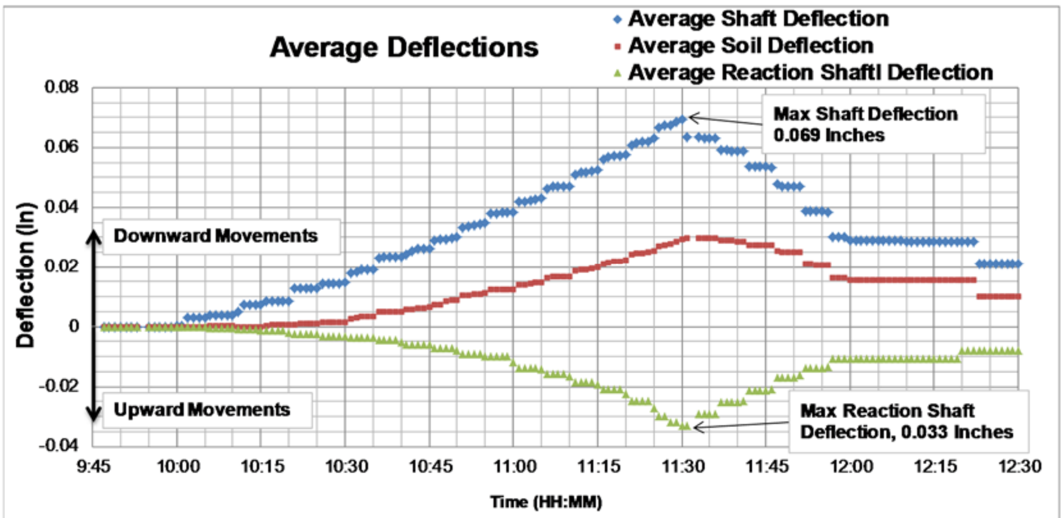

Figure 4-27: Displacements during static load test of long shaft

Using the embedded strain data and Young's modulus (concrete samples taken during shaft construction), the internal force distribution was calculated (Figure 4-28 and 4-29 - left). During the maximum applied load (380 kip), the internal force above the side grouted zone was 335 kip, and the internal force below the side grouted zone was 180 kip (shaft tip). Recall calculations made for the mobilized side resistance during tip grouting, the difference in the applied load and internal force above the side grouted zone was equal to the mobilized side friction above the side grouted zone and shown in Figure 4-29 (right). Similarly, the difference in the internal force above and below the side grouted zone was equal to the mobilized side friction along the side grouted zone.

This gives a mobilized side resistance above the side grouted zone of 45 kip (similar to the side resistance observed during tip grouting), and a mobilized side resistance along the side grouted zone of 155 kip. The internal force below the side grouted zone (180 kip) was the remaining load being carried by the shaft's tip (i.e., end bearing). During the top-down test, the side grouted zone (bottom ⅓ of shaft) mobilized three and a half times the side resistance as above the side grouted zone (top ⅔ of shaft), or the bottom third of the shaft carried 40.8% of the total load during the top-down test.

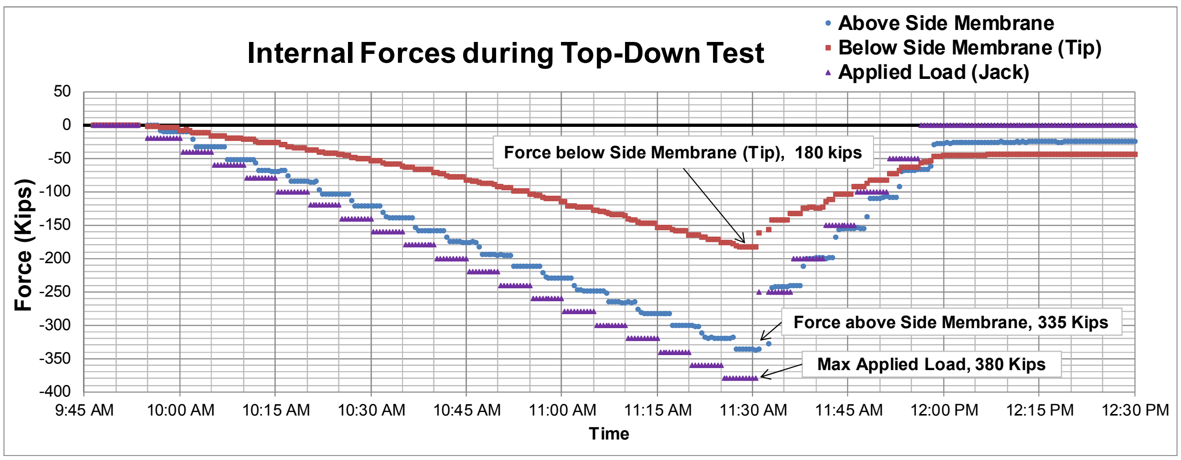

Figure 4-28: Load distribution during static load test of long shaft

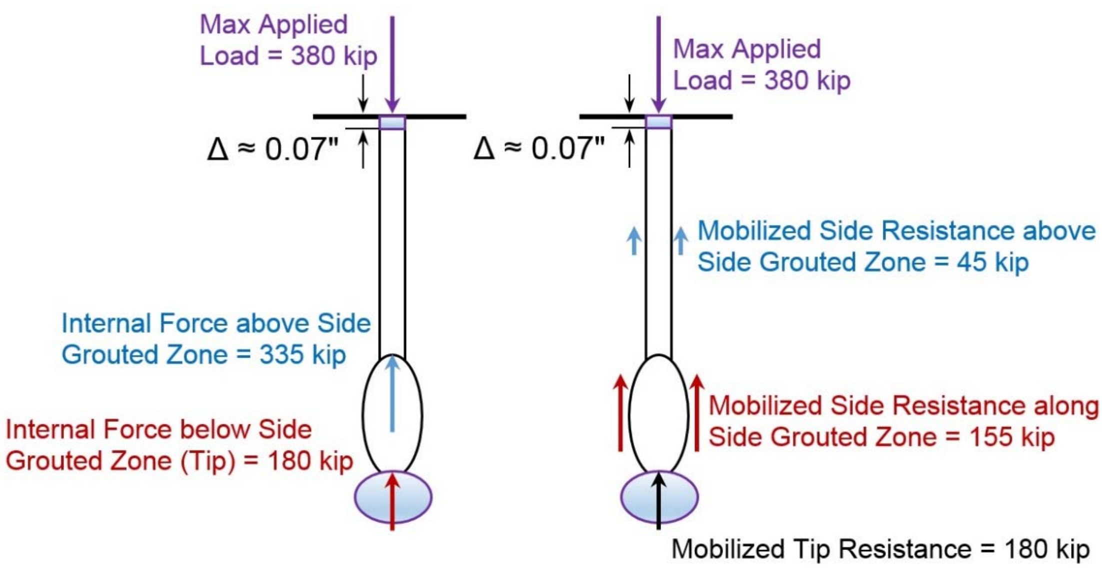

Figure 4-29: Measured internal force (left) and mobilized side and tip resistance (right) during static load test of long shaft

The load-displacement behavior of the long test shaft during static loading is shown in Figure 4-30. The elastic shortening of the shaft during the maximum applied load was estimated to be 0.0284", calculated using a Young's modulus of 3,950,000 psi (tested concrete specimens). Consequently for the applied load of 380 kip, only 0.04" of displacement (0.1% D) may be attributed to yielding of the soil. Note, the soil below the tip was already compressed during the tip grouting phase, so little displacement would be associated with its mobilization.

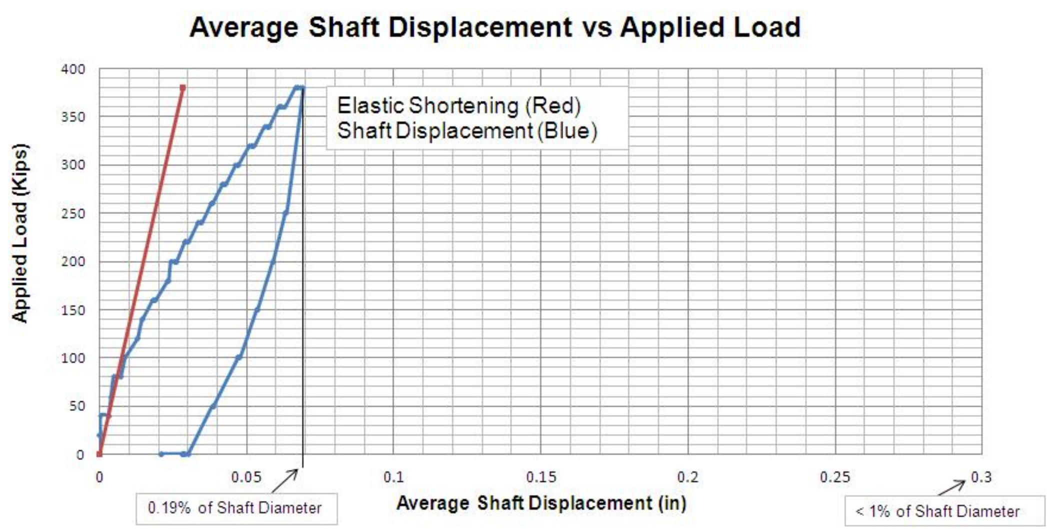

Figure 4-30: Load-displacement behavior of long shaft under axial loading

4.3 Field Shaft (42" x 25')

4.3.1 Shaft Construction and Membrane Seal Grouting

The top membrane seal was 16 feet long (cut length) with an estimated volume of grout of 25 gallons (3.34 cubic feet), so once grouted (fully inflated), the OD of seal and side membrane would be 5.09 feet (i.e., seal expands 9.56 inches away from shaft into surrounding soil). Before 100% volume of the seal could be reached, the grout pressures exceeded the allowable limits (150 psi rated working pressure), so grouting was stopped before rupturing of the seal occurred. The volume of grout pumped into the top seal was 24 gallons (2.8 cubic feet), which corresponded to an OD of 4.54 feet (i.e., seal expanded 6.2 inches away from shaft into the surrounding soil). The grout volumes and recorded pressure while grouting the membrane seals are given in Table 4-2. Given the length of hose used to fabricate the bottom membrane seal (15 feet) and hose diameter, the estimated volume of grout to fill the seal was 24.25 gallons (3.24 cubic feet), which corresponds to an OD of about 4.77 feet (i.e., seal expands 7.65 inches away from shaft into surrounding soil). Before 100% volume could be reached, the grout pressures started to exceed allowable limits (310 psi rated working pressure), so the grouting stopped before rupturing the seal. The actual volume of grout pumped in the bottom seal was about 22 gallons (2.54 cubic feet), which corresponds to an outside diameter of about 4.12 feet (i.e., seal expands 3.7 inches away from shaft into surrounding soil).

Table 4-2: Grout pressures during membrane seal grouting of field shaft

Membrane Seal	Pump Stroke #	Volume during Stroke (gal)	Pressure during Stroke (psi)	Hole Pressure after Stroke (psi)	Cumulative Volume (gal)
Top Seal	1	3.5	0	0	3.5
	2	3.5	10	0	7
	3	3.5	100	40	10.5
	4 (Partial)	1	145	100	11.5
	(Prime*)	2	N/A	N/A	13.5
	5	3.5	100	40	17
	6	3.5	105	80	20.5
	7	3.5	145	120	**24**
Bottom Seal	1	3.5	0	0	3.5
	2	3.5	20	0	7
	3	3.5	100	5	10.5
	4	3.5	160	130	14
	5	3.5	200	20	17.5
	6	3.5	270	160	21
	7 (Partial)	1	320	210	**22**

4.3.2 Side Grouting

The estimated volume of grout needed to create the side grout bulb with a height of nine-and-a-half feet and an outside diameter of 5.25 feet (1 ½ D) was 855 gallons. The grout pressure, grout volume, and upward movements of the shaft and surrounding soil during the side grouting phase can be seen in Figures 4-31 through 4-33. 425 gallons of grout were pumped using AFT's grout pump (blue curves), and 190 gallons of grout were pumped using UF's grout pump (red and green curves). While grouting with AFT's pump, there was an increase in grout pressure and a slowing in grout flow after pumping about 200 gallons of grout, (see erratic pumping description in section 3.1.3); therefore, pumping was stopped around 250 gallons, the grout pump was cleaned out, and pumping resumed with the higher pressure setting on the pump (flow rate around four gpm). With the higher flow rate, the grout pressure dropped from 600 psi to less than 300 psi over one hour (additional 175 gallons pumped). Looking at Figures 4-33 and 4-34, the shaft moved upwards, and the soil stresses increased by 20 to 40 psi two feet away from the shaft. Given the lateness of the day (i.e., need to switch grout delivery lines, clean out pump, etc.), it was decided to stop grouting and continue shortly after (day or two later). Two days later, 190 gallons of grout were pumped using UF's grout pump (red and green curves). After pumping 85 gallons of grout (red curves), a two hour break was taken to switch delivery lines and allow grout to hydrate before pumping more grout. Following the break (green curve), another 105 gallons of grout were pumped when grouting was stopped with upward vertical movement of approximately 0.5".

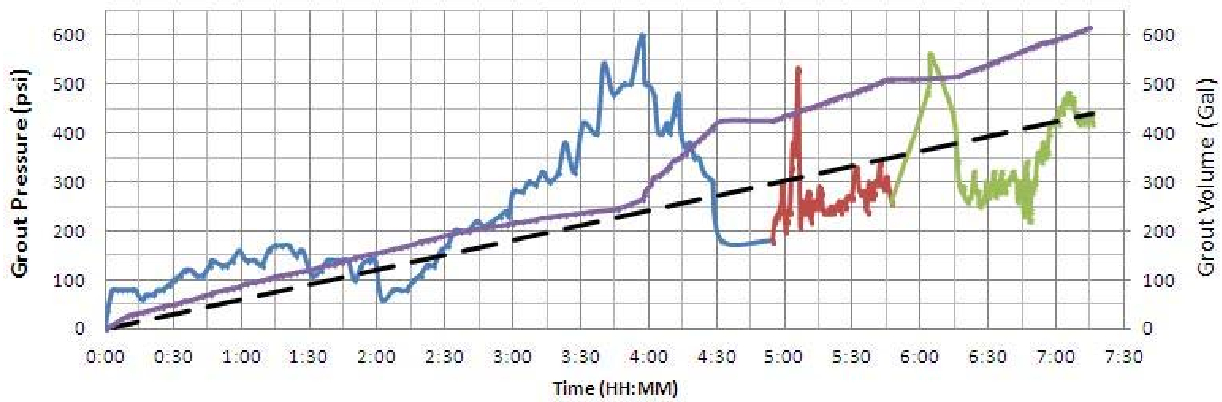

Figure 4-31: Grout volume (purple curve) and grout pressure using AFT pump (blue curve) and UF pump (red and green curves) during side grouting of field shaft

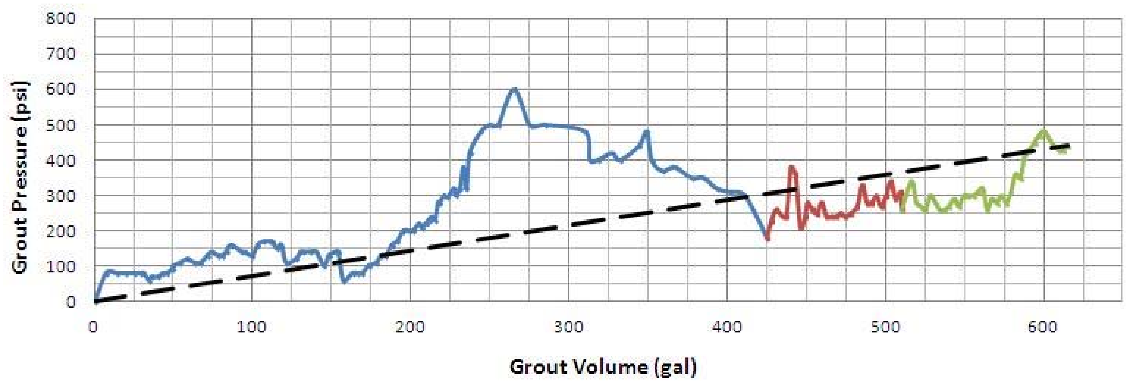

Figure 4-32: Volume vs. pressure using AFT pump (blue curve) and UF pump (red and green curves) during side grouting of field shaft

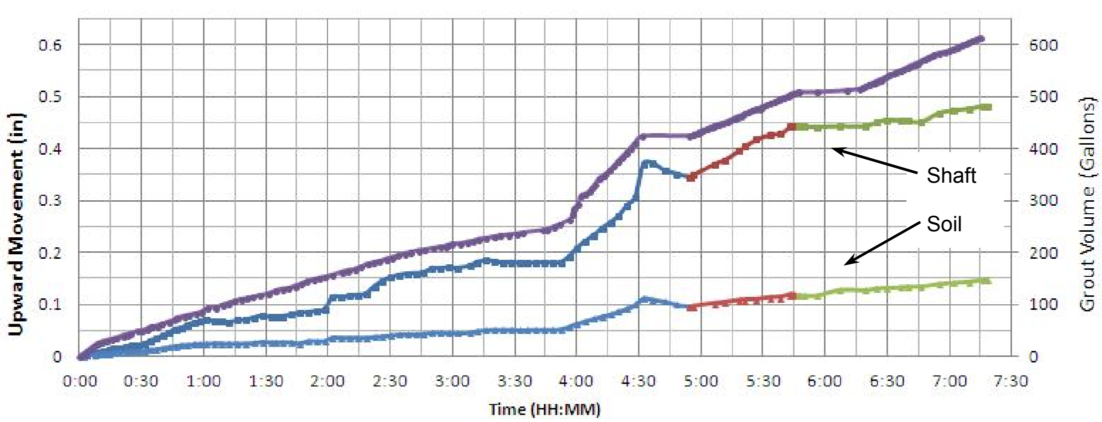

Figure 4-33: Grout volume (purple curve) and displacements using AFT pump (blue curve) and UF pump (red and green curves) during side grouting of field shaft

The change in horizontal stresses at the center of the membrane (2' and 4' away) varied during side grouting, as shown in Figure 4-34. Using AFT's grout pump (0 to 425 gallon of grout), the horizontal pressure increased immediately after side grouting began, which suggested radial grout flow (i.e., cylindrical cavity expansion). Pressure cells #2 and #3 (red and green curves) show similar change in stress despite being located at different distances away from the cavity expansion, for pressure cell #2 was two feet away from shaft and pressure cell #3 was four feet away from the shaft (both located on the north side of the shaft).

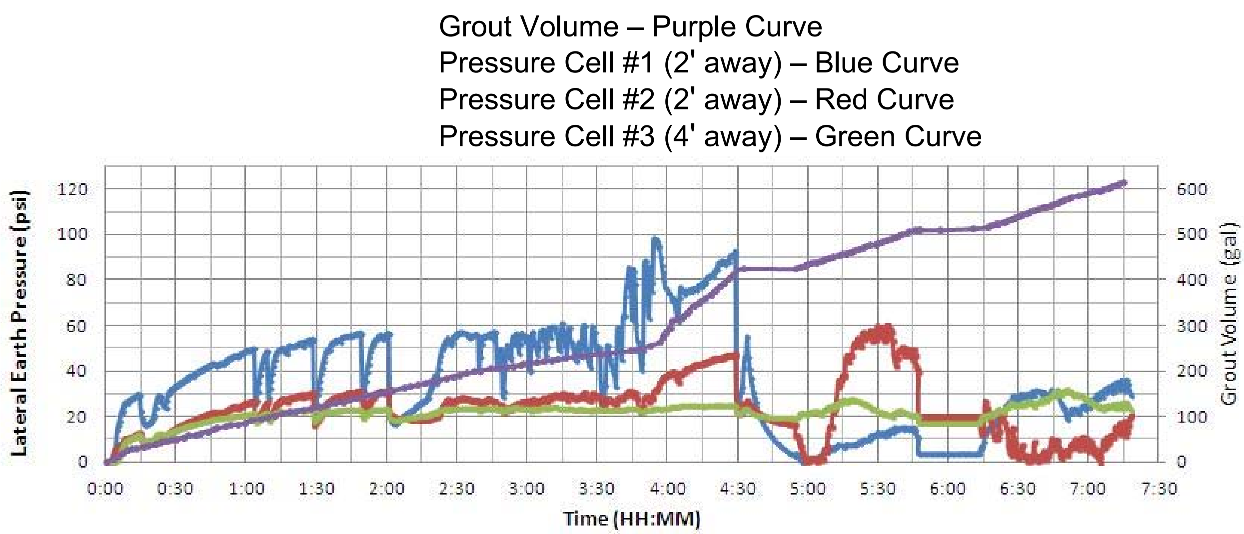

Figure 4-34: Grout volume (purple curve) and horizontal stress during side grouting of field shaft

As expected, pressure cell #2 showed a greater horizontal stress increase (closer to cavity expansion), but the effects during the side grouting process were nearly identical in magnitude at the further gauge location (i.e., pressure cell #3). Pressure cell #1 was located on the north side of the shaft (other side) and showed a greater change in horizontal stress during the side grouting using AFT's pump (up to 425 gallons of grout). This suggests grout flow and cavity expansion in this direction (south). Then when additional grout was pumped using UF's pump (through orthogonal side-manchettes), the grout flow and cavity expansion was predominate on the other side of the shaft (north), which was reflected by the change in horizontal stress using UF's pump (425 to 615 gallons of grout). While side grouting with UF's grout pump (85 + 105 gallons), the side-manchette was changed after the break, so grout was being delivered in a new direction. Again, the side grout flowed in the direction of least resistance and cavity expansion was predominate on the southeast side. Note that during certain time periods, the soil stresses dropped and can be seen in Figure 4-34 (e.g., 5:00). This is attributed to switching grout delivery pipes and the stress gauges being attached to a stiff/rigid CPT rod, so as the soil mass moves, the CPT rod and pressure cell deform. At the time of stopping however, the observed pressure in the soil 2' and 4' away from the grout membrane was about 20 psi greater then when the process began (e.g. 4:30, 5:45, and 7:15).

4.3.3 Tip Grouting

The total volume of grout pumped during the tip grouting phase was 77.6 gallons, as shown in Figure 4-35. Approximately 61 gallons of grout was pumped through the first tip-manchette (blue curves) before switching to the second tip-manchette (red curves). While the remaining 16.6 gallons of grout was pumped (red curves), the grout pressure, grout volume, and upward movements of the shaft and surrounding soil continued to increase as shown in Figures 4-36 and 4-37. The maximum vertical displacement observed at the top of the shaft was 0.3422" and the soil moved upward 0.0715". The maximum differential displacement between the shaft and the soil was 0.2707" (0.64% D). Because the upward movement of the shaft was approaching the limits (i.e., < 1% D to fully mobilize side resistance), tip grouting was stopped. At no time during grouting (side or tip) was there observed grout flow up alongside the soil-shaft interface to the ground surface or through any of the open grout delivery pipes (e.g., tip or side).

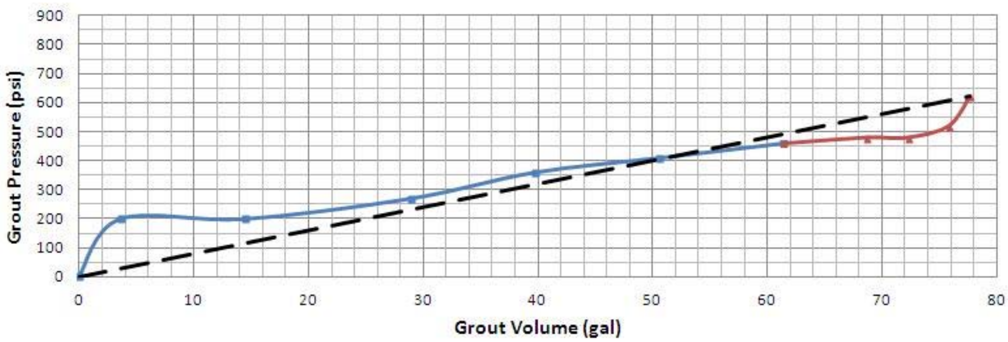

Figure 4-35: Grout volume vs. grout pressure during tip grouting of field shaft (blue curve – first tip-manchette; red curve – second tip-manchette)

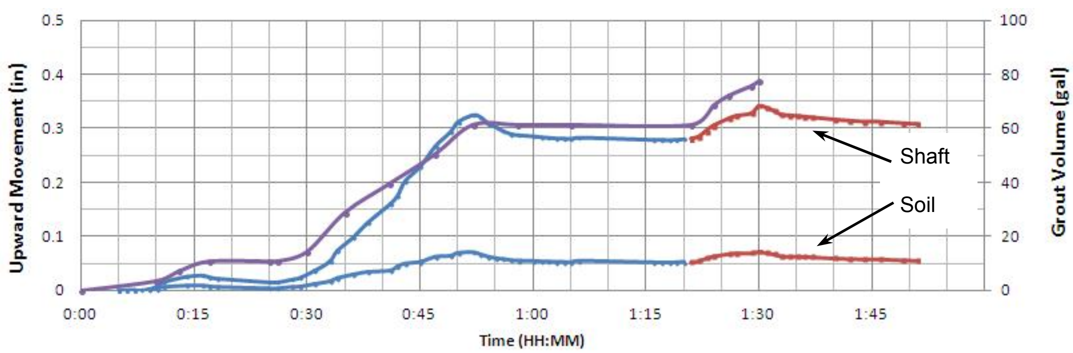

Figure 4-36: Grout volume (purple curve) and displacements during tip grouting of field shaft

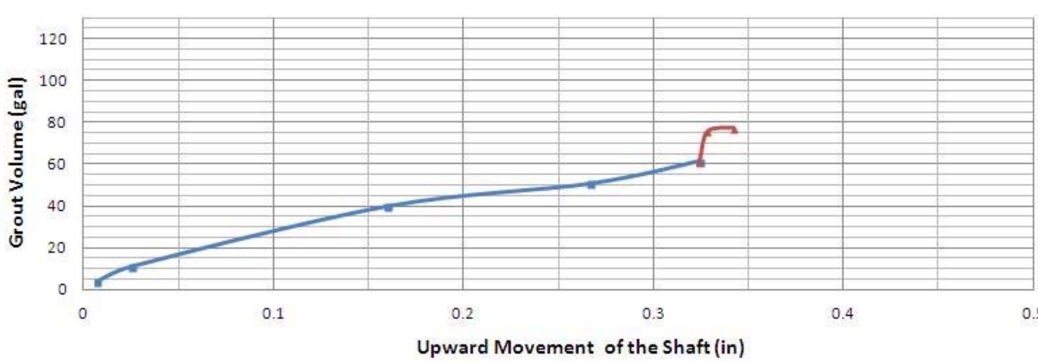

Figure 4-37: Displacement of shaft vs. grout volume during tip grouting of field shaft

Of great interest was the change in the horizontal soil stress near the tip during tip grouting. Shown in Figure 4-38 is the change in pressure cell #4, which was located 25.5 feet below the ground surface and two feet away from the shaft. As expected, the lateral earth pressure grew with increased grout volume. After grouting through the first tip-manchette had stopped (around 0:53), steady state pressure was observed at 25 psi. Similarly after grouting through the second tip-manchette stopped (around 1:31), the lateral earth pressure stabilized at about 30 psi, so the horizontal stress was greater than before tip grouting began (similar to side grouting). Note, the peak stresses (e.g., 50 psi) were less than the maximum observed grout pressures (600 psi); however, the stresses were expected to drop quadratically with distance away from the grout bulb.

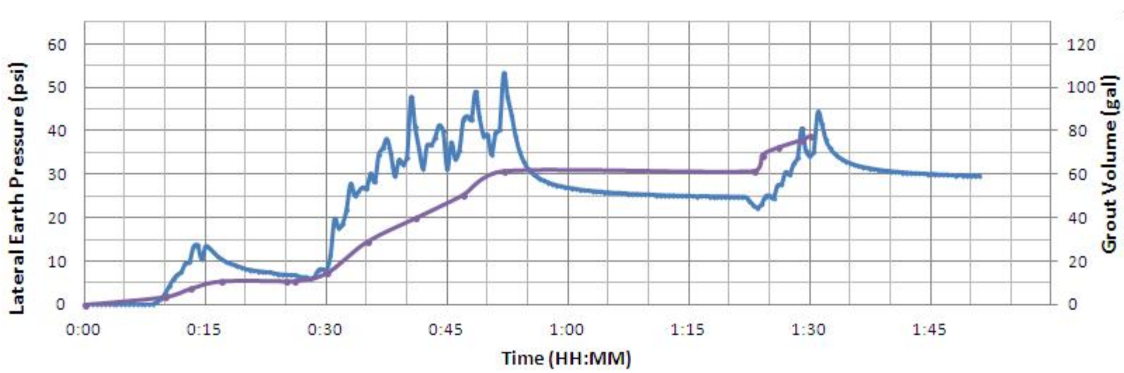

Figure 4-38: Grout volume (purple curve) and lateral earth pressure near tip of field shaft during tip grouting

Also of significance was the mobilized side resistance along the shaft during tip grouting, and more specifically, a comparison of the side grouted vs. ungrouted zones of the shaft. The internal strain data during tip grouting is shown in Figure 4-39 (strain below the side grouted zone; raw data – black curve; max reading – purple curve; average – red curve). Following the same procedure as explained in section 4.2.2, the tip strain data was converted into forces and shown in Figures 4-40, 4-41, and illustrated in Figure 4-43 - left. For the internal force calculations (Figures 4-40 and 4-41), the laboratory modulus of the concrete was employed with a shaft cross-sectional diameter of 42". Similarly, the calculated tip force from the observed grout pressure was calculated using a tip area given the base plate diameter of 40".

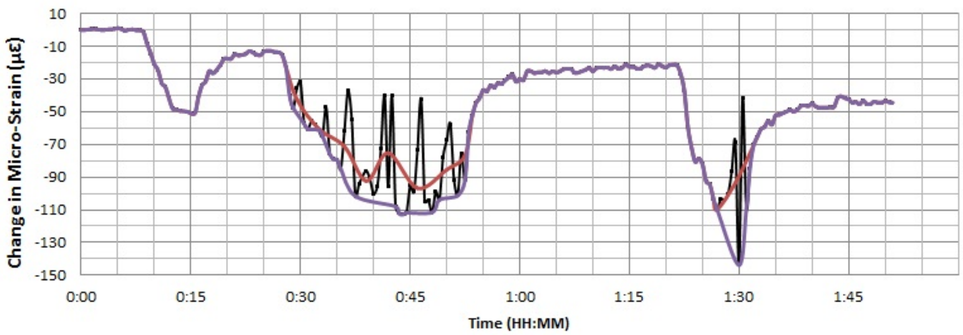

Figure 4-39: Tip strain data during tip grouting of field shaft (raw data – black curve; max reading – purple curve; average – red curve)

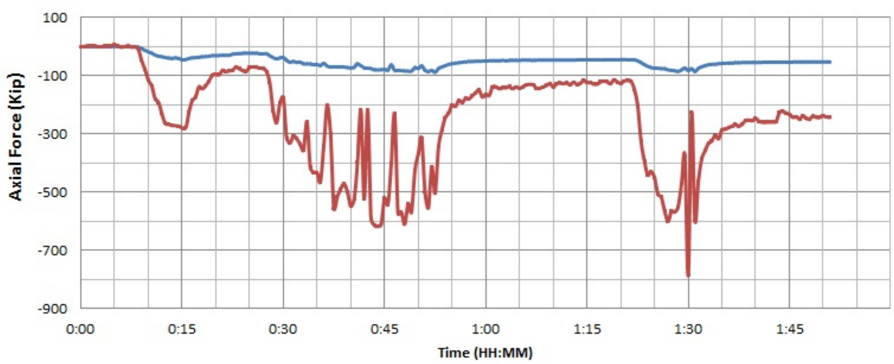

Figure 4-40: Internal force above (blue curve) and below (red curve) the side grouted zone (tip) during tip grouting of field shaft

The tip force calculated using grout pressures (green curve in Figure 4-41) agrees with the embedded strain data and was used with the upward displacements of the shaft to generate Figure 4-42, which illustrates the load vs. upward movement of the shaft during tip grouting. Note in Figure 4-42, the blue line was the tip resistance when grouting through one tip-manchette and red line was through the second tip-manchette. The maximum internal force below the side grouted zone (tip) was 787 kip, and the maximum internal force above the side grouted zone was 83 kip, as shown in Figures 4-41 (1:30) and 4-43 (left). Given the maximum observed grout pressure of 620 psi, the back calculated tip area for which the grout pressure was acting was about 1,269.23 in^2 (D = 40.2"), which agreed with the diameter of the steel base plate (D = 40"). A peak force of 787 kip was measured at the shaft tip with an upward movement of 0.34" at the top, as illustrated in Figure 4-43 (left). Following the same calculation described in sections 4.2.3 and 4.2.4 (i.e., difference between internal force), the side grouted zone mobilized 704 kip and 83 kip of side resistance was mobilized above the side grouted zone (Figure 4-43 - right). The side grouted zone mobilized over eight times the side resistance that was mobilized above the side grouted zone, or the bottom third of the shaft mobilized 80.9% of the total side resistance during tip grouting.

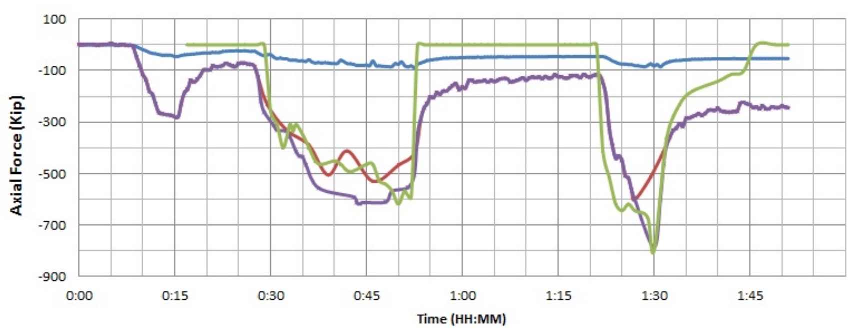

Figure 4-41: Internal force above (blue curve) and below the side grouted zone (max strain – purple curve; average strain – red curve; grout pressure – green curve)

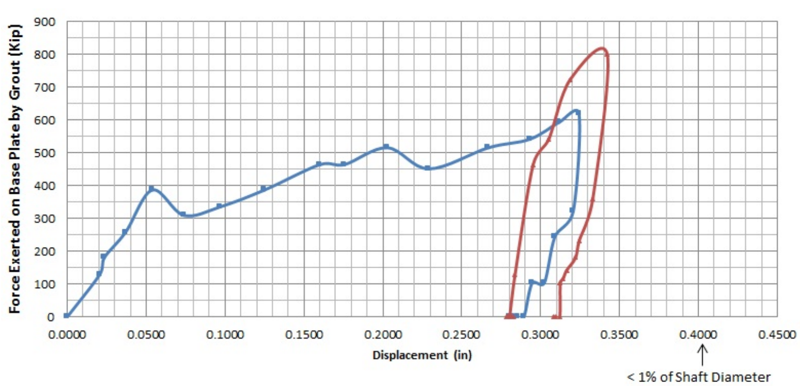

Figure 4-42: Tip force vs. upward displacement during tip grouting of field shaft

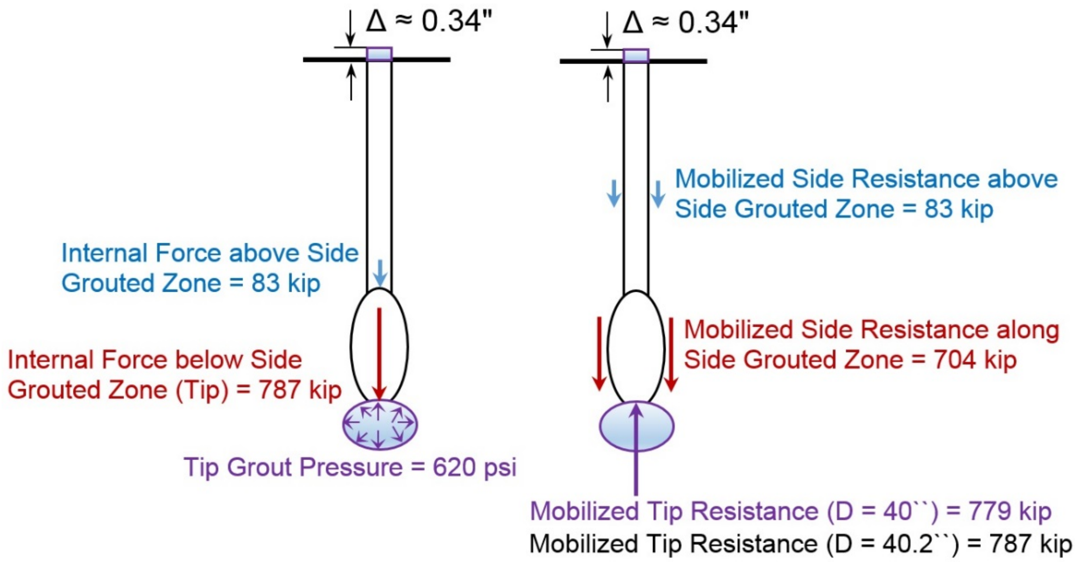

Figure 4-43: Measured internal force and grout pressure (left) and mobilized side and tip resistance (right) during tip grouting of field shaft

4.3.4 Static Load Test

The maximum applied load during the static load test was 850 kip. The test was stopped due to excessive upward displacement of one of the reaction shafts (south shaft). Under the max load of 850 kip, the maximum upward displacement of the north reaction shaft was 0.3734" and the south was 0.5763" (Figure 4-44). At maximum load of 850 kip, the maximum downward displacement of the test shaft was only 0.18" as shown in Figure 4-45 (average digital level data). The movement of the wooden frame (dial gauges attached) was also collected (digital level) and corrections to dial gauges data were made. Note, the wooden frame moved downward throughout testing, i.e., the uncorrected dial gauge readings were under estimating the downward movement of the test shaft. After corrections, dial gauge readings agreed closely with the digital level readings as shown in Figure 4-45.

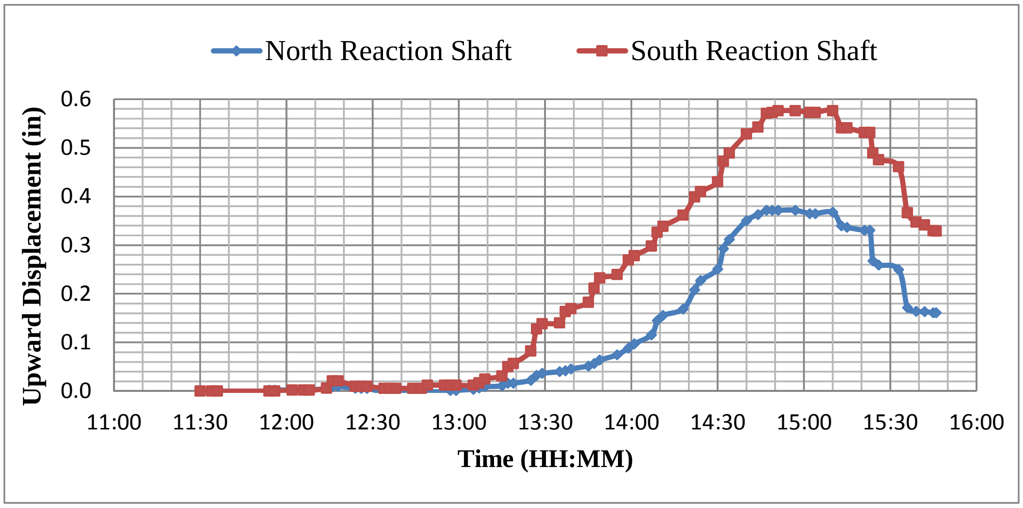

Figure 4-44: Upward displacement of reaction shafts during static load test of field shaft

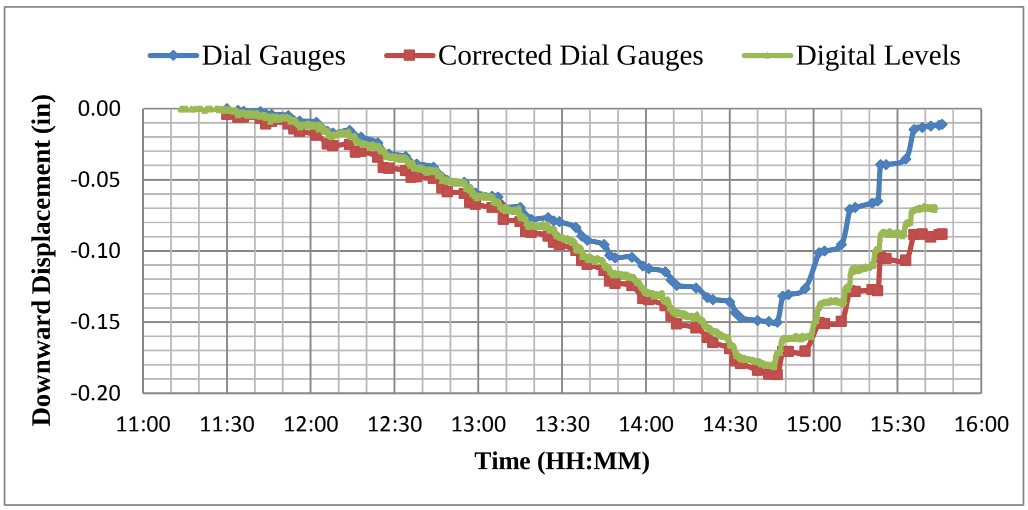

Figure 4-45: Downward displacement during static load test of field shaft

Using the same cross-sectional area (D = 42") and Young's modulus that was used above (tip grouting data reduction), the embedded strain data collected during the top-down test was used to calculate the internal forces above and below the side grouted zone (Figure 4-46 and illustrated in Figure 4-48 - left). Following the same calculation procedure (difference between internal forces), the mobilized side resistance above and along the side grouted zone as well as the mobilized tip resistance is shown in Figure 4-47 and illustrated in Figure 4-48 (right). During the max applied load of 850 kip, the force above the side grouted zone was 764 kip, and the force below the side grouted zone (shaft tip) was 241 kip. Thus, the mobilized side resistance was 86 kip above side grouted zone (top 15 feet of shaft) and 523 kip along the side grouted zone (bottom 10 feet of shaft), with 241 kip being mobilized at the shaft tip (i.e., end bearing). During the top-down test, the side grouted zone (bottom ⅓ of shaft) mobilized six times the side resistance as above the side grouted zone (top ⅔ of shaft), or the bottom third of the shaft carried 61.5% of the total load during the top-down test.

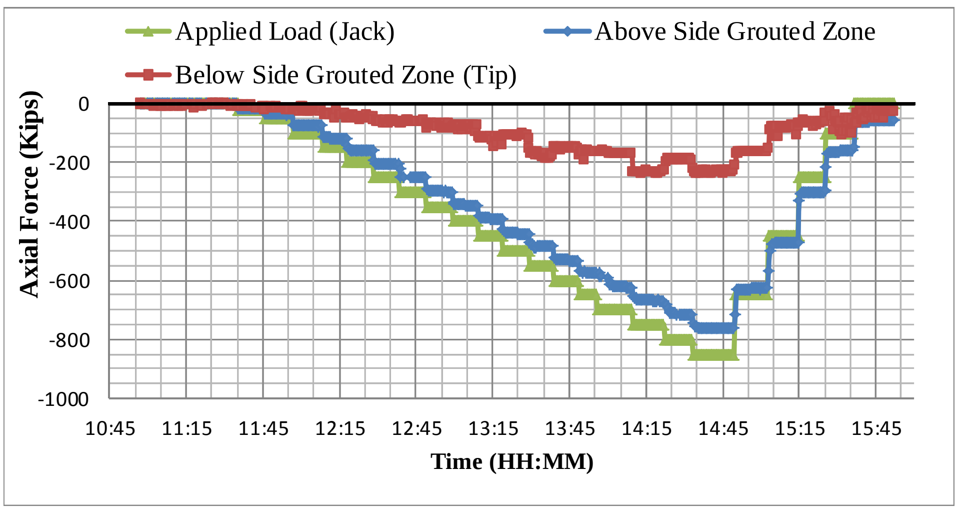

Figure 4-46: Force along shaft during static load test of field shaft

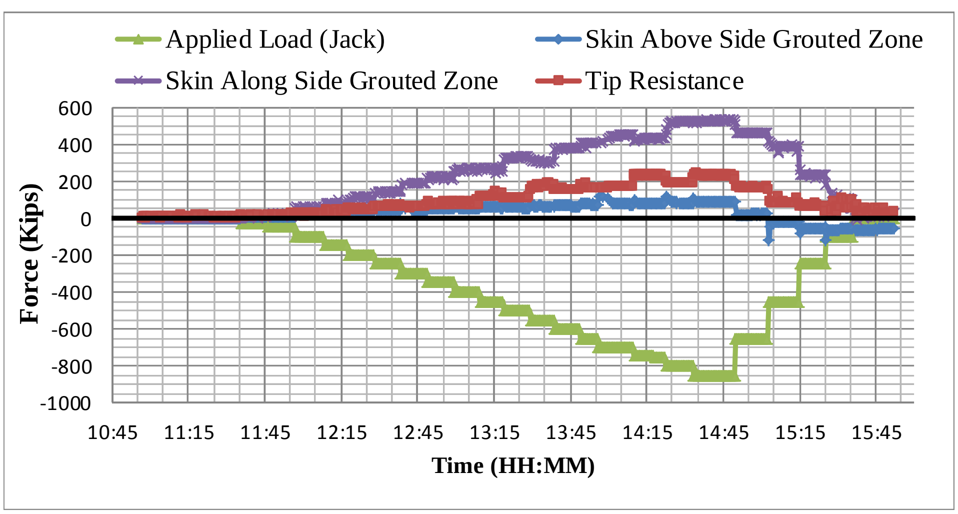

Figure 4-47: Mobilized resistance during static load test of field shaft

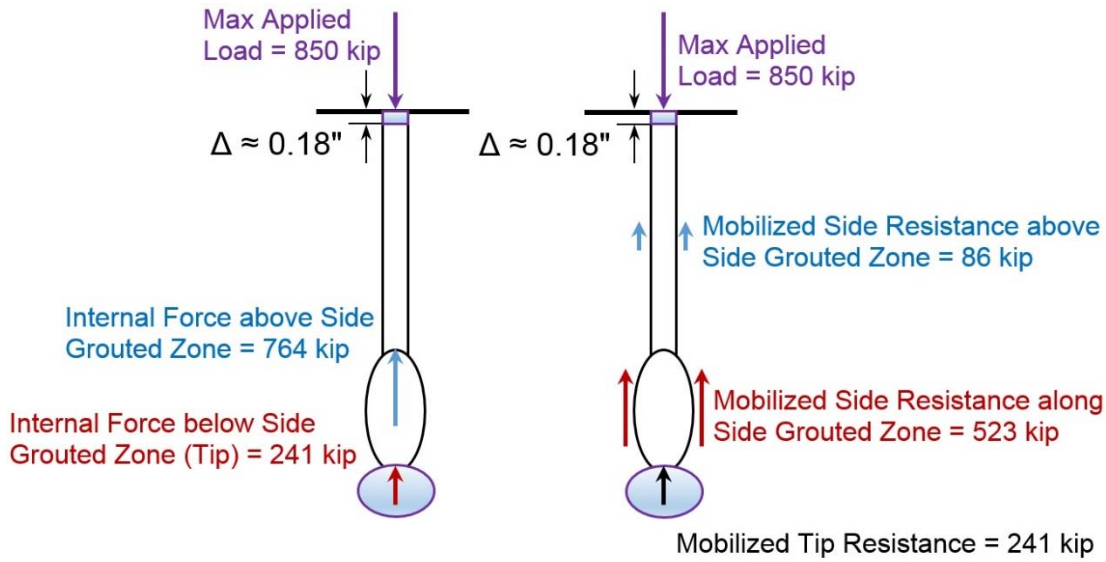

Figure 4-48: Measured internal force (left) and mobilized side and tip resistance (right) during static load test of field shaft

The load distribution at various load increments is shown in Figure 4-49. As the load increased, the lines above the side grouted zone become parallel which suggests that the side resistance was fully mobilized above the side grouted zone. The lines within the side grouted zone appear to be not parallel, suggesting that the resistance along this zone was not fully mobilized. Also since the load is mobilized along the shaft from the top-down, the tip resistance of 241 kip was not fully mobilized either.

The applied load vs. top displacement of the side-and-tip-grouted drilled shaft is plotted in Figure 4-50. Under the max load of 850 kip, the downward displacement of the top of the shaft was 0.18 inch (< 0.5%) with the elastic shortening estimated as 0.0462". After unloading, the shaft had a permanent displacement of 0.0695" (< 0.2% shaft diameter) with a rebound of 0.11".

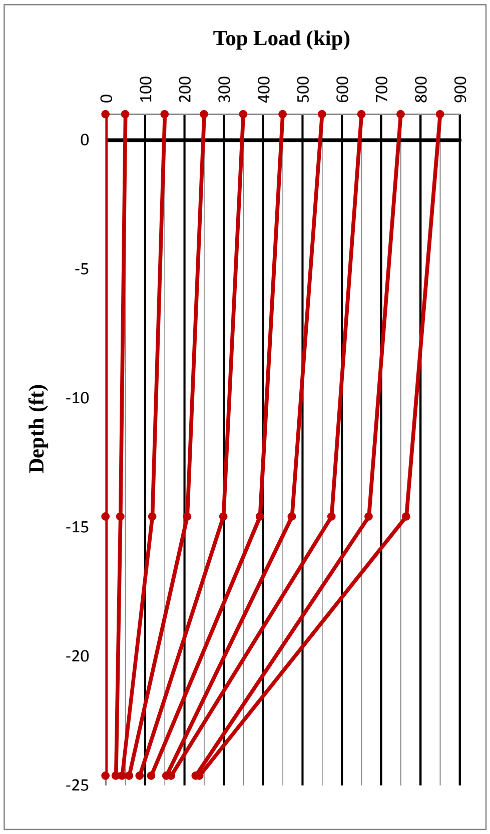

Figure 4-49: Load distribution during static load test of field shaft

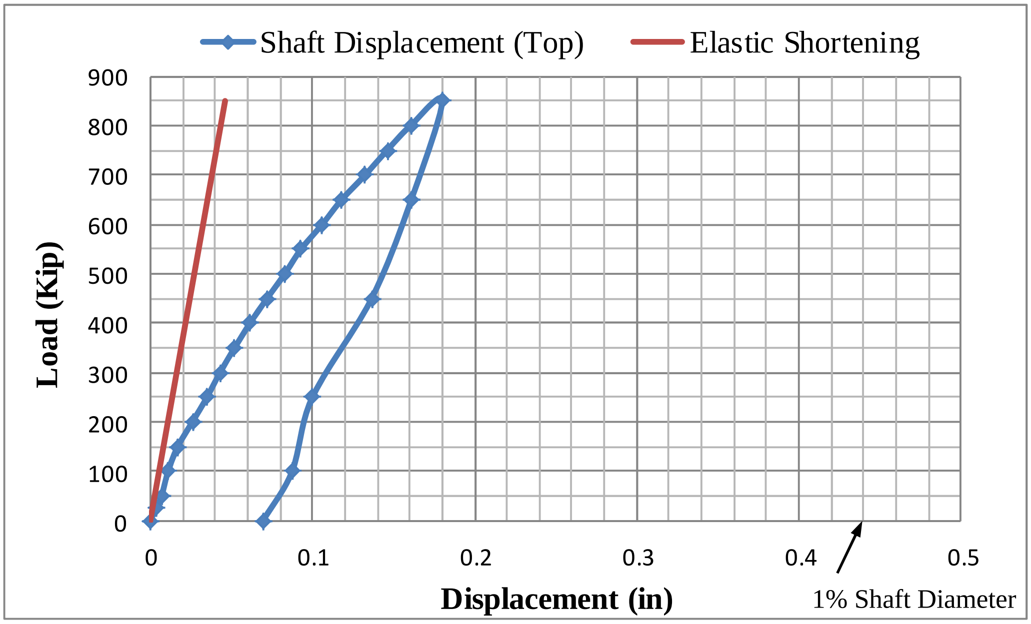

Figure 4-50: Load displacement behavior of field shaft under static axial loading

4.3.5 Statnamic Load Test

The statnamic load test was conducted by AFT along with data collection and analysis (static resistance). Referring to the field shaft as the “Jet Grouted Drilled Shaft,” the measured statnamic load vs. displacement response reported by AFT is shown in Figure 4-51. Using the installed strain gauges (see section 3.1.5) and top accelerometers, the segmental unloading point (SUP) method (Mullins et al., 2002) was used by AFT to compute the static force distribution within the shaft as shown in Figure 4-52. Note, the SUP method does not use bottom accelerometer data (i.e., accelerometer located at shaft tip).

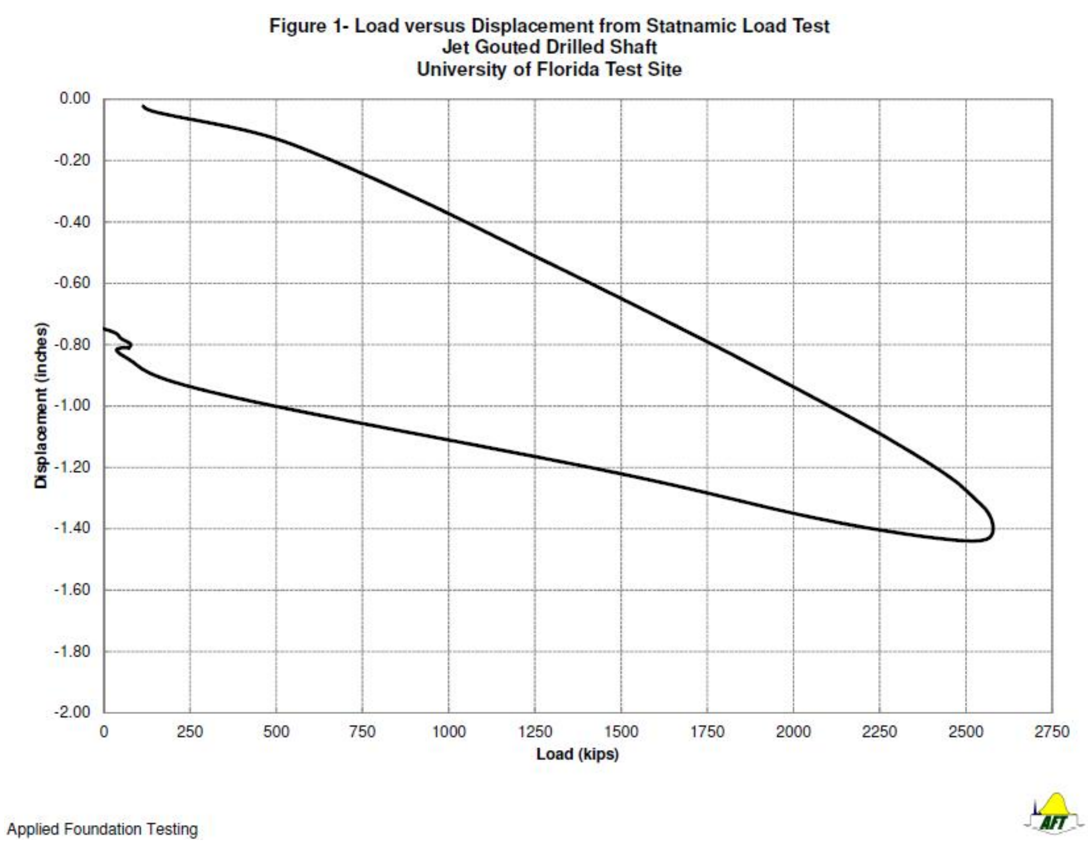

Figure 4-51: Applied load (Statnamic load) and displacement of field shaft during Statnamic load test

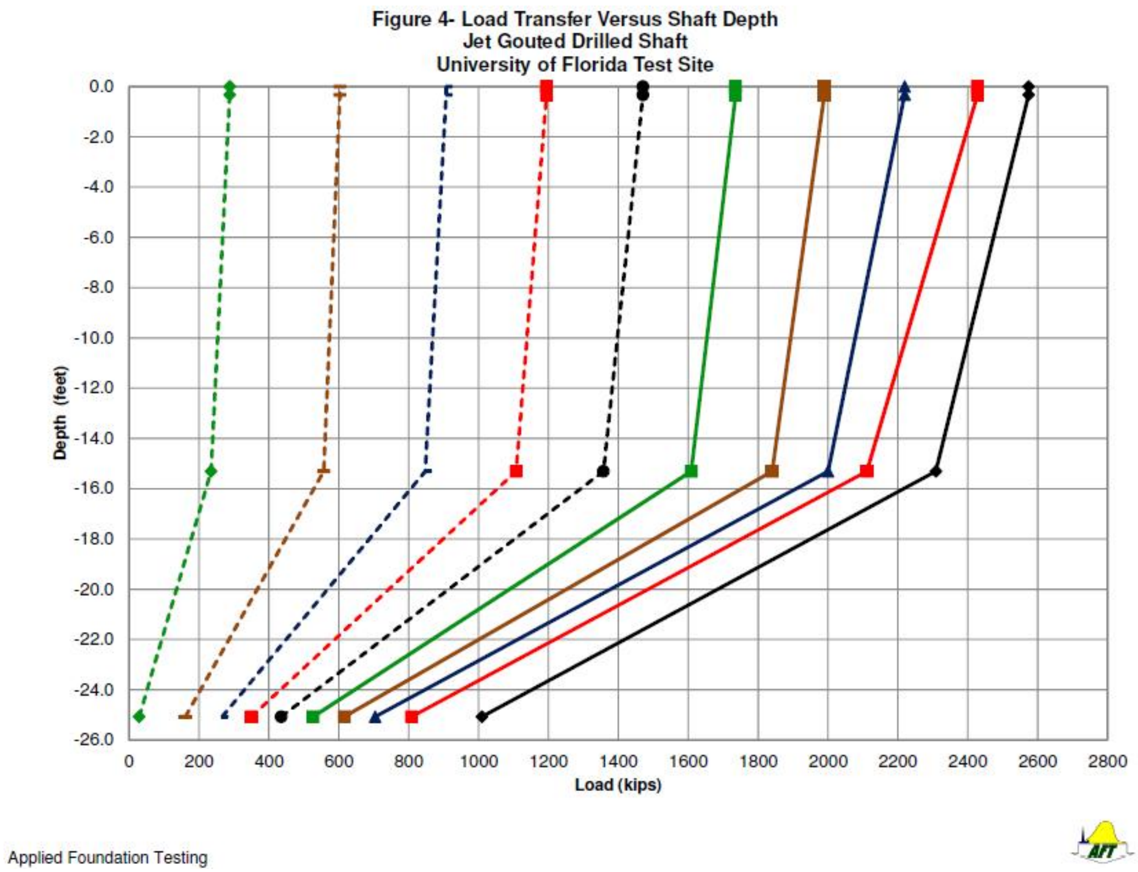

Figure 4-52: Load distribution (static load) during Statnamic load test of field shaft

Their results suggested that the side resistance of the whole shaft was fully mobilized during the test, which is shown by the parallel line in Figure 4-52 above. AFT's maximum static load applied was 2,600 kip with 1.45" of displacement, and the load distribution was separated as 1,600 kip attributed to side friction and 1,000 kip to end bearing. The 1,600 kip mobilized side resistance was further separated into 1,300 kip along the side grouted zone and 300 kip above the side grouted zone. Note the fully mobilized side friction in the top portion of the shaft (i.e., no side grouting; top ⅔ of shaft) during tip grouting and the top-down static load test was around 100 kip as shown in Figures 4-43 and 4-48. Interestingly in Figure 4-52 for the case of 920 kip static load (blue dashed line), the mobilized side friction above the side grout zone was approximately 70 kip, mobilized side friction along the side grout zone was approximately 575 kip, and the mobilized tip resistance was approximately 275 kip (similar to Figure 4-49 for the case of 850 kip static load).

The raw data collected by AFT (i.e., embedded strain and accelerometers) was also analyzed by UF and compared with AFT's analysis. Using the embedded strain and accelerometer data (top and bottom; Figure 4-53), nonlinear side friction algorithm was employed, and the static side resistance along the shaft was computed (Tran et al., 2011a) and shown in Figure 4-54. Note for the analysis, different cross-sectional areas (ungrouted and grouted) shaft sections were considered. Compared to 1,600 kip using the SUP method (300 kip – ungrouted; 1,300 – grouted zone), the ungrouted zone showed 200 kip of side resistance and the side grout zone mobilized 1,150 kip for a total of 1,350 kip of side resistance, as shown in Figure 4-54.

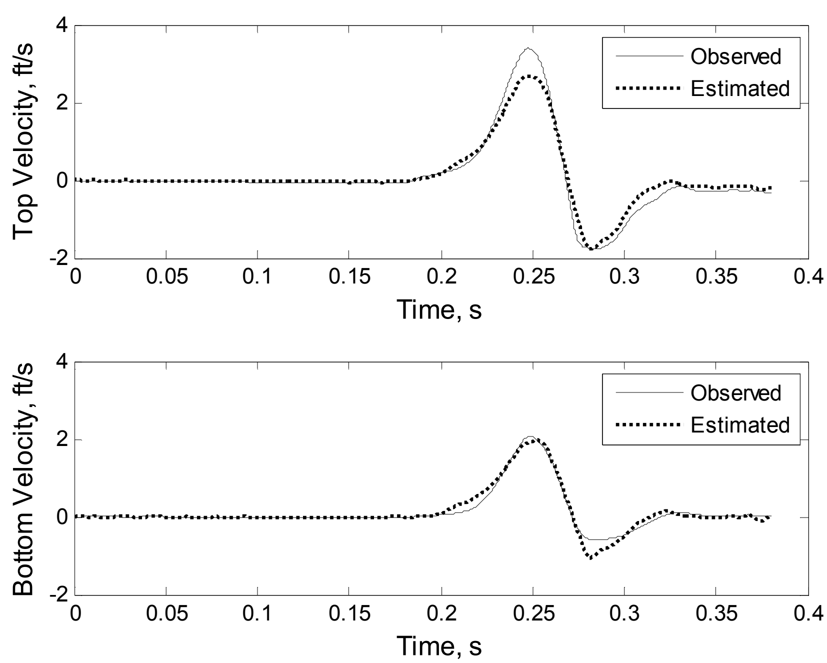

Figure 4-53: Match of measured vs. predicted velocities at top and bottom of shaft (Tran et al., 2011a)

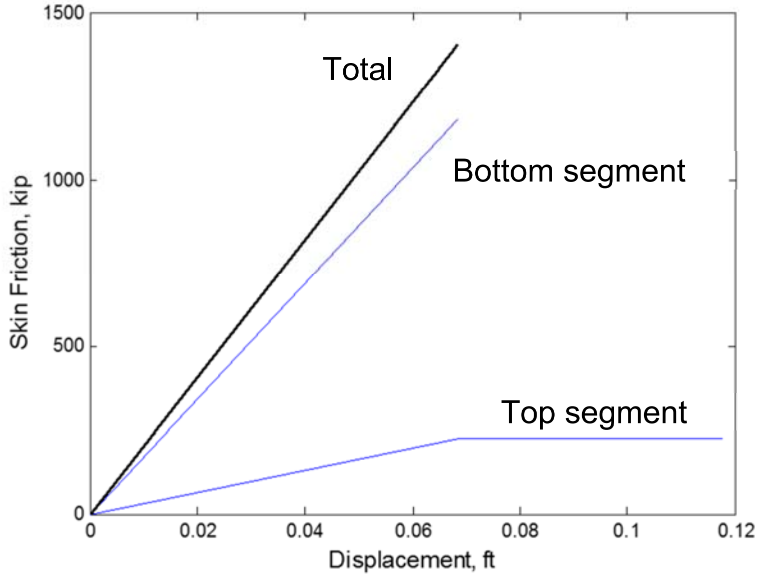

Figure 4-54: Mobilized side resistance during Statnamic load test using nonlinear side friction algorithm (Tran et al., 2011a)

Also using force and energy conservation algorithm (Tran et al., 2011b), the mobilized forces at the bottom of the shaft (tip) are shown in Figure 4-55. Here, two static load segments (loading and unloading) were employed. The peak static resistance (red line) from the algorithm was 1,200 kip.

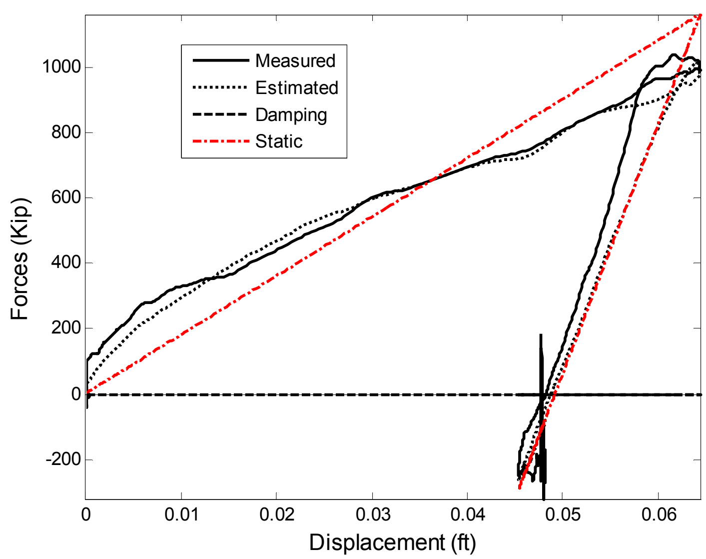

Figure 4-55: Mobilized tip resistance during Statnamic test using force and energy conservation algorithm (Tran et al., 2011b)

Due to the slight mismatch of the measured and estimated static force during unloading (right side of Figure 4-55), it was decided to perform a simple excel spreadsheet solution as shown by Figure 4-56. The excel spreadsheet used two segments for static loading and one segment for unloading. Evidently, the match between measured and predicted total forces (strain at tip) was quite good, even for the unloading phase (loop on the right). Note, the loop on the right is due the rapid loss of inertia force during the unloading phase. Also after unloading, a tension force of 200 kip existed one foot above the bottom of the shaft, which was accompanied with further unloading (i.e., displacement from -0.55" to -0.47"). This tension force supports the existence of a grout bulb at tip of the shaft and upward movement of the shaft/side grout zone relative to the tip movement. Note, the predicted static tip resistance (190 kip – excel; 300 kip – algorithm) were in good agreement with the static load test for the tip values of 241 kip at 0.18" of top movement (Figure 4-48).

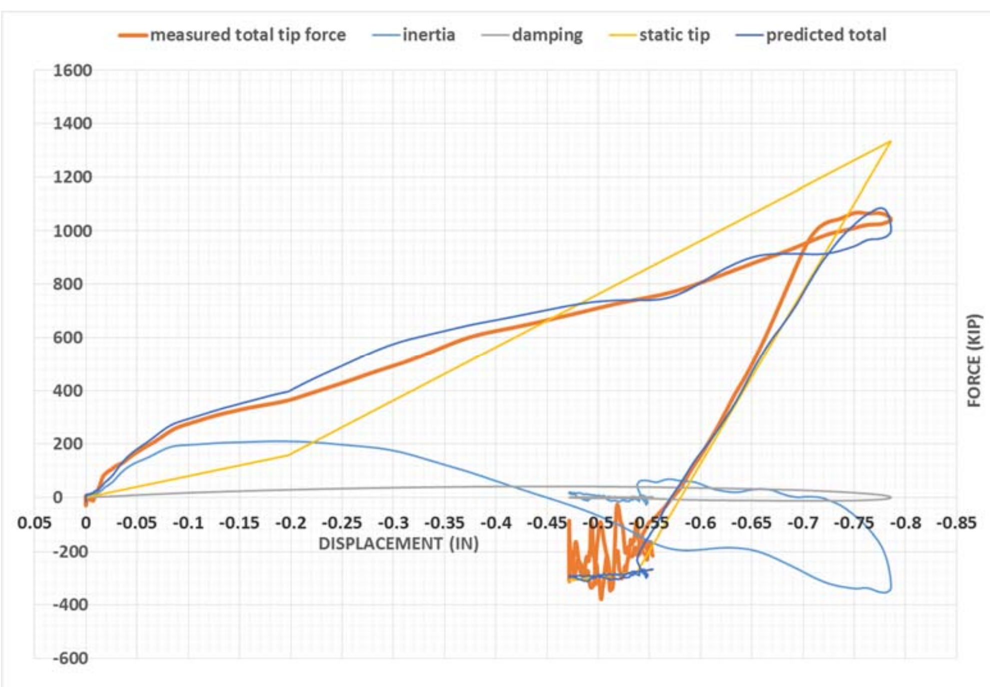

Figure 4-56: Tip forces using Excel spreadsheet

Using Tran's algorithms, a total resistance of 2,550 kip was estimated (1,350 kip side; 1,200 kip tip), whereas using the excel spreadsheet for tip (1,300 kip) and Tran's side resistance (1,350 kip), a total static resistance of 2,650 kip was computed. Applying the unloading point method to the whole shaft (Middendorp et al., 1992), an uncorrected static resistance of 2,850 kip was obtained and shown in Figure 4-57. Using a rate factor of 0.95 (Statnamic rate factor for sand = 0.91; FHWA, 2010), a total capacity of 2,700 kip was computed. It needs to be emphasized that even though the SUP method and newer algorithms gave similar total capacities of about 2,600 kip, their distribution were different (1,600 side; 1,000 tip – SUP vs. 1,350 side; 1,300 tip – algorithms). This difference is believed to be the results of using both top and tip strain gauges and accelerometer data to estimate shaft velocities, especially acceleration at the shaft's tip. It is highly recommended that independent top and bottom strain gauges and accelerometer be used when testing grouted shafts under Statnamic and/or dynamic loading conditions.

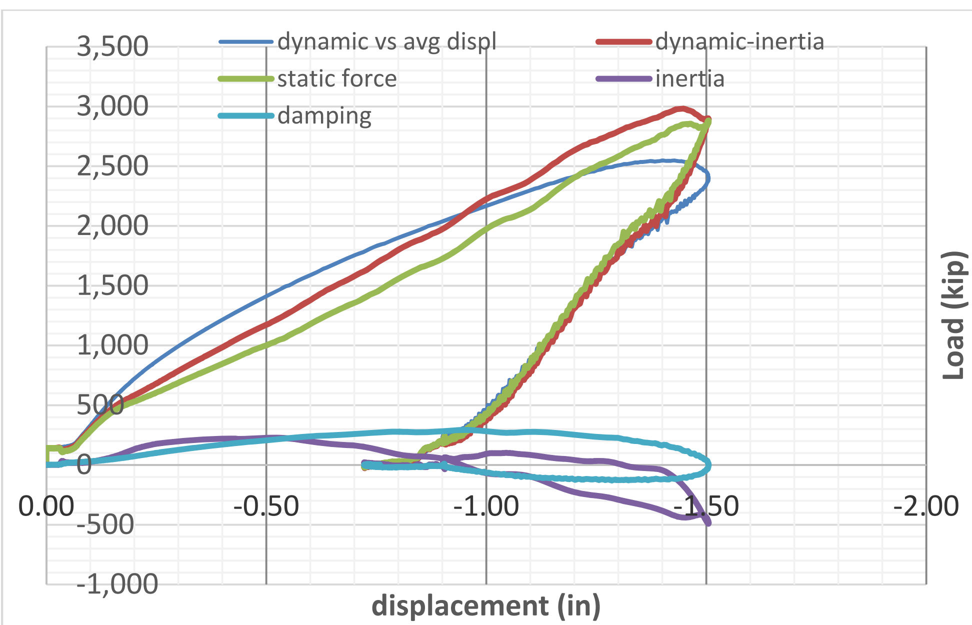

Figure 4-57: Statnamic analysis using unloading point method (Middendorp et al., 1992)

CHAPTER 5
PREDICTION OF GROUTING PRESSURES AND SHAFT RESISTANCES BASED ON IN SITU AND LABORATORY DATA

5.1 Side-and-Tip-Grouted Long Test Shaft (36" x 25')

The shaft had a total length of 26 feet with an embedment length of 25 feet, and the side grout zone length was nine feet (approximate bottom ⅓ of shaft). The original cross-sectional area was 1,018 in^2 (casing ID = 36"), and the planned grouted diameter along the side grouted zone was 54" (1 ½ D) or cross-sectional area of 2,290 in^2. The weight of the ungrouted shaft was estimated to be 14.3 ton (unit weight of concrete = 150 pcf).

5.1.1 Properties of Soil in Test Chamber

The FDOT test chamber was filled with a typical homogeneous Florida soil and compacted to have specified properties (i.e., moisture content, ω, relative density, D_r, and moist unit weight, γ_m). The soil used in the test chamber was a silty-sand (A-2-4) obtained from District 2 and used in previous research (FDOT BD545-031). The grain size distribution of the soil is shown in Figure 5-1 on the next page. The soil was placed in 18 inch lifts (see section 2.2.2) to obtain the following soil properties: moisture content of 7.5%, compacted relative density of 56%, average moist unit weight of 110 lb/ft^3, peak internal friction angle, Φ_p, of 33°, and a constant volume friction angle, Φ_{cv}, of 30° (direct shear testing). Three nuclear density tests were performed every four to five lifts by SMO personnel to verify the moisture content and wet and dry densities, and the average of the three tests are shown in Table 5-1 and plotted in Figure 5-2. For a maximum dry density of 110.4 lb/ft^3 (laboratory) and a placed average dry density of

102.3 lb/ft^3 (average nuclear density), the relative density, D_r, of the soil within the test chamber was estimated to be 56% (Table 5-2).

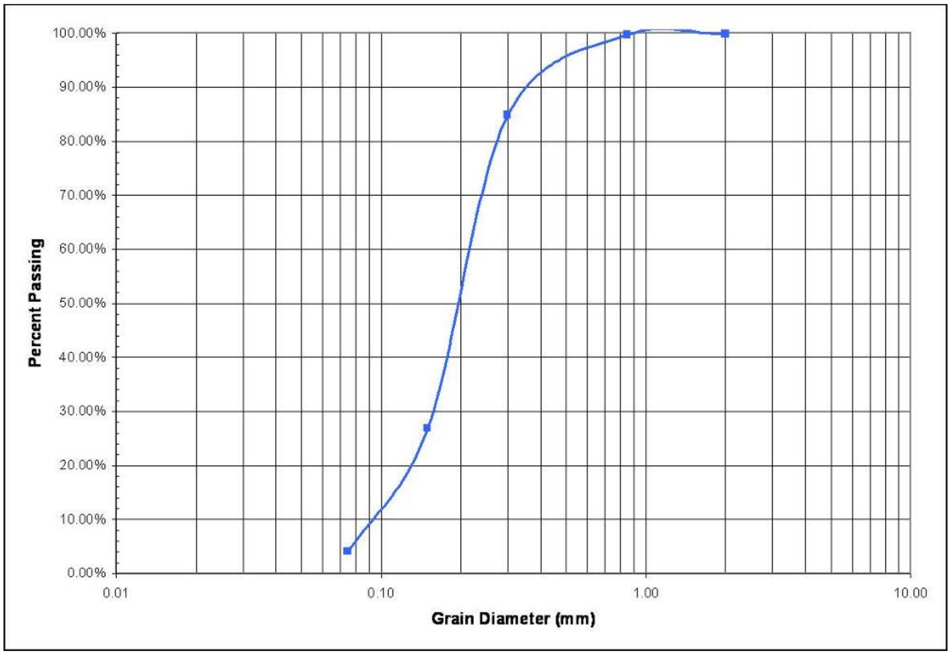

Figure 5-1: Grain size distribution of the soil used to fill FDOT test chamber (A-2-4)

Table 5-1: Nuclear density tests throughout soil placement in FDOT test chamber

FDOT 12" Nuclear Density Test

Site Visit	Soil Lift	Depth to Soil Lift (ft)	Test #	Wet Density (lb/ft^3)	Dry Density (lb/ft^3)	Moisture Content (%)
1	3	20	1	108.6	102.8	5.7
			2	109.4	101.4	8
			3	109.5	101.5	8
			4	109.1	102.8	6.1
			Avg.	**109.2**	**102.1**	**7.0**
2	8	11.375	1	108.7	100.7	7.9
			2	108.5	101.3	7.1
			3	108.9	102.3	6.5
			4	109.6	102.7	6.7
			Avg.	**108.9**	**101.8**	**7.1**
3	12	5.1667	1	111.4	102.9	8.2
			2	112.8	103.9	8.5
			3	112.5	103.7	8.5
			4	110.2	101.5	8.6
			Avg.	**111.7**	**103.0**	**8.5**

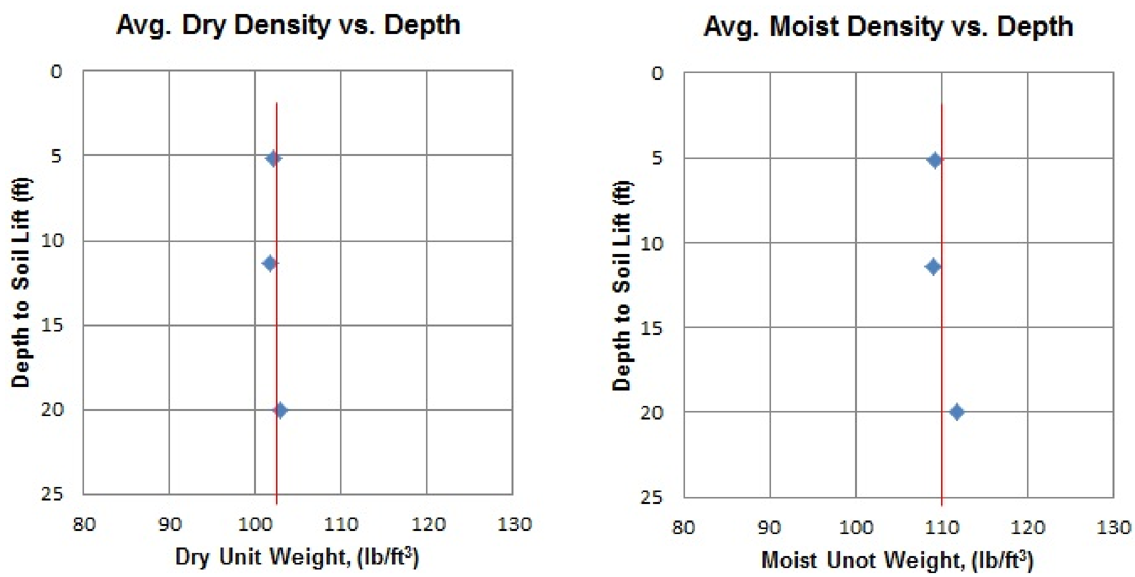

Figure 5-2: Average results for nuclear density tests with depth in chamber

Table 5-2: Calculation of relative density throughout test chamber

Compacted:											**Maximum**
Container	dry wt(g)	full wt (g)	wt of soil	ht-1	ht-2	ht-3	ht-4	Avg. ht	Vol (m^3)	Unit Wt (kg/m^3)	Unit Wt (lb/ft^3)
"1-2"	3604	7746	4142	24	25	29	27	26.25	0.002352	1761.300	109.954
"1-1"	3690	8150	4460	18	21	19	15	18.25	0.002498	1785.574	111.470
"1-1"	3690	7878	4188	25	23	25	25	24.5	0.002384	1756.979	109.685
										Average	110.4

Loose:						**Minimum**
Container	dry wt (g)	full wt (g)	wt of soil (g)	Vol (m^3)	Unit Wt (kg/m^3)	Unit Wt (lb/ft^3)
"1-2"	3604	7797	4193	0.002831	1481.029	92.458
"1-1"	3690	7978	4288	0.002831	1514.585	94.552
					Average	93.5

Dry Density	**Relative Density**
102.3	**56.2**

5.1.2 Estimated Axial Capacity of Ungrouted Shaft

Using the average moist unit weight (109.9 lb/ft^3) and peak internal friction angle (33°), the lateral earth pressure coefficient for the at rest condition was given by equation 5.1 and shown in Table 5-3 on the next page. The vertical, lateral, and mean stresses were estimated down to a depth of 26 feet using equations 5.2 to 5.4 and shown in Table 5-4. The calculated geostatic stresses were found to be comparable to the measured values (pressure cells) and within ± two psi. Next, the relative density and overburden pressures (vertical stresses) were used to estimate SPT blow counts every two feet along the depth of the test chamber (Holtz and Kovacs, 1981), as shown in Figure 5-4 on the next page.

$$K_0 = 1 - \sin \Phi_p \tag{5.1}$$

Table 5-3: Final in situ soil properties within FDOT test chamber

Moist Unit Weight, γ (lb/ft^3)	109.9
Peak Friction Angle, Φ_p (°)	33
Constant Volume Friction Angle, Φ_{cv} (°)	30
At Rest Lateral Earth Pressure Coefficient*, K_0	0.46

$$Overburden\ Pressure,\ \sigma_v\ \left({}^{lb}/_{in^2}\right) = \frac{\gamma\ x\ z}{144\left({}^{in^2}/_{ft^2}\right)} \tag{5.2}$$

$where$:

$\gamma\ is\ the\ soil\ unit\ weight\ \left({}^{lb}/_{ft^2}\right)$

$z\ is\ the\ depth\ below\ soil\ surface\ (ft)$

$$Lateral/Horizontal\ Earth\ Pressure,\ \sigma_h\ = K_0\ x\ \sigma_v \tag{5.3}$$

$where$:

$K_0\ is\ given\ by\ equation\ 5.1$

$$Mean\ Earth\ Pressure,\ \sigma_m\ = \frac{(2\ x\ \sigma_h) + \sigma_v}{3} \tag{5.4}$$

Table 5-4: Initial stress state within FDOT test chamber

Depth, z (ft)	Overburden Pressure, σ_v (lb/in^2)	Lateral Earth Pressure, σ_h (lb/in^2)	Mean Earth Pressure, σ_m (lb/in^2)
0	0	0	0
2	1.5	0.7	1.0
4	3.1	1.4	1.9
6	4.6	2.1	2.9
8	6.1	2.8	3.9
10	7.6	3.5	4.9
12	9.2	4.2	5.8
14	10.7	4.9	6.8
16	12.2	5.6	7.8
18	13.7	6.3	8.7
20	15.3	7.0	9.7
22	16.8	7.6	10.7
24	18.3	8.3	11.7
26	19.8	9.0	12.6

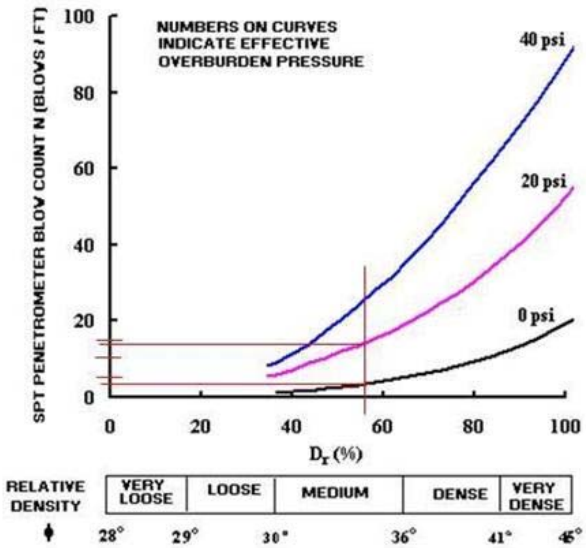

Depth, z (ft)	Overburden Pressure, σ_v (lb/in^2)	SPT Blow Count, N (blows/ft)
0	0	0
2	1.5	2
4	3.1	3
6	4.6	4
8	6.1	5
10	7.6	6
12	9.2	7
14	10.7	8
16	12.2	9
18	13.7	10
20	15.3	11
22	16.8	12
24	18.3	13
26	19.8	14

Figure 5-4: Estimated SPT blow counts within FDOT test chamber

Generally for a conventional ungrouted drilled shaft (3' x 25'), the SPT blow counts are used to estimate the unit side resistance, e.g., beta method (FDOT, 2012; FHWA, 2010), and unit end bearing (Reese and O'Neill, 1988). For the analysis, the shaft was divided into seven sections, having four sections above the side grouted zone (each four foot thick) and three sections along the planned side grouted zone (two four foot thick and a single one foot thick). Using equations 5.5 to 5.9, the average unit side friction for each section was estimated at the midpoint of layer (i.e., depth of two, six, 10, 14, 18, 22, and 24.5 foot), as shown in Table 5-6. The estimated ultimate side resistance was 28.9 ton above the side grouted zone (top ⅔ of shaft) and 63.9 ton along the side grouted zone (bottom ⅓ of shaft) for a total side resistance of 92.7 ton.

Table 5-5: Shaft dimensions before grouting

Shaft Diameter, D (ft)	3
Shaft Embedment Length, L_E (ft)	25
Circumference of Shaft, Ci (ft)	9.42
Surface Area of Shaft, SA (ft^2) (4 Foot Length)	37.70
Surface Area of Shaft, SA (ft^2) (1 Foot Length)	9.42

$$Beta\ Value,\ \beta\ =\ 1.5 - 0.135\sqrt{z} \tag{5.5}$$

$where:$

$z\ is\ the\ depth\ below\ soil\ surface\ (ft)$

$$Corrected\ Beta\ Value,\ \beta_1\ =\ \frac{N}{15}\ x\ \beta \tag{5.6}$$

$where:$

$N\ is\ the\ SPT\ Blow\ Count\ Number\ \left(\frac{blows}{foot}\right)$

$$Unit\ Skin\ Friction,\ f_s\ \left({}^{lb}/_{ft^2}\right) =\ \sigma_v\ x\ \beta_1 \tag{5.7}$$

$where:$

$\sigma_v\ is\ Overburden\ Pressure\ \left({}^{lb}/_{ft^2}\right)$

$$Mobilized\ Side\ Resistance,\ F_s\ (ton) = \frac{f_s\ x\ SA}{2000\ ({}^{lb}/_{ton})} \tag{5.8}$$

$where:$

$SA\ is\ the\ Shaft\ Surface\ Area\ (ft^2)$

$$Total\ Side\ Resistance,\ Q_s\ (ton) =\ \sum F_s \tag{5.9}$$

Table 5-6: Side resistance of long shaft before grouting

Considering 4 Foot Thick Soil Layers along Shaft (Last Soil Layer is 1 Foot Thick)								
Depth, z (ft)	SPT Blow Count, N (blows/ft)	Beta Values, β	Corrected Beta Values, β_1	Depth to Mid-Point of Soil Layer (ft)	Overburden Pressure, σ_v (lb/ft^2)	β_1 at Mid-Point of Soil Layer	Unit Side Resistance, f_s (lb/ft^2)	Mobilized Side Resistance, F_s (ton)
0	0	1.2	0	2	219.8	0.16	35.17	0.7
2	2	1.2	0.16					
4	3	1.2	0.24					
6	4	1.17	0.31	6	659.4	0.31	205.61	3.9
8	5	1.12	0.37					
10	6	1.07	0.43	10	1099	0.43	471.73	8.9
12	7	1.03	0.48					
14	8	0.99	0.53	14	1538.6	0.53	816.38	15.4
16	9	0.96	0.58					
18	10	0.93	0.62	18	1978.2	0.62	1222.85	23.1
20	11	0.90	0.66					
22	12	0.87	0.69	22	2417.8	0.69	1676.59	31.6
24	13	0.84	0.73					
26	14	0.81	0.76	24.5	2692.6	0.73	1957.00	9.2
Total Side Resistance, Q_s (tons) =								**92.7**

Reese and O'Neill (1988) expressed mobilized tip resistance of drilled shafts as a function of the shaft diameter and permissible settlement (Figure 1-2). At a defined settlement of 5% the shaft diameter, the unit end bearing of the shaft is given by equation 5.10. The total end bearing is simply the unit end bearing multiplied by the tip area. An uncorrected SPT blow count of 14 was used to estimate the bearing capacity (58.9 ton). Note, the nine feet of soil between the tip of the shaft and concrete bottom of the test chamber was considered sufficient to not affect tip resistance. The estimated total capacity of the ungrouted shaft was 151.6 ton (side - 92.7 ton; tip - 58.9 ton).

$$Mobilized\ End\ Bearing,\ q_b\ (MPa) = 0.057\ x\ N \tag{5.10}$$

$$where:$$

$$N\ is\ the\ SPT\ Blow\ Count\ Number\ \left(\frac{blows}{foot}\right)$$

5.1.3 Estimated vs. Measured Grout Volumes

The volume of grout needed to fully inflate the membrane seals were estimated given the known dimensions of the layflat hose (i.e., six inch ID and cut length). The length of the lay flay hose used to fabricate both seals was 170 inches, so the estimated volume of grout needed was 2.8 ft^3 (20.9 gal). To avoid seal failure, it was planned to stop grouting once the volume approached 90% of the calculated volume (18.8 gal). The actual volume of grout pumped into the bottom seal was 17.5 gal and actual volume of grout pumped into the top seal was 18.1 gal.

The volume of grout needed to generate the desired side grout zone was estimated assuming a perfectly cylindrical shape from an initial shaft diameter of three feet to a final grout bulb diameter of four-and-a-half feet (1 ½ D). The area of grout needed to expand ($Area_{D = 4 \frac{1}{2} feet}$ – $Area_{D = 3 feet}$) multiplied by the side grout zone height of nine feet gave a volume of grout as 79.5 ft^3 (594.8 gal). Since both the top and bottom of the membrane were pleated (connected to rings cast in shaft), there was 10% to 20% of the theoretical calculated volume lost. To avoid the possibility of failure of the side membrane due to pleats, irregularities in membrane expansion, etc., pumped volumes in excess of 70% of the theoretical calculated volume, i.e., 55.7 ft^3 (416.4 gal), were considered acceptable. Recalling from the actual construction when side grouting stopped, the pumped volume was 425 gal (i.e., 71% of theoretical), excessive upward movement of the shaft had occurred, and side grout pressures were in excess of 600 psi were observed. The additional side grout (425 gal) adds 20% to the self-weight of the grouted shaft (i.e., 4.1 ton for a total of 18.4 ton after side grouting).

The volume of grout needed to grout the tip was estimated assuming a perfectly spherical grout bulb and a final grout bulb diameter of four-and-a-half feet (1 ½ D or a diameter equivalent to the side grout zone) and calculate to be 47.7 ft^3 (357 gal). To limit the influence of bearing effects of the enlarged side grout zone (i.e., ledge/shelf at the top of side grouted zone), tip grouting was to be stopped if upward shaft displacement exceeded 1%. That is, upward movements less than 0.3" to 0.4" would only mobilize side friction along the soil-membrane interface and not the end bearing on the enlarged grout zone. The actual volume of grout pumped was 180 gal (50%) when upward movement of the shaft were between 0.3" and 0.4". Interestingly, the grout tip pressure did approach the spherical cavity limit pressure due to rigid boundary effects (see section 5.1.4).

5.1.4 Estimated vs. Predicted Grout Pressures

The expansion of the membrane seals are not perfectly spherical or cylindrical due to their deformed shape and stress distribution. For instance, spherical expansion results in equal all around stresses, whereas cylindrical expansion results in stresses that are equal in two directions. Membrane seals expand outward as a wedge (i.e., bearing capacity) with resistance less than cylindrical cavity expansion, unless the seal pushes the membrane outward forming a cylinder. Consequently, a conservative estimated stress was the cylindrical cavity expansion values (i.e., > max stresses). Considering the top seal, the soil's initial lateral stress was 5.2 psi (36 kPa) at a depth of 15 feet (depth to top seal). For the bottom seal, the initial lateral stress was 8.7 psi (59.9 kPa) at a depth of 25 feet (depth to bottom seal). From Figure 5-6 (Salgado and Randolph, 2001), the predicted cylindrical cavity limit pressure was 204 psi (1,400 kPa) for the top seal and 297 psi (2,050 kPa) for the bottom seal. The measured maximum pressure while grouting the top seal was 110 psi (< 204 psi) and maximum pressure while grouting the bottom seal was 220 psi (< 297 psi). Note, even though the seals did not expand outward fully, i.e., 86% of the theoretical calculated maximum volume, the cylindrical cavity expansion estimation for seals were reasonable and are recommended for layflat hose selection (i.e., estimate pressure of membrane seals).

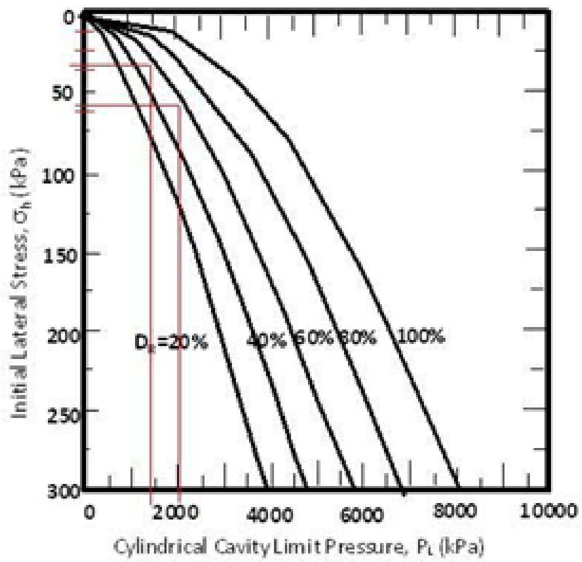

Figure 5-5: Cylindrical cavity limit pressure at depth of 15' and 25'

In the case of side grouting, cylindrical cavity expansion was also employed. Note, the top and bottom of the bag have seals beneath the membranes, which expanded once grouted to form upper and lower boundaries, i.e., rigid and soil (see sections 4.2.1 and 4.3.1). The predicted side grout pressure was estimated from the cylindrical cavity expansion limit pressure chart (Salgado and Randolph, 2001) at the mid-depth of the side membrane and shown in Figure 5-6. The initial soil's lateral stress was 7.3 psi (50.3 kPa) at a depth of 21 feet (depth to the middle of the side grouted zone), and the estimated limit pressure was 261.1 psi (1,800 kPa), as shown in Table 5-7. Recall, the maximum measured grout pressure at the end of side grouting of the long shaft was in excess of 600 psi, which was greater than the cylindrical cavity limit pressure. The high recorded grout pressure vs. theoretical limit pressure was attributed to boundary effects of the test chamber wall. This was identified in section 4.2.2 with large upward movement of the soil with the shaft and small relative movement between the shaft and soil (i.e., 0.076" at three feet away from the shaft).

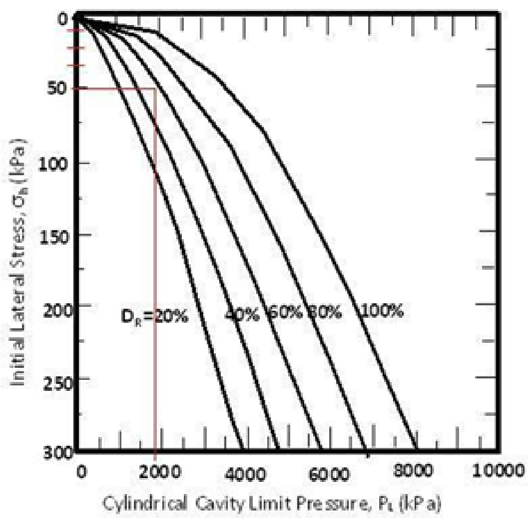

Figure 5-6: Cylindrical cavity limit pressure at depth of 21 feet

Table 5-7: Cylindrical cavity limit pressure during side grouting

Depth to Middle of Side Zone (ft)	Overburden Pressure, σ_v (lb/in^2)	Lateral Earth Pressure, σ_h (lb/in^2)	Lateral Earth Pressure, σ_h (kPa)	Cylindrical Cavity Limit Pressure (kPa)	Cylindrical Cavity Limit Pressure (lb/in^2)
21	16.0	7.3	50.3	1800	261.1

In the case of tip grouting, spherical cavity expansion chart (Salgado and Randolph, 2001) was used to estimate expected tip grout pressures based on an assumed shape. Using the initial mean stress of 12.1 psi (83.8 kPa) at a depth of 25 feet (depth to shaft tip), the spherical cylindrical cavity limit pressure of 783 psi (5,400 kPa) was found from Figure 5-7 and shown in Table 5-8.

During the design phase, a total upward resistance of 189.9 ton (171.5 ton - side resistance after side grouting; 18.4 ton - self-weight of side grouted shaft) was estimated based on the K_g method, see section 5.1.5 below. Consequently, the maximum expected grout pressure acting on the shaft's tip before upward movement occurs was 373 psi, which was less than the spherical cavity limit pressure. However as a result of the test chamber wall effects, the actual side grout pressure was 600 psi (i.e., doubling of side friction), which increased the required tip pressures to move the shaft upward. The recorded maximum tip grout pressure was 700 psi which closely agrees with the predicted spherical cavity limit pressure of 783 psi. Note, the measured stresses clearly illustrate the change in soil stress state at the tip of the shaft as identified in Figure 1-4, suggesting a significant increase in tip resistance over a conventional drilled shaft or even a shaft with only tip grouting.

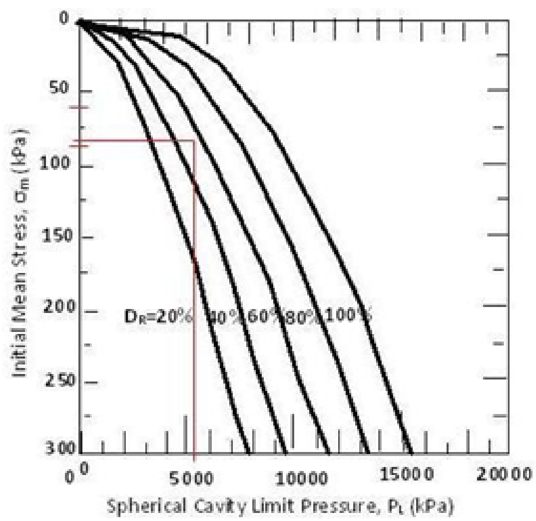

Figure 5-7: Spherical cavity limit pressure at depth of 25 feet

Table 5-8: Spherical cavity limit pressure during tip grouting

Depth to Tip (ft)	Overburden Pressure, σ_v (lb/in^2)	Lateral Earth Pressure, σ_h (lb/in^2)	Mean Earth Pressure, σ_m (lb/in^2)	Mean Earth Pressure, σ_m (kPa)	Spherical Cavity Limit Pressure (kPa)	Spherical Cavity Limit Pressure (lb/in^2)
25	19.1	8.7	12.2	83.8	5400	783.2

5.1.5 Estimated vs. Predicted Axial Capacity after Side Grouting

Assuming a side grouted zone from a depth of 16 feet to 25 feet (bottom ⅓ of shaft), the estimated side resistance of the shaft was calculated using the K_g method (Thiyyakkandi et al, 2013a; McVay et al., 2009; Figure 5-8). The increase in side resistance was calculated based on the in situ vertical stress at the center of three sections along the side grouted zone (two four foot soil layers and a single one foot layer), i.e., 18, 22, and 24 ½ feet depths. Given an increased surface area along the side grouting (1 ½ D), the resulting unit side resistance was calculated using equations 5.11 to 5.13 and 5.8 and 5.9 above, as shown in Tables 5-9 and 5-10. The mobilized side resistance along the side grouted zone was estimated to be 171.5 ton (142.7 ton along the side grouted zone; 28.8 ton along ungrouted zone). The total upward resistance of the shaft was estimated to be 189.9 ton (171.5 ton side resistance; 18.4 ton total self-weight after side grouting). As described in section 5.1.4 above, the measured side resistance during tip grouting was 385 ton (770 kip) and approximately two times the estimated, which was attributed to twice the expected side stresses due to the chamber wall effects.

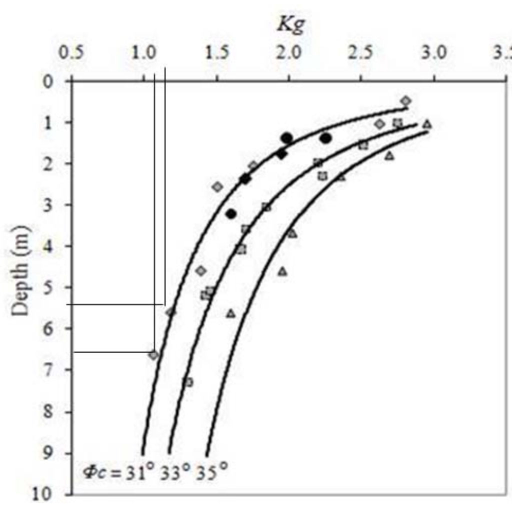

Figure 5-8: K_g coefficient chart (Thiyyakkandi et al., 2013a)

Table 5-9: Shaft dimensions after side grouting

Constant Volume Friction Angle, Φ_{cv} (°)	30
Shaft Diameter, D (ft)	4.5
Circumference of Shaft, Ci (ft)	14.14
Surface Area of Shaft, SA (ft^2) (4 Foot Length)	56.55
Surface Area of Shaft, SA (ft^2) (1 Foot Length)	14.14

$$Vertical\ Stress\ Coefficient,\ K_g = f(z, \Phi)\ (see\ above\ plot) \tag{5.11}$$

$$Vertical\ Stress\ Increase,\ \sigma_{vg} = K_g\ x\ \sigma_v \tag{5.12}$$

$$Unit\ Side\ Resistance,\ f_s = \sigma_{vg}\ x \left[\frac{\sin \Phi_{cv}}{1 - \sin \Phi_{cv}}\right] x\ \sin(90 - \Phi_{cv}) \tag{5.13}$$

Table 5-10: Side resistance of long shaft after side grouting

Depth, z (ft)	SPT Blow Count, N (blows/ft)	Beta Values, β	Corrected Beta Values, β_1	Depth to Mid-Point of Soil Layer (ft)	Overburden Pressure, σ_v (lb/ft^2)	Vertical Stress Coefficient, K_g	Vertical Stress Increase, σ_{vg} (lb/ft^2)	β_1 at Mid-Point of Soil Layer	Unit Side Resistance, f_s (lb/ft^2)	Mobilized Side Resistance, F_s (ton)
0	0	1.2	0	2	219.8	N/A	N/A	0.16	35.17	0.7
2	2	1.2	0.16							
4	3	1.2	0.24							
6	4	1.17	0.31	6	659.4	N/A	N/A	0.31	205.61	3.9
8	5	1.12	0.37							
10	6	1.07	0.43	10	1099	N/A	N/A	0.43	471.73	8.9
12	7	1.03	0.48							
14	8	0.99	0.53	14	1538.6	N/A	N/A	0.53	816.38	15.4
16	9	0.96	0.58							
18	10	0.93	0.62	18	1978.2	1.21	2393.6	N/A	2072.94	58.6
20	11	0.90	0.66							
22	12	0.87	0.69	22	2417.8	1.12	2707.9	N/A	2345.14	66.3
24	13	0.84	0.73							
26	14	0.81	0.76	24.5	2692.6	1.08	2908.0	N/A	2518.36	17.8
									Total Side Resistance, Q_s (tons) =	**171.5**

5.1.6 Estimated Axial Capacity of Side-and-Tip-Grouted Shaft

As was identified in Figure 4-26, the measured side resistance was 385 ton (770 kip). Since the grout exerts a bi-directional force, the mobilized tip resistance during tip grouting was at least 385 ton, and the total shaft capacity was least 770 ton (1,540 kip) or two times the observed mobilized side resistance. Due to the limited uplift capacity of the reaction shafts at the FDOT/UF test chamber (600 kip or 300 ton total uplift capacity), the ultimate capacity of the long shaft was never validated during the static load test (i.e., only 380 kip or 190 ton maximum applied load).

5.2 Side-and-Tip-Grouted Field Test Shaft (42" x 25')

5.2.1 Shaft Dimensions and Field In Situ Soil Properties

The constructed field test shaft had a diameter of three-and-a-half feet and an embedment length, L_E, of 25 feet (42" x 25') with a total length of 26 feet (one foot above soil surface). The predicted volume of concrete for shaft construction was 9.3 cubic yards (cy), but 10.3 cy of concrete was actually used to cast the field shaft with an estimated ungrouted shaft weight of 19.7 ton (concrete and steel). The length of the side grouted zone was about nine-and-a-half feet (approximate bottom ⅓ L_E). The proposed final diameter of the membrane seals, side membrane, and tip grout bulb was five-and-one-quarter feet (1 ½ D) or a final circumference of 16.5 ft.

The stratigraphy and soil properties were estimated using in situ test data (i.e., SPT, CPT, PMT, and DMT) and laboratory test results (i.e., tri-axial and direct shear tests). An open stand pipe located on site was used to estimate the depth of the water table which was approximately eight feet below the soil surface during shaft construction and load tests (static and Statnamic).

The in situ tests were performed by SMO personnel, and a plan view of SPT and CPT locations relative to the test shaft are shown in Figure 5-9. To minimize error due to the spatial variability, the SPT in the shaft footprint (B11) was used to identify various soil types and layer depths (i.e., stratigraphy; Table 5-11). Additional layer breaks were introduced at depths of 15 and 25 feet to separate soil above and alongside the grouted zone and below the shaft tip (i.e., zones along the shaft). The four layer breaks can be identified by the applicable color (e.g., blue = clay layer, rest are silty-sand), and the layer breaks and elevations along the field shaft were illustrated using an excel spreadsheet and shown in Figure 5-10. The first eight feet of soil (depth 0 – 8 ft) consisted of clayey sand mixtures with clays (fines greater than 50%) having a high plasticity index (PI), resulting in the first layer being treated as a clay (i.e., cohesive material). The soil at depths greater than eight feet consists of poorly graded sands and sand-silt mixtures, so all other layers were treated as sand (i.e., cohesionless material).

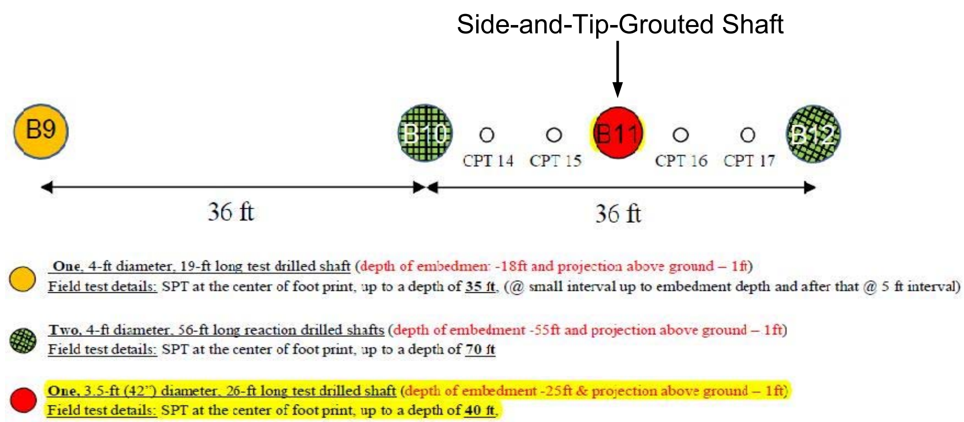

Figure 5-9: Plan view of SPT and CPT locations

Table 5-11: SPT in footprint of shaft (B11)

SAMPLE NUMBER	SAMPLE DEPTH (ft)	PERCENT MOISTURE	Percent Passing #10	#40	#60	#100	#200	LL / PI	ORGAN %	AASHTO CLASS	UNIFIED CLASS	SPT N-Value	Avg SPT N-Value	Soil Layers
B11														
1	1.0 - 2.5	15.9	100	98.3	92.9	48.3	33.1	26 / 11		A-2-6	SC	5	6.0	1
2	2.5 - 4.0	17.9	100	97.8	94.4	72.6	60.3	50 / 34		A-7-6	CH	7		
3	4.0 - 5.5	33.5	100	99.1	98.3	90.4	86.2	72 / 51		A-7-6	CH	5		
4	5.5 - 7.0	108.2	100	99.0	93.9	51.3	38.6	25 / 12	1.4	A-6	SC	6		
5	7.0 - 8.5	14.9										7		
6	8.5 - 10.0	19.7	100	99.5	94.8	26.7	7.8	N.P.		A-3	SP-SM	6	5.5	2
7	13.5 - 15.0	28.8	100	99.9	96.7	22.5	3.6	N.P.		A-3	SP	5		
8	18.5 - 20.0	27.6	100	100	99.0	32.3	5.1	N.P.		A-3	SP-SM	19	16.0	3
9	23.5 - 25.0	28.8	100	100	97.6	21.2	4.0	N.P.	2.7	A-3	SP	13		
10	28.5 - 30.0	27.1	100	99.3	95.8	29.5	3.8	N.P.	2.8	A-3	SP	27	55.0	4
11	33.5 - 35.0	26.2	100	99.0	90.6	23.2	5.2	N.P.	2.5	A-3	SP-SM	54		
12	38.5 - 40.0	28.3	100	99.3	94.4	24.5	4.6	N.P.		A-3	SP	84		

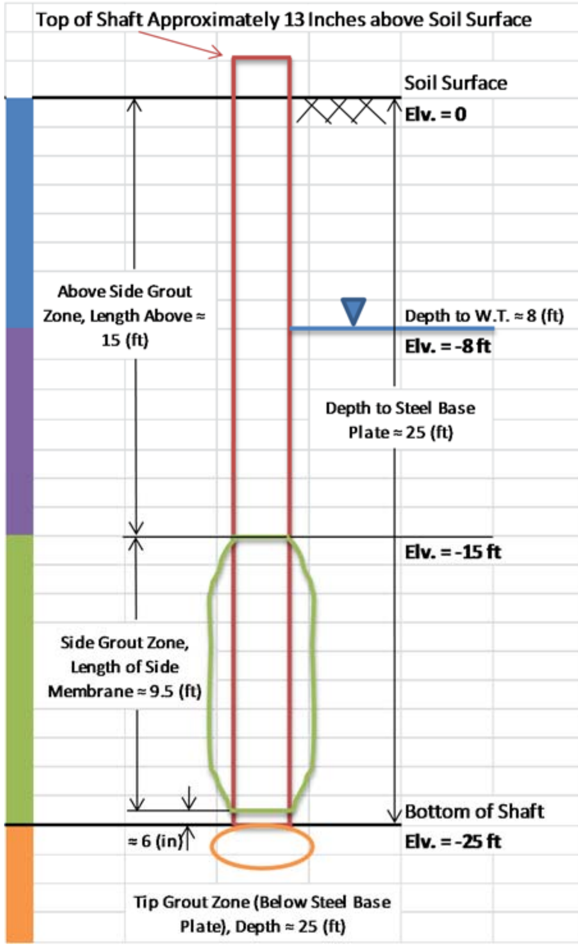

Figure 5-10: Illustration of soil stratigraphy and field test shaft with proposed side and tip grouted zones

The SPT data (B11) was used in conjunction with the four closest CPT (CPT 14, 15, 16, and 17) and DMT logs (DMT 1, 2, and 3) to estimate the soil properties. The assessment started with the DMT to estimate the unit weight of each soil layer (DMT results reported by SMO; Table 5-12). The final moist unit weights assigned to each soil layer is given in the last column in Table 5-12.

Table 5-12: DMT correlated friction angle and unit weight

		Phi				Unit Weight (psi)				
Layer	Depth	DMT 1	DMT 2	DMT 3	Avg.	DMT 1	DMT 2	DMT 3	Avg.	**Approx.**
1	0 - 8ft	39.1	37.1	39.8	38.7	115	115	113	114	**115**
2	8ft - 15ft	38	37.5	36	37.2	119	119	119	119	**120**
3	15ft - 25ft	39.7	39.9	38.8	39.5	126	124	122	124	**125**
4	> 25ft	---	40	40.4	40.2	---	131	131	131	**130**

Shown in Table 5-13 are the in situ estimations for each soil layer using direct shear and tri-axial test results that were performed on reconstructed spoon samples recovered from the site by SMO. Also shown in Table 5-13 are the calculated and estimated (graphically) fiction angles and relative densities. Using the estimated unit weights obtained from the DMT data, the initial effective vertical stress (i.e., overburden pressure) was computed. With the overburden stresses, the SPT data (corrected SPT blow counts) for each layer was used to calculate the angle of internal friction (Schmertmann, 1975) and relative density (Meyerhof, 1957). In addition to calculating soil properties, the friction angle and relative density was estimated graphically using plots presented in FB-MultiPier (Holtz and Kovacs, 1981). There was general agreement between the laboratory and the calculated/estimated results (Table 5-13).

Table 5-13: SPT correlated friction angle

Soil Layer (#)	Depth (ft)	Avg. Uncorrected Blow Count (N-Value)	Avg. Corrected Blow Count (N_{60})	(1) Direct Shear Ultimate Friction Angle, ϕ_u	(2) Tri-Axial Peak Friction Angle, ϕ_p	(3) Tri-Axial Ultimate Friction Angle, ϕ_u	(4) Calculated Friction Angle, ϕ'	(5) Relative Density (%)	(6) Friction Angle, ϕ	(7) Relative Density (%)
1	0 - 8	6	6	27.1	---	---	35.3	52	---	---
2	8 - 15	5.5	5.83	27.9	---	---	32.1	44	35	60
3	15 - 25	16	19	---	41.2	36.2	41.3	73	39	75
4	25 - 40	55	72.73	---	---	---	51.9	127	45	> 100

(1) Ultimate Friction Angle Calculated from Direct Shear Test (SPT Lab Results)

(2) Peak Friction Angle Calculated from Tri-Axial Test (A-3 Sand)

(3) Ultimate Friction Angle Calculated from Tri-Axial Test (A-3 Sand)

(4) Schmertmann (1975), ϕ' (°) = $\tan^{-1}[N_{60}/(12.2 + 20.3*(\sigma_v'/P_a))]^{0.34}$

(5) Meyerhof (1957), D_r (%) = $[N_{60}/(17 + 24*(\sigma_v'/P_a))]^{0.5}$

(6) Friction Angle Obtained Graphically (MultiPier)

(7) Relative Density Obtained Graphically (MultiPier)

Note: Atmospheric Pressure, P_a = 14.70 psi

The CPT data closest to the test shaft (CPT 14, 15, 16, and 17) was also considered. The data was divided into four soil layers (same as SPT soil layers) and averaged across each layer (Figure 5-11). The average cone tip resistance, q_c, for each layer was calculated and used to estimate the peak friction angle for each layer (Kulhawy and Mayne, 1990; Table 5-14). The peak friction angle calculated from Kulhawy and Mayne (1990) agreed with the friction angles found using the SPT data. The average cone tip resistance and DMT data were also used to estimate the OCR for each soil layer using an iterative process (Mayne, 2007; Kulhawy and Mayne, 1990). The average OCR from the DMT data was used as an initial input and the at-rest lateral earth pressure coefficient, K_0, and the final OCR was calculated using the two equation defined by Kulhawy and Mayne (1990). A summary of all in situ property estimations, e.g., friction angles using SPT, CPT, and DMT, is shown in Table 5-15. Based on the different estimates, the final friction angles and in situ stresses used to calculate grout stresses (i.e., cavity expansion limit pressures), shaft capacities (before and after grouting), and other data reduction is presented in Table 5-16. Note, the values are shown at the center of the layers and represent average values.

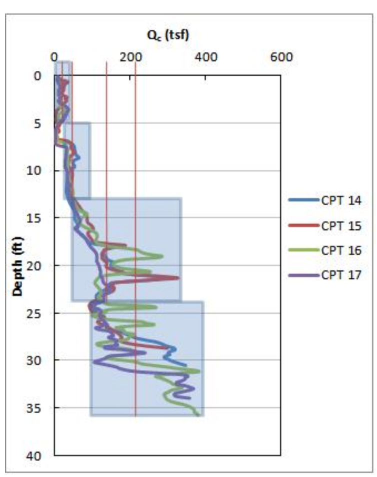

Figure 5-11: CPT data collected near test shaft

Table 5-14: CPT correlated friction angle

Layer (Depth)	CPT	Avg. Tip Resistance, Q_c (tsf)	Avg. Side Resistance, F_c (tsf)	Avg. Friction Ratio, F_c/Q_c (%)	(1) Peak Friction Angle, Φ_{tc}
Layer 1 (0 - 8 ft)	CPT 14	20.36	0.54	3.95	35.4
	CPT 15	20.58	0.74	4.83	35.4
	CPT 16	15.20	0.51	4.20	34.0
	CPT 17	16.11	0.53	5.09	34.2
	Avgersge	**18.06**	**0.58**	**4.52**	**34.8**
Layer 2 (8ft - 15ft)	CPT 14	44.39	0.52	1.18	37.0
	CPT 15	52.85	0.63	1.19	37.8
	CPT 16	48.55	0.56	1.14	37.4
	CPT 17	41.43	0.59	1.40	36.6
	Avgersge	**46.80**	**0.57**	**1.23**	**37.2**
Layer 3 (15ft - 25ft)	CPT 14	128.05	1.68	1.23	41.1
	CPT 15	135.11	1.85	1.24	41.4
	CPT 16	145.38	1.58	1.05	41.7
	CPT 17	107.89	1.15	1.10	40.3
	Avgersge	**129.10**	**1.57**	**1.15**	**41.2**
Layer 4 (> 25ft)	CPT 14	232.34	2.76	1.14	43.0
	CPT 15	167.34	1.77	1.02	41.4
	CPT 16	252.39	3.04	1.15	43.4
	CPT 17	209.49	2.43	1.07	42.5
	Avgersge	**215.39**	**2.50**	**1.10**	**42.6**

(1) Kulhawy and Mayne (1990), $\Phi_{tc} = 17.6 + \{11.0 * \log[(Q_c/P_a)/(\sigma_v'/P_a)^{0.5}]\}$

Note: Atmospheric Pressure, P_a = 14.70 psi

Table 5-15: Summary of correlated properties

Soil Layer (#)	Depth (ft)	(1) SPT			(2) CPT				(3) DMT		
		ϕ (Lab)	ϕ (Calc.)	ϕ (Graph)	ϕ (Calc.)	ϕ (Graph)	OCR (Iter.)	K_0 (Calc.)	Avg. ϕ	Avg. OCR	Avg. K_0
1	0 - 8	---	35.3	---	34.8	40	2.7	0.75	38.7	19.2	1.8
2	8 - 15	---	32.1	35	37.2	40	2.2	0.67	37.2	8.7	1.1
3	15 - 25	41.2	41.3	39	41.2	43	4.2	0.88	39.5	10.5	1.2
4	> 25	---	51.9	45	42.6	43	4.1	0.86	40.2	14.3	1.4

(1) Estimated Friction Angle - Tri-Axial Test Resuts (Lab), Schmertmann 1975 (Calculated), & MultiPier (Graphically)

(2) Estimated Friction Angle - Kulhawy and Mayne 1990 (Calculated) and MultiPier (Graphically)

Estimated OCR - Kulhawy and Mayne 1990 (Iterative) and Estimated K_0 - Mayne and Kulhawy 1982 (Calculated)

(3) Average DMT Data - OCR and K_0

Table 5-16: Final soil properties and in situ stresses

Soil Layer (#)	Depth (ft)	Depth to Mid-Point of Soil Layer (ft)	Peak Friction Angle, ϕ_p	Ultimate Friction Angle, ϕ_u	Final Unit Weight (lb/ft^3)	Vert. Effective Stress, σ_v' (lb/ft^2)	Vert. Effective Stress, σ_v' (lb/in^2)	(1) Lateral Earth Pressure Coef., K_0	Horiz. Effective Stress, σ_h' (lb/ft^2)	Horiz. Effective Stress, σ_h' (lb/in^2)
1	0 - 8	4	35	---	115	460	3.2	0.43	196.2	1.4
2	8 - 15	11.5	35	---	120	1122	7.8	0.43	478.3	3.3
3	15 - 25	20	41.2	36.2	125	1636	11.4	0.34	558.5	3.9
4	25 - 40	32.5	41.2	---	130	2456	17.1	0.34	838.3	5.8

(1) Lateral Earth Pressure Coefficient (Jaky 1960), $K_0 = 1 - \sin(\phi_p)$

5.2.2 Estimated Axial Capacity of Ungrouted Drilled Shaft

Capacity calculations were made for a similar sized ungrouted conventional drilled shaft (i.e., 42" x 26' with 25' embedment depth) and compared to the side-and-tip-grouted drilled shaft (side grout bulb along the bottom 10'). For the ungrouted conventional drilled shaft, unit side resistance was calculated using the alpha method for the top clay layer and beta method for the sand layers (FHWA 2010; AASHTO, 2010). These calculations are given in Table 5-17 (alpha) for the clay and Table 5-18 (beta) for the sands. The estimated total side resistance of an ungrouted drilled shaft was 243 kip (Table 5-19). The side resistance in the clay layer was q_{s1} (0' to 8'), first sand layer was q_{s2} (8' to 15'), and second sand layer was q_{s3} (15' to 25').

Table 5-17: Alpha method

Layer (#)	Soil Type	Depth (ft)	Depth to Mid-Point of Zone, z (ft)	Avg. Cone Tip Resist., Q_c (ton/ft^2)	Vertical Stress, σ_v (lb/ft^2)	Undrained Shear Strength, C_u (kip/ft^2)	(1) Alpha Value, α	(2) Unit Side Resistance, f_{su1} (kip/ft^2)	Surface Area (Top 8 ft), A_{side1} (ft^2)	Side Resistance (Top 8 ft), (kip)	
1	Clay	0 - 8	4	18.06	460	1	0.55	0.55	87.96	48	$= q_{s1}$

(1) $\alpha = 0$ (if z < 5 ft); $\alpha = 0.55$ (if z > 5 ft); $\alpha = 0$ (bottom of shaft for 1 diameter length & length of casing)

(2) Ultimated Unit Load Transfer in Side Resistance, $f_{su} = \alpha * C_u$

Table 5-18: Beta method

Layer (#)	Soil Type	Depth (ft)	Depth to Mid-Point of Zone, z (ft)	Avg. Uncorrected Blow Count (N-Value)	Vertical Effective Stress, σ_v' (lb/ft^2)	(1) Beta Value (β_0)	(2) Corrected Beta Value (β)	(3) Unit Side Resistance, f_s (kip/ft^2)	Surface Area, A_{side} (ft^2)	Side Resist., q_s (kip)	
2	Sand	8 - 15	11.5	5.5	1122	1.0422	0.3821	0.43	77	33	$= q_{s2}$
3	Sand	15 - 25	20	16	1636	0.8963	0.8963	1.47	110	161	$= q_{s3}$
4	Sand	25 - 40	32.5	55	2456	0.7304	0.7304	1.79	N/A	N/A	

(1) $\beta_0 = 1.2$ (if z < 5 ft); $\beta_0 = 1.5 - 0.135\sqrt{z}$ (if 5 ft < z < 86 ft); $\beta_0 = 0.25$ (if z > 86 ft)

(2) Corrected Beta, $\beta = (N/15)*\beta_0$ (if N < 15)

(3) Unit Side Resistance, $f_s = \beta*\sigma_v'$

Table 5-19: Summary of side resistance for ungrouted drilled shaft

Side Resistance above Side Grouted Zone, $Q_{s\text{-}above}$ (kip)	81	$= q_{s1} + q_{s2}$
Side Resistance along Side Grouted Zone, $Q_{s\text{-}along}$ (kip)	161	$= q_{s3}$
Total Side Resistance, $Q_{s\text{-}Total}$ (kip)	**243**	$= q_{s1} + q_{s2} + q_{s3}$

The estimated tip resistance (settlement 5% of diameter) was 323 kip, estimated using the average of SPT blow counts one and a half diameters above and three diameters below the shaft's tip (AASHTO, 2010) as shown in Table 5-20. Summing the side and tip resistance, the capacity of the ungrouted shaft was 566 kip and will be used in later sections for comparison with the grouted shaft response.

Table 5-20: Estimated tip resistance for ungrouted drilled shaft

Tip Area, A_T (in^2)	1385.44
Tip Area, A_T (ft^2)	9.62
(1) Avgerage Tip N-Value	28
(2) Unit Tip Resistance, q_T (ton/ft^2)	16.8
(3) Tip Resistance, Q_T (kip)	323
(1) Average N-Value of Soil 1.5*D above Tip down to 3*D below Tip	
(2) Unit Tip Resistance (AASHTO 2007), q_T (ton/ft^2) = 0.6*N	
(3) Tip Resistance, Q_T (kip) = A_T(ft^2)*q_T(ton/ft^2)*2(kip/ton)	

5.2.3 Estimated vs. Measured Grout Volumes

The predicted grout volumes for the field shaft were calculated using the same method as with the long shaft predictions presented above, which were discussed in section 5.1.3. The predicted grout volumes for side and tip grouting were calculated given the shaft geometry and final cavity expansions (i.e., expand to 1 ½ D). The side grout bulb was modeled as a cylindrical cavity expansion, and the tip grout bulb was modeled as a spherical cavity expansion. The volume of grout needed to create a cylindrical side grout bulb (i.e., 9 ½ feet long by 1 ½ D) was 114.25 ft^3 (855 gal), and the volume of grout needed to create a spherical tip grout bulb (i.e., expand to 1 ½ D) was 75.78 ft^3 (567 gal).

The actual grout pumped during side grouting was 615 gallons (Figure 4-32), which was 72% of the calculated theoretical value (855 gallons). As identified in section 5.1.3, pleating (top and bottom of the membrane) may result in loss of 10% to 20% of the theoretical volume. Consequently if the pumped volumes exceed 70% of the theoretical volume and grout pressures were equal to or greater than that of the cylindrical cavity expansion limit pressures, grouting may be suspended. Note, the actual grout pressures exceeded this estimated value, thus grouting was stopped. This will be discussed further in section 5.2.5.

In the case of tip grouting, a theoretical spherical volume of 567 gallons corresponded to the spherical limit pressure of 1,160 psi. However, pumping stopped at a volume of about 80 gallons (77.6 gallons measured), tip grout pressure of only 600 psi (Figure 4-35), and upward movement of the shaft in excess of 0.35" (0.8% D). The upward movement was limited to estimate side friction between membrane/shaft and soil (i.e., upward movement < 1% D to fully mobilized side resistance). Again, due to end bearing effects on the side grout zone (42" vs. 54"), side resistance of the shaft was actually greater (see section 4.3.5). Consequently, it is expected that higher tip volumes and grout pressures could have been mobilized.

5.2.4 Estimated vs. Predicted Grout Pressures

Expected grout pressures were again estimated for the field test shaft using cylindrical and spherical cavity limit pressure charts published by Salgado and Randolph (2001). The estimated in situ stresses were used to calculate the lateral and mean stresses at the appropriate depths (i.e., middle of side grout zone and tip grout zone). During cavity expansion, the soil strains are large, so the ultimate friction angle should be used with the cavity limit pressure charts. An ultimate friction angle of 36.2° was used to estimate cavity limit pressures in the charts (Salgado and Randolph, 2001). The predicted side grout pressures are given in Figure 5-12 and Table 5-21, and on the next page, the predicted tip grout pressure are given in Figure 5-13 and Table 5-22.

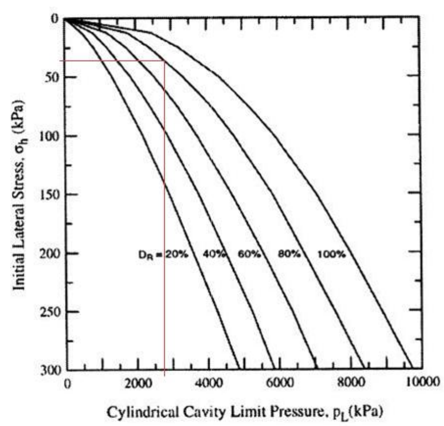

Figure 5-12: Cylindrical cavity limit pressure at a depth of 20 feet for φ = 36°

Table 5-21: Cylindrical cavity limit pressure during side grouting

Depth to Middle of Side Grouted Zone (ft	20	
W.T. Depth (ft)	8	
Vertical Effective Stress, σ_v' (lb/ft^2)	1636	
*Lateral Earth Pressure Coef., K_0	0.34	
Horizontal Effective Stress, σ_h' (lb/ft^2)	558	
**Horizontal Effective Stress, σ_h' (kPa)	26.7	= Initial Lateral Stress, σ_h (kPa)
Cylindrical Cavity Limit Pressure (kPa)	2750	
Cylindrical Cavity Limit Pressure (lb/ft^2)	57435	
Cylindrical Cavity Limit Pressure (lb/in^2)	**399**	

*Low strain, so peak friction angle should be used (Jaky 1960, $K_0 = 1 - \sin(\phi_p)$)

**1 (lb/ft^3) = 47.8803 (Pa)

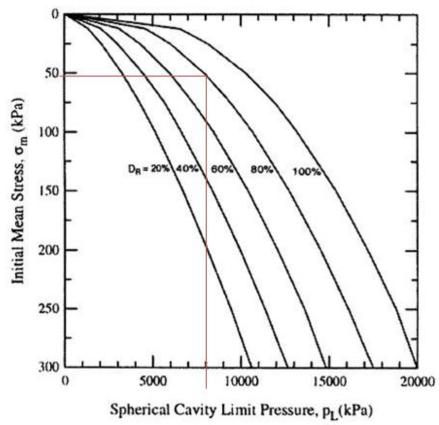

Figure 5-13: Spherical cavity limit pressure at a depth of 25 feet for φ = 36°

Table 5-22: Spherical cavity limit pressure during tip grouting

Depth to Tip (ft)	25
W.T. Depth (ft)	8
Vertical Effective Stress, σ_v' (lb/ft^2)	1949
Coefficient of Lateral Earth Pressure, K_0	0.34
Horizontal Effective Stress, σ_h' (lb/ft^2)	665
*Initial Mean Stress, σ_m' (lb/ft^2)	1093
**Initial Mean Stress, σ_m' (kPa)	52
Spherical Cavity Limit Pressure (kPa)	8000
Spherical Cavity Limit Pressure (lb/ft^2)	167083.3
Spherical Cavity Limit Pressure (lb/in^2)	**1160**

*Initial Mean Stress, $\sigma_m' = (2*\sigma_h' + \sigma_v')/3$

**1 (lb/ft^3) = 47.8803 (Pa)

The estimated cylindrical cavity expansion stress of 399 psi agrees closely with the maximum pumped side grout pressure of 420 psi (Figure 4-31). Note, this was contrast with the observed chamber test results of 600 psi (Figure 4-12) vs. its theoretical value of 261 psi (Table 5-7), i.e., the chamber results were greatly impacted by chamber wall (boundary effects). The field shaft results support the concept that the side grout zone was expanding outward as cylindrical cavity.

In the case of the tip grout pressures, the linearly increasing grout pressure vs. volume (Figure 4-35) supports the cavity expansion concept. In addition, the limiting tip pressure of 600 psi, pumped volume of 78 gallons, and shaft movement of 0.35" (Figure 4-37), suggests that higher tip pressures may be achievable (Table 5-22). It should be noted that the volume pumped (78 gallons) exceeded the volume to fill the base plate (i.e., 20 gallons), and the grout could have expanded either radially or vertically. To be conservative all subsequent calculations (e.g., tip force) will assume a tip area that is based on original diameter of the steel base plate (D = 40").

5.2.5 Estimate Side Resistance of Shaft after Grouting

For the case of the field grouted drilled shaft, the side resistance (after side grouting) was estimated using four methods: (1) K_g method (Thiyyakkandi et al., 2013b; McVay et al., 2009); (2) in situ Pressuremeter Test (PMT); (3) measured in situ soil pressure cell data; and (4) measured tip grouting pressures during construction (i.e., final grouting stage). Comparison of the capacity estimations versus the observed mobilized side resistance during load testing will be presented in section 5.2.6.

The first method used to assess the unit side resistance of side-grouted shaft was the K_g method (Thiyyakkandi et al., 2013b; McVay et al., 2009), as shown in Table 5-23. This method requires the calculation of both K_g and unit side friction factor, f_s (see equations below Table 5-23). For the mobilized side resistance, f_s, the ultimate/peak friction angle (i.e., 41.2°) is generally considered, and for cavity expansions (i.e., Salgado and Randolph, 2001) or estimation of K_g, the ultimate/critical friction angle (i.e., 36.2°) is generally recommended (Thiyyakkandi et al., 2013b; McVay et al., 2009). To estimate the K_g coefficient, lines were drawn corresponding to the top and bottom of the side grouted zone, as shown in Figure 5-14 (blue lines). Then, the coefficient K_g of 1.85

at the midpoint of the side grouted zone (red lines) was selected (linear between top and bottom of the side grouted zone). The estimated side resistance along the side grouted zone after side grouting was estimated to be 689 kip using the K_g method (Table 5-23). The total side resistance of the shaft after side grouting was estimated to be 770 kip (689 kip in grout zone and 81 kip above).

Table 5-23: K_g method

Soil Layer (#)	Depth (ft)	Depth to Mid-Point of Soil Layer (ft)	Peak Friction Angle, ϕ_p	Post Grout Surface Area, A_{sg} (ft^2)	Vertical Effective Stress, σ_v' (lb/ft^2)	(1) K_g	(2) Post Grout Vertical Stress, σ_{vg}' (lb/ft^2)	(3) Post Grout Unit Side Resist., $f_{s3\text{-}Kg}$ (kip/ft^2)	(4) Post Grout Side Resist., $q_{s3\text{-}Kg}$ (kip)	
3	15 - 25	20	41.2	156.69	1636	1.85	3027	4.40	689	$= q_{s3\text{-}Kg}$
(1) Use $\phi_c = \phi_u = 36.2°$ (See Plot Below)				**(5) Total Side Resistance (Post Side Grout), $Q_{sg\text{-}Total\text{-}Kg}$ =**					**770**	
(2) Post Side Grout Vertical Effective Stress, $\sigma_{vg}' = K_g*\sigma_v'$										
(3) Post Grout Unit Side Resistance along Side Grouted Zone, $f_{s3\text{-}Kg} = \sigma_{vg}'*[\sin\phi_p/(1-\sin\phi_p)]*\sin(90-\phi_p)$										
(4) Post Grout Side Resistance along Side Grouted Zone, $q_{s3\text{-}Kg} = f_{s3\text{-}Kg}*A_{sg}$										
(5) Total Side Resistance after Side Grouting, $Q_{sg\text{-}Total\text{-}Kg} = Q_{s\text{-}above} + q_{s3\text{-}Kg}$										

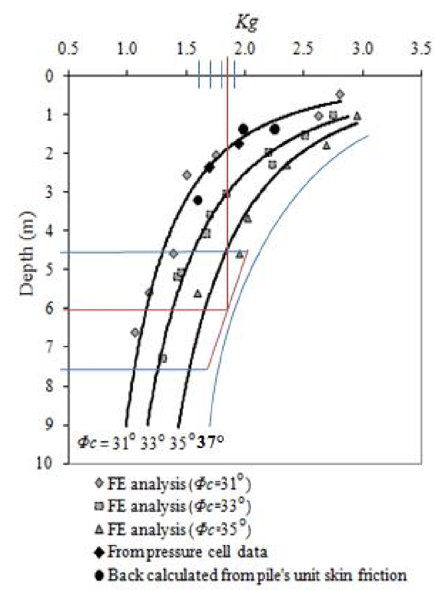

Figure 5-14: K_g coefficient chart (Thiyyakkandi and McVay, 2013)

The second method used to assess side friction of the side-grouted shaft is the PMT approach (Thiyyakkandi et al., 2013b; McVay et al., 2009). This method requires the estimate of both the lateral stress alongside the grout zone and Columbic friction between the soil and the grout membrane. Generally, Columbic friction angles of ⅔ that of the peak resistance, ϕ_p (41.2°) are used in the literature. However, laboratory shear tests on the sand-RPP interface (section 2.2.1) suggested that the interface friction angle between soil and polypropylene may be greater than ⅔ and closer to ⅘ of the peak friction angle. Therefore for the PMT analysis, an interface friction, δ_i', between the soil and the side membrane of 33° was used (i.e., $\delta_i' = ⅘ \times \phi_p$ (triaxial); Table 5-24).

Table 5-24: Interface friction angle

(1) Peak Friction Angle, ϕ_p	41.2
(2) Interface Friction Angle (Recomended), δ_i	27.5
(3) Ultimate Friction Angle, ϕ_u	35
(4) Interface Friction Angle, ϕ_i	28
(5) Interface Friction Ratio, Δ_i	0.80
(6) Interface Friction Angle (Measured), δ_i'	33

(1) Peak Friction Angle Calculated from Tri-Axial Test (A-3 Sand)
(2) Interface Friction Angle Recommended with Beta Method, $\delta_i = ⅔ * \phi_p$
(3) Ultimate Friction Angle from Direct Shear Test (A-3 Sand), ϕ_u
(4) Interface Friction Angle from Direct Shear Test (A-3 Sand & RPP), ϕ_i
(5) Interface Friction Ratio, $\Delta_i = \phi_i/\phi_u$
(6) Interface Friction Angle given Direct Shear Results , $\delta_i' = \Delta_i * \phi_p$

To estimate the lateral stresses after side grouting, the PMT results were used. Recall, the PMT was performed in the footprint of the shaft at a depth equal to the midpoint of the side grouted zone (section 3.1.2; Figure 3-20). Tangent lines were used to estimate the residual stress after a cavity expansion pressure and was estimated to be 3.5 bars or 14.5 psi, as shown in Figure 5-15 and Table 5-25. Note, the residual stresses alongside the device are used to represent the expected grout-soil stresses long-term. Using the interface friction angle of 33° and residual lateral stress, the side resistance alongside grouted zone was estimated and shown in Table 5-25 (see equations below table). The estimated side resistance along the grout zone was 743 kip, and the total side resistance was 824 kip (743 kip along grouted zone; 81 kip above).

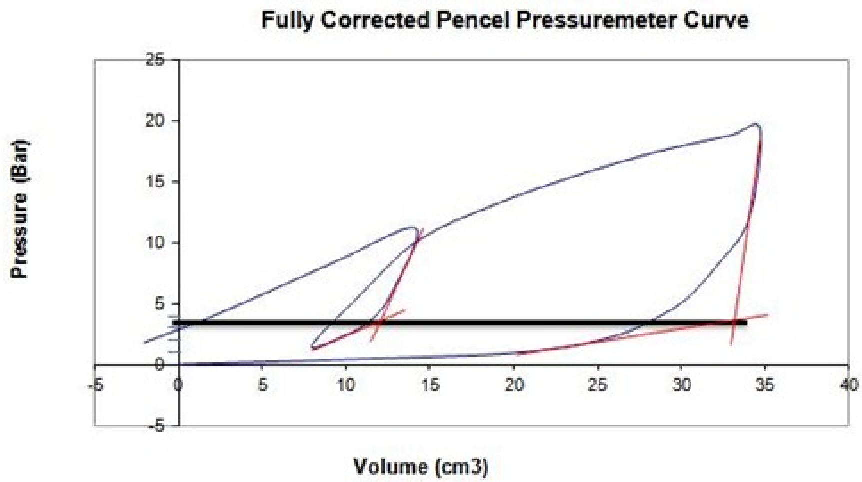

Figure 5-15: PMT in footprint of field shaft

Table 5-25: PMT method

Residual Stress (Bar)	Residual Stress (lb/in^2)	Peak Friction Angle, ϕ_p	Post Grout Surface Area, A_{sg} (ft^2)	(1) Unit Side Resist. along Side Grouted Zone, $f_{s3\text{-}PMT}$ (ksf)	(2) Friction along Side Grouted Zone, $q_{s3\text{-}PMT}$ (kip)	(3) Total Side Resist., $Q_{sg\text{-}Total\text{-}PMT}$ (kip)
3.5	50.76	41.2	156.69	4.74	743	824
(1) Post Grout Unit Side Resistance along Side Grouted Zone, $f_{sg\text{-}PMT}$ = ("Residual Stress")*tan(δ_i')						
where: Interface Friction Angle, $\delta_i' = \Delta_i * \phi_p = 33°$						
(2) Post Grout Side Resistance along Side Grouted Zone, $q_{s3\text{-}PMT} = f_{s3\text{-}PMT} * A_{sg}$						
(3) Total Side Resistance after Side Grouting, $Q_{sg\text{-}Total\text{-}PMT} = Q_{s\text{-}above} + q_{s3\text{-}PMT}$						

The third method for estimating side resistance was the use of pressure cell data collected just before the tip grouting phase which reflects the lateral stress state after shaft construction and side grouting (i.e., direct measurement of horizontal earth pressures). Using pressure cells #2 and #3, the lateral earth pressure on the side membrane was estimated graphically, as shown in Figure 5-16. That is, the lateral earth pressures were plotted against the pressure cell locations (i.e., distance away from shaft divided by the shaft diameter). A third point was added that corresponds to the in situ lateral stress of 3.88 psi at a distance of four diameters away. The residual stress on the interface of the side grouted zone before tip grouting was estimated to be 54.55 psi, as shown in Table 5-26 (see equations below table). Using the interface friction angle of 33°, the estimated side resistance along the side grouted zone after side grouting was 798 kip, and the total resistance was 879 kip (798 kip along grouted zone; 81 kip above).

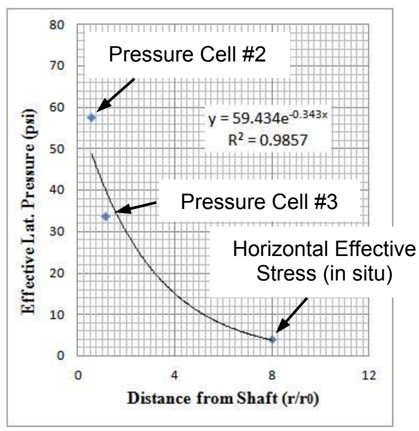

Figure 5-16: Push-in pressure cell readings (lateral stress) vs. pleasure cell location

Table 5-26: Pressure cell method

(1) Lateral Stress (lb/in^2)	Peak Friction Angle, ϕ_p	Post Grout Surface Area, A_{sg} (ft^2)	(2) Unit Side Resist. along Side Grouted Zone, $f_{s3\text{-}PCell}$ (ksf)	(3) Friction along Side Grouted Zone, $q_{s3\text{-}PCell}$ (kip)	(4) Total Side Resist., $Q_{sg\text{-}Total\text{-}PCell}$ (kip)
54.55	41.2	156.69	5.09	798	879

(1) Final Lateral Stress on Side Membrane (psi), $y = 59.434 * e^{-0.343x}$

where: x = Location of Side Membrane/Shaft Diemeter = 10.5/42 = 0.25

(2) Unit Resistance, $f_{sg\text{-}PCell}$ = ("Lateral Stress")*tan(δ_i')

where: Interface Friction Angle, $\delta_i' = \Delta_i * \phi_p = 33°$

(3) Friction along Side Grouted Zone, $q_{s3\text{-}PCell} = f_{s3\text{-}PCell} * A_{sg}$

(4) Total Side Resistance, $Q_{sg\text{-}Total\text{-}PCell} = Q_{s\text{-}above} + q_{s3\text{-}PCell}$

The final estimate of the side-and-tip-grouted shaft capacity was based on the observed tip grout pressure of 620 psi multiplied by the original base plate area of 1,256.6 in^2 (D=40"), for total side resistance of 779 kip (i.e., grouted zone and above; Figure 4-43 - right). Note again that since the upward displacement of the shaft was 0.34 inch, approaching 1% of the shaft diameter, the side resistance should have been fully mobilized; however, no consideration was given to the bearing at the ends of side membrane. Using the assumption that the shaft capacity should be at least twice the mobilized side resistance during tip grouting, then the total capacity of the shaft was estimated to be 1,558 kip.

5.2.6 Comparison of Measured and Predicted Shaft Capacities

Of interest was a comparison of measured and predicted capacities for the field constructed drilled shaft (42" x 25') at Keystone Heights and is shown in Table 5-27. Row one describes the case of an ungrouted shaft (section 5.2.2), which has an estimated total capacity of 566 kip (243 kip - side; 323 kip - tip). The second row shows the case for a drilled shaft (42" x 25') that was just tip grouted following conventional methods, i.e., no side grouting prior to tip grouting. Table 5-28 shows the estimation procedure for conventional tip-grouted shafts (FDOT Soils and Foundations Handbook, 2012; Mullins et al, 2006). In Table 5-27 (row two), the side resistance of 243 kip (ungrouted) was added to the estimated tip resistance of 464 kip (conventional tip-grouted shaft) for a total resistance of 707 kip; however, conventional tip-grouted shafts are limited by the available resistance during tip grouting (i.e., side resistance and self-weight), so the ultimate capacity of conventional tip-grouted shaft is limited to twice the mobilized side resistance during tip grouting (i.e., no side grouting prior). Therefore, the ultimate capacity given for a conventional tip-grouted shaft in Table 5-27 was over estimated. The next four rows in Table 5-27 (i.e., row three to six) are the estimated shaft resistance for the new side-and-tip-grouted drilled shaft (section 5.2.5). Note that the total capacities ranged from 1,540 kip to 1,782 kip. Rows seven and eight are the measured/calculated mobilized static side and tip resistance of the side-and-tip-grouted drilled shaft tested in the field (i.e., static and Statnamic load test results).

Evident from the Table 5-27, side grouting has a significant impact on improvement of both the side and tip resistance of the drilled shaft. Specifically, the Statnamic testing indicated that the total static resistance of the shaft was 2,650 kip at a mobilized top shaft movement of 1.5". The higher side resistance of 1,350 kip vs. 770 kip to 891 kip (rows three to six) may be attributed to bearing resistance developed on the bottom end of the grouted membrane, which is currently neglected (i.e., conservative).

Table 5-27: Measured and predicted field shaft capacities

	Above Side Grouted Zone (Top 15 ft of Shaft)		Along Side Grouted Zone (Bottom 10 ft of Shaft)					
	Unit Side Resistance (ksf)	Side Resistance (Kip)	Unit Side Resistance (ksf)	Side Resistance (Kip)	Total Side Resistance (Kip)	Tip Resistance (Kip)	Ultimate Load (Kip)	
Ungrouted Drilled Shaft (Include Tip Resist.)	0.49	81	1.47	161	243	323	566	
(1) Conventional Tip Grouted Shaft (No Side Grouting)	0.49	81	1.47	161	243	464	707	
Side & Tip Grouted Drilled Shaft, Kg Method	---	---	4.40	689	770	---	1540	
Side & Tip Grouted Drilled Shaft, PMT Method	---	---	4.74	743	824	---	1648	
Side & Tip Grouted Drilled Shaft, Pressure Cell Data	---	---	5.09	798	891	---	1782	
(2) Mobilized during Tip Grouting (Max)	---	---	---	---	779	779	1558	
(3) Mobilized during Static Load Test (Max)	0.52	86	3.34	523	609	241	850	(5)
(4) Mobilized during Statnamic Test (Max)	1.21	200	7.33	1150	1350	1300	2650	(6)
(1) Donwward Displacement (Top of Shaft) = 5% of Shaft Diameter (2.1 Inch)								
(2) Upward Displacement (Top of Shaft) = 0.34 Inch (0.81% of Shaft Diameter)								
(3) Downward Displacement (Top of Shaft) = 0.18 Inch (0.43% of Shaft Diameter)								
(4) Downward Displacement (Top of Shaft) = 1.5 Inch (3.6% of Shaft Diameter)								
(5) Maximum Applied Load during Static Load Test so Not an Ultimate Load								
(6) Maximum Static Load during Statnamic Load Test using UF Method								

Table 5-28: Conventional tip-grouted shaft resistance (FDOT Soils and Foundations Handbook, 2012; Mullin et al., 2006)

Tip Area, A_T (ft^2)	9.62
(1) Grouted Tip Area, $A_{T\text{-}Grouted}$ (ft^2)	8.30
Avgerage Tip N-Value	28
(2) Unit Tip Resistance, q_{tip} (ton/ft^2)	16.8
Side Resistance, Q_s (ton)	121.5
(3) Maximum Grout Pressure, GP_{max} (ton/ft^2)	12.6
(4) Grout Pressure Index, GPI	0.75
Maximum Displacement, %D (%)	3.6
(5) Tip Capacity Multiplier, TCM	1.67
(6) Grouted Unit Tip Resist., $q_{grouted}$ (ton/ft^2)	27.97
(7) Grouted Tip Resistance Q_t (ton)	232.07
(8) Unltimate Resistance (ton)	**353.57**

(1) Tip Area of the Shaft $after\ Grouting, A_{grouted-tip} = \pi \text{ x } (r - 3 \text{ in})^2$

(2) Ungrouted Unit Tip Resistance, $q_{tip}(\text{tsf}) = 0.6 \text{ x N}$
where: $N = 28\ (AASHTO, 2010)$

(3) Maximum Grout Pressure, $GP_{max} = {}^{Q_s}/_{A_{tip}}$
$where{:}\ Q_s(ton) = {}^{Q_{s-Total}\,(kip)}/_{2}$

(4) Grout Pressure Index, $GPI = {}^{GP_{max}}/_{q_{tip}}$

(5) Tip Capacity Multiplier, $\text{TCM} = 0.713 \text{ x GPI x } (\%D^{0.364}) + \frac{\%D}{(0.4 \text{ x } \%D)+3.0}$
$where{:}\ \%D = 3.6\%\ (observed\ during\ Statnamic\ test)$

(6) Grouted Unit Tip Resistance, $q_{grouted} = TCM \text{ x } q_{tip}$

(7) Grouted Tip Resistnace, $Q_t = q_{grouted} \text{ x } A_{grouted-tip}$

(8) Ultimate Resistnace $= Q_t + Q_s$

CHAPTER 6
DISCUSSION AND CONCLUSION

6.1 Background and Objectives

Drilled shafts are used as a foundation beneath structures (bridges, buildings, etc.) and common in urban areas (e.g., vibration issues) or where large lateral loading is expected in limited right of way areas (e.g., barge impact on bridge pier). Unfortunately in sands and silts, the axial resistance of drilled shafts is generally lower than that of similar sized driven large-displacement piles. To increase the axial capacity of drilled shafts, conventional methods of post grouting drilled shaft tips/bottoms are seeing increased use in Florida and throughout the US (Mullins et al., 2006). The technique involves attaching a steel plate with welded ring to the bottom of the drilled shaft's reinforcement cage. Passing through the plate from the top of the shaft are PVC pipes used in the tip grouting. Also covering the bottom steel ring and PVC pipes is a rubber membrane for protection. The shaft is cast in situ, allowed to hydrate, and then tip grouted. The grouting of the shaft tip via conventional methods serves two functions (Thiyyakkandi et al., 2013; McVay et al, 2009): (1) it preloads the tip or it increases the shaft tip mobilization at the onset of axial top loading; and (2) it gives an estimate of axial shaft capacity (i.e., grout pressure times cross-sectional tip area). Unfortunately during tip grouting, it has been found that grout first fills the ring void beneath the shaft and then flows in the weakest direction, which is usually up alongside the soil-shaft interface (low radial stress around shaft) thus reducing side friction (fluid grout) during grouting process (McVay et al, 2009).

However, the FDOT readily recognized that grouting had the potential to significantly increase the axial capacity of a drilled shaft. Specifically if the stress states (side and tip) could be increased (e.g., cavity expansion), a significant side and tip resistance could be developed vs. ungrouted or conventional tip-grouted drilled shaft approaches.

Consequently the focus of this research was to develop/introduce materials and construction practices which would allow a traditional drilled shaft to be cast (e.g., drill hole, rebar cage placement, and concreting), subsequently side grouted, followed by tip grouting with sufficient wait times for concrete and grout hydration. As with the development of any new technology, the experimental effort was scaled up from small proof test of concept experiment to larger tests in a controlled environment (i.e., FDOT test chamber), finally to full-scale testing at an FDOT field site. For any future applications, the methods of design (e.g., in situ tests) and validation (grout pressures and volumes) during construction were needed. Presented is the summary of materials, construction steps, grouting practices, and recommended design approach for side-and-tip-grouted drilled shafts.

6.2 Constructing a Side-and-Tip-Grouted Drilled Shaft

The final side-and-tip-grouted drilled shaft is expected to look like Figure 6-1. It includes two separate grouting systems: (1) side and (2) tip. The side grout system is composed of the following components: (1) tube-a-manchettes for grout delivery; (2) flexible top and bottom seals; (3) polypropylene side membrane; (4) colloidal grout (cement, fly ash, and water); and (5) multiple sets of steel rings (hold side membrane, seals, etc.). The tip grouting system has the following components: (1) tube-a-manchettes for grout delivery; (2) steel base plate and bottom ring; (3) steel feet (cage support and bottom manchette protection); (4) bottom membrane; and (5) colloidal grout (cement, fly ash and water). A summary discussion of each follows.

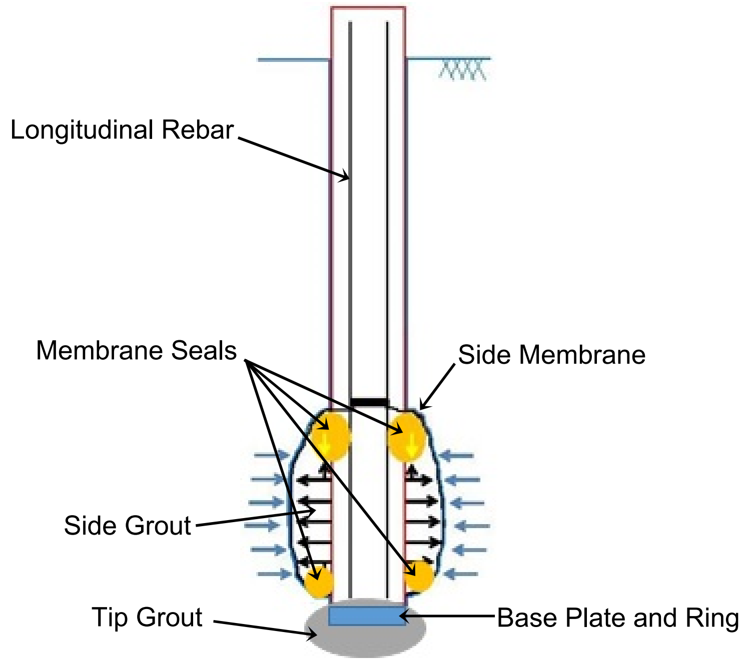

Figure 6-1: Side-and-tip-grouting system

For the side grout system, the polypropylene side membrane has two main functions: (1) prevents mixing of grout and soil (loss of grout strength and grout-shaft concrete bond); and (2) limits grout flow to form a cylindrical shape/expansion (i.e., impermeable membrane). The top and bottom membrane seals have three important functions: (1) inflated with air during shaft construction, they prevent concrete from flowing outside of the membrane (i.e., embedding side membrane within shaft); (2) separate the membrane from the concrete shaft in the first stage of grouting (i.e., grout membrane seals); and (3) help anchor the shaft and provide top and bottom constraints during side grouting (i.e., upper and lower boundaries).

In the case of the tip grouting system, separate tube-a-manchettes from the top to the bottom of the shaft are required. The pipes exiting the top and bottom of the shaft should be constructed from schedule 80 steel pipes due to the large tip grout pressures (> 1,000 psi). A steel base plate, steel ring, and steel feet are strongly recommended for the tip grout system. The side-and-tip grouted cage (i.e., rebar cage with grout systems attached) is designed to sit on the bottom of the drilled hole, so the steel feet provide support to limit settlement of the cage during concrete placement. The shaft feet along with steel ring and bottom membrane protection the tip-manchette (tube-a-manchette) from becoming clogged with soil, embedded during concrete placement, or being damaged due to excessive settlement of the cage; in addition, the steel base plate, steel ring, and bottom membrane create a void below the shaft tip for grout pressures to develop and provides a good contact area with known surface area between the shaft tip and grout.

The evolution of both the side and tip grouting systems evolved from the small scale experiments (small shaft) up to the large scale (large shaft) and finally the full scale field test (field shaft). For instance, the membrane seals started from using only one seal at the top of the side grouted zone and evolved to using two membrane seals (top and bottom of the side grouted zone). Also, changes in material type were made to accommodate higher grout pressures, connection type was changed to improve reliability and stop air leaks, air/grout delivery system was improved, steel rings were added to support the seals (i.e., minimize intrusion onto rebar to ensure adequate concrete cover), flexible hoses to allow membrane seal to expand away from shaft during grouting, and so on.

6.3 Design/Validation Results

The main focus of this research was to improve the axial capacity of drilled shafts installed in cohesionless soils. One way to accomplish this was by introducing cavity expansion stresses around the shaft. Specifically by first developing cylindrical cavity expansion stress state alongside the shaft, two important outcomes were accomplished: (1) shaft side friction increased, which is a function of significant lateral stress increased and increased surface area where side grouting occurred; and (2) allows for development of spherical cavity expansion at the tip of the shaft during subsequent tip grouting if sufficient upward shaft resistance is available. The development of spherical cavity expansion at the tip was possible due to the increase in mean stresses alongside the shaft and an enlarged side grouted boundary constraint; that is, the side grouted zone provided greater resistance to upward movement (i.e., increased side resistance and self-weight) and restricted grout flow vertically upwards (i.e., side grout bulb acted as a rigid boundary and mean stresses above the tip were greater than below). The development of spherical cavity limit stress at the tip of a drilled shaft (i.e., tip grouting) will mobilize significant tip resistance beneath a drilled shaft with small vertical movements during reloading, especially if the area of the tip is enlarged.

Validation of the cylindrical cavity expansion during side grouting was observed in both the large shaft (36" x 25') in the test chamber and field shaft (42" x 26') at the test site. For instance, side grout pressures in the test chamber of 600 psi exceeded the cylindrical cavity expansion values of 261 psi (Salgado and Randolph, 2001). The greater measured side grout pressures were attributed to chamber wall effects (confirmed with soil movements). Excavation of the large shaft did reveal cylindrical expansion had occurred. In the case of the field shaft, measured side grout pressures of 420 psi agreed closely with the predicted cavity expansion pressures of 399 psi (Salgado and Randolph, 2001).

In the case of tip grouting after side grouting, the large shaft exhibited a peak grout pressure of 700 psi which compared favorably with cavity spherical cavity expansion stress of 783 psi (Salgado and Randolph, 2001). For the field shaft, peak tip grout pressure of 620 psi was observed vs. spherical cavity expansion stress of 1,160 psi (Salgado and Randolph, 2001). Upward vertical movement of the field shaft was limited to only 0.3" to quantify friction between the side membrane and soil. If further side resistance was mobilized (e.g., Statnamic test), larger tip stresses (i.e., grout pressures) and grout volumes would have been achievable.

Successively, the side resistance (after side grouting) was estimated using one of four methods: (1) K_g method (Thiyyakkandi et al., 2013; McVay et al, 2009); (2) in situ PMT; (3) measured in situ pressure cell data; and/or (4) measured tip grouting pressures during construction. Total capacity was estimated as at least twice the estimate side resistance that was mobilized during tip grouting. Comparison of capacity estimations versus the observed mobilized side (Chapter 5) generally showed them to be conservative (i.e., under predict side friction). This was attributed to the increased diameter of the side grout zone (58" vs. 42") and mobilization of end bearing on the end of the side grouted zone (i.e., end bearing on ledge/shelf).

Finally, a comparison between conventional ungrouted drilled shafts response with the side-and-tip-grouted drilled shaft response is shown in Figure 6-2. Presented is a comparison between the back calculated static response from the Statnamic test (Middendorp et al., 1992) vs. predicted FB-Deep response (42 inch and 58 inch drilled shaft). The predicted FB-Deep analysis used SPT boring B11 (Table 5-10) and considered two shaft diameters: (1) 42 inch diameter (ungrouted shaft); and (2) 58 inch diameter (diameter of side grouted zone; see Chapter 5). Evident at service deformations (e.g., 1"), the side-and-tip-grouted drilled shaft has over three times the capacity of the conventional drilled shaft.

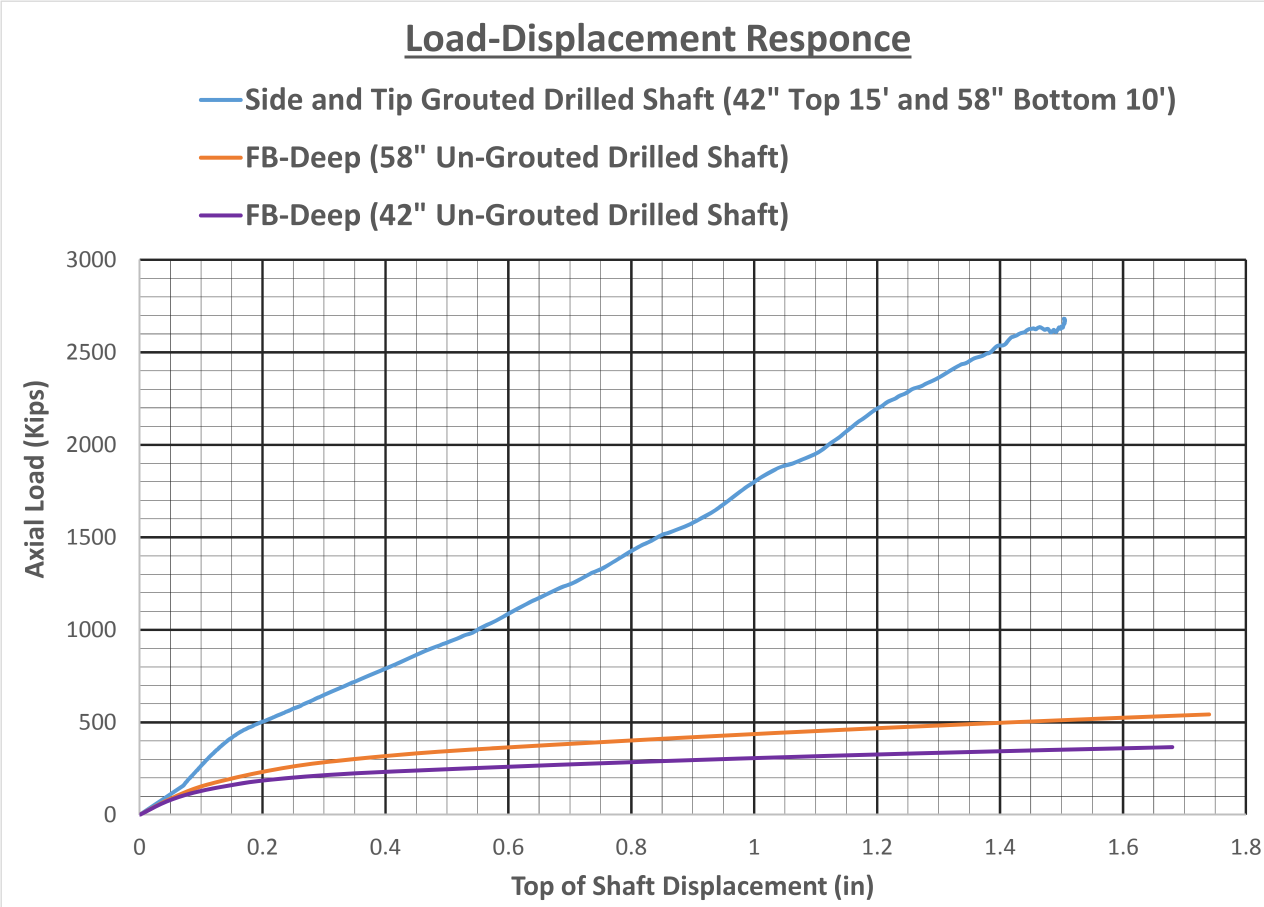

Figure 6-2: Comparison between side-and-tip-grouted drilled shaft with conventional ungrouted shafts (42" and 58")

REFERENCES

American Association of State Highway and Transportation Officials [AASHTO] (2010). *LRFD bridge design specifications*, 5th Edition, AASHTO.

American Society for Testing and Materials [ASTM] D 1143/D 1143M (2007). Standard test methods for deep foundations under static axial compression load, ASTM.

Bruce, D.A. (1986). “Enhancing the performance of large diameter piles by grouting,” Parts 1 and 2, *Ground Engineering*, May and July, respectively.

Florida Department of Transportation [FDOT] (2012). *Soils and Foundations Handbook*. FDOT State Materials Office Gainesville, Florida

Kulhawy, F.H., and Mayne, P.H. (1990). “Manual on Estimating Soil Properties for Foundation Design.” Report EL-6800, Final Rep. Submitted Electric Power Research institute [EPRI], August 1990.

Holtz, R. D. and Kovacs, W. D. (1981). *An Introduction to Geotechnical Engineering*. Prentice Hall, N.J.

Marchetti, S., and Craps, D. (1981). “Flat dilatometer manual,” Internal report of G.P.E. Inc.

Marchetti, S. (1997). “The flat dilatometer: design applications.” Proc. Third International Geotechnical Engineering Conference, Keynote lecture, Cairo University, Jan., 421-448.

Mayne, P.W., and Kulhawy, F.H. (1982). “K0-OCR relationships in soil.” *Journal of Geotechnical Engineering*, Vol. 108 (GT6), pp.851-872.

Mayne, P.W. (2007). “National Cooperative Highway Research Program [NCHRP] Synthesis 368: Cone Penetration Testing.” Transportation Research Board, National Research Council, Washington, D.C., 117 pages.

McVay, M., Bloomquist, D., Forbes, H., and Johnson, J. (2009). “Prestresses Concrete Pile Installation – Utilized Jetting and Pressure Grouting.” Final Rep. Submitted Florida Department of Transportation, Fla.

McVay, M. C. and Thiyyakkandi, S. (2010). “Group Efficiencies of Grout-Tipped Drilled Shafts and Jet-Grouted Piles.” Final Rep. Submitted Florida Department of Transportation, Fla.

Meyerhof, G.G. (1957). “Discussion on Research on determining the density of sands by penetration testing.” Proc. 4th Int. Conf. on Soil Mech. and Found. Eng., Vol. 1: 110.

Middendorp, P., Bermingham, P., and Kuiper, B. (1992). "Statnamic Load Testing of a Foundation Pile." Proceedings, 4th International Conference on Application of Stress-Wave Theory to Piles, The Hague, pp. 581-588

Mullins, G., Dapp, S., Fredrerick, E., and Wagner, R. (2001). "Pressure grouting drilled shaft tips - Phase I final report." Final Rep. Submitted Florida Department of Transportation, Fla.

Mullins, G., Dapp, S., and Lai, P. (2000). "Pressure-grouting drilled shaft tips in sand." New technological and design developments in deep foundations, N. D. Dennis, R. Castelli, and M. W. O'Neill, eds., ASCE, Reston, Va.

Mullins, G., Lewis, C. L. & Justason, M. D (2002). "Advancements in Statnamic data regression techniques." Proceedings of the ASTM International Deep Foundations Congress, ASTM Geotechnical Special Publication No. 116, Vol. 2, pp. 915–930. West Conshohocken, PA: ASTM International.

Mullins, G., and Winters, D. (2004). "Post grouting drilled shaft tips - Phase II final report." Final Rep. Submitted Florida Department of Transportation, Fla.

Mullins, G., Winters, D., and Dapp, S. (2006). "Predicting End Bearing Capacity of Post Grouted Drilled Shafts in Cohesionless Soils." ASCE *Journal of Geotechnical and Geoenvironmental Engineering*, Vol. 132, No. 4. pp. 478-487

O'Neil, M. W., and Reese, L. C. (1999). "Drilled shafts: Construction procedures and design methods." FHWA, Publication No. FHWA-IF-99-025.

Reese, L. C., and O'Neill, M. W. (1988). "Drilled shafts: Construction and design." FHWA, Publication No. HI-88-042.

Robertson, P.K., and Campanella, R.G., (1983). "Interpretation of cone penetration tests - part I: sand." *Canadian Geotechnical Journal*, 20(4); 718-733.

Schmertmann, J. H., (1975). "Measurement of in-situ shear strength." Proceedings of the Specialty Conference on in-situ Measurement of Soil Properties, ASCE, Raleigh, Vol. 2 pp. 57-138.

Salgado, R., and Prezzi, M. (2007). "Computation of Cavity Expansion Pressure and Penetration Resistance in Sands." *International Journal of Geomechanics*, Vol. 7, No. 4, pp. 251-265.

Salgado, R. and Randolph, M. (2001). "Analysis of Cavity Expansion in Sands." *The International Journal of Geomechanics*, Vol. 1, No. 2, p. 175-192

Thiyyakkandi, S., McVay, M., Bloomquist, D., Lai, P. (2013a). "Measured and predicted response of a new jetted and grouted precast pile with membranes in cohesionless soils." *Journal of Geotechnical and Geoenvironmental Engineering*, 139 (8), 1334-1345.

Thiyyakkandi, S., McVay, M., Bloomquist, D., Lai, P. (2013b). “Experimental study, numerical modeling of and axial prediction approach to base grouted drilled shafts in cohesionless soils.” *Acta Geotechnica*, Springer. DOI: 10.1007/s11440-013-0246-3.

Tran K. T, McVay M., Herrera R., and Lai P. (2011a). “A New Method for Estimating Driven Pile Static Skin Friction with Instrumentation at the Top and Bottom of the Pile.” *Soil Dynamics and Earthquake Engineering*, Vol. 31, pp. 1285-1205.

Tran K. T, McVay M., Herrera R., and Lai P. (2011b). “Estimating Static Tip Resistance of Driven Piles with Bottom Pile Instrumentation.” *Canadian Journal of Geotechnical Engineering*, Vol. 49, pp. 381-393.

U.S. Department of Transportation Federal Highway Administration [FHWA] (2010). *Drilled Shafts: Construction Procedures and LRFD Design Methods*. FHWA-NHI-10-016, FHWA GEC 010